SERI/CP-252-2714
DE86014506

August 1986

Proceedings: Workshop on Solar Applications of Energy Conversion Technology

February 19, 1985
Golden, Colorado

SERI

Solar Energy Research Institute
A Division of Midwest Research Institute

1617 Cole Boulevard
Golden, Colorado 80401-3393

Operated for the
U.S. Department of Energy
under Contract No. DE-AC02-83CH10093

SERI/CP-252-2714
UC Category: 62
DE86014506

Proceedings: Workshop on Solar Applications of Energy Conversion Technology

February 19, 1985
Golden, Colorado

Workshop Coordinators:

David H. Johnson
Ren Anderson
Solar Energy Research Institute

Alan Haught
United Technologies, Inc.

August 1986

Prepared under Task No. 5115.21
FTP No. 5-510-85

Solar Energy Research Institute
A Division of Midwest Research Institute

1617 Cole Boulevard
Golden, Colorado 80401-3393

Prepared for the
U.S. Department of Energy
Contract No. DE-AC02-83CH10093

SERI

PREFACE

The workshop described in this document was sponsored by the U.S. Department of Energy's Solar Thermal Technology Program. The goal of this program is to advance the engineering and scientific understanding of solar thermal technology and to establish the technology base from which private industry can develop solar thermal power production options for introduction into the competitive energy market.

Solar thermal technology concentrates the solar flux using tracking mirrors or lenses onto a receiver where the solar energy is absorbed as heat and converted into electricity or incorporated into products as process heat. The two primary solar thermal technologies, central receivers and distributed receivers, employ various point and line-focus optics to concentrate sunlight. Current central receiver systems use fields of heliostats (two-axis tracking mirrors) to focus the sun's radiant energy onto a single, tower-mounted receiver. Point focus concentrators up to 17 meters in diameter track the sun in two axes and use parabolic dish mirrors or Fresnel lenses to focus radiant energy onto a receiver. Troughs and bowls are line-focus tracking reflectors that concentrate sunlight onto receiver tubes along their focal lines. Concentrating collector modules can be used alone or in a multimodule system. The concentrated radiant energy absorbed by the solar thermal receiver is transported to the conversion process by a circulating working fluid. Receiver temperatures range from 100°C in low-temperature troughs to over 1500°C in dish and central receiver systems.

The Solar Thermal Technology Program is directing efforts to advance and improve each system concept through solar thermal materials, components, and subsystems research and development and by testing and evaluation. These efforts are carried out with the technical direction of DOE and its network of field laboratories that works with private industry. Together they have established a comprehensive, goal-directed program to improve performance and provide technically proven options for eventual incorporation into the Nation's energy supply.

To successfully contribute to an adequate energy supply at reasonable cost, solar thermal energy must be economically competitive with a variety of other energy sources. The Solar Thermal Program has developed components and system-level performance targets as quantitative program goals. These targets are used in planning research and development activities, measuring progress, assessing alternative technology options, and developing optimal components. These targets will be pursued vigorously to ensure a successful program.

The workshop was organized to establish the potential of conversion concepts which do not include moving parts and evaluate their applicability to Solar Thermal Technology. Todays' systems use Rankine, Brayton or Stirling cycle engines for conversion of thermal energy to electricity. Advances in the field of energy conversion and the need in the

SERI

solar program to search for more reliable and efficient conversion approaches led to the conduct of this workshop as a preliminary step in deciding an appropriate course of action.

The workshop coordinators would like to acknowledge the helpful comments and suggestions made by the external reviewers of these proceedings.

David H. Johnson, Manager
Thermal Sciences Research Branch

Approved for

SOLAR ENERGY RESEARCH INSTITUTE

Larry J. Shannon, Director
Solar Heat Research Division

SUMMARY

SERI, within its responsibility to look for new and innovative ideas to help Solar Thermal Technologies reach long term goals, assessed the potential energy conversion technologies for use in solar energy applications. A workshop on solar applications of conceptual conversion technologies, which may lead to nonmoving parts conversion of thermal energy to electricity, was organized in conjunction with the 1985 Solar Thermal Research Program Annual Review. The participants in the workshop included experts whose collective knowledge covered the full range of direct conversion technologies. The aims of the workshop were to

(1) discuss the interface between energy conversion technologies and the solar thermal resource to determine the technologies which are best suited for solar applications

(2) review the state of the art of energy conversion technologies to determine the technologies that are ready for full-scale development, and

(3) establish lines of communication between researchers working on energy conversion technology and researchers working on solar thermal energy systems to encourage further development of conversion technologies which show future promise.

The participants in the workshop were asked to prepare a short paper describing the state of the art of a particular technology and the relation of the technology to solar energy applications. The comments prepared by each participant are reproduced on the following pages. Several of the invited participants were unable to attend the workshop, but were asked to submit written comments so that their technology could be covered in the final proceedings. The papers presented in the proceedings which were not presented during the workshop are indicated with asterisks in the Table of Contents.

The primary emphasis of the workshop was technologies which convert heat directly to electricity. However, two technologies examined nonconventional means of converting light directly to electricity. One technology examined the conversion of thermal energy to light, and one participant examined recent advances in the thermodynamics of heat engines operating under realistic (non-Carnot) rather than ideal (Carnot) conditions. A summary of the technologies considered by the contributors to the workshop is presented in Table 1. In addition to the individual summaries of each technology, which appear on the following pages, each participant was asked to respond to a questionnaire that asked specific questions about each conversion technology. The responses to this questionnaire are included in a separate section which follows the individual summary papers. The proceeding concludes with an evaluation of the usefulness of the conversion technologies for solar applications and makes several recommendations for future research efforts. Because of the qualitative nature of the information provided at the workshop, the conclusions are preliminary and are intended to form the basis for a continuing dialogue between researchers working on direct energy conversion technologies and the DOE Solar Thermal Program. On the basis of the information available, it appears that none of the direct conversion technologies considered during the workshop offer a significant advantage as "stand alone" conversion devices relative to the current state-of-the-art Brayton, Rankine, or Stirling heat engine conversion systems. However, several of the technologies do offer promise for use in combined cycles with other conversion systems. It is recommended that an analysis of the efficiency of direct conversion technologies be carried out from a consistent fundamental, thermodynamic, and engineering basis to provide a quantitative measure of the usefulness of conversion cycles in solar thermal applications.

Table 1. Summary of Conversion Technologies

Technology	Summary
Surface Plasmon	Converts light to electricity by coupling sunlight to longitudinal oscillations of the conduction electron gas at the surface of a metal or semiconductor.
Submicron Antenna/Rectifier	Converts light to electricity through the use of submicrometer dipole antennas that absorb light waves.
Black Body Pumped Laser	Converts thermal radiation from a solar-heated blackbody into light by optical pumping of a laser.
Pyroelectric	Electrical analog of a conventional heat engine with the thermodynamic variables of charge and voltage replacing the thermodynamic variables of volume and pressure that occur in a conventional heat engine.
Sodium Heat Engine	Converts heat to electricity by extracting electrical energy from the electrochemical expansion of sodium vapor across a beta-alumina solid electrolyte membrane.
Thermionic	Converts heat to electricity by "boiling" electrons from a heated emitter electrode. The emitted electrons cross a narrow interelectrode gap and "condense" on a condensor electrode.
High-Temperature Thermoelectric	Converts heat to electricity by utilizing the Seebeck effect (thermocouples).
Regenerable Fuel Cell	Uses heat to regenerate the products of a fuel cell reaction.
Thermomagnetic	Magnetic analog of a conventional heat engine with the thermodynamic variables of magnetic field strength and magnetization replacing the thermodynamic variables of volume and pressure.

Table 1. Summary of Conversion Technologies (Concluded)

Technology	Summary
Thermoacoustic	Converts heat to acoustic energy via nonlinear coupling of pressure changes in a fluid to a temperature gradient in a stack of conducting plates.
Electrohydrodynamic	Converts heat to electricity by using an expanding gas to transport charged particles between electrodes.
Magnetohydrodynamic	Converts heat to electricity by using pressure differences to drive a conducting fluid through a magnetic field.

TABLE OF CONTENTS

---

*Participants who were unable to attend the workshop.

WORKSHOP ON SOLAR APPLICATIONS OF DIRECT ENERGY CONVERSION TECHNOLOGY
FEBRUARY 19, 1985

WORKSHOP PARTICIPANTS

B

BOURKE, EDGAR R.
PHOTOTHERM, INC.
141 Canal Street
Nashua, NH 03060
603/889-8611

C

CARASSO, MEIR
SERI
1617 Cole Blvd., Bldg. 15/3
Golden, CO 80401
303/231-1353

CHRISTIANSEN, WALTER
UNIVERSITY OF WASHINGTON, SEATTLE
Dept. of Aeronautics & Astronautics
Seattle, WA 98195
206/543-6224

CHUBB, DONALD
NASA LEWIS RESEARCH CENTER
Solar Conversion Branch
MS-302-2 21002 Brookpark Road
Cleveland, OH 44135
216/433-6000 (Ext. 5114)

CHUM, HELENA
SERI
1617 Cole Blvd., Bldg. 16/2
Golden, CO 80401
303/231-7249

F

FISHER, ELIZABETH
SERI
1617 Cole Blvd., Bldg. 15/3
Golden, CO 80401
303/231-7673

G

GUNN, MARVIN
U.S. DEPARTMENT OF ENERGY
ECUT Program, CE-142
Forrestal Bldg., 5E-091
1000 Independence Ave., S.W.
Washington, DC 20585
202/252-1484

GUPTA, BIM
SERI
1617 Cole Blvd., Bldg. 15/3
Golden, CO 80401
303/231-1760

H

HAUGHT, ALAN
UNITED TECHNOLOGIES RESEARCH CENTER
Silver Lane
East Hartford, CT 06108
203/727-7389

HOLMES, JOHN
SANDIA LABS
Division 6222
Albuquerque, NM 87185
505/844-6871

HUNT, TOM
FORD SCIENTIFIC LABORATORY
Room 2016, Box 2053
Dearborn, MI 48121
313/323-1509

J

JOHNSON, DAVID H.
SERI
1617 Cole Blvd., Bldg. 15/3
Golden, CO 80401
303/231-1752

K

KIROL, LANCE
EG&G IDAHO, INC.
MS/WCB-E3, Box 1625
Idaho Falls, ID 83414
208/526-1474

L

LUDWIG, FRANK
HUGHES AIRCRAFT COMPANY E1/F150
P.O. Box 902
El Segundo, CA 90245
213/616-6035

M

MARTINEZ, JESUS
SANDIA NATIONAL LABORATORIES
Division 6227
P.O. Box 5800
Albuquerque, NM 87185
505/846-7508

MISKOLCZY, GABOR
THERMO ELECTRON CORPORATION
101-1st Avenue
Waltham, MA 02254
617/890-8700

N

NIX, GERRY
SERI
1617 Cole Blvd., Bldg. 15/3
Golden, CO 80401
303/231-1757

O

OLSEN, RANDALL B.
CHRONOS RESEARCH LABORATORIES, INC.
3025 Via DeCaballo
Olivenhain, CA 92024
619/756-1447

S

SALAMON, PETER
SAN DIEGO STATE UNIVERSITY
Math Department
San Diego, CA 92182
619/265-6862

SWIFT, GREG
LOS ALAMOS NATIONAL LABORATORY
Mail Stop: K764
Los Alamos, NM 87545
505/667-4133

W

WANG, KUANG-YU
SERI
1617 Cole Blvd., Bldg. 15/3
Golden, CO 80401
303/231-1880

WILKINS, FRANK
U.S. DEPARTMENT OF ENERGY
STT PROGRAM, CE-314
Forrestal Bldg., 5H-041
1000 Independence Ave., S.W.
Washington, DC 20585
202/252-1684

WOOD, CHARLES
JET PROPULSION LABORATORY
MS 277-102
4800 Oak Grove Drive
Pasadena, CA 91109
818/354-4036

SURFACE PLASMON CONVERSION

Anne Arrison and Donald Chubb
NASA Lewis Research Center

SURFACE PLASMON CONVERSION

Anne Arrison

National Aeronautics and Space Administration
Lewis Research Center
Cleveland, Ohio 44135

The broad goal of advanced thin film device research at NASA Lewis Research Center is to survey the many advances in the field of optoelectronics and apply these new developments to devise high efficiency (greater than 30%) photovoltaic and non-photovoltaic solar cell concepts. One such concept that has received considerable attention is the surface plasmon solar cell (ref. 1) Due to the growing power demands of future NASA missions, increased cell efficiency along with a reduction of array area and weight are of exceptional importance for space power systems. It is well known that two of the major loss mechanisms in a typical solar cell are that light with an energy below the semiconductor bandgap cannot be utilized, and that electron-hole pairs that are created by photons with energies greater than the bandgap will convert their excess energy to heat. Spectral splitting photovoltaic concepts are one attempt to partially overcome these losses. A three-cell cascade solar cell, for example, will have an AM0 (air mass zero) efficiency of approximately 30% (ref. 2).

The surface plasmon solar cell was conceived with the goal of surmounting the above-mentioned difficulties to an even greater extent. In-house and grant theoretical studies began on this concept in 1980, and an in-house and grant experimental program was begun in 1983. The device involves parallel processing of surface plasma waves on a metal film, and energy conversion by tunneling in metal-oxide-semiconductor-metal (MOSM) diodes. Broadband, unpolarized sunlight would be coupled by some means to surface plasmons on the metal film adjacent to the semiconductor, plasmons of the appropriate energies would be directed to the proper diode for maximum energy conversion in an array of tunnel diodes, and energy conversion would result by an electron in the semiconductor absorbing a plasmon and tunneling across the oxide into the second metal film. The diodes would each be tuned by operating voltage so that maximum power could be generated by the plasma wave. The primary advantage of this device, if it could be realized, is that the solar spectrum would be better utilized. This is true for two reasons. First, many common metals support surface plasmons throughout the solar spectrum so ideally all the incident sunlight could be absorbed. Second, there would be a number of energy channels which would all be fabricated from the same materials.

One way to discuss the progress made on determining the feasibility of this concept is to separate the problem into four technical barriers: coupling broadband sunlight to surface plasmons, energy transfer of plasmons along the metal film, coupling energy into the tunnel diodes, and extracting electrical energy out of the tunnel diodes.

Broadband Coupling of Light to Surface Plasmons

A surface plasma wave is the longitudinal oscillation of the conduction electron gas at the surface of a metal or semiconductor. A metal or semiconductor can be viewed as a solid state plasma due to the equal number of positive and negative charges and the ability of the electrons to move with respect to the ion cores. Plasmons can be excited by both photons and

electrons and they interact strongly with them. The surface plasma wave is a transverse magnetic wave and using a prism coupler method, p-polarized monochromatic light can excite plasmons on a metal film with 99% efficiency (ref. 3). Metals such as silver and aluminum can support surface plasmons with frequencies across the solar spectrum, and both coherent and incoherent light will excite these relativistic waves (ref. 4). The difficulty in utilizing surface plasmons in a solar cell concept is that broadband coupling of unpolarized light is required at a single angle of incidence.

The two most common coupling methods, a prism or a surface grating, require a specific angle of incidence as a function of frequency in order for the wavevector of the incoming light to be matched to the surface plasmon wavevector. In order to overcome this restriction, two alternative methods of exciting surface plasmons have been investigated under grant. One of these is 'end-fire' coupling, a common technique in the optics field used to match the field pattern of the incident light to that of a guided wave (ref. 5). It involves focussing the light into the end of a given waveguide structure, and experiments are currently being conducted to match the electric field distribution of incoming light of a given frequency to that of the corresponding surface plasmon on a thin metal film. Theoretical calculations for a silver film show that greater than 80% of the light, $\lambda = .4$ μm to 1.2 μm, can be coupled in this way and even though pointing is necessary, all the light would be coupled in at a single angle. However, again this method is only applicable to p-polarized light, since the surface plasmon is a TM wave, and the coupling efficiency would be limited to less than 50%.

The second means of broadband coupling which is being studied involves metal island films (ref. 6). A lithium fluoride spacer layer (250Å) is deposited on top of a silver film, (500Å) and a silver or gold island film (30Å mass thickness) is then deposited on top of the spacer layer. The metal islands have a plasma resonance and both p and s-polarized light can be coupled to this structure. Energy is transferred from the island plasma resonances to surface plasmons on the metal film and it is a way of broadening the angle and wavelength of the absorption maximum. By incorporating metal island film experimental data into a well developed theory for molecular dipoles near a conducting surface, it is predicted that the maximum amount of energy transfer from the island film resonance to the surface plasmon on the metal film is 40%. This may be increased somewhat by changing the shape of the islands, however, as with the end-fire coupler technique, even though it is more broadband than previous coupling methods, the fact that the surface plasma wave has a single polarization seems to limit this method.

Plasmon Range

In many device configurations that might be imagined it is important to have long surface plasmon propagation lengths so that plasmons may be directed the proper energy conversion diode. Surface plasmons on metal films typically have a range of 75 μm to 5000 μm across the solar spectrum . A long-range plasmon mode has been identified which has millimeter ranges at solar frequencies and this mode has been observed experimentally (ref. 7). This mode is the mode of a thin metal film (< 500 Å) with a dielectric on either side such that both dielectrics have the same refractive index. A device configuration has not yet been envisioned which incorporates this geometry. Studies are underway to find a geometry which supports a long-range mode but also provides an efficient tunneling structure.

Coupling Energy into the Tunnel Diodes

The surface plasmon solar cell concept is based on the tunable light emitting metal-oxide-metal tunnel diode. This light emission can be observed in a darkened room and was first reported by Lambe and McCarthy in 1976 (ref 8). Much theoretical and experimental work has been done to increase the output intensity of these diodes and explain why they seem to be limited to a quantum efficiency on the order of 10^{-4} (ref. 9). Conflicting theories exist as to whether the electrons tunnel through the barrier inelastically, losing their energy to a plasma wave, or whether they tunnel through as hot electrons and couple to surface plasmons after they have traversed the oxide. If the former theory is accepted, the efficiency limitations have been explained by a weak degree of energy overlap in one step of the two-step excitation process: in which step one is the coupling of electrons to the plasma wave and step two is the coupling of the plasma wave to light.

Electrons have a strong coupling to the junction plasmon mode or slow mode. This wave is a coupled mode of the two plasma waves that exist along the metal-oxide interface at either side of the oxide layer. The energy of this mode is concentrated in the oxide which facilitates the strong interaction with tunneling electrons. However, it propagates so slowly, with velocities on the order of one-eighth the speed of light, that wavevector matching the wave to light by standard methods is quite difficult. If a grating were used, periodicities on the order of one-seventh the wavelength of light would be required. On the other hand, the surface plasmon on the metal-air interface has most of its energy outside the structure in the air and thus has a strong coupling to light, but a weak coupling to tunneling electrons. In order to solve this problem in the solar cell concept, it was proposed that a method to permit strong coupling of junction and surface plasmons was necessary (ref 1). This issue has been studied and theoretical calculations have shown that for a given frequency, a grating coupler could transfer as much as 90% of the surface plasmon energy into the junction plasma wave (ref. 10). Even though this is an encouraging result, two difficulties still remain. The necessary periodicity for surface plasmon/junction plasmon coupling is still on the order of slightly less than one-seventh the wavelength of light because the surface plasma wave progagation velocity is close to that of light (98%). Since the innate surface roughness of the structure has a periodicity on that order, the roughness will cause this coupling to occur but it will be difficult to control. Also, the junction plasmon will not necessarily exist in a MOSM structure, and would only exist under certain conditions, one of which is that the semiconductor must be thin enough for the two waves on the inner metal surfaces to couple to one another to form the mode. How this limits the operation of the device has not been studied. Thus, the energy overlap of the plasma wave and tunneling electrons still poses a problem in this device, and this issue is also under investigation.

Extracting Energy from the Tunnel Diodes

The fourth technical barrier, that of extracting energy from the tunnel diodes is perhaps the most difficult to overcome. The unbiased metal-oxide-metal tunnel diode appears too symmetrical to be an efficient rectifier, which is why the MOSM structure was suggested (ref. 1). The desired transition is for an electron from the valence band of the semiconductor to be excited by the plasmon and tunnel across the oxide to a state just above the fermi level of the metal. Other transitions are

possible, however, such as the creation of an electron-hole pair in the semiconductor or an electron in the metal absorbing a plasmon and tunneling into the conduction band of the semiconductor. The bandgap of the semiconductor serves to limit the number of available states for tunneling in the reverse direction. Studies are continuing on tunneling probabilities and whether the reverse tunneling mechanisms will overwhelm tunneling in the desired direction. Also, the junction plasmon mode is so heavily damped, with a range of tenths of microns, how much of its energy can be transferred to tunneling electrons before it is lost to heat has not yet been determined. To avoid this and other difficulties, novel device structures, substantially different from the original concept, are now under investigation (ref. 11).

It is still not known whether this device can be operated efficiently as it has been conceived, and whether all the above-mentioned difficulties may be overcome. In the meantime, we are looking at other new device ideas based on developments in the field of optoelectronics that may lead to high efficiency solar-to-electricity conversion. We hope to report on these ideas in the not too distant future.

REFERENCES

1. L. M. Anderson, Proc. 17th Intersociety Energy Conversion Engineering Conf., pp. 125-130 (1982); and Proc. 16th I.E.E.E. Photovoltaic Specialists Conf., pp. 371-377 (1982).

2. T. J. Maloney, Solar Energy Mat. 4, 359 (1981).

3. G. T. Sincerbox and J. C. Gordon II, App. Optics 20, 1491 (1981); M. R. Philpott and J. D. Swalen, J. Chem. Phys. 69, 2912 (1978); M. R. Philpott, A. Brillante, I. R. Pockrand, and J. D. Swalen, Ml. Cryst. Liq. Cryst. 50, (1979).

4. For a complete discussion of surface plasmons see H. Raether, Excitation of Plasmons and Interband Transitions by Electrons, Springer Tracts in Modern Physics, Vol. 88 (Springer Verlag, NY 1980).

5. G. I. Stegeman and J. J. Burke, NASA Grant NAG 3-392 (U. of Arizona) 1983-1985 and G. I. Stegeman, R. F. Wallis, and A. A. Maradudin, "Excitation of Surface Polaritons by End-fire Coupling" paper JH3, Proc. Am. Phys. Soc, March 1983.

6. D. G. Hall, NASA Grant NAG 3-414 (U. of Rochester) 1983-1985; W. R. Holland and D. G. Hall, Phys. Rev. B27, 7765 (1983); W. R. Holland and D. G. Hall, Phys. Rev. Lett. 52, 1041 (1984).

7. G. I. Stegeman and J. J. Burke, NASA Grant NAG 3-392 (U. of Arizona) 1983-1985; G. I. Stegeman, J. J. Burke, D. G. Hall, Appl. Phys. Lett. 41, 906 (1982); G. I. Stegeman and J. J. Burke, Appl. Phys. Lett. 43, 221 (1983).

8. J. Lambe and S. L. McCarthy, Phys, Rev. Lett. 37, 923 (1976).

9. For a review and extensive bibliography see P. Dawson, D. G. Walmsley, H. A. Quinn, and A. J. L. Ferguson, Phys. Rev. B 30, 3164 (1984).

10. G. I. Stegeman and J. J. Burke NASA Grant NAG 3-392 (U. of Arizona) 1983.

11, R. Schwartz and S. Datta, NASA Grant NAG 3-433 (Purdue University) 1984-1985.

SURFACE PLASMON CONVERSION

ANNE ARRISON

&

DONALD L. CHUBB

NASA LEWIS RESEARCH CENTER

CLEVELAND, OHIO

SOLAR ENERGY CONVERSION

NASA
Lewis Research Center

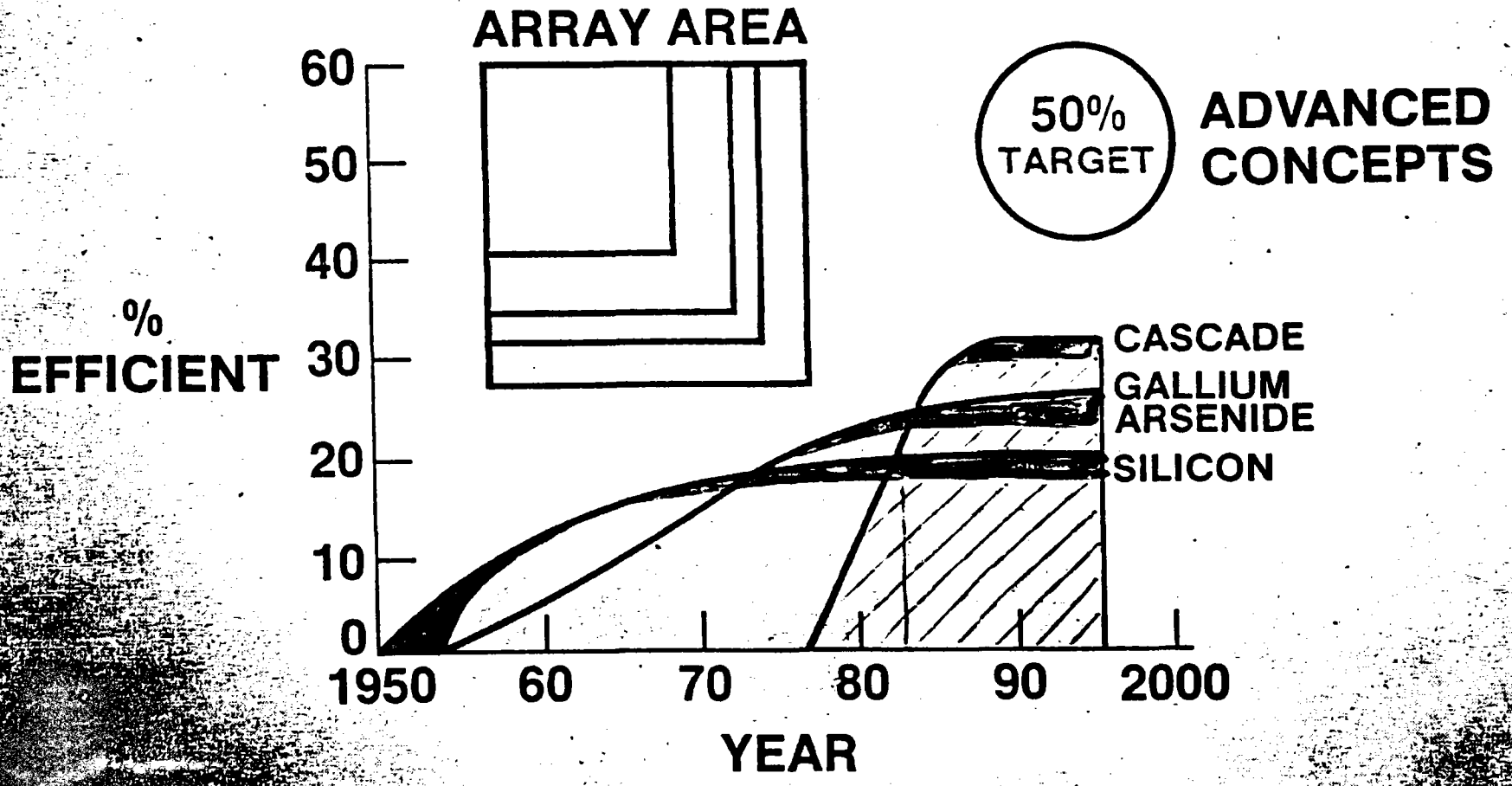

SOLAR CELL LOSSES

NASA

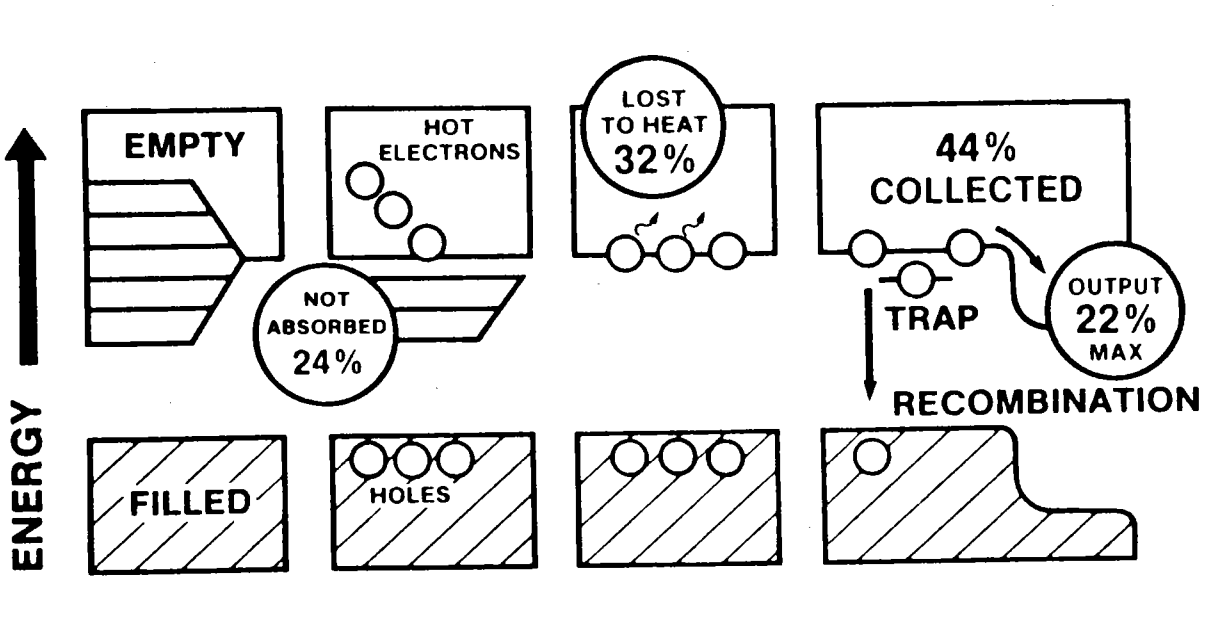

SURFACE PLASMA WAVES

NASA
Lewis Research Center

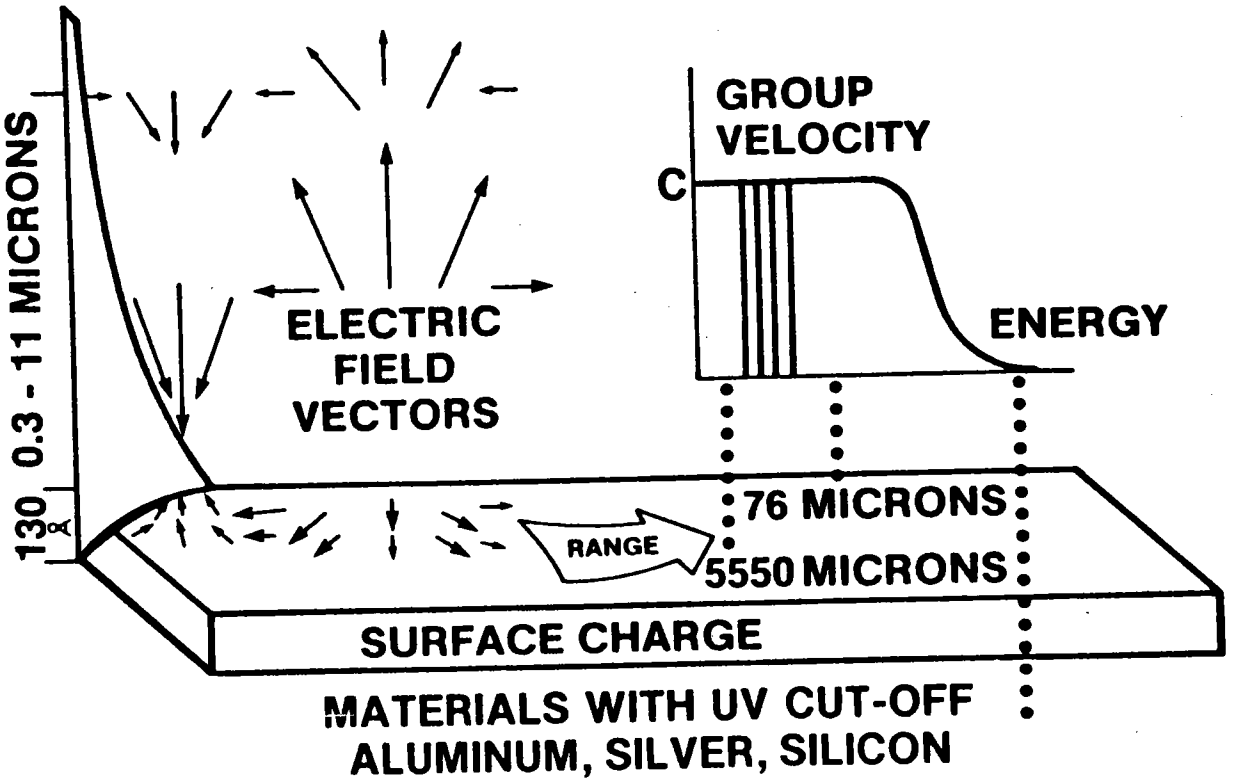

PARALLEL PROCESSING WITH SURFACE PLASMA WAVES

NASA
Lewis Research Center

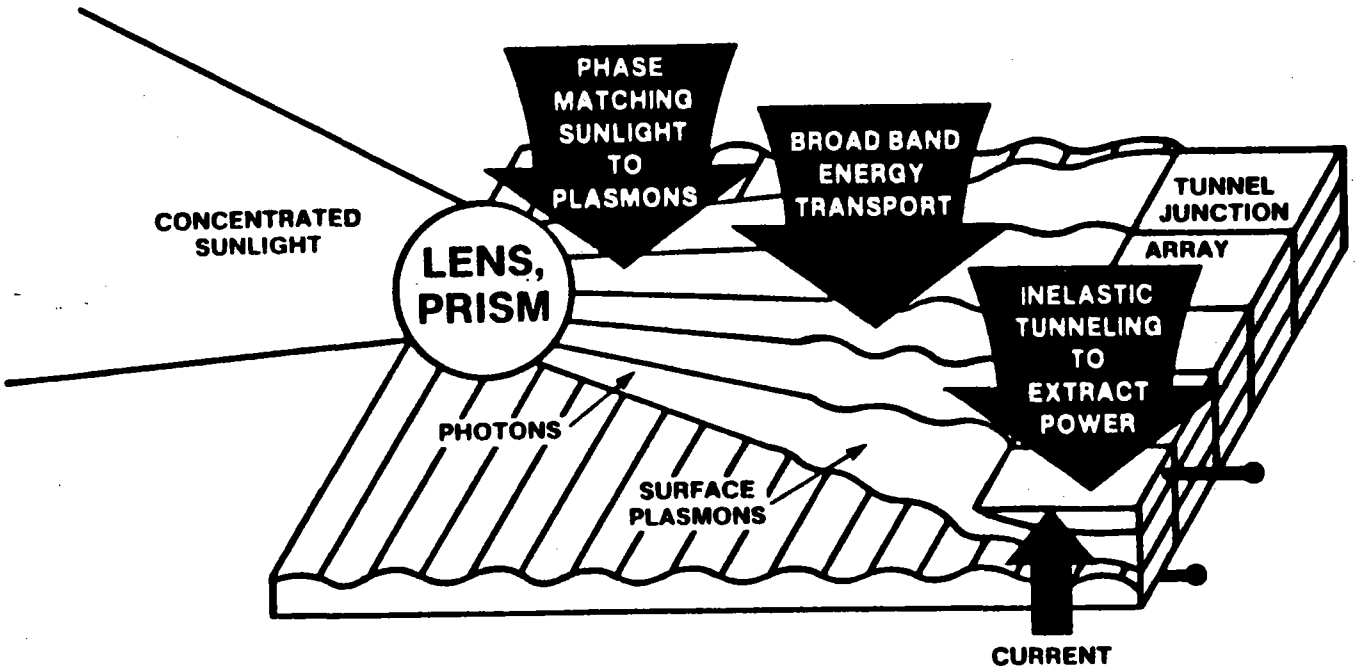

STATUS: EARLY CONCEPTUAL PHASE

SURFACE PLASMON RESEARCH

COUPLING INTO TUNNEL DIODES

- >90% EFFICIENT SURFACE TO JUNCTION PLASMON CONVERSION

COUPLING TO SUNLIGHT

- BROADBAND, BROADANGLE COUPLING FOR BOTH POLARIZATIONS

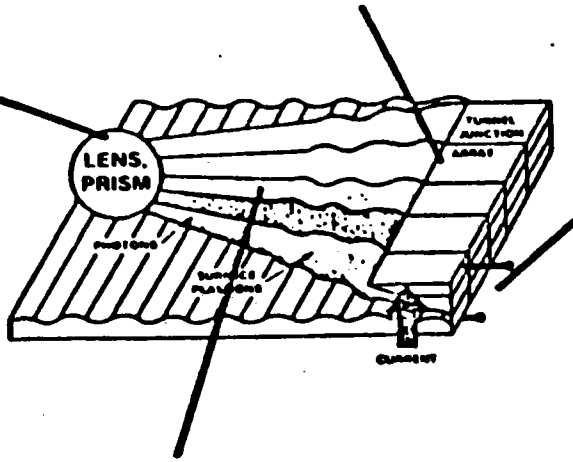

ENERGY CONVERSION DIODES

- PREVENT BACKFLOW
- ENHANCE PLASMON CAPTURE BY TUNNELING ELECTRONS

ENERGY TRANSFER

- REDUCE OHMIC LOSS, RERADIATION

ISLAND FILM STRUCTURE

DENNIS HALL U. OF ROCHESTER

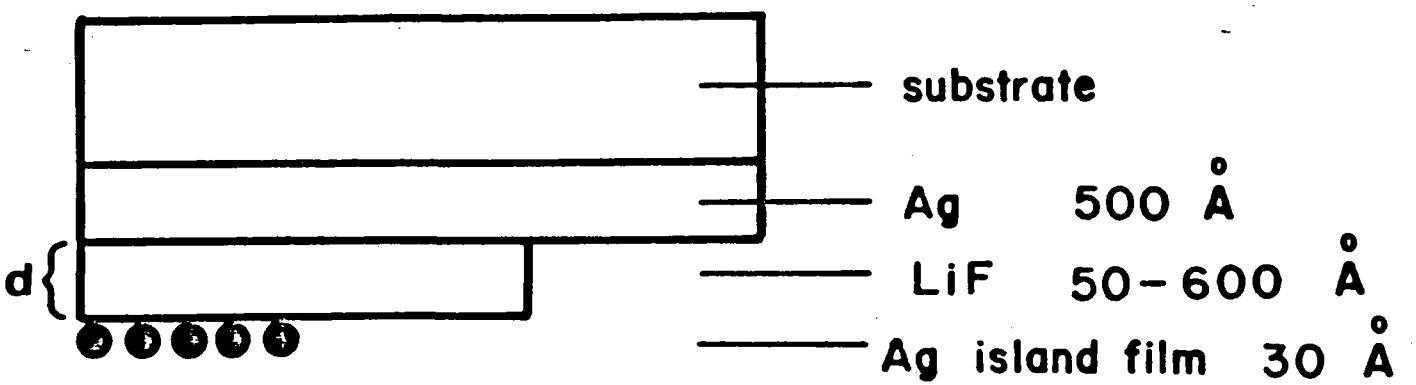

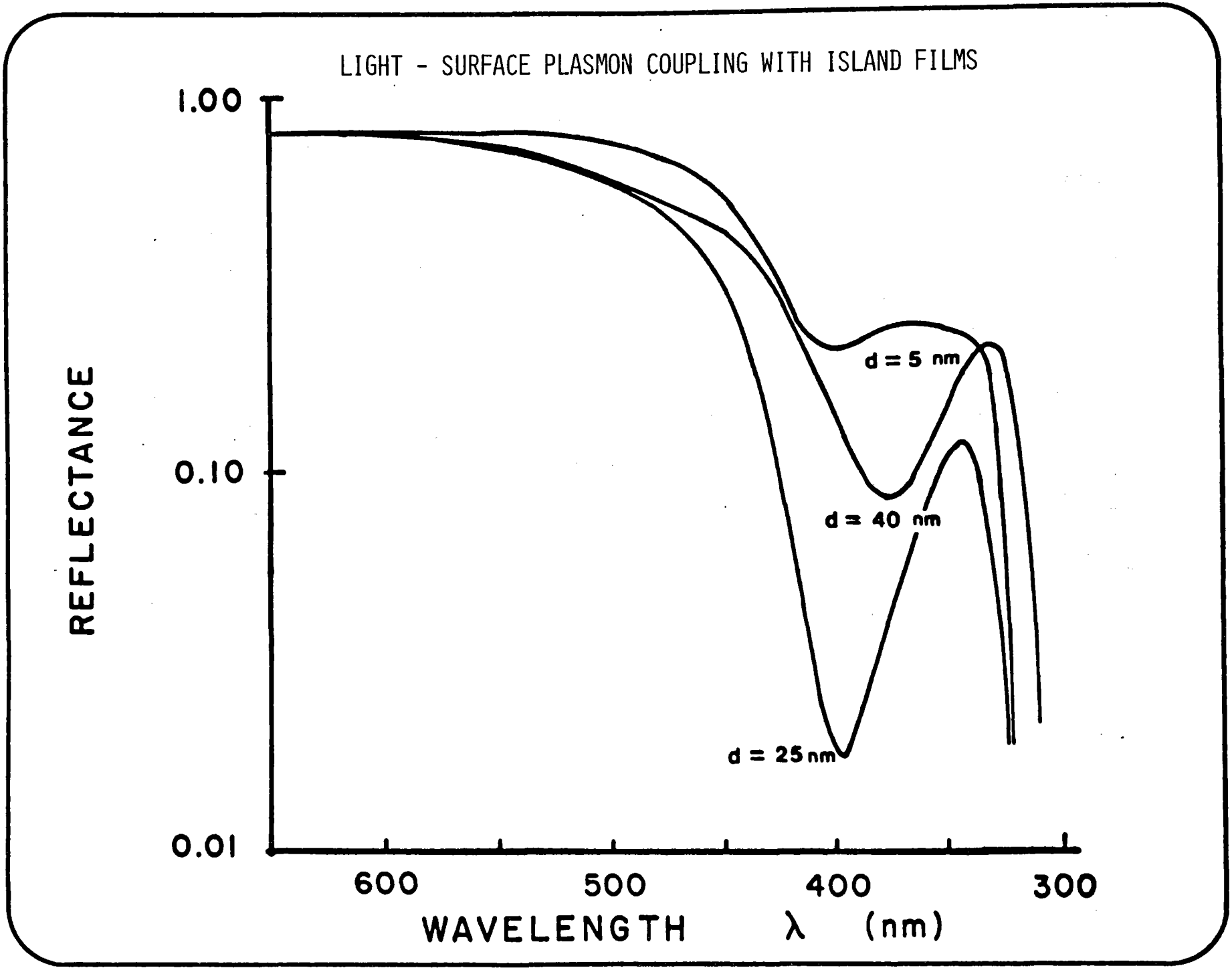
LIGHT - SURFACE PLASMON COUPLING WITH ISLAND FILMS
1.00
0.10
0.01
REFLECTANCE
d = 5 nm
d = 40 nm
d = 25 nm
600
500
400
300
WAVELENGTH λ (nm)

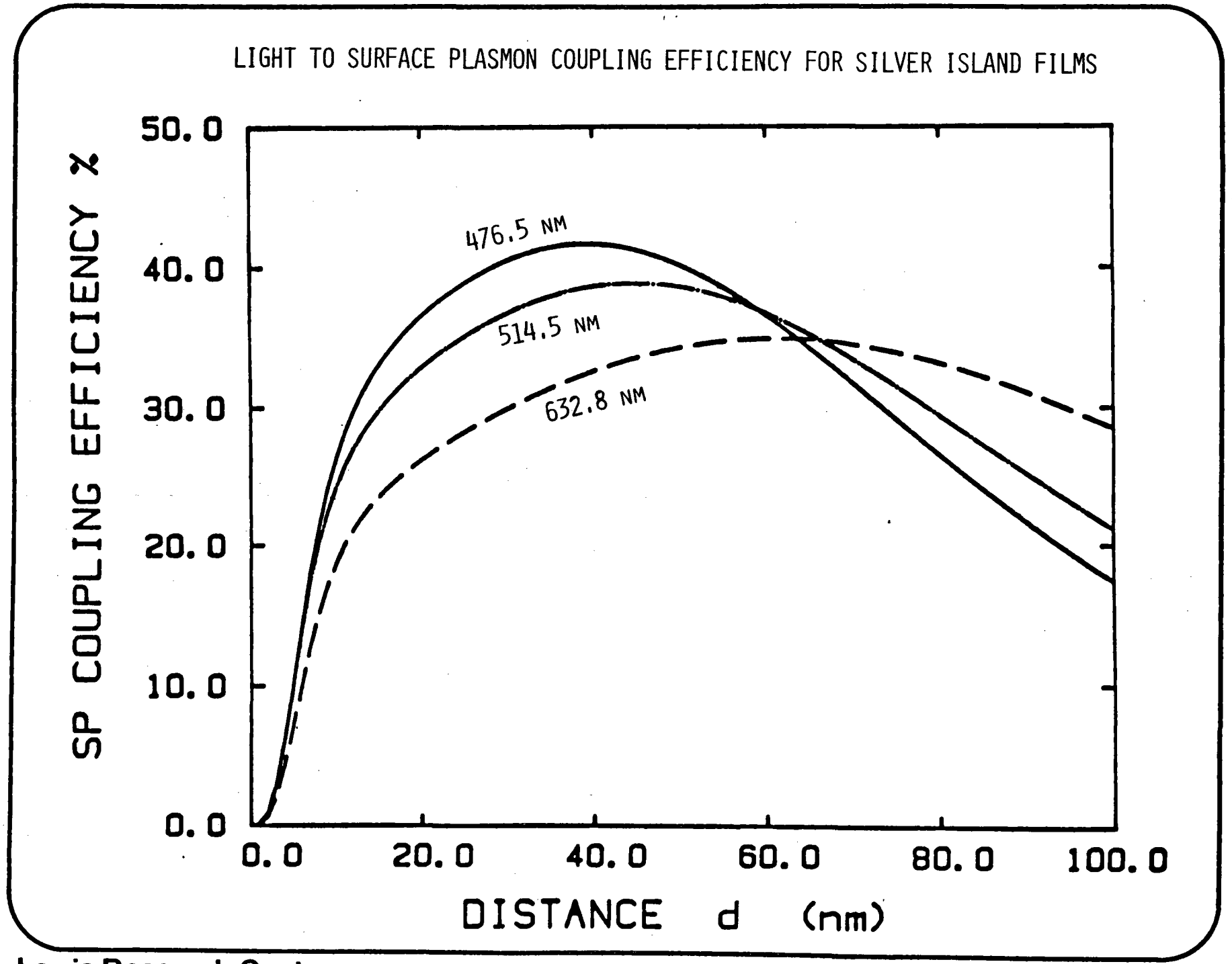
LIGHT TO SURFACE PLASMON COUPLING EFFICIENCY FOR SILVER ISLAND FILMS
SP COUPLING EFFICIENCY %
50.0
40.0
30.0
20.0
10.0
0.0
476.5 NM
514.5 NM
632.8 NM
0.0
20.0
40.0
60.0
80.0
100.0
DISTANCE d (nm)

ENDFIRE COUPLER
U. OF ARIZONA

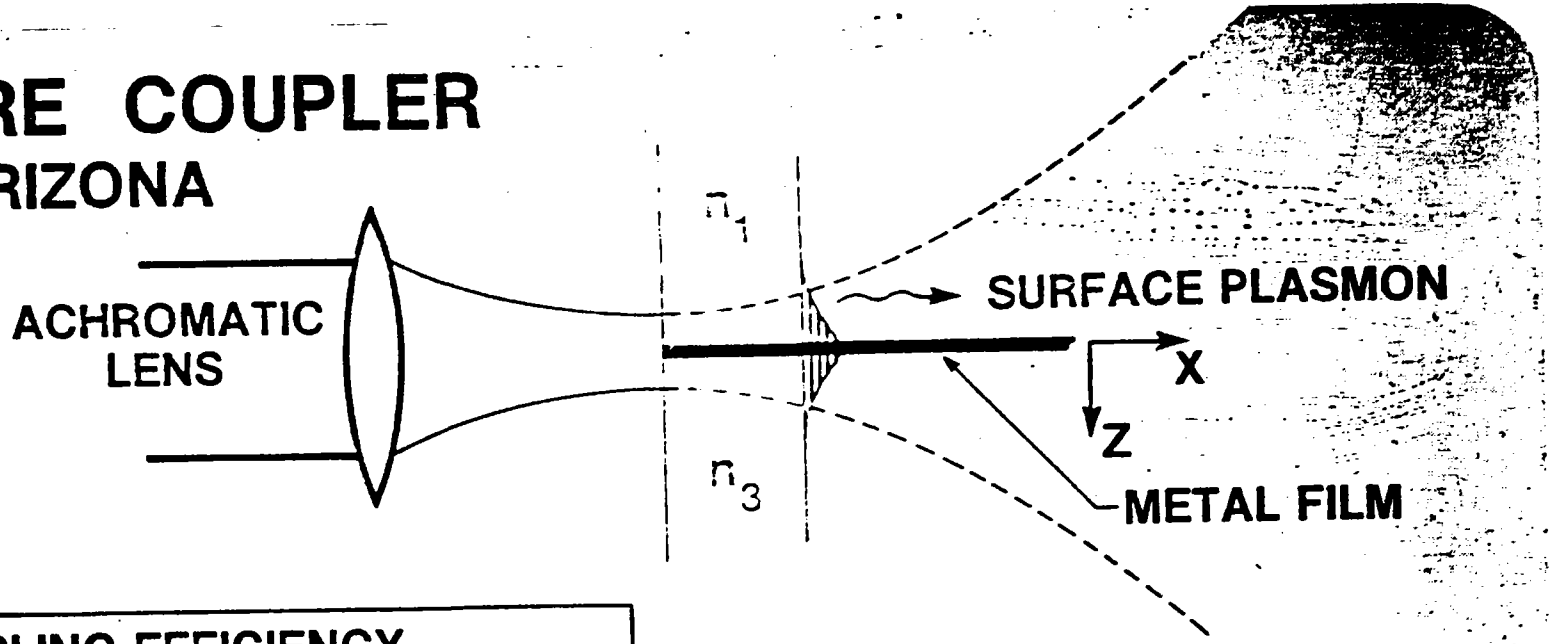

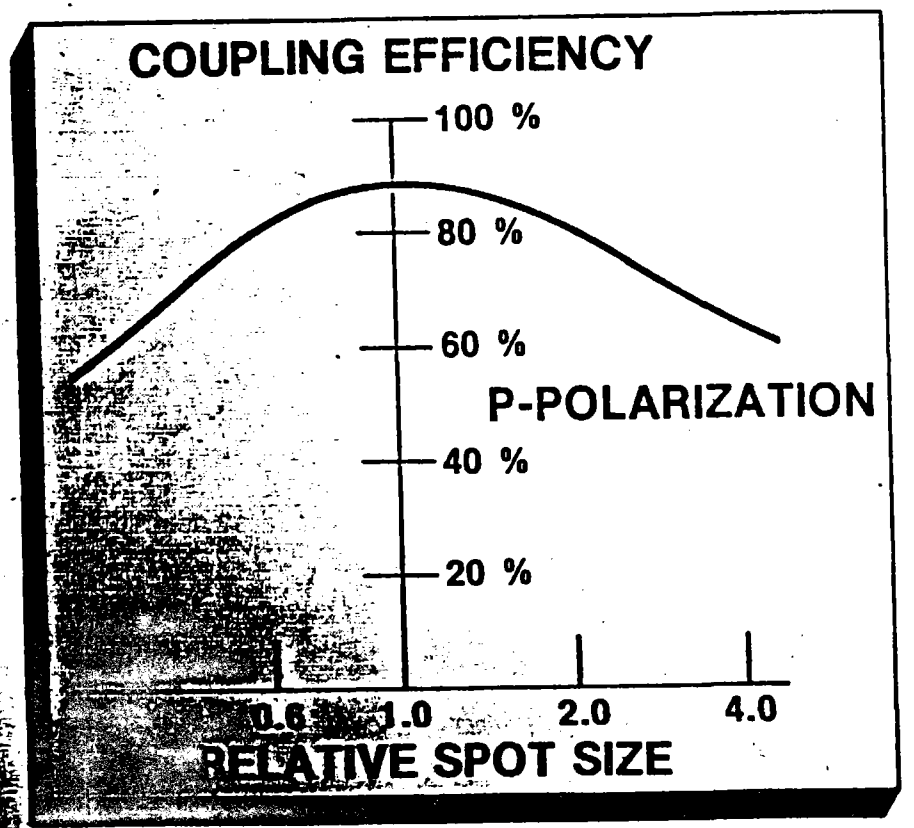

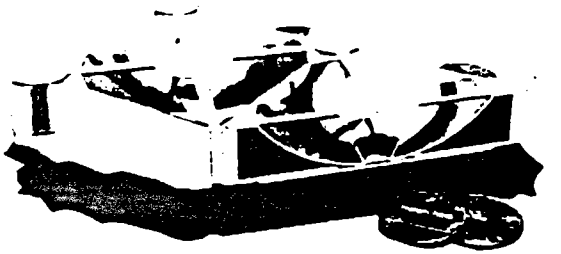

MINIATURE CONCENTRATOR
125X, 4MM CELL DIAMETER

CD-83-13760

CALCULATIONS SHOW THAT THE SURFACE PLASMON RANGE CAN BE INCREASED A HUNDRED TIMES BY USING VERY THIN FILMS. THE PLASMONS COULD TRAVEL FROM 10 MICRONS TO OVER A CENTIMETER DEPENDING ON FREQUENCY. EXPERIMENTS ARE PLANNED.

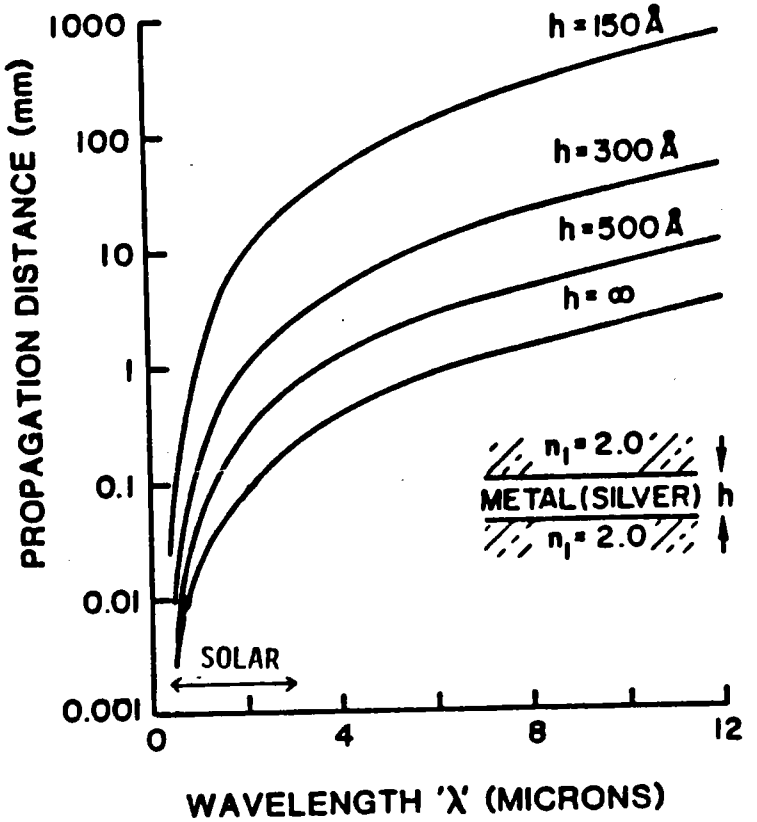

GEORGE STEGEMAN, JIM BURKE U. OF ARIZ., OPTICAL SCI. CEN.

COUPLING INTO THE TUNNELS

WEAK LINK IN EFFICIENCY CHAIN

BELIEVED RESPONSIBLE FOR VERY LOW (10^{-5} %) EFFICIENCY OF TUNABLE LEDS USING PLASMONS

SOLUTION: USE GRATINGS FOR MODE CONVERSION

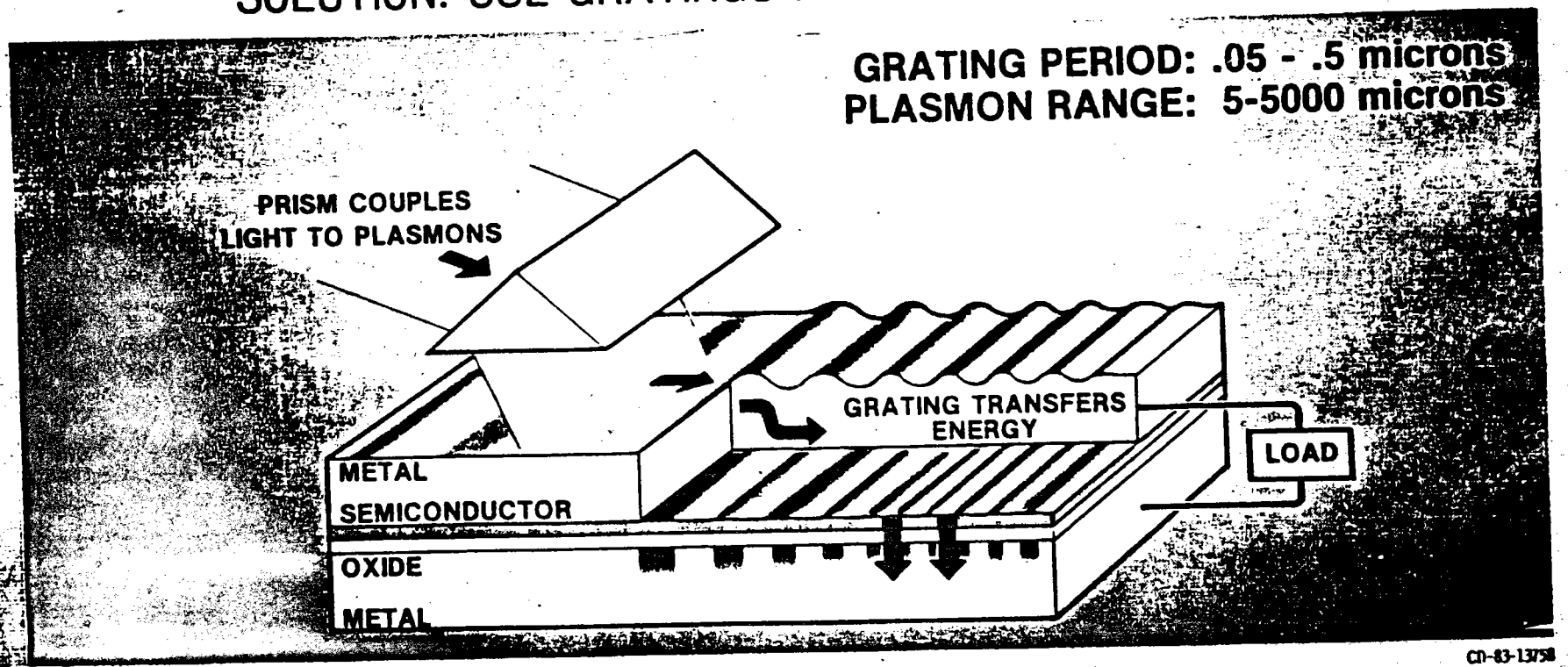

LEPCON - LIGHT/ELECTRIC POWER CONVERSION

Alvin Marks and Edgar Bourke II
Phototherm, Inc.

INNOVATIONS

PATENTS, PROCESSES, AND PRODUCTS

Solar-power converter

An array of submicrometer antennas deposited on a glass substrate can directly convert solar energy into electric power, with four times the efficiency and at a tenth of the cost of traditional photovoltaic converters, according to Alvin M. Marks, chief scientist of Phototherm Inc. of Nashua, N.H. Mr. Marks was awarded U.S. patent number 4 445 050 in April of this year for his invention of the device, trade-named the Lepcon (for light electric power converter).

Traditional photovoltaic cells are semiconductor devices consisting of a sandwich of two materials with differing electrical properties. Incoming solar photons are absorbed at the junction of the two materials, creating pairs of electrons and electron vacancies (holes) that flow through the material as the generated electric current. Practically speaking, the most advanced working photovoltaic cells operate at only 15- to 20-percent efficiency.

In the Lepcon solar converter, however, needlelike metallic dipole antennas 0.18 micrometer long—half as long as the wavelength of light—are deposited and oriented on a glass substrate. Incoming electromagnetic radiation (light from the sun) sets up an oscillation in the submicrometer-size dipoles just as radio waves set up an oscillation in a much larger radio antenna. This oscillation sets up an alternating current whose resonant frequency depends on the length of the antenna. A rectifier then converts the alternating current into a direct current. According to Mr. Marks, the efficiency of the solar-conversion process is 75 to 80 percent.

Similar attempts have been made in past years but only within the last year or so have techniques such as X-ray lithography become available for fabricating structures narrower than a hundredth of a micrometer—small enough to make the process work at the wavelengths of visible light.

Phototherm Inc. expects to produce a prototype panel sometime in 1985.

LCD color television

overcoming two major hurdles. First, liquid crystals commonly used in watch and calculator displays are too slow to respond to the rapid electrical signals of video displays. Second, conventional liquid-crystal displays are low in contrast and are limited to black images on a light background.

The Epson Elf television circumvents both hurdles by incorporating thin-film transistors, made of polycrystalline silicon deposited on a glass substrate, to turn on and off each of the 52 800 pixels in the Elf display and to activate microscopic color filters over each pixel.

The Elf uses nematic liquid crystals, in which the long axes of the rod-shaped molecules lie in parallel lines, although not in layers [see illustration]. The liquid

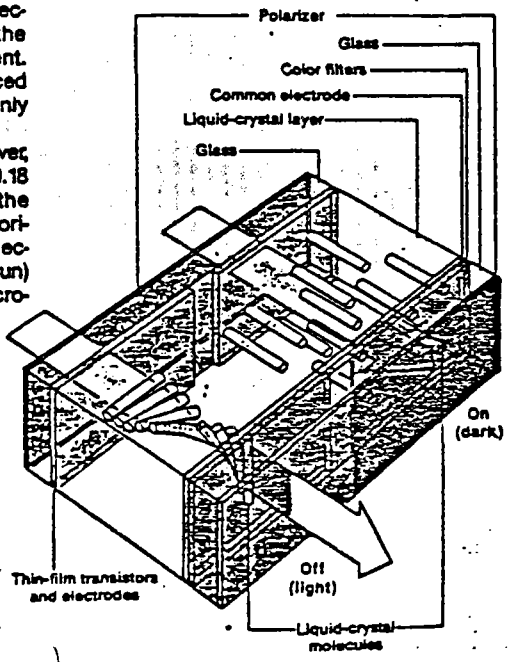

crystals are sandwiched between polarizers, one with its axis of polarization placed at a right angle to that of the other. When no electric field is present, the liquid crystals rotate light from a small fluores-

pixel respond. Because many rows must be quickly addressed by a single electric pulse, the time-weighted voltage is low, resulting in slow response and poor contrast.

In the Elf television, however, both the 240 rows and the 220 columns of electrodes are deposited on a single glass substrate on one side of the liquid-crystal layer; on the opposite side is a common electrode. Thin-film transistors, placed at each junction of a row and column, turn on whenever a pixel is to be activated. Thus, each pixel experiences the full voltage, not a time-weighted average, so it reacts quickly and exhibits good contrast.

The color in the Elf television is created by microscopic red, blue, and green color filters placed over each pixel electrode. Shades of color are created by varying the voltage to the thin-film transistors at each of the filters to let through various mixtures of red, green, and blue.

The Elf television is scheduled to be available for sale in October.

IEEE SPECTRUM
VOLUME 21 ☐ NUMBER 8 ◈ AUGUST 1984

The Boston Herald

Wednesday, December 26, 1984

Scientist's idea for cheap electricity

By JEFF KRASNER

INVENTOR Alvin Marks of Athol says cheap electricity is the key to such diverse goals as saving endangered animal species, ending Third World poverty, preventing nuclear war and, not incidentally, making his stockholders rich.

And Marks, who holds a doctorate, claims to have invented the key to cheap electricity — the femto diode.

The femto diode is the basis for Lepcon, a solar power converter that Marks patented earlier this year. A Lepcon panel consists of tiny antennae that convert light energy directly into AC current.

Marks says Lepcon reduces the cost of solar electricity from $5 a watt to 50 cents a watt. Lumeloid, a cheaper plastic version of Lepcon, brings the cost down to 1 cent a watt, or as Marks says, "Power would become almost free."

Besides electricity, the Lepcon panel generates a fair amount of skepticism, particularly from prospective investors in Phototherm, a Nashua, N.H.-based firm licensed to use the new technology.

"It was a little bit like pulling teeth in the beginning," says Marks. "If the idea is that spectacular, then they're automatically suspicious. They think it's a scam."

Marks and William Zebuhr, Phototherm's president, have been able to instill confidence in a group of private investors who put up several hundred thousand dollars to bring Lepcon closer to production. The company plans a $150 public offering by next summer.

Meanwhile, Phototherm is seeking a partnership with a large manufacturing company. Dow Chemical has signed a preliminary agreements with Marks to evaluate Lepcon and Marks hopes to have a development contract within a month.

The first product based on Lepcon technology is a solar cooker — an ungainly device that looks like a cross between a personal computer and a microwave oven. Marks says the SunCooker, which heats foods using sunlight, can end deforestation for cooking fuel in the Third World. That, in turn, will save dozens of threatened species.

The SunCooker will be in production within six months, with a $600 price for an upscale suburban model, Marks says.

But the cooker is just the appetizer in a full meal of femto diode-based products.

DR. Alvin Marks shows a model of the Elcon satellite weapon system, which he says could end the threat of nuclear war by vaporizing missiles in orbit and melting missile silos.

Staff Photo by Nancy Lane

Satellite-mounted Lepcon panels could generate a laser beam that could vaporize nuclear missiles and melt missile silos. Marks and his associates unabashedly suggest that their "Peace Ray" defense system could end the threat of nuclear war.

Another byproduct of the Lepcon, Marks says, is a matrix that can replace traditional computer semiconductors with chips that are five times faster, 25 times smaller and non-toxic to boot.

Marks says the most influential use of the Lepcon panel will be rural electrification in the Third World.

Patents are his credentials

ALVIN Marks, 74, says the Lepcon panel is the culmination of a lifetime of work in electricity and optics. He invites skeptics to review his other inventions.

"I don't work on gadgets — all my ideas have some scale to them and they're all very sensible," he says. "There's no perpetual motion machines here."

Marks' more than 100 patents include:

- Polarized sunglasses;
- The 3-D movie process used in "Friday the 13th, Part III;"
- The Incredible Power Fence, a 500-foot tall fence which would generate electricity from the wind;
- Superhard transparent coatings as used on airplane windshields;
- The charged-aerosol air purifier, which Marks says could solve the acid rain problem.

1984 TECHNOLOGY
STORIES OF THE YEAR

• Out to break the distance barrier, aircraft wizard Bert Rutan readied his oddly graceful Voyager (wingspan, 110 feet; fuselage, 25 feet) for a 12-day, nonstop round-the-world flight. Built of graphite composites, it weighs a mere 1,858 pounds, carries nearly 9,000 pounds of fuel.

• The Statue of Liberty is getting a $30 million, high-tech face-lift. Supercold nitrogen is spraying the corrosion from her copper skin; she will get 1,200 new stainless steel ribs; and her sagging torch arm is being buttressed—all in time for her July 4, 1986, centennial.

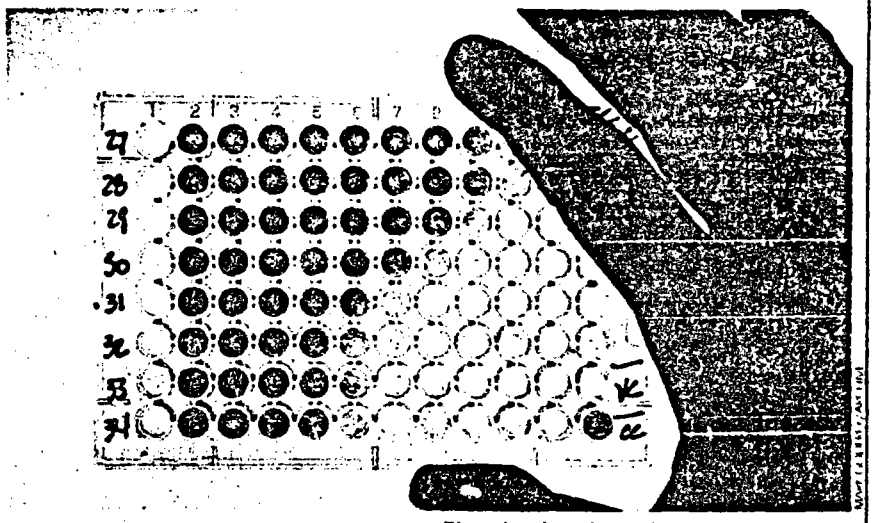

Biotechnology boom begins:
Here, a test of engineered bacteria.

Mac attack:
The invasion of the friendly computers.

INVENTIONS OF '84

The 67,000 patents granted last year attest to the ingenuity of science. Among the patent holders, Stanford University maintained its proprietary position in basic methodology used throughout the biotechnology industry with a patent for compositions that transform microorganisms, particularly bacteria, and lead to the production of hormones and antibiotics. The inventors, who assigned the patent to their universities, were Stanley Cohen, Stanford genetics professor, and Herbert Boyer, professor of genetics at the University of California, San Francisco.

A system enabling a robot to track and pick up specific objects was invented by Joseph La Russa of Farrand Optical Co., Valhalla, New York. Using it, a robot can select objects with its hand that match a stored image. The hand is guided by a camera placed in its center.

Cheap electricity from the sun's rays can be produced by equipment patented by Alvin Marks of Athol, Massachusetts. Trademarked Lepcon, Marks's equipment utilizes submicron antennas arrayed on glass plates to transform high-frequency alternating current to direct current. Marks estimates Lepcon-produced power at 50 cents per watt; photovoltaic power is about $5 per watt.

IBM received two patents: one for a system to check spelling and hyphenation in documents written in more than one language; the other for a system of proofreading a document and suggesting replacements for words exceeding the level of an audience's understanding.

The Patent and Trademark Office also reported progress. Patent processing time has been cut from 25 months to 18 months.

United States Patent [19]

Marks

[11] **4,445,050**

[45] **Apr. 24, 1984**

[54] DEVICE FOR CONVERSION OF LIGHT POWER TO ELECTRIC POWER

[76] Inventor: **Alvin M. Marks**, Bigelow Rd., Athol, Mass. 01331

[21] Appl. No.: **330,791**

[22] Filed: **Dec. 15, 1981**

[51] **Int. Cl.**[3] **H02M 7/02**

[52] **U.S. Cl.** **307/145**; 136/244; 307/151

[58] **Field of Search** 307/151, 145; 136/256, 136/244

[56] **References Cited**

U.S. PATENT DOCUMENTS

3,310,439	3/1967	Seney	136/256
3,475,609	7/1966	Schneider	136/256
4,251,679	2/1981	Zwan	136/244
4,360,741	11/1982	Fitzsimmons et al.	307/151

Primary Examiner—L. T. Hix

Assistant Examiner—Todd E. DeBoer

[57] **ABSTRACT**

This invention relates to a high efficiency device for the direct conversion of light power to electrical power. Present photocells for accomplishing this purpose are well known to the art and have a theoretical efficiency not exceeding about 20%. In practice, realization of efficiency of about 10% has been achieved, but ultimately the theoretical limitation is an upper limit which cannot be exceeded by devices utilizing known construction. The present device differs from the prior art devices in that it utilizes a plurality of dipole antennae for absorbing light photons, employing an alternating electrical field of said photons to cause electrons in the dipole antenna to resonate therewith and absorb electrical power therefrom, with means for rectifying said AC power to DC, said DC being accumulated on conducting busbars from the plurality of antennae and associated rectifying circuits.

12 Claims, 3 Drawing Figures

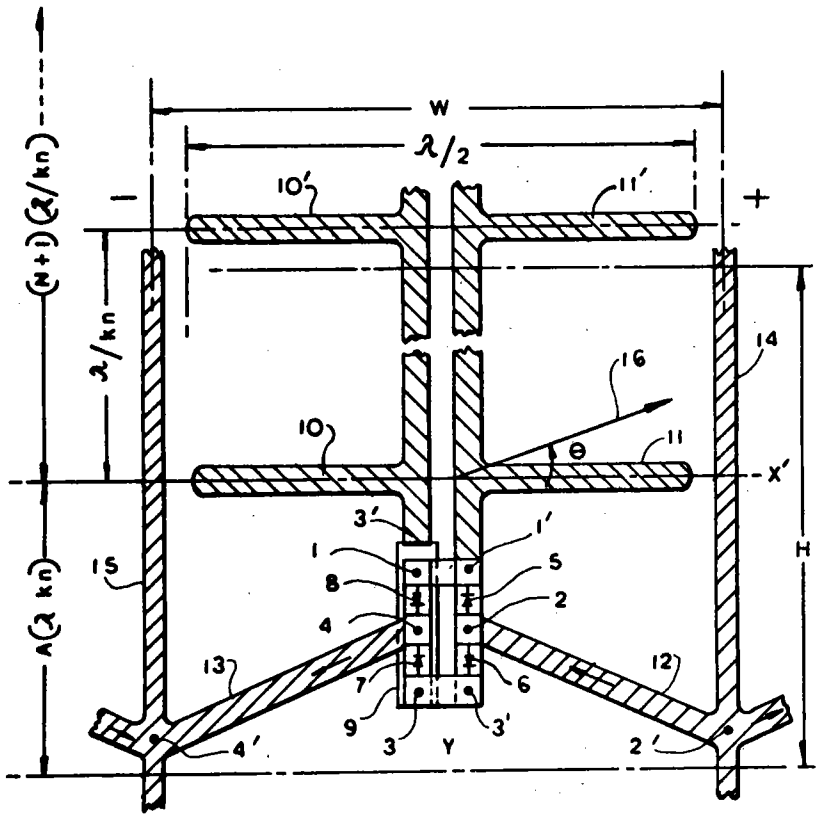

FIG. 3

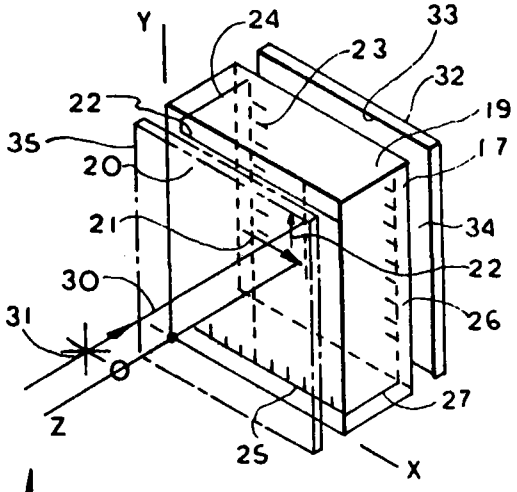

FIG. 1
(PRIOR ART)

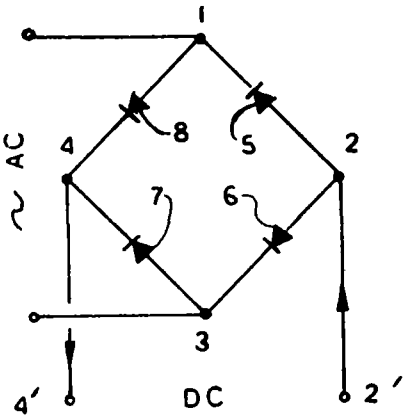

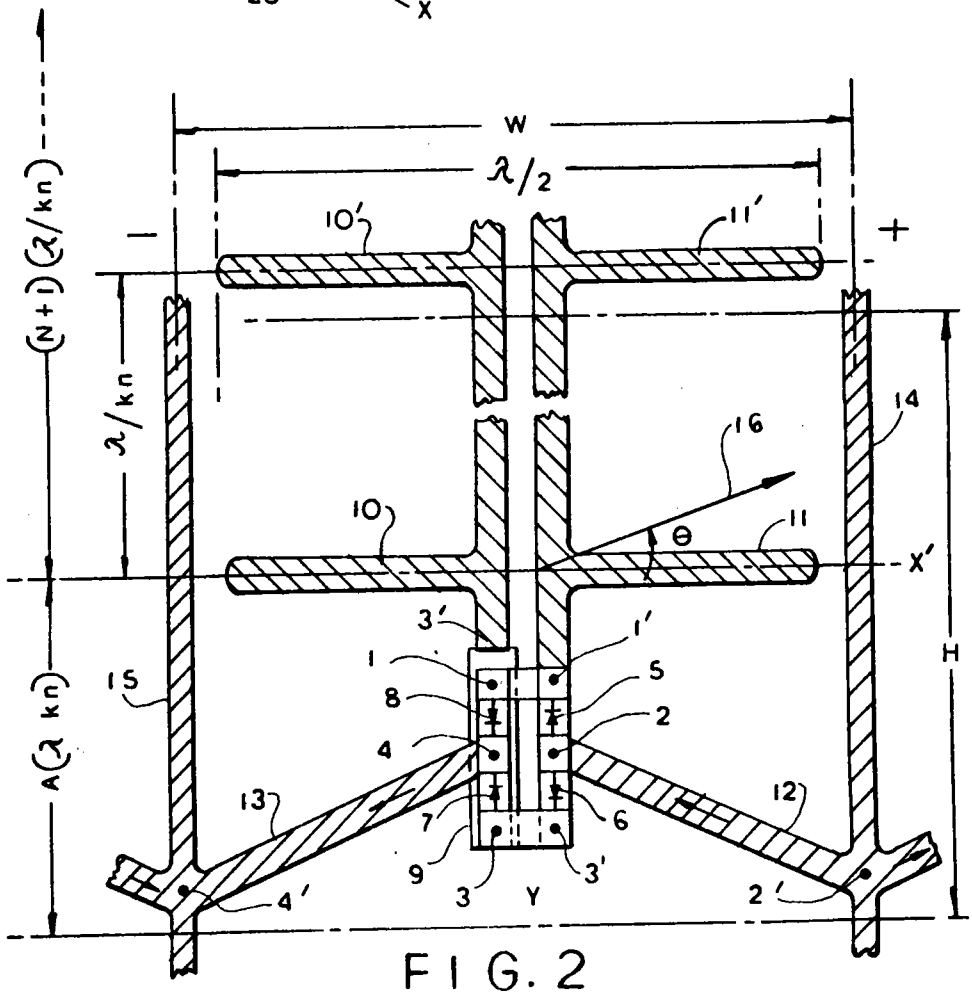

FIG. 2

DEVICE FOR CONVERSION OF LIGHT POWER TO ELECTRIC POWER

BACKGROUND

Present efforts in the conversion of light power directly to electric power employ "photo voltaic" devices. Various types of photo voltaic devices have been proposed. Amongst these are photo voltaic cells which comprise layers of conductors, insulators and semi-conductors. The best ones are made from single crystal silicon appropriately "doped" with small quantities of other elements. These have a theoretical efficiency not exceeding about 20% and actual values of 8 to 10% have been realized.

The green leaves in every plant or algae cell contain structures[1] for converting photon energy to chemical energy comprising carbon, hydrogen, oxygen, and small amounts of other elements such as magnesium.

These structures have become well known. Electron microscope pictures depict structures whose function is to absorb the energy of a light photon which is electromagnetic, and to utilize this energy to break up a water molecule and to free an electron and protonic hydrogen. Four photons must be absorbed by the molecular structure. An electron is transported by each absorption of a photon to a higher potential. The protonic hydrogen liberated combines with atmospheric carbon dioxide and liberates free oxygen to the atmosphere. The protonic hydrogen and carbon dioxide form starches and other compounds which are the basis for the living process, known as photosynthesis. The conversion of photon energy to chemical energy by the separation of H^+ and e^- charges occurs in a manner similar to that of a p-n junction in a semi-conductor photovoltaic cell, and which has about the same efficiency. There have been attempts to emulate this process with varying degrees of success in the laboratory. However, the starches produced then have to be burned in some other converter to produce electric power.

Other prior art processes employ the photo electrochemical potential, to directly produce electric power; efficiency: 6 to 7%, theoretical: 20%[2].

DEFINITIONS

Microarray: A set of N dipole antennae connected to a single pair of conductors.

Rectenna: N antennae connected to a pair of conducting leads and to a rectifier to provide a DC output.

A NASA Tech Brief[3] describes a "rectenna"; for example, a 10-cm long dipole reactive to microwaves and a single diode rectifier to convert the micro wave induced AC power to DC power. This system converts about 82% of the beamed microwave power directly to DC electric power. A space platform is proposed to gather sun power, convert it to microwave power and beam it to earth from a stable orbit. This microwave power will then be directly converted to electric power using a rectenna array over several square kilometers.

In outer space conventional photo voltaic cells are proposed to convert the sun power to electric power to actuate the microwave transmitters which beam the microwave power to earth. Such photo voltaic devices are only about 10% efficient. Using the light/electric power conversion device disclosed herein, the space platform would be 8 times smaller in area for the same power, and less expensive.

This invention uses a new, novel and different approach based on the direct conversion of photon energy to DC electric energy employing microarrays of submicron antennae connected to a submicron rectifier.

The microarray comprises a submicron rectenna array in which each antenna element has a length of 1800 Å and a width of about 100 Å. These elements are split in the center and the output directly rectified using a semi-conductive material as a diode rectifier. The submicron rectenna array described hereinafter reacts with light waves instead of microwaves. Light has a wavelength from about 0.35 to 0.8 μm, from the near ultraviolet through the visible spectrum to the near infrared.

The device of the present invention will produce electric power at an efficiency of about 75%, an improvement by a factor of 8 over existing systems. The device of the present invention is less expensive than present photovaltaic devices since large single expensive crystals of silicon are not used. We propose to substitute a miniaturized metal structure deposited on an insulating substrate, which is within the State of the Art on submicron structures[4].

FIGURES

In the figures,

FIG. 1 shows a conventional AC-DC rectifier device having 4 diodes.

FIG. 2 shows a light/electric power converter using a dipolar array and rectifier according to the present invention.

FIG. 3 shows a perspective view of a light/electric power converter comprising two dipolar arrays, each at right angles to the other, on opposite faces of a transparent insulating plate.

FIG. 1 shows a conventional rectifying circuit commonly employed in electrical technology. Rectifiers **5**, **6**, **7**, and **8** enable the conversion of the AC to DC. The AC power is applied to terminals **1** and **3** and the DC power is taken from terminals **2** and **4**.

Referring to FIG. 2, the diode elements, connected as shown in FIG. 1, are again identified with the same numbers, now rearranged in a straight line configuration but having the same electrical connections. The configuration shown in FIG. 2 is made possible by the use of an insulating barrier **9** shown as a dashed rectangular area. This enables point **3** to be connected to point **3'** by passing over the point **4** and the rectifiers **7** and **8** without being in electrical contact therewith. The dipole elements **10** and **11** are shown as an array of linear dipoles; **10'** and **11'**; etc.

Although only two dipoles are shown in FIG. 2, it will be understood many such dipoles may be employed, for example, 25. The criterion is that only 1 photon should impinge on the array, spaced in time from the next photon to enable the conversion of its electromagnetic wave to DC, without interference from the simultaneous incidence of a second photon. The dipole elements **10** and **11** absorb photon energy, resolving it in the direction of the dipole. The electric vector of polarization of the input photo wave **16** is shown at an angle θ to the horizontal axis X X' on the drawing.

By the "resolved component" of the electromagnetic energy of the photon, it is now understood according to the quantum theory, that the photon energy is either entirely absorbed or entirely transmitted, the proportion of photon energy absorbed or transmitted being the

same as computed using classical theory for the resolved electric vector. The dipole antenna is about $\lambda/2n \approx 2000$ Å in length. The diagram FIG. 2 is drawn to scale at a magnification of 500,000 at a scale: 1 cm = 200 Å. Such a small dimension can be obtained using electron or ion beams as presently used in the smallest semiconducting elements[4]. The rectifier elements 5, 6, 7, and 8 comprise semi-conductors which are amorphous, crystalline or epitaxial[5], each about 100 to 200 Å in diameter. These semi-conductor areas are suitably doped to obtain a p/n junction to provide the uni-directional flow of electrons. Leads 12 and 13 connect points 2 and 2' and 3 and 4' respectively, providing DC power to the busbars 14 and 15; n = index of refraction of coating 17. Adjacent elements may be repeated along the X axis and along the Y axis. The dipoles in the array repeat at λ/k (or λ/kn) intervals and are connected together as shown. It is preferred that in elements repeating along the X axis, the direction of the rectifiers is reversed, whereby there is a common positive busbar 14 and a common negative busbar 15. Each array is contained within a rectangular space; for example, of height $(N+1)(\lambda/kn)+A(\lambda/kn)$ and width about 2200 Å, where N = number of dipole antennae in a microarray and where A (λ/kn) is the space between it and the next microarray. These dimensions may vary somewhat in accordance with the wavelength of light employed. Generally, light from the middle of the spectrum (green) will require that the length of the dipole be $\lambda/2n = 5600/2 \times 1.5 = 1867$ Å (instead of 2000 Å). Other dimensions are decreased in the same proportion. The value $2 \leqq k < 8$.

Without a transparent insulating coating over the dipole structure, the dimensions are increased 50% to $\lambda/2 = 5600$ Å$/2 = 2800$ Å (instead of 1800 Å). The line width is then 300 Å instead of 200 Å. This will facilitate fabrication but increase its fragility.

This device may be fabricated upon a transparent slab by the deposition of one or more metal coatings in a known manner. The various rectifier elements are first prepared by opening appropriate windows in the metal coating utilizing an electron beam and suitably coating and doping the rectifying areas. An electron or ion beam cuts the shape and connections shown. The connections are completed after deposition of the insulating coating 9. The circuit is then the same as that shown in FIG. 1.

The common positive busbars 14 from alternate groups of antennae are all connected at one end of the array of dipoles. Similarly, the common negative busbars 15 are all connected at the other end of the device. In this manner all of the positive terminals are brought out on one side and all of the negative terminals are brought out on the other side of the device.

An array of dipole elements in a 2-dimensional area convert light power directly to electrical power from photons of visible light emitted by the sun impinging on the area.

This device has a theoretical efficiency of about 80%; thus avoiding the problems encountered by the conventional methods of the prior art.

FIG. 3 shows a device which enables the utilization of the randomly oriented polarization of the incident photons. The device shown in FIG. 3 comprises a transparent insulating sheet supporting member 19 such as polished glass. Mounted on the faces thereof are dipole arrays and rectifying elements such as shown in FIG. 2 and described hereinabove.

The dipoles on the front face 20 of the sheet 19 are oriented with their long axis horizontal and parallel to the X axis, as shown by the arrow 21; and the dipoles on the rear face 23 of the sheet 20 are oriented vertically and parallel to the Y axis as shown by the arrow 22. Incident light 30, with its electromagnetic waves oriented at random, as shown by the symbol 31*, are then resolved, absorbed, and converted by the dipoles on both faces of the sheet.

Photons are not only random in polarization direction, but fluctuate in time. However, the oscillations of the electric field from a single photon are coherent within a small time interval so that the result is a rectification of the photon AC electric field to DC.

A methematical physics analysis of the random polarization and random impact of light photons has determined that there will be no net cancellation of the light/electric conversion due to the great number of photons having random wave phases impinging simultaneously on the device.

The rectifier elements shown herein may utilize relatively expensive silicon crystal slabs experimentally employed for computer chips. However, it is preferred to prepare amorphous or epitaxial rectifying elements by epitaxial growth and ion implantation upon a glass surface.

An insulating coating may be placed over the first layer dipole-rectifier device shown in FIG. 2, and over this an identical device may be placed in a second layer offset with respect to the first layer device, so as to absorb incident photons which may pass unabsorbed between the spaced antennae microarrays in the first layer. This same two-layer structure may be placed on the opposite face of the transparent sheet 23 but at right angles, thus absorbing substantially all the incident photon-power and converting it to electric power with an efficiency of about 80%, based on measurements with the microwave analogue.

In another embodiment of this invention, in lieu of the multiple layers of dipoles to more fully absorb and convert the incident radiation to electricity, a sheet 32 having a reflecting surface 33 may be placed behind the sheet 19 so as to reflect back that portion of the radiation which is transmitted through the sheet. The sheet 32 optionally may be held in proximity or may be laminated to the sheet 19 by a transparent adhesive layer 34. The reflector 33 may be specular or may scatter the light.

The dipole antennae microarray on the front face 20 may be coated with a protective transparent coating 17, or may be laminated or fused to a front protective sheet 35, which results in a durable composite structure.

Solar energy is distributed over wavelengths λ from the near ultraviolet at about 3800 Å through the visible spectrum from 4000 Å to 7000 Å to the near infrared at 8500 Å; along a "black body" curve with an energy peak in the blue-green region.

Consequently, the antennae must be broad band or of a variety of lengths to respond to this range of wavelengths. The antenna dipole is broad banded by increasing its width to length ratio; for example, to 5. Alternately, or in combination with a broad banded antenna, adjacent dipoles may have a variety of lengths, and be spaced closely from each other; the lengths varying for a medium of n = 1.5 from $3800/3 = 1267$ Å to $8500/3 = 2833$ Å.

The effective cross section of an antenna is about $(\lambda^2/8n^2) = (\lambda/2n)(\lambda/4n)$. Hence, a spacing of $(\lambda/4n)$

between antennae (k=4) is sufficient to absorb all photons whose electric vectors are resolved in the direction of the antenna length. However, in an antennae array other design factors must be considered, such as directivity, gain, etc., as is well known in the art[6,7].

TABLE OF SYMBOLS

c=Velocity of light 2.9979×10^8 m/s
h=Plancks Constant=6.626×10^{-34} J.s.
n=Index of refraction
p=Light power watts/m^2
k=Numerical constant which determines the distance between dipoles in the microarray. It is usually chosen=2; but may be a design value between 2 and 8
$B_a=B_1B_2$=Packing factor
B_1=Packing factor along X axis
B_2=Packing factor along Y axis
E=Energy of photon, Joules
N=Number of dipoles on a microarray; for example 1 to 25
λ=Wavelength of photon m
ν=Frequency of photon cycles/s.

MATHEMATICAL PHYSICS ANALYSIS

Data on Photometric Units

1. Photon Frequency, Wavelength and Energy

1.1	5320 Å → 5.6×10^{14}	Hz (cycles/sec) frequency
1.2	$\lambda\nu=c$	wavelength
1.3	$E=n\nu$ Joules	energy
1.4	Normal levels of room illumination 10 ft lamberts (reflection)	
1.5		$\sim10^{14}$ photons/cm^2-sec.
1.6	Daylight 10^2 ft lamberts	$\sim10^{15}$ photons/cm^2-sec.

2. At 0.555 μm→5555 Å; 5.37×10^{14} Hz there are:

2.8×10^{12} photons/s≈1 μW=680 μlumens

2.8×10^{18} photons/s≈1 watt.

3. For daylight from (1.5) and (2.1)

p=Light power/$cm^2=10^{15}/2.8\times10^{12}=0.357\times10^3$ $\mu W/cm^2$ (photons/cm^2−sec)/(photons/sec μW)=3.57×10^{-4} W/cm^2

$p=3.57$ W/m^2 (by reflection).

4.

4.1	Solar Constant	=	2 gm cal/min-cm^2
		=	(1/30) gm cal/sec-cm^2
4.2	Cal/gm-sec	=	4.183 Watts
4.3	Hence, Solar constant outside the atmosphere		
	(1/30) × 4.184 = 0.1395 W/cm^2		
	= 1395 W/m^2		

System Analysis

1. Photon Impact Rate

Assuming direct sunlight at 25% of the solar constant; the available solar power is:

$0.25\times1395\approx350$ W/m^2

From 2:

$350\times2.8\times10^{18}\approx1.0\times10^{<}$photons/$m^2$−sec.

For each element embedded in a material having an index of refraction of 1.5 length of dipole is:

λ/2n	=	λ/3 = 5555/3 = 1850 Å
	=	1850×10^{-10} m

Assuming 1 element per 2000 Å×2000 Å area=$(2000\times10^{-10})^2=4\times10^{14}$ elements/m^2.

Photons/sec-element=$10^{21}/4\times10^{14}=2.5\times10^6$ photons/s per dipole.

Each ¼ μs (0.25×10^{-6} sec) a photon will impinge on a dipole antenna. Since each photon at 5555 Å has a frequency of 0.54×10^{14} Hz (cycles/s) in each ¼ μs interval there can be $0.54\times10^{14}\times0.25\times10^{-6}\approx14\times10^6$ discrete cycles.

This is adequate to individually actuate each rectifier unit and produce a DC output without cancellation due to simultaneous random impingement of too many photons.

2. Conversion Efficiency

The dipolar microarrays require a packing factor along the X axis of:

$$B_1=(\lambda/2n)/[(\lambda/2n)+(\lambda/4n)]=0.75$$

and a packing factor along the Y axis of:

$$B_2=N(\lambda/kn)/[N(\lambda/kn)+A(\lambda/kn)]$$

if N=25; and A=2, then:

$$B_2=25/27\approx0.925.$$

The B_a packing factor for this rectenna array is:

$$B_a=B_1B_2=0.75\times0.925=0.693.$$

The composite plate array in FIG. 3 then acts like a filter having a % transmission=100−69.3=31.7%. Two such plates have a % transmission=100 $(0.317)^2=10\%$ of the incident light; and, if the DC electric conversion efficiency=82%, the % efficiency of the composite=100 (0.75×0.90)=67.5%.

3. Results of Calculations

3.1. The impinging photons will be so well spaced in time that they will not overlap and their phases will not cancel each other. Each photon will be separately absorbed, and its energy converted to DC electric current pulse. The many photons will produce a steady DC electric power.

3.2 The output power of each dipole antenna is:

$(350/4\times10^{14})=0.875\times10^{-12}$ Watts/dipole

3.3 Since the overall conversion efficiency of light/electric power of a 2-side composite with reflector is about 67%, the output electric DC power will be about $350\times0.67\approx235$ W/m^2.

It will be understood that various modifications of the antennae structures[67], described herein may be made, such modifications being within the State of the Art and included within the scope of this invention.

REFERENCES

1. "The Photosynthetic Membrane", Kenneth R. Miller, *Scientific American,* October 1979, pp 102–113, Bibliography, p 186.

2. Nozik, A. J., Solar Energy Research Institute, Faraday Discussion No. 70, Sept. 8-10, 1980, Oxford University, England.
3. *NASA Tech Brief,* Winter 1978, Vol. 3, Number 4 "Efficient Rectifying Antenna", pp 497-8.
4. *Science,* Vol. 214, Nov. 13, 81, "Cornell Submicron Facility Dedictated".
5. Proceedings of the Ninth International Conference on Amorphous and Liquid Semiconductors, Grenoble, France, 7/81, to appear in *Le Journal de Physique.*
6. *Antennas,* John D. Kraus, McGraw-Hill Book Co., Inc., 1950, New York.
7. *Antenna Engineering Handbook,* Henry Jasik, Editor, McGraw-Hill Book Company, Inc., 1961, New York.

Having thus fully described my invention, what I wish to claim as new is:

1. In a light/electric energy converter an insulating sheet, a dipole antenna on said sheet to intercept light photons and convert the resolved electric vector of the alternating electromagnetic energy of said photons to an alternating current in said dipole antenna, a first pair of conducting leads connected to the center of said dipole antenna, an alternating current to a direct current rectifier connected to said leads, a second pair of leads from said rectifier, a pair of output terminals connected to a load, said second pair of leads being connected to said terminals to provide DC power to the said load.

2. In a light/electric energy converter according to claim 1, an antennae microarray comprising a plurality of said dipole antennae which are spaced λ/kn apart and connected to said first pair of conductors, λ being the wavelength and n the index of refraction of the medium in which said dipole is located, and k a number from 2 to 8.

3. In a light/electric energy converter according to claim 1, said rectifier comprising a full wave rectifier having 4 diodes.

4. In a light/electric energy converter according to claim 1, and rectifier comprising a full wave rectifier having 4 diodes, in which each of said diodes comprises a p/n junction on a crystalline semiconductor surface.

5. In a light/electric energy converter according to claim 1, said rectifier comprising a full wave rectifier having 4 diodes, in which each of said diodes comprises a p/n junction in an epitaxial differentially doped semiconductor area.

6. In a light/electric energy converter according to claim 1, said rectifier comprising a full wave rectifier having 4 diodes, in which each of said diodes comprises a p/n junction in an amorphous, differentially doped semiconductor area.

7. In a light/electric energy converter according to claim 2, said dipole antennae microarrays being arranged with their axes at right angles to each other on opposite faces of said insulating sheet which is transparent to said light photons, whereby electric vectors of said light photons are absorbed along both axes.

8. In a light/electric energy converter according to claim 2, said dipole antennae microarrays being arranged with their axes at right angles to each other on opposite faces of said insulating sheet which is transparent to said light photons, whereby electric vectors of said light photons are absorbed along both axes, in which at least two layers are coated on each face of said transparent insulating sheets said layers having a transparent insulating spacer between them; whereby substantially all of the incident light-power is converted to electric power.

9. In a light/electric energy converter according to claim 2, said dipole antennae microarrays being arranged with their axes at right angles to each other on opposite faces of said insulating sheet which is transparent to said light photons, whereby electric vectors of said light photons are absorbed along both axes, a reflecting layer on a sheet located behind said insulating sheet, whereby light not absorbed in said light converter is transmitted to said reflecting sheet, and returned to said light converter, whereby a substantial proportion of said light energy is absorbed and converted to electric energy.

10. In a light/electric energy converter according to claim 1, a transparent protective sheet, said protective sheet being laminated onto the front surface of said insulating sheet and over the dipole antennae microarrays thereon, which results in a durable composite.

11. In a light/electric energy converter according to claim 2, in which said dipole antennae are broad banded to respond to a range of light wavelengths.

12. In a light/electric energy converter according to claim 2, in which said plurality of dipole antennae are closely spaced and vary in length from 1267 Å to 2833 Å.

* * * * *

BLACK BODY PUMPED LASERS

Walter Christiansen
University of Washington

BLACK BODY PUMPED LASERS

Walter H. Christiansen
University of Washington

Direct conversion of sunlight into laser light without the need for a complicated intermediate step of energy conversion is a significant advantage for high-power solar pumped CW lasers. While the principle of broadband optical pumping using flashlamps to achieve a working laser is well known and has been put into practice with the ruby laser and dye laser, broadband pumping of gas lasers has not been so extensively studied. Recently, however, an optically pumped iodine laser has been demonstrated at NASA Langely Research Center using a solar simulator.

Solar pumping of bound-bound absorption transitions, typical of infrared lasers, is also a possibility. This approach normally would be very inefficient, and therefore of little interest, due to the fact that the absorption bandwidths of many potential gas laser media are small in relation to the effective bandwidths of the solar spectrum. Consequently, only a very small fraction of the solar energy can be absorbed and converted into laser light. A concept for efficient optical pumping of an infrared laser medium has evolved which has the potential of making these solar-pumped lasers very efficient (see figs. 1-6). In this method, a blackbody heated by focused sunlight is used as the optical pumping source. The basic idea is shown in fig. 2 wherein an insulated body provides the intermediate radiation field. If an optically active medium contained in a transparent vessel is inserted into the insulated cavity, the overall thermodynamic efficiency can be markedly improved. In fact, the potential efficiency of this approach is orders of magnitude greater than utilizing sunlight directly in narrow band absorption media. This improvement allows the entire solar flux to contribute to the lasing because of the thermodynamics of the cavity. If the cavity radiation is withdrawn via the pumping bands of the laser medium, the nonequilibrium part of the radiation field in the cavity is returned to a distribution by thermal re-emission of the hot walls (fig. 3). In this way the pumping radiation of these type lasers are continuously replenished and all of the energy source is utilized.

This laser system seems well suited for space applications, particularly in view of new concepts of waste heat rejection. Utilizing this pumping concept, heat balance studies of the overall efficiency of conversion of solar radiation to laser radiation has been made and shown to be 10-20 percent provided transparent materials are available as shown in fig. 8. See also figs. 7-10.

Because of the potential of the blackbody pumped laser, experiments to demonstrate the physics of lasing such a device are being carried out at the University of Washington. One such experiment utilizes an electrically heated blackbody cavity which simulates the equivalent solar heated blackbody cavity (figs. 11-12). Carbon dioxide (fig. 7) was selected as the initial lasing media since its properties are well understood and it is a good candidate for testing of the blackbody pumping concept. (A recent astronomical discovery showed the existence of a sun-pumped CO_2 laser in the Martian atmosphere.) Prior experiments have shown the level of gain and its relationship to the blackbody pump temperature. These results showed that one should reach threshold conditions fairly easily in the laboratory. Recent gain calculations and power measurements (figs. 13-15) confirm these results. The results of these experiments clearly demonstrate our ability to convert broadband blackbody radiation into laser light. The experimental results fully illustrate the physcial principle of the radiation conversion process.

Utilizing the basic blackbody pumping ideas, scaled up versions of the laboratory laser have been made (fig. 16). A higher power density device, possibly using CO gas as the energy storage medium is shown in fig. 17.

The use of blackbody to pump a laser has other possible advantages. The blackbody cavity may be heated in any number of ways in addition to solar heating without affecting the laser performance if the appropriate blackbody temperature is maintained. Perhaps, in some instances, solar light may not be available in large quantities or the collector may be too far from the sun. In that case, alternate power in the form of heat (perhaps excess heat from a chemical source) could be used to help power the cavity. Other future possibilities (fig. 18) may include blackbody pumping with thermo photovoltaics, in chemical processing, or possibly as a narrow frequency lamp - all energized by solar power.

METHOD 1

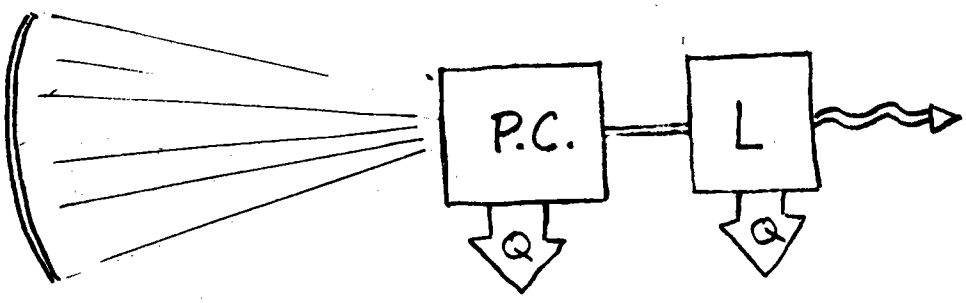

EDL
GDL
SDL
OTHER

METHOD 2
(DOPL)

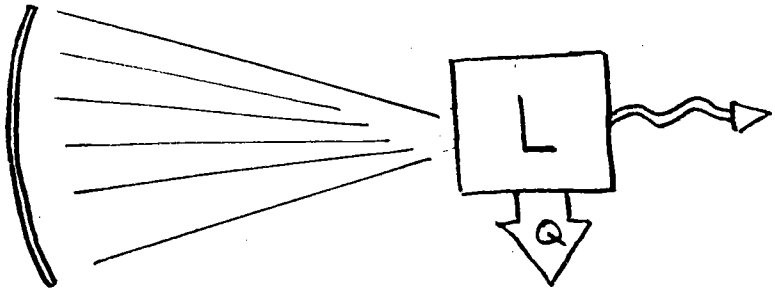

I^*, Br^*, Dyes,
DIMERS

INFRARED
LASERS

METHOD 2'
(IOPL)

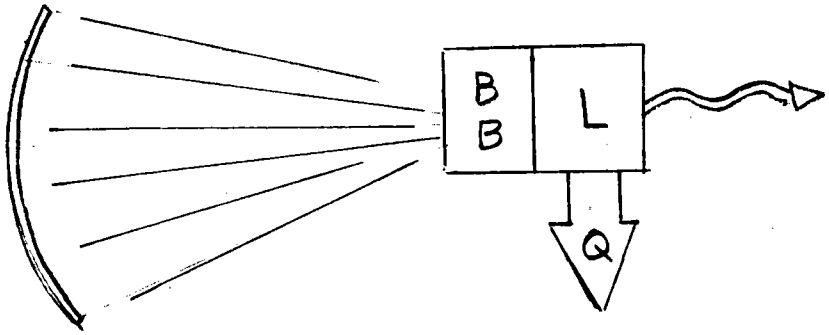

Fig 1

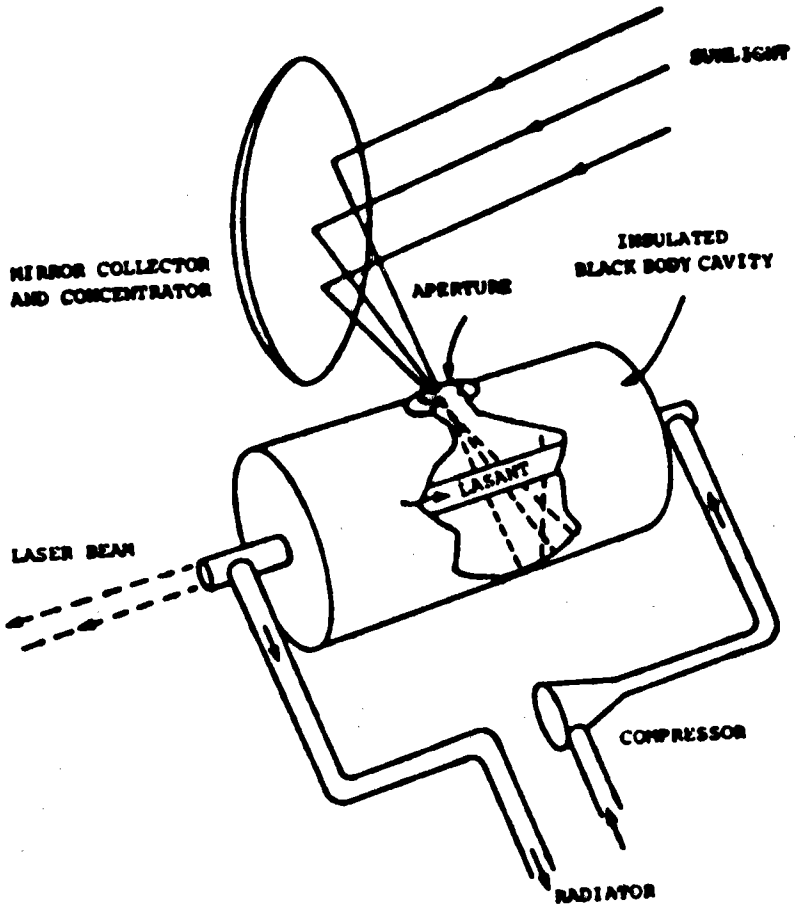
SUNLIGHT
MIRROR COLLECTOR
AND CONCENTRATOR
APERTURE
INSULATED
BLACK BODY CAVITY
LASANT
LASER BEAM
COMPRESSOR
RADIATOR

FIG 2

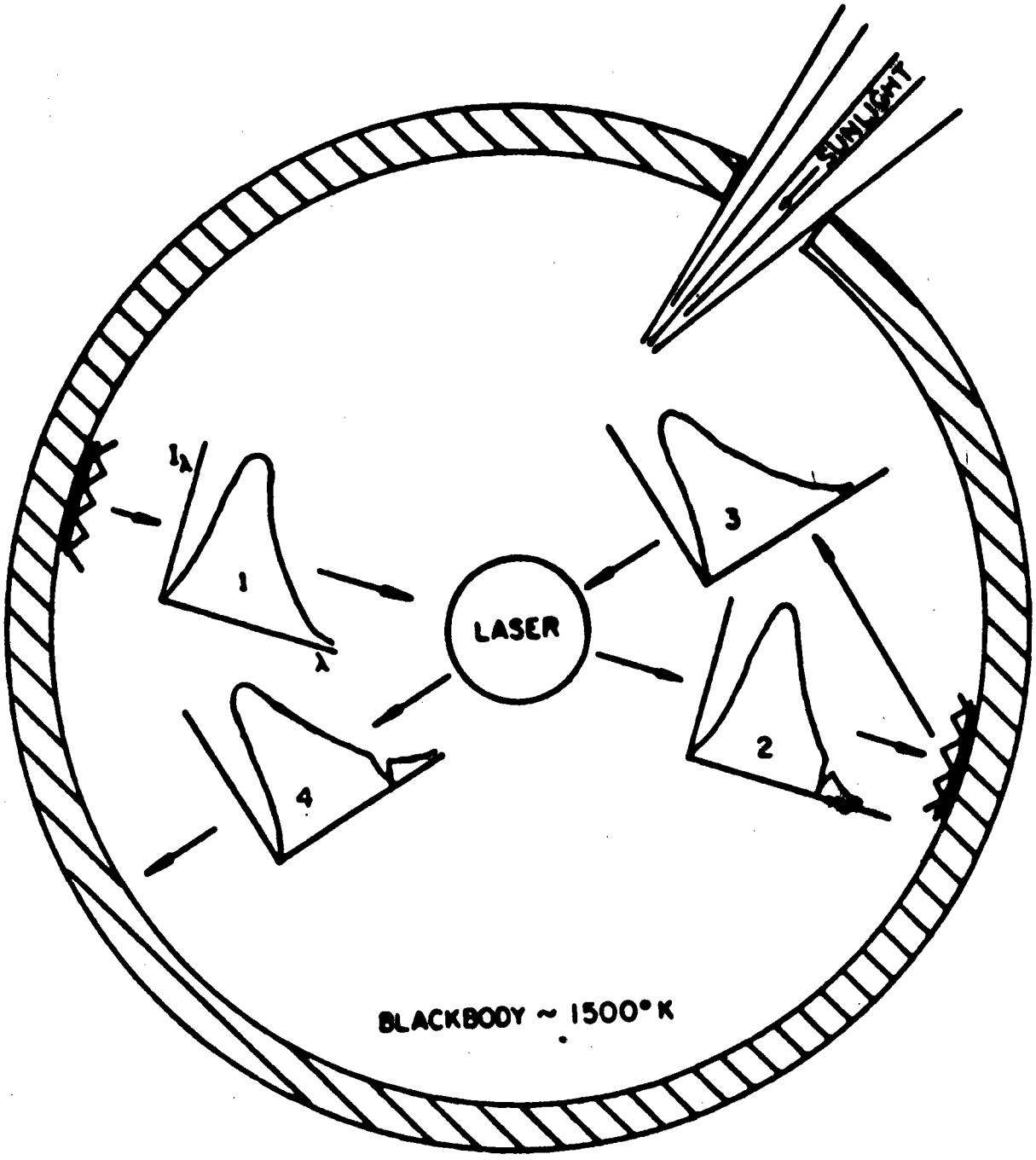

FIG 3

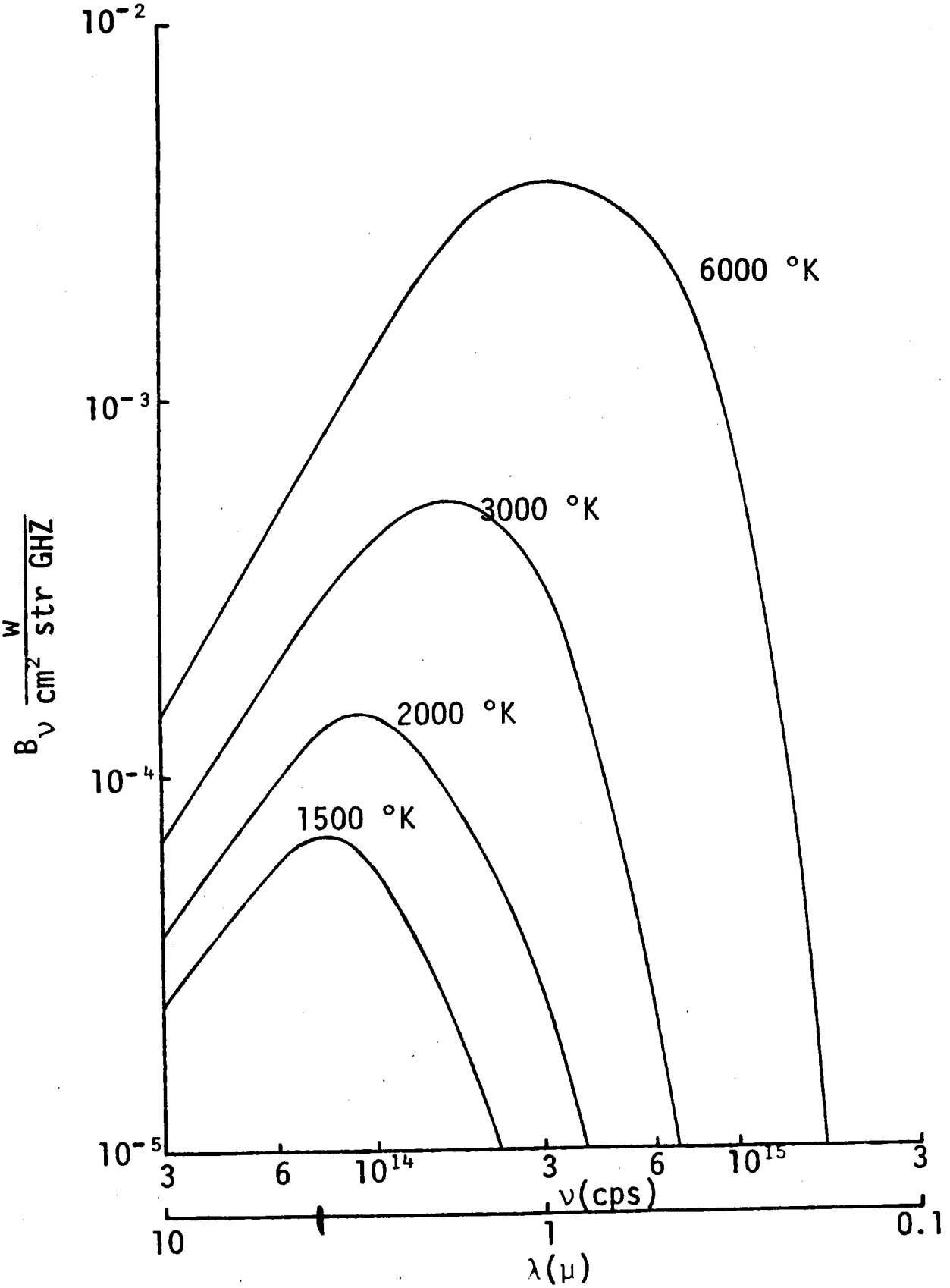
10^{-2}
10^{-3}
10^{-4}
10^{-5}
$B_\nu \frac{W}{cm^2\ str\ GHZ}$
6000 °K
3000 °K
2000 °K
1500 °K
3
6
10^{14}
3
6
10^{15}
3
ν(cps)
10
1
0.1
λ(μ)

FIG 4

BLACKBODY PUMPED LASERS

- CAN USE SOLAR RADIATION TO HEAT

  BLACKBODY CAVITY TO 1000 K → 3000 ^{o}K

- EXCITE OR ENERGIZE GAS VIA

  BLACK BODY RADIATION

- CONCEPT USES ENTIRE SOLAR SPECTRUM

- MOST LIKELY AN I.R. LASER,
  V-V TRANSFER LASER POSSIBLE

FIG 5

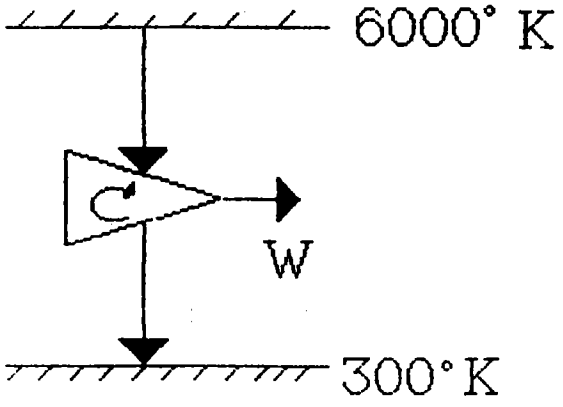

$$\eta_c = 1 - \frac{300}{6000} = 0.95$$

$$\eta_{pract} = 1 - \sqrt{\frac{300}{6000}} = 0.78$$

IDEAL DIRECT METHOD

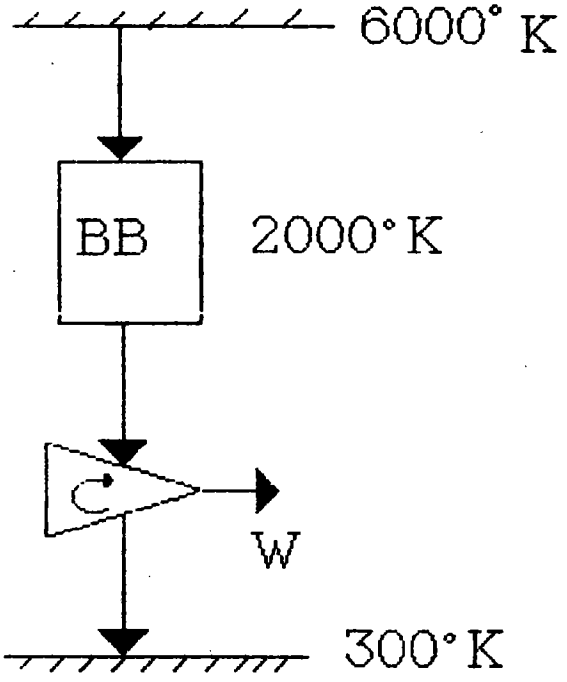

$$\eta_c = 1 - \frac{300}{2000} = 0.85$$

$$\eta_{pract} = 1 - \sqrt{\frac{300}{2000}} = 0.61$$

IDEAL INDIRECT METHOD

BLACKBODY SOLAR-PUMPED LASERS

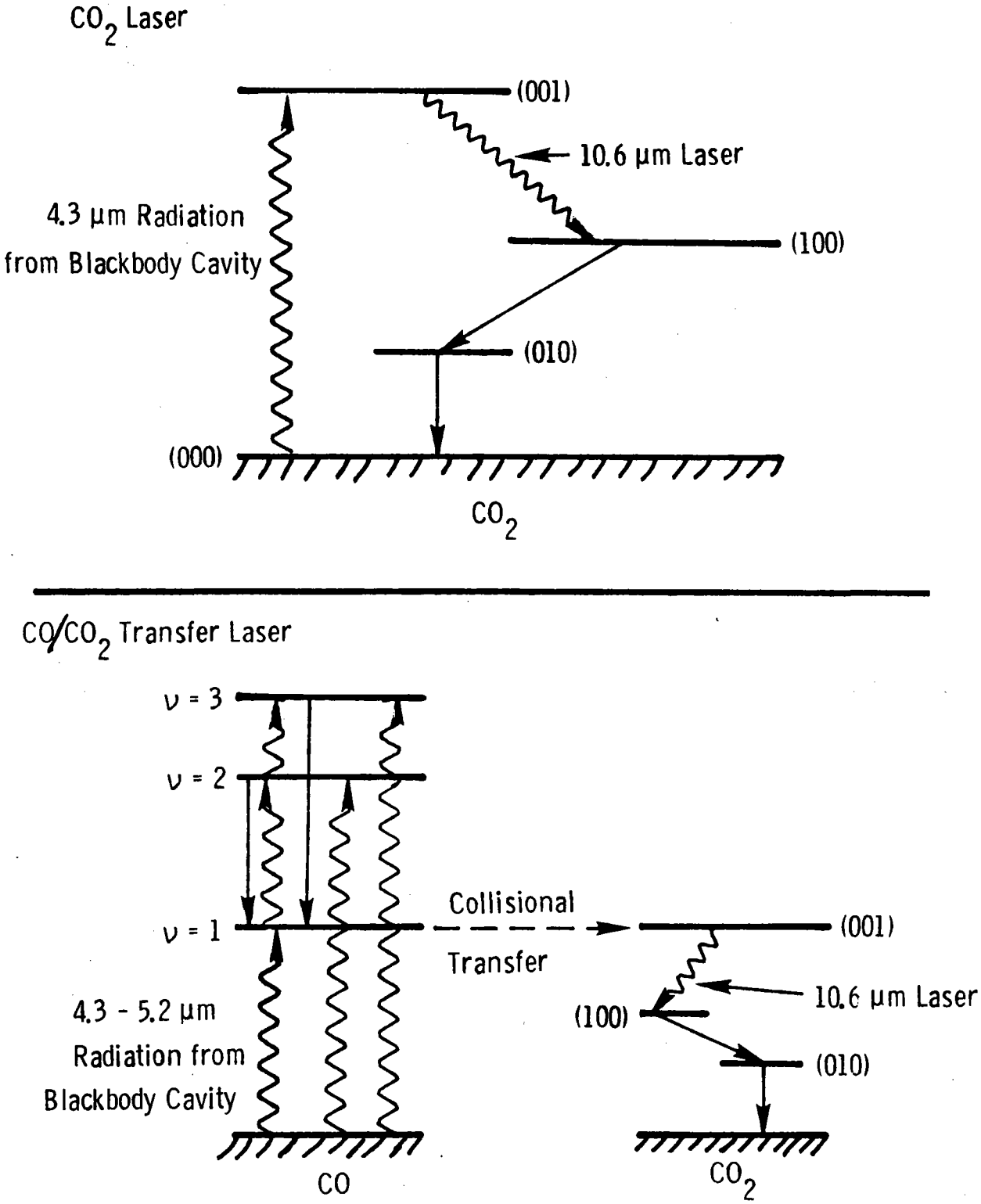

FIG 7

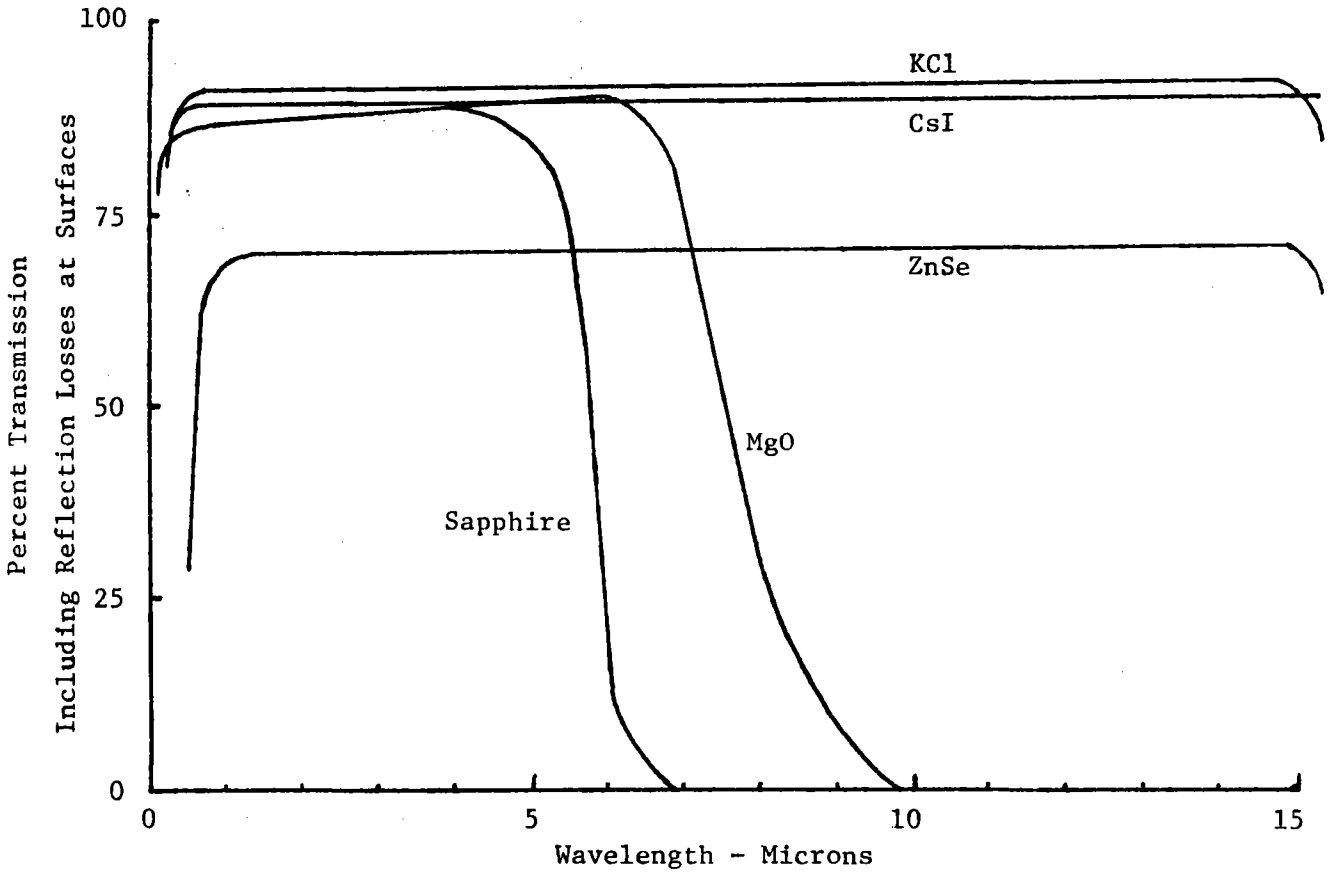
100
75
50
25
0
Percent Transmission
Including Reflection Losses at Surfaces
KCl
CsI
ZnSe
MgO
Sapphire
0
5
10
15
Wavelength - Microns

FIG 8

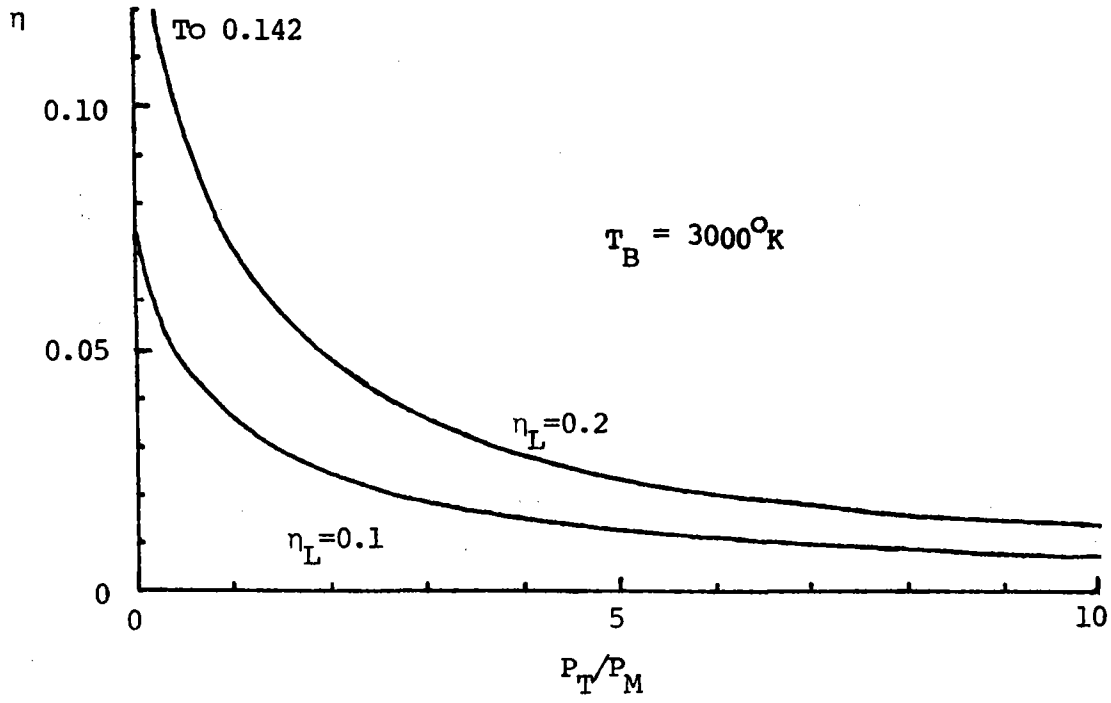
η
To 0.142
0.10
0.05
0
$T_B = 3000^oK$
η_L=0.2
η_L=0.1
0
5
10
P_T/P_M

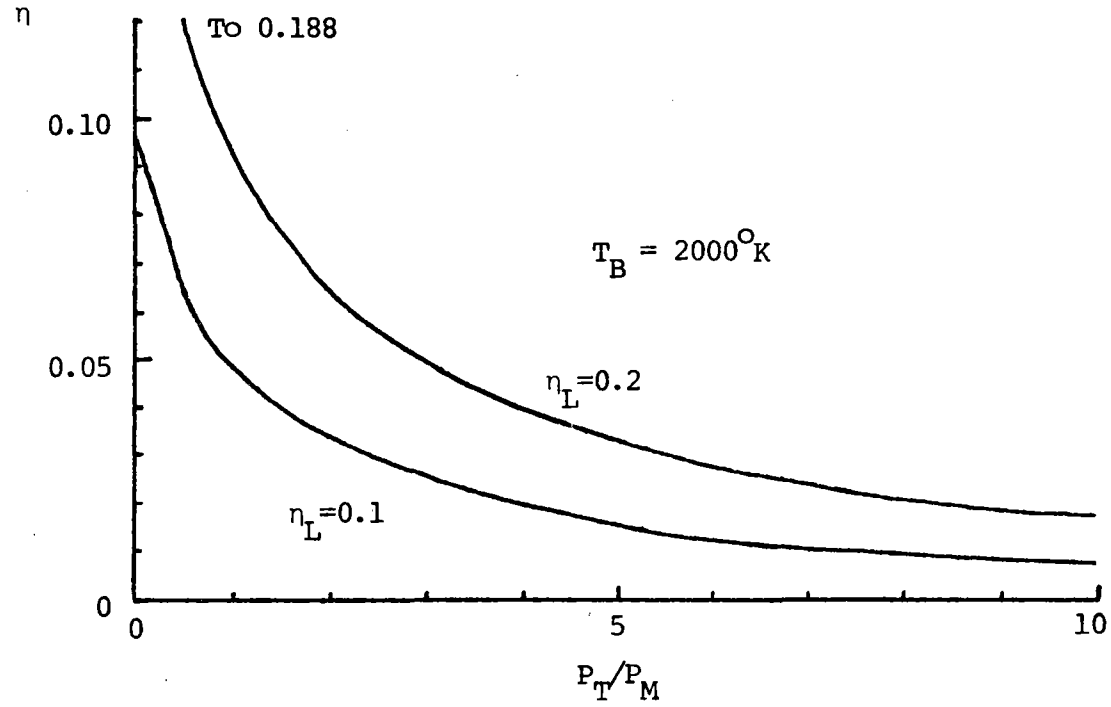
η
To 0.188
0.10
0.05
0
$T_B = 2000^oK$
η_L=0.2
η_L=0.1
0
5
10
P_T/P_M

FIG 9

ADVANTAGES

- η > 10% ARE POSSIBLE
- NO CHEMICAL PROBLEMS
- DUTY CYCLE POSSIBLE
- KNOWN LASER MEDIUM
- SIMULTANEOUS DIRECT & INDIRECT O.K.
- NO LARGE TECHNOLOGY BREAKTHRU REQ'D

DISADVANTAGES

- LONG λ
- OPTICAL MATERIALS?
- CONSTRAINTS ON PUMPING, λ_p
- EARLY STAGE OF DEVELOPMENT
- NO DEMONSTRATION OF SCALING OR η YET
- LOW POWER DENSITY IN DEVICE

FIG 10

CW Blackbody Laser Setup

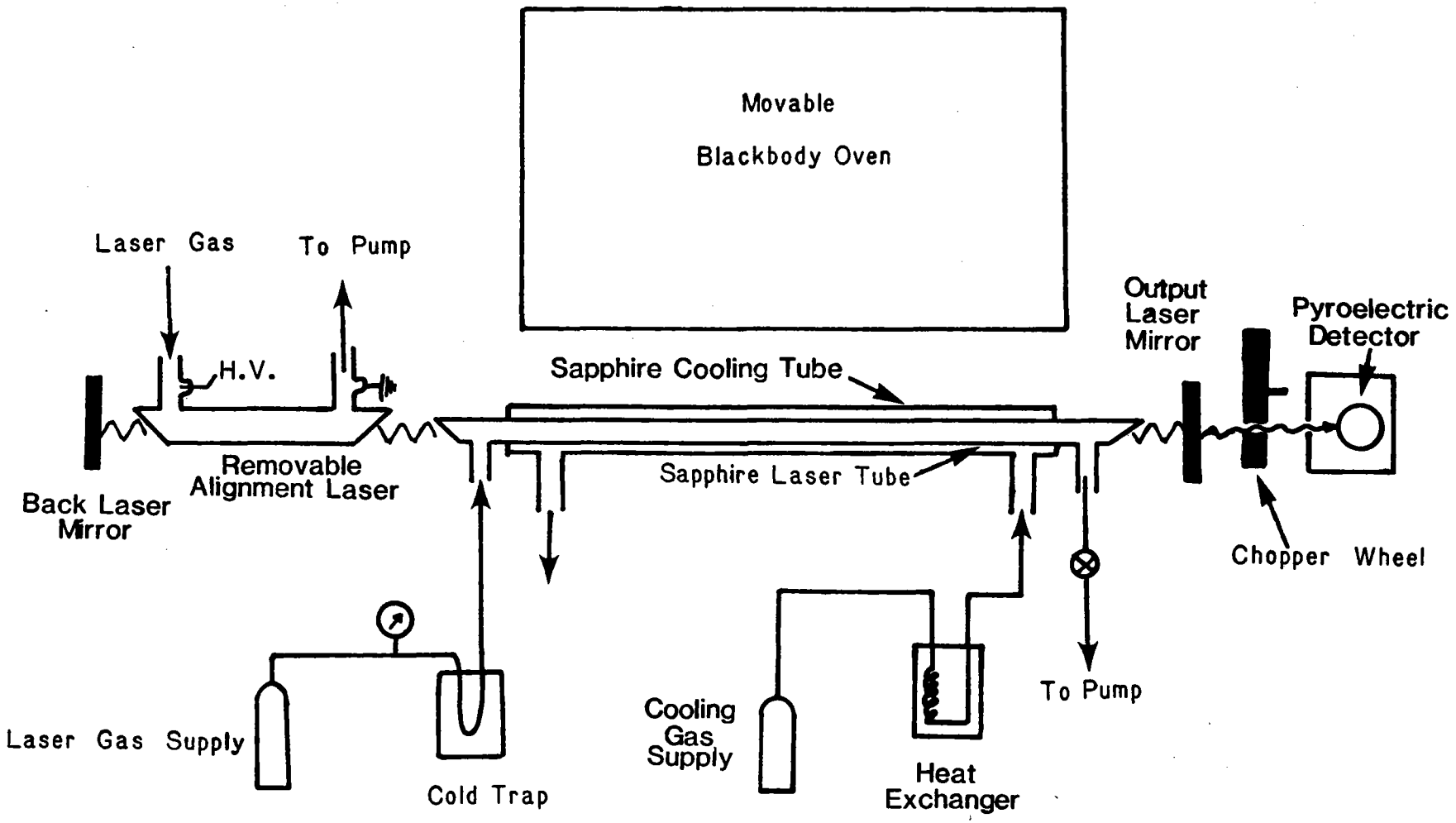

Fig 11

CW Blackbody Pumped CO_2 Laser

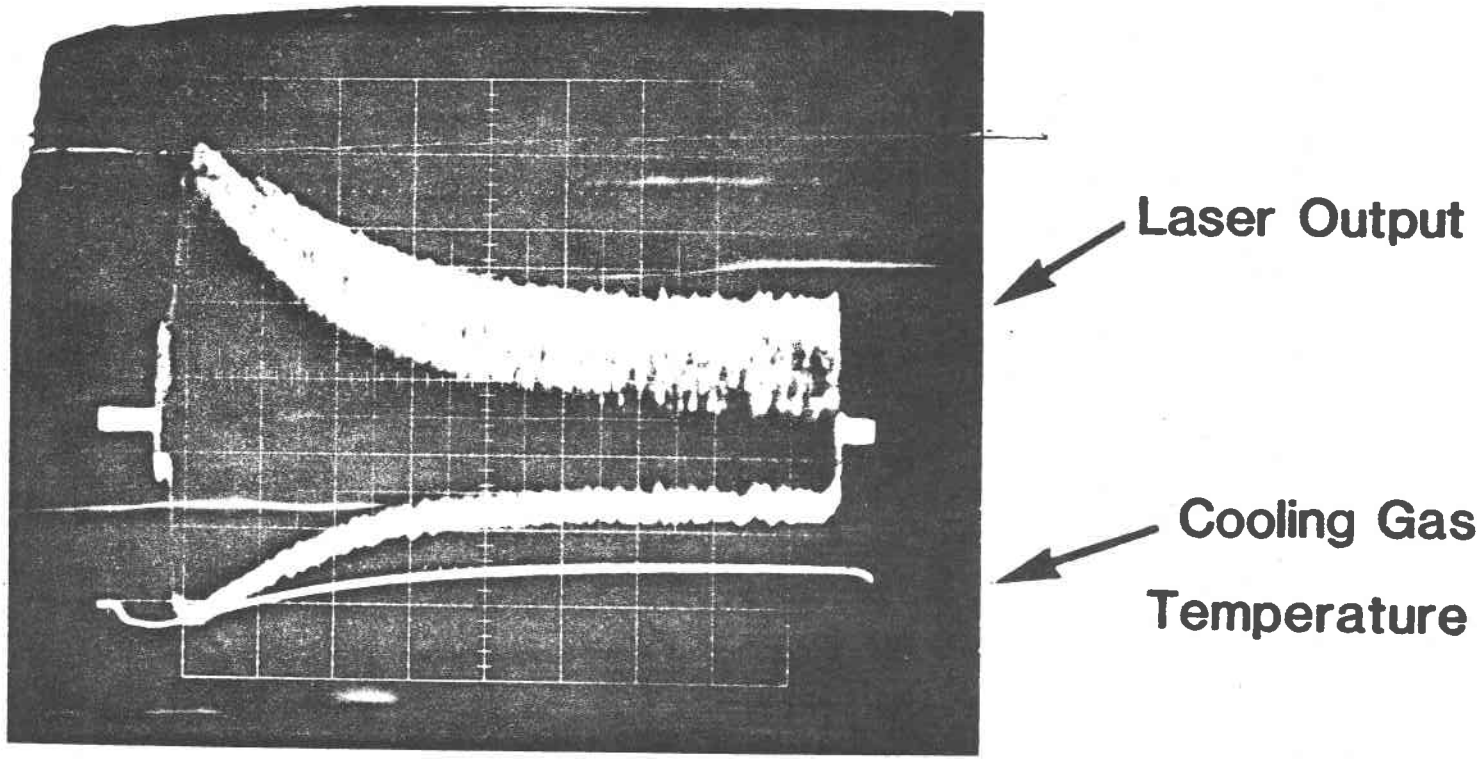

Blackbody-pumped CO_2 laser signal chopped at 30 Hz. The upper trace is the laser power 2 mW/div The lower trace is the cooling gas outlet temperature 100°C/div. The horizontal axis is 5 sec/div and the total pressure is 10 torr.

UPPER LEVELS:

$$\begin{cases} D\nabla^2 N_3 - \frac{1}{\tau_B}\left(N_3 - \bar{N}_3\right) + S + \frac{1}{\tau_4}\frac{\theta_2'}{\theta_3}\left(\psi N_3' - \psi' N_3 e^{-\Delta E/T}\right) = 0 \\ D'\nabla^2 N_3' - \frac{1}{\tau_B'}\left(N_3' - \bar{N}_3'\right) + S' - \frac{1}{\tau_4}\left(\psi N_3' - \psi' N_3 e^{-\Delta E/T}\right) = 0 \end{cases}$$

re $$S = \frac{(.85)^2}{\tau_{4.5} Q_V}\left[N_3(T_{BB})\, e^{-\alpha(R-R_W)} - N_3\right]$$

LOWER LEVELS:

$$D\nabla^2 N_2 - \frac{1}{\tau_1}\left(N_2 - \bar{N}_2\right) + \frac{3}{\tau_B}\left(N_3 - \bar{N}_3\right) = 0$$

$$D'\nabla^2 N_2' - \frac{1}{\tau_1'}\left(N_2' - \bar{N}_2'\right) + \frac{3}{\tau_B'}\left(N_3' - \bar{N}_3'\right) = 0$$

GAIN:

$$g_0(J) = \frac{G(J)}{n_t}\left(N_3 - N_1\right)$$

$$\frac{G^0(J)}{n_t} = \frac{\lambda_0^2 (\ln 2)^{1/2}}{4\pi^{3/2}\tau_{10.6}\Delta\nu_D}\,\frac{2\theta_r}{T}\left(2J+1\right) e^{-J'(J+1)\theta_r/T}$$

$$g_\nu(J) = g_0(J)\, \exp(a^2)\,\mathrm{erfc}(a) \quad ; \quad a = \frac{\Delta\nu_c}{\Delta\nu_D}(\ln 2)^{1/2}$$

FIG 13

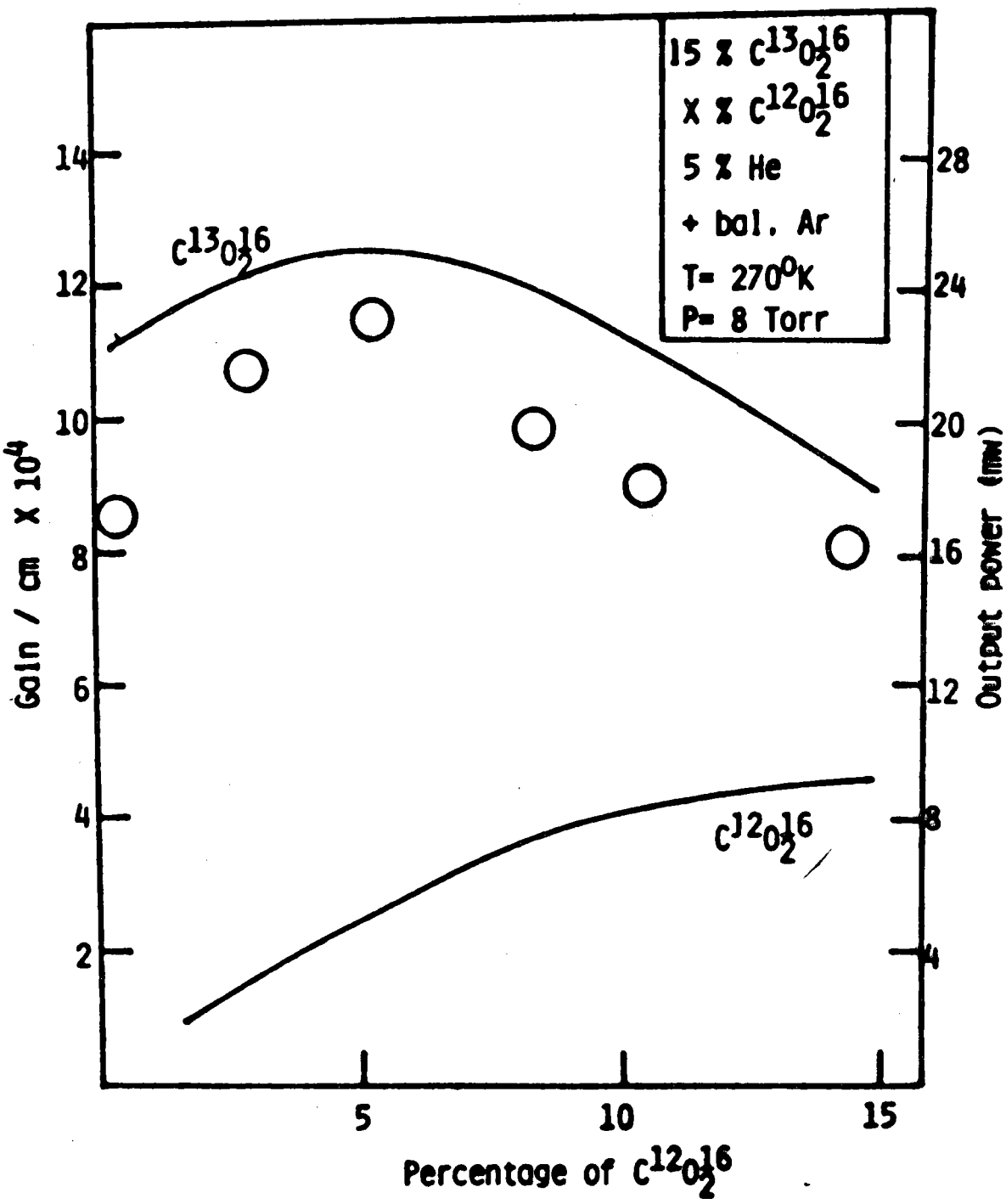
15 % $C^{13}O_2^{16}$
X % $C^{12}O_2^{16}$
5 % He
+ bal. Ar
T= 270°K
P= 8 Torr
$C^{13}O_2^{16}$
$C^{12}O_2^{16}$
Gain / cm X 10^4
Output POWER (mW)
14
12
10
8
6
4
2
28
24
20
16
12
8
4
5
10
15
Percentage of $C^{12}O_2^{16}$

FIG 14

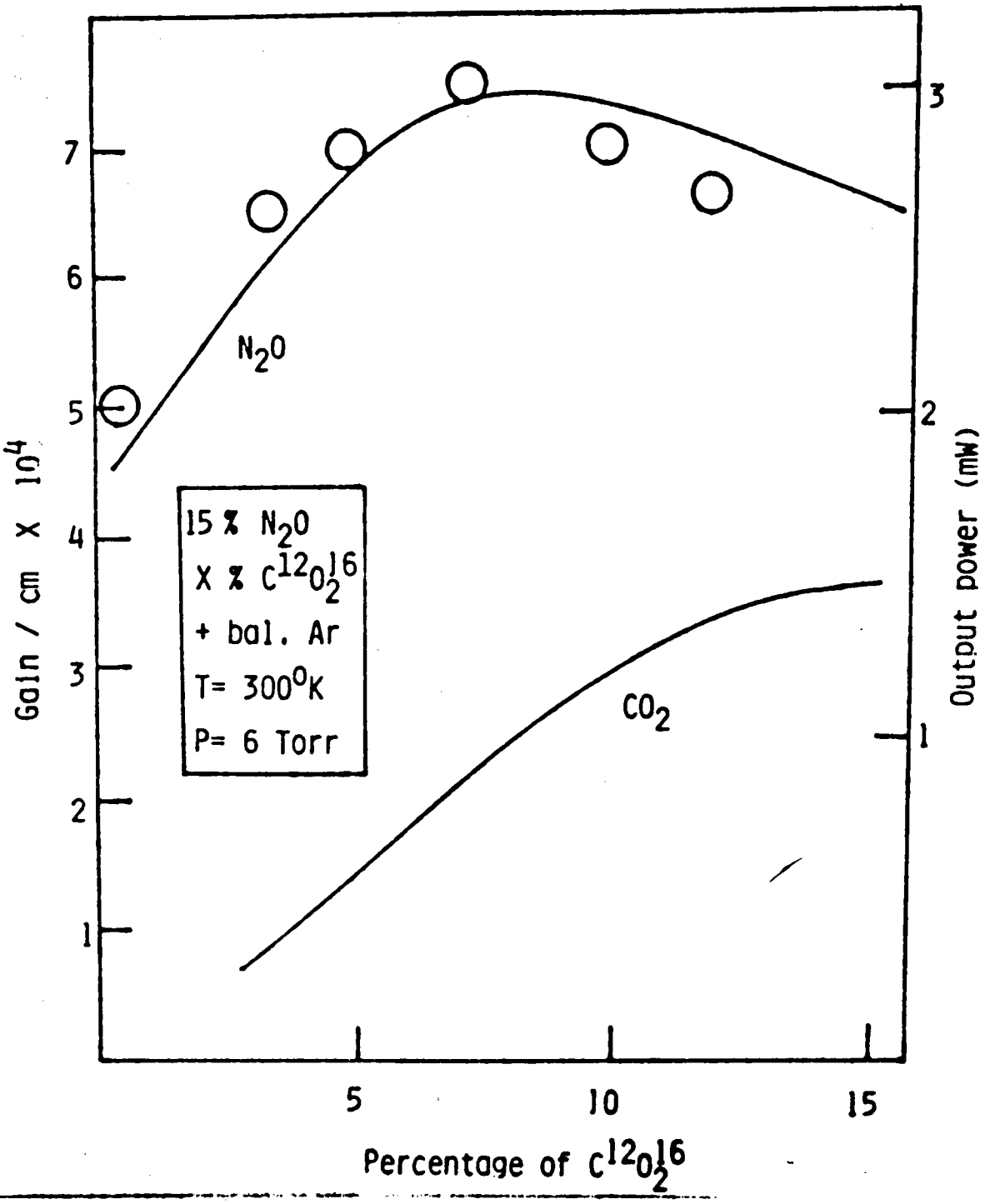
Gain / cm X 10^4
Output power (mW)
Percentage of $C^{12}O_2^{16}$
N_2O
CO_2
15 % N_2O
X % $C^{12}O_2^{16}$
+ bal. Ar
T= 300°K
P= 6 Torr
1
2
3
4
5
6
7
5
10
15

Fig 15

STATIC INDIRECT OPTICALLY PUMPED GAS LASER

LASANT: 12 ISOTOPES OF CO_2 AND HELIUM (24 TORR, 300 °K)

GAIN: $g_0 \approx 0.13\ M^{-1}$

LASER EFFICIENCY: $\eta_L = 36\%$

BLACK BODY TEMP.: $T_B = 2000$ °K

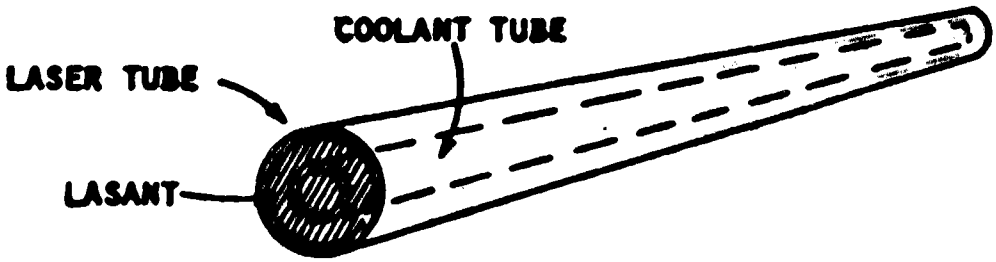

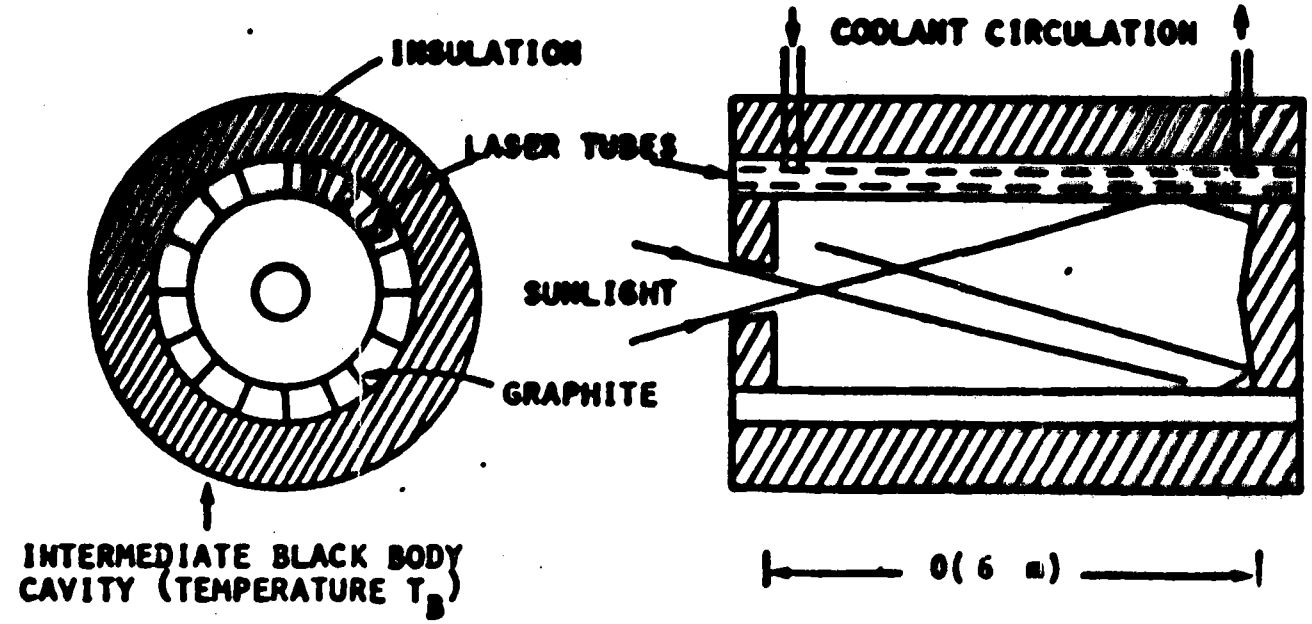

78 01503

FIG 5

(a) ISOMETRIC VIEW

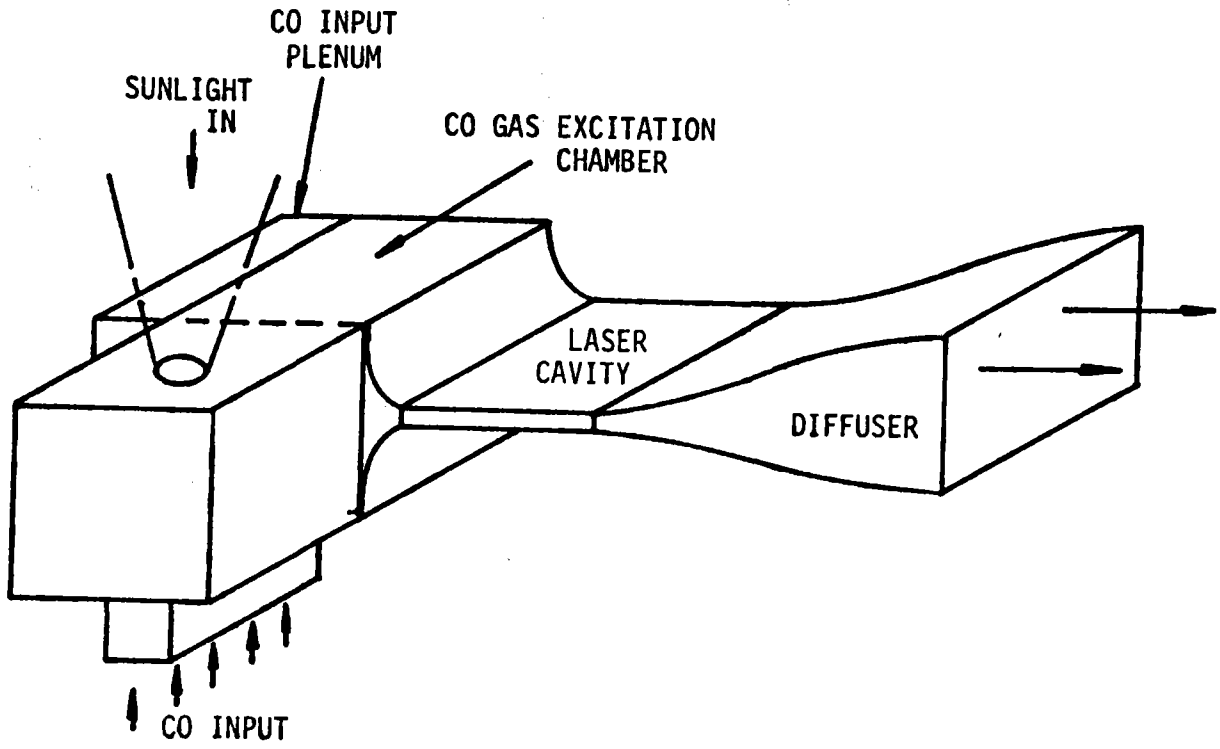

(b) ENLARGED SIDE VIEW OF BLACKBODY AND LASER CAVITIES

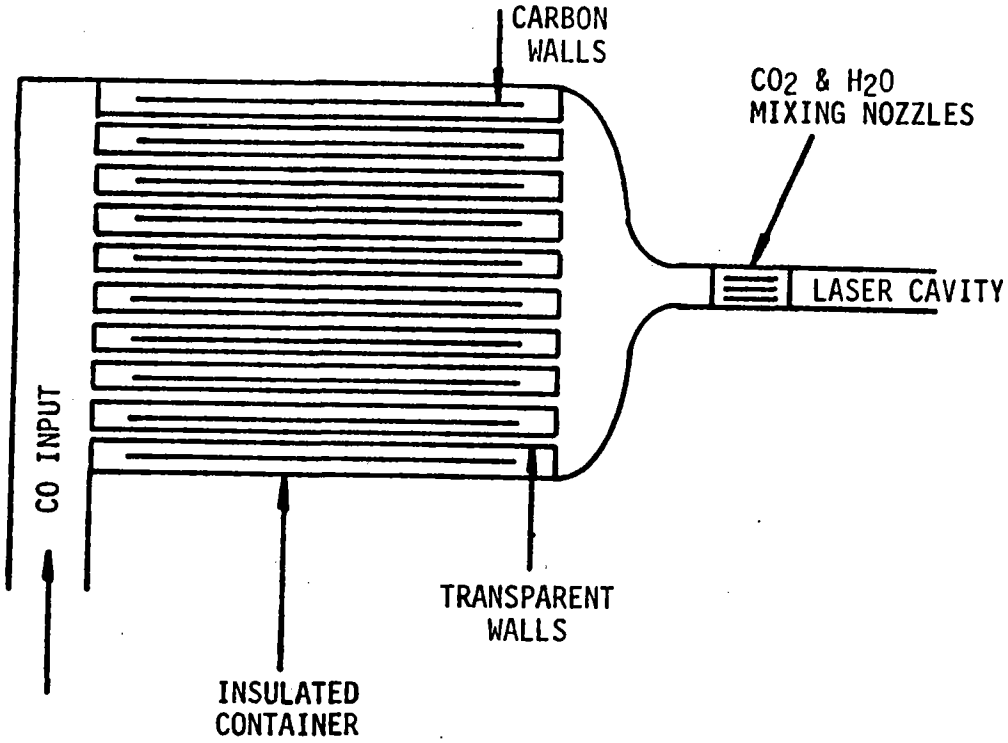

FIG 17

CURRENT RESEARCH TOPICS

- Use of isotopes, effect on Lasing, Kinetics
- Other IR lasers, CO?
- Scaling
- η
- Optical Materials/Coatings

FUTURE POSSIBILITIES

- Multiple λ lasing
- Shorter λ lasing
- Other systems
- Solar pumped mixing system

Fig 12

PYROELECTRIC CONVERSION

Randall B. Olsen
Chronos Research Laboratories, Inc.

PYROELECTRIC CONVERSION

Randall B. Olsen

Chronos Research Laboratories, Inc.

Pyroelectric conversion is the electrical analog of the familiar steam engine. The thermodynamic variables charge and voltage are analogous to volume and pressure. Special (ferroelectric) materials show large couplings between thermal and electrical properties near their (ferroelectric to para-electric) phase transitions.

Ceramic pyroelectric converters have been demonstrated with efficiencies of about one tenth of the Carnot limit at 1.8 Watt power level.

A recently discovered polymer promises a factor of 35 increase in the electrical output per unit volume over the older ceramic materials. In addition to low cost ($0.05 per Watt), the new polymer is expected to permit operation at greater than half the Carnot limit.

After the polymer properties are developed it is anticipated that complete pyroelectric conversion systems costing less than one dollar per Watt will convert 150C heat (solar or industrial waste) into electricity at about 15% efficiency.

SPECIAL CHARACTERISTICS OF THE PYROELECTRIC CONVERTER

- DIRECT CONVERSION OF HEAT TO ELECTRICAL ENERGY
- HIGH ADAPTABILITY: MODULARITY AND FLEXIBILITY OF CONFIGURATION
- LOW OPERATING PRESSURE (SAFE)
- LOW FREQUENCY PUMP. THIS MAY LEAD TO:
  - QUIET OPERATION
  - HIGH RELIABILITY - LOW MAINTENANCE
  - LOW OPERATING COST
- LOW SPECIFIC VOLUME
- NO STRATEGIC METALS

PYROELECTRIC CONVERTER
HOLDS PROMISE FOR:

HIGH EFFICIENCY

LARGE FRACTION (75%) OF CARNOT EFFICIENCY IS POSSIBLE.

HIGH POWER DENSITY

5 KILOWATT/LITER (FE) OR GREATER.

LOW CAPITAL COST

POTENTIALLY LESS THAN $1/WATT (PAYBACK TIME 2-3 YEARS).

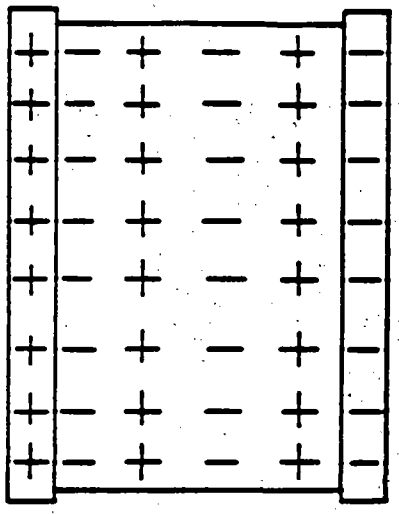

LOW VOLTAGE CHARGE

COLD (T < CURIE T)

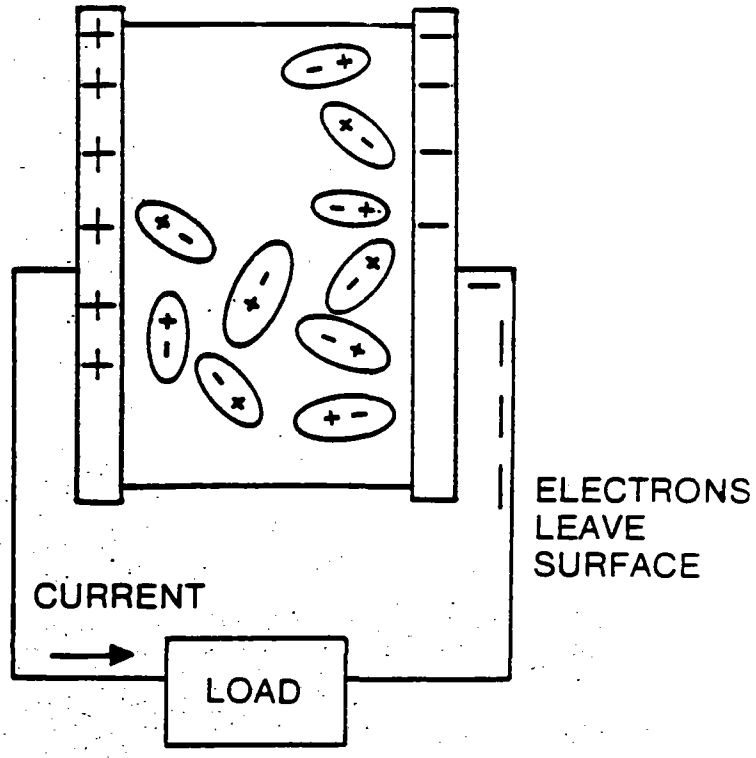

HIGH VOLTAGE DISCHARGE

HOT (T > CURIE T)

PYROELECTRIC

STRESS

ELECTRIC FIELD.

STRAIN

ELECTRIC DISPLACEMENT, (POLARIZATION).

ADVANTAGE

ELECTRIC WORK.

DISADVANTAGE

INTERACTIONS BETWEEN ELECTRIC FIELD AND CONDUCTING HEAT EXCHANGE FLUID.

SOLAR

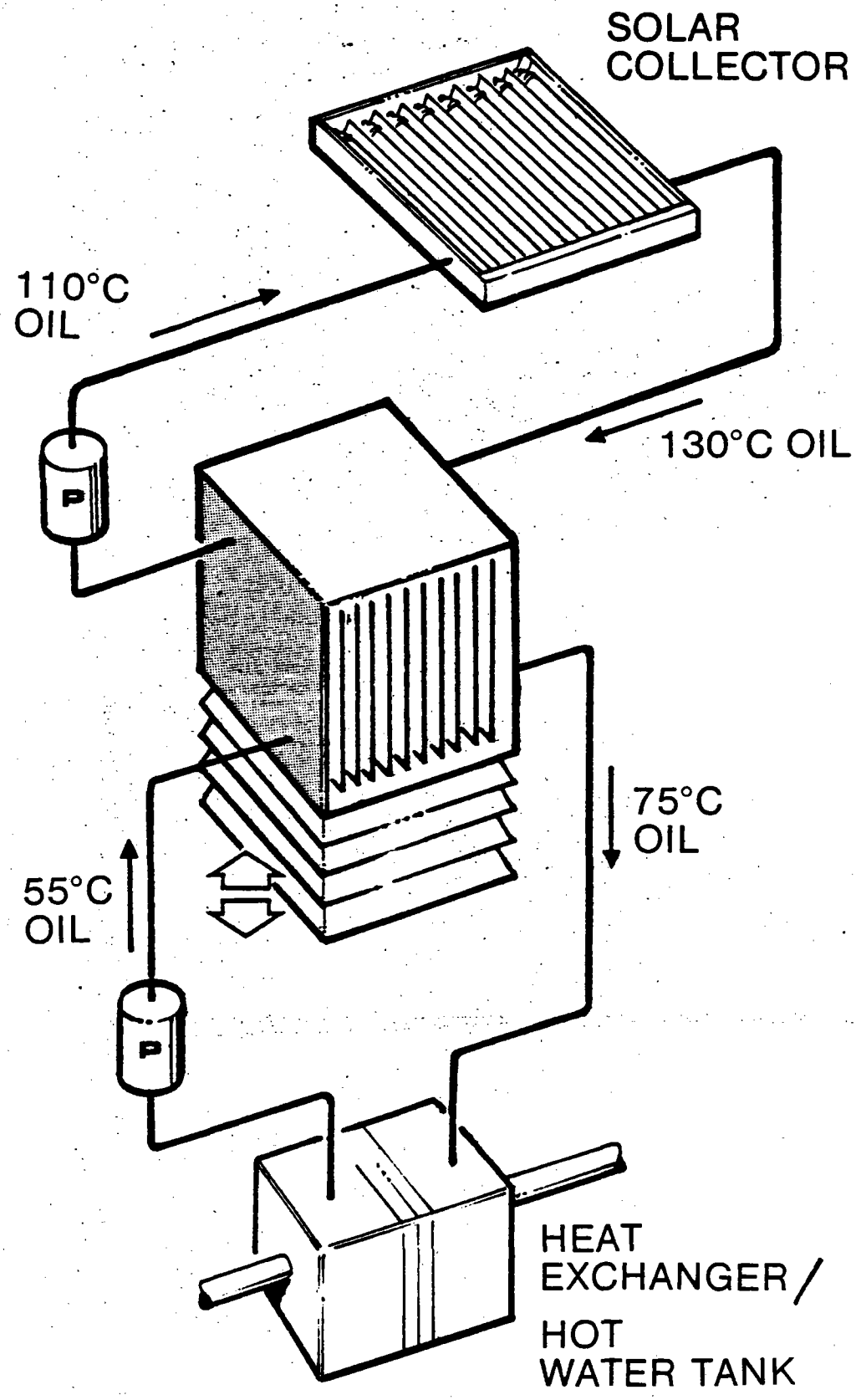
SOLAR
COLLECTOR
110°C
OIL
130°C OIL
P
75°C
OIL
55°C
OIL
P
HEAT
EXCHANGER /
HOT
WATER TANK

COST OF SOLAR PYROELECTRIC CONVERTER

5 KILOWATT (PEAK ELECTRICAL) SYSTEM

PLASTIC SHEET	$100	
METALIZING, ASSEMBLY AND CONTAINER	150	
PUMP	100	
CONTROL SYSTEM AND POWER CONDITIONING	500	
SUBTOTAL	$850	($0.17/WATT PEAK) (0.68/WATT AVERAGE)
ADDED COLLECTORS (20% MORE COLLECTORS)		
$100/m² x 20% x 100m²	2,000	(.40/WATT PEAK) (1.60/WATT AVERAGE)
TOTAL	2,850	(.57/WATT PEAK) (2.28/WATT AVERAGE)

TOTAL ELECTRICAL POWER OUTPUT FOR EXPERIMENTAL PYROELECTRIC CONVERTERS

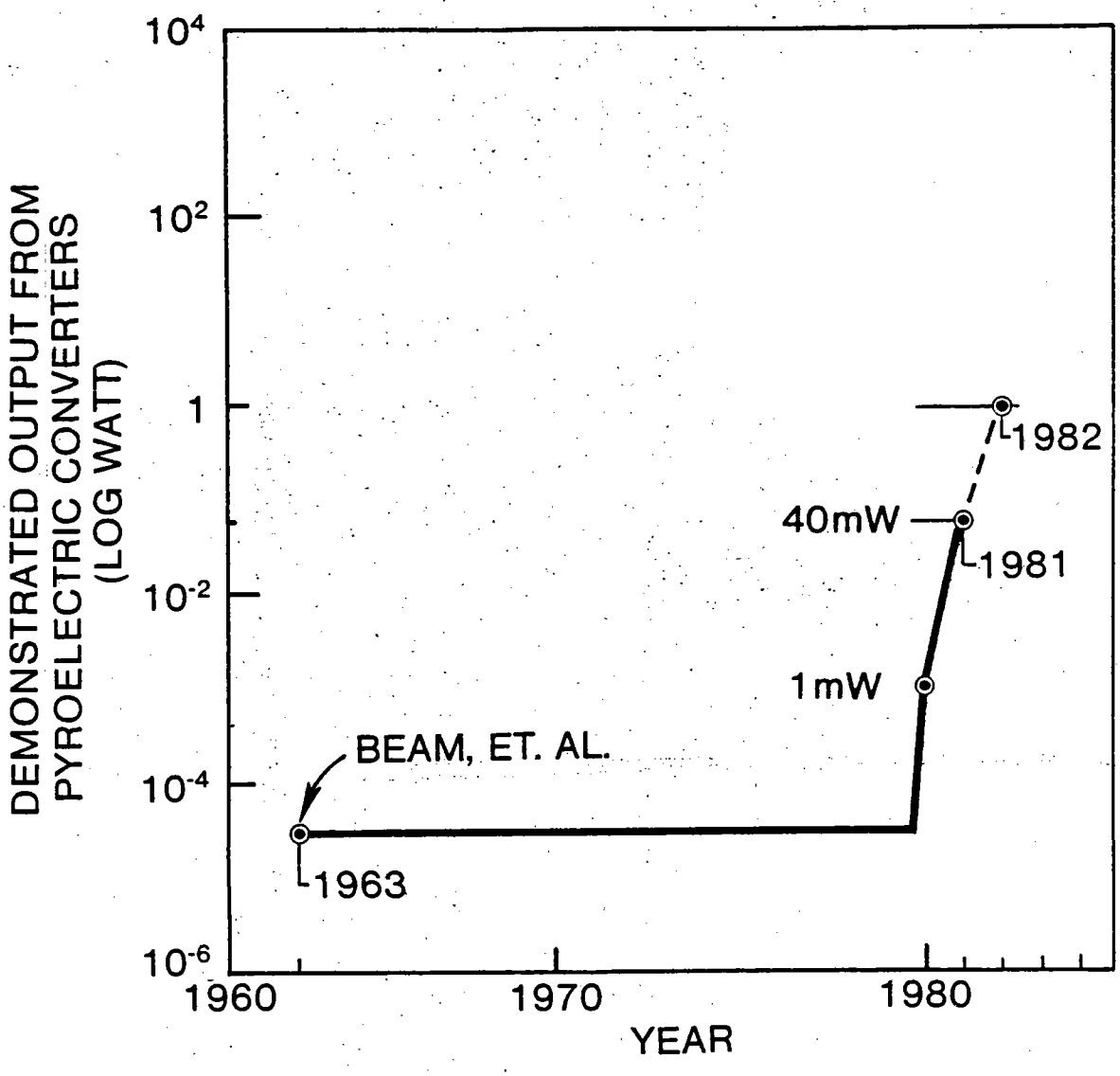

SHOWS 30,000 FOLD INCREASE IN DEMONSTRATED CONVERTER POWER OUTPUT

RELATIVE EFFICIENCY ADVANCES

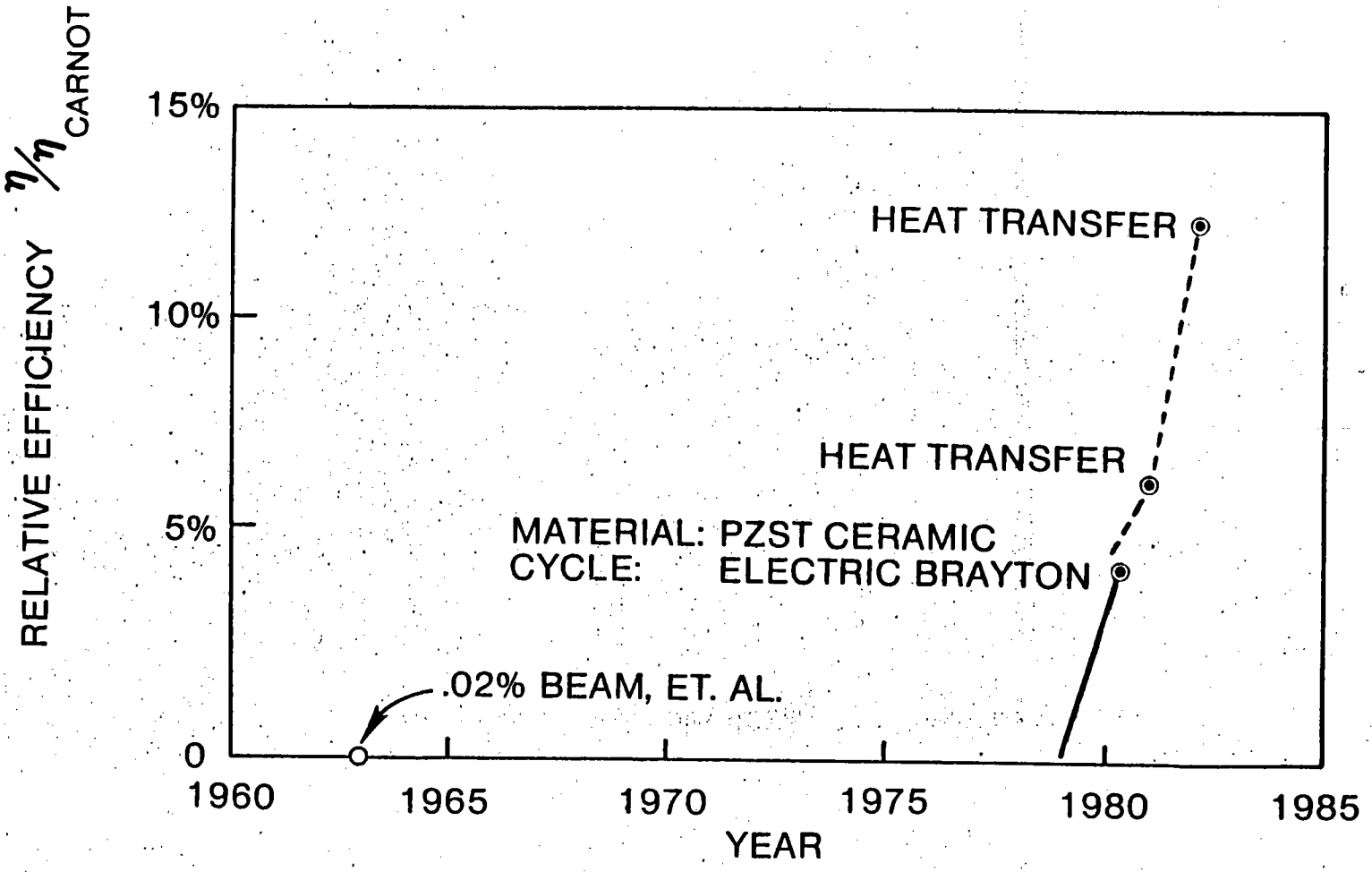

SHOWS 600 FOLD INCREASE IN MEASURED RELATIVE EFFICIENCY

REFERENCES

1. Olsen, R.B., and Brown, D.D., "High efficiency direct conversion of heat to electrical energy--related pyroelectric measurements," Ferroelectrics 40 pp. 17-27 (1982).

2. Olsen, R.B., Evans, D.,"Pyroelectric Energy Conversion - Hysteresis Loss and Temperature Sensitivity of a Ferroelectric Material," J. Appl. Phys. 54 p 5941 (1983).

3. Lines, M.E. and Glass, A.M., Principles and Applications of Ferroelectrics and Related Materials,Clarendon, Oxford (1977).

4. Drummond, J. E., "Dielectric power conversion," 10th IECEC, p. 569, (1975).

5. Gonzalo, J. A., "Ferroelectric materials as energy converters," Ferroelectrics 11,423 (1976).

6. Olsen, R. B.,"Ferroelectric conversion of heat to electrical energy--a demonstration," J. Energy, p. 91 March/April (1982).

7. Olsen, R. B., Briscoe, J. M., Bruno, D. A., and Butler, W. F., "A pyroelectric energy converter which employs regeneration," Ferroelectrics 38,975 (1981).

8. Olsen, R. B., Briscoe, J. M., and Bruno, D. A.,"Performance of a 1-watt pyroelectric converter," 17th IECEC (1982).

9. Beam, B. H., "An exploratory study of thermoelectrostatic power generation for space flight applications," NASA TN-D336 (1960).

10. Beam, B. H., Fry, J. and Russel, L., "Experiments on radiant energy conversion using thin dielectric films," Progress in Astronautics and Aeronautics, Vol. 16, Space Power Systems Engineering, Editors: G. Szego and J. Taylor, Academic Press, 1964.

11. Margosian, P. M., "Parametric study of a thermoelectrostatic generator for space applications," Lewis Research Center, NASA, Cleveland, Ohio, Jan. 4, 1965.

12. Furukawa, T., Date, M., Fukada, E., Tajitsu, Y. and Chiba, A., "Ferroelectric behavior in the copolymer of vinylidene fluoride and trifluoroethylene," Jap. J. Appl. Phys. 19 (1980).

13. Furukawa, T., Johnson, G. E., Bair, H. E., Tajitsu, Y., Chiba, A., and Fukada, E., "Ferroelectric phase transition in a copolymer of vinylidene fluoride and trifluoroethylene," Ferroelectrics 32,61 (1981).

14. Higashihata, Y., Sako, J. and Yagi, T., "Piezoelectricity of vinylidene fluoride-trifluoroethylene copolymers," Ferroelectrics, 32, 85 (1981).

15. Yamaka, T., Ueda, T. and Kitayama, T., "Ferroelectric-to- paraelectric phase transition of vinylidene fluoride-trifluoroethylene copolymer," J. Appl. Phys. 52, 2 (1981).

16. Yamada, T. and Kitayama, T., "Ferroelectric properties of vinylidene fluoride-trifluoroethylene copolymers," J. Appl. Phys. 52, 6863 (1981).

17. Hicks, J.C., Jones, T.E., Burgener, M.L., and Olsen, R.B., "High temperature hysteresis in polyvinylidene fluoride," Ferroelectrics Letters, 44 pp. 89-92 (1982).

18. Olsen, R.B., Hicks, J.C., Broadhurst, M.G., and Davis, G.T., Temperature Dependent Ferroelectric Hysteresis Study of Poly(vinylidene fluoride) App. Phys. Let., 43, 127-129 (1983).

19. Sawyer, C.B., and Tower, C.H., Phys. Rev. 35, pp. 269-273 (1930).

20. Olsen, R.B., Butler, W.F., Payne, D.A., Tuttle, B.A., and Held, P.C., "Observation of a polarocaloric (electrocaloric) effect of 2C in lead zirconate modified with Sn4+ and Ti4+," Phys. Rev. Lett. 45p. 1436 (1980).

21. Olsen, R.B., "Condensed state heat engines," DOE workshop on thermall / regenerative electrochemical systems (TRES), Alexandr a, Virginia, Dec. 3-4 (1981).

22. Olsen, R.B., Bruno, D.A., and Briscoe, J.M., "Pyroelectric conversion cycles," submitted to J. Appl. Phys.

23. Olsen, R.B., Bruno, D.A., Briscoe, J.M., and Dullea, J. "Cascaded pyroelectric energy converter," Ferroelectrics (in press).

24. Olsen, R.B., Butler, W.F., Drummond, J.E., Bruno, D.A., and Briscoe, J.M., "Heat flow in a pyroelectric converter," submitted to IECEC (1985).

25. Olsen, R.B., "Pyroelectric conversion in space," 19th IECEC p. 224 (1984).

26. Olsen, R.B., Bruno, D.A., Briscoe, J.M., and Jacobs, W.E., "Quasi-irreversible changes in the polarization of vinylidene fluoride - trifluoroethylene," submitted to Ferroelectrics Letters.

27. Olsen, R.B., Bruno, D.A., Briscoe, J.M., and Jacobs, W.E., "Pyroelectric conversion cycle of vinylidene fluoride - trifluoroethylene," J. Appl. Phys. (in press).

28. "Method and apparatus for pyroelectric power conversion," U.S. Patent No. 4,425,540 (1984)

REGENERABLE FUEL CELLS

Frank Ludwig
Hughes Aircraft Company

Report not available at time of publication

SOLAR THERMAL/ELECTRIC CONVERSION USING THE SODIUM HEAT ENGINE

Thomas K. Hunt
Ford Motor Company

Solar Thermal/Electric Conversion Using the Sodium Heat Engine

Thomas K. Hunt
Research Staff, Ford Motor Company
Dearborn, Michigan 48121

Introduction

The Sodium Heat Engine (SHE) is a high efficiency energy conversion device capable of the direct conversion of heat to electricity using thermal input at temperatures in the range from 700 to 1000°C. The SHE operates by extracting electrical energy from the electrochemical expansion of sodium vapor across a beta''-alumina solid electrolyte (BASE) membrane[1]. Because the efficiency of the SHE system should be essentially independent of size, it is anticipated that most systems will be constructed from modules of modest output, probably in the range from 1 to 10 kW. Experiments performed thus far suggest that efficiencies in the range from 25 to 35% will be possible in fully developed SHE systems[2]. Modular system fabrication appears to offer a number of particular advantages for solar thermal conversion.

Early SHE experiments emphasized confirmation of the basic process and verification that all the components required for a general system could be made to work. A second research phase focussed on the electrode system and showed that it is possible to achieve performance very nearly at the limits predicted for perfect electrodes[2] (output at 1.1 W/cm^2 at 900°C has been observed). Unfortunately, such performance levels do not endure for more than a few hundred hours at 900°C for the refractory metal electrodes considered to be the reference system. Such electrodes suffer a reduction in output which appears to reach an asymptotic value of 0.2 to 0.5 W/cm^2. Further experiments showed that in operation at temperatures up to 900°C, the beta''- alumina does not suffer deterioration of its bulk ionic/electronic conduction properties to a degree which would impair SHE performance. The mechanisms generally proposed to explain the degradation of beta''-alumina as observed in the sodium sulfur battery system are not expected to apply in the SHE system for which liquid sodium never appears at the exit electrode-electrolyte interface.

A third phase of SHE research currently is aimed at construction and testing of a 100-200 watt system which can run from a combustion or focussed solar heat source. Concurrently, progress is being made on a number of approaches aimed at improving the high performance endurance of SHE electrodes.

Demonstrated SHE system performance includes operation of complete self-pumped recirculating cells at constant output (20 A and 8 watts) for over 10,000 hours and operation at thermal to electrical conversion efficiencies as high as 19%. High temperature series connection of individual SHE cells within a common condenser chamber has been demonstrated successfully thus paving the way for improvement of system efficiency by the reduction of parasitic thermal conduction down the output leads. While the first experiments using a focussed solar thermal heat source have not yet been performed, combustion heating of a SHE system has been successfully demonstrated. In such tests a two tube SHE device has been heated from room temperature to 600°C in less than 8 minutes several times, with no apparent adverse consequences to the BASE tubes.

It has also been established experimentally that heating of a sodium-core SHE by radiation from the outside can be accomplished in geometries for which the condenser has a large view factor for the electrode. This opens up a large range of possible configurations for high performance radiatively heated SHE systems. Radiative heat transfer also promises heating rates consistent with avoiding thermal shock damage to the BASE tubes.

At Ford, we have made an attempt to assess the utility of the SHE relative to various alternatives for use in a point focus distributed receiver[3]. It was concluded that on the basis of efficiency, the SHE can be very competitive with Stirling, organic Rankine and Brayton systems and that advantages in operating and maintenance costs may well be possible in a fully developed SHE system. The relative assessments in that report do not yet appear to require revision. An effort is now being made at Sandia to engineer a SHE system specifically tailored for such an installation.

Research Directions:

Since the ultimate utility of the SHE system clearly depends in considerable measure on its durability, investigation of the endurance/performance properties of SHE electrode materials continues to be important. With our improved understanding of the mechanisms leading to the remarkably good initial performance of sputtered, refractory metal electrodes we now have an important opportunity to explore new methods for stabilizing them.

The electromagnetic pump systems used for recirculation in 'conventional' SHE systems appear to work reliably once primed, but this operation often is time consuming. Improved procedures for assuring prompt sodium wetting of all the circulation loop components are desirable. A related issue involves the presence of hydrogen introduced into the sodium cycle by reaction of sodium with residual water, some of which appears to survive bake-out of the beta''-alumina at temperatures up to 800°C. Build-up of hydrogen pressure within the BASE tube can forcible empty the EM pump and starve the cell. Development of methods for removing or immobilizing this hydrogen remains a practical consideration in SHE designs.

Collection of the large currents produced by SHE cells also requires further attention. The reduction of parasitic resistance is crucial since the internal impedance of single SHE cells is of order 1 to 2 milliohms. Investigation of the proper compromises between electrode sheet resistance and the spacing of the bus wires should lead to better designs and higher overall performance.

References

1. 'A Thermoelectric Device Based on Beta-Alumina Solid Electrolyte', Neill Weber, Energy Conversion, 14, 1 (1974).

2. 'Research on the Sodium Heat Engine', T.K. Hunt, Neill Weber and Terry Cole Proceedings of the 13 Intersociety Energy Conversion Engineering Conference, p2011 (1978).

3. 'Solar Thermal/Electric Power Conversion Using the Sodium Heat Engine', K. Subramanian and T.K. Hunt, Proceedings of the ASME Solar Energy Division Fifth Annual Conference. p288 (1983).

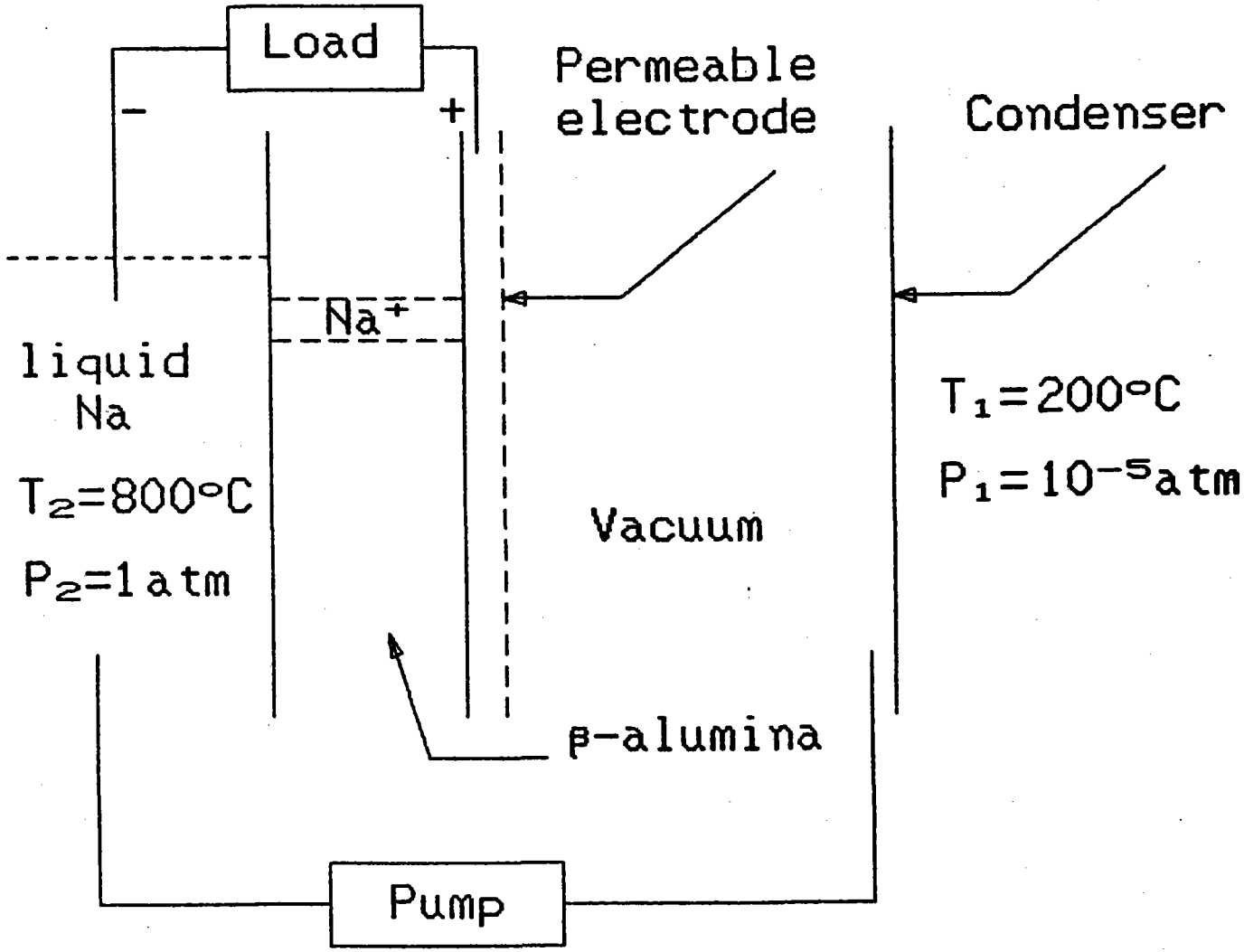
Load
−
+
Permeable
electrode
Condenser
Na+
liquid
Na
T2=800°C
P2=1 atm
Vacuum
T1=200°C
P1=10−5atm
β-alumina
Pump

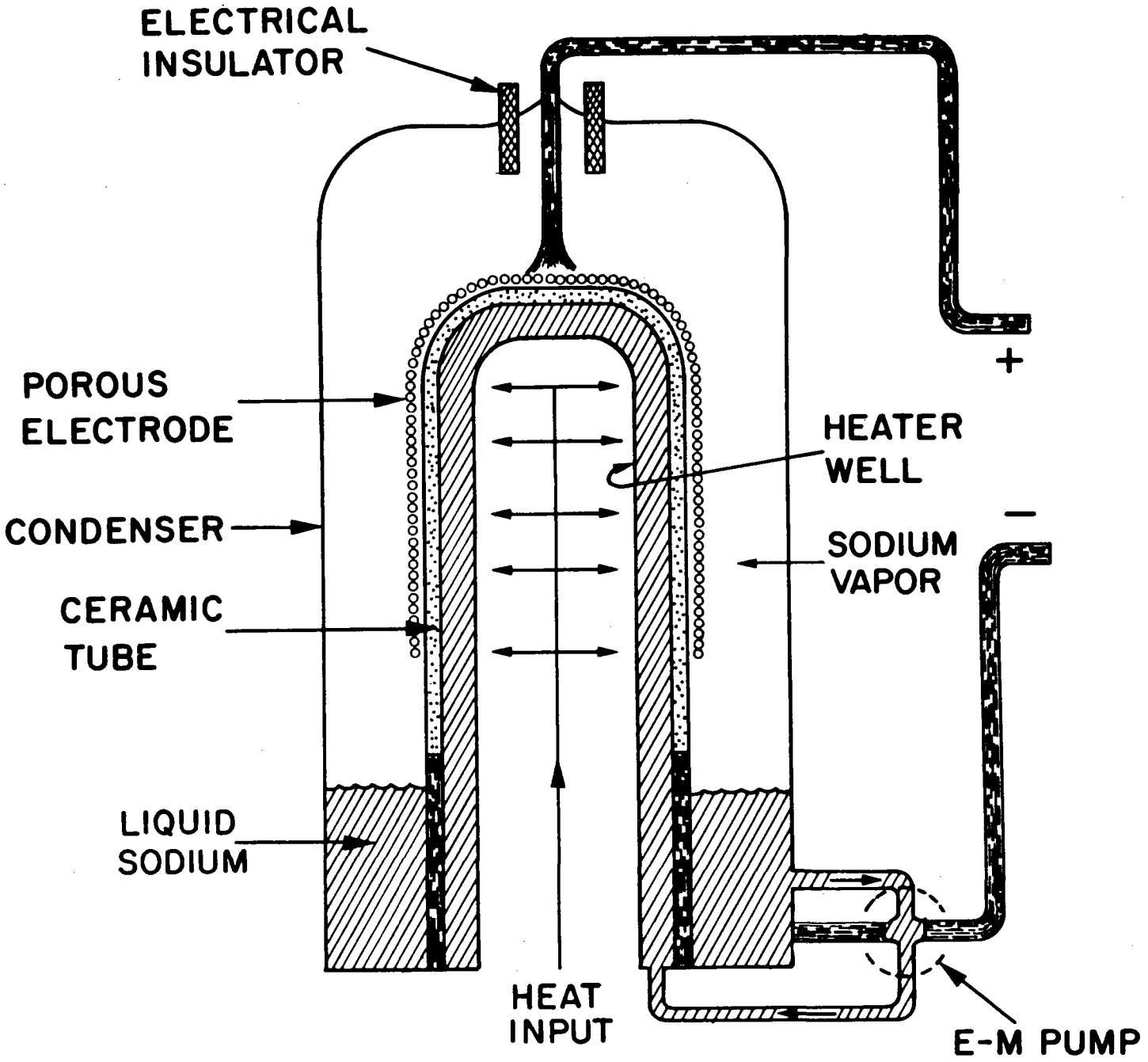
ELECTRICAL
INSULATOR
+
POROUS
ELECTRODE
HEATER
WELL
CONDENSER
SODIUM
VAPOR
−
CERAMIC
TUBE
LIQUID
SODIUM
HEAT
INPUT
E-M PUMP

Voltage - Current

$$V = \frac{RT_2}{F} \ln\left[\frac{P_v(T_2)}{(T_2/T_1)^{1/2}P_v(T_1) + aT_2^{1/2}i}\right] - iR_o$$

$$= A - \frac{RT_2}{F} \ln i \; - iR_o$$

Efficiency

$$\eta = \frac{iV}{i[V+L/F+C_p(T_2-T_1)/F]+\sigma(T_2^4-T_1^4)/Z+K(T_2+T_1)}$$

↑ Latent Heat ↑ Enthalpy ↑ Radiation ↑ Conduction

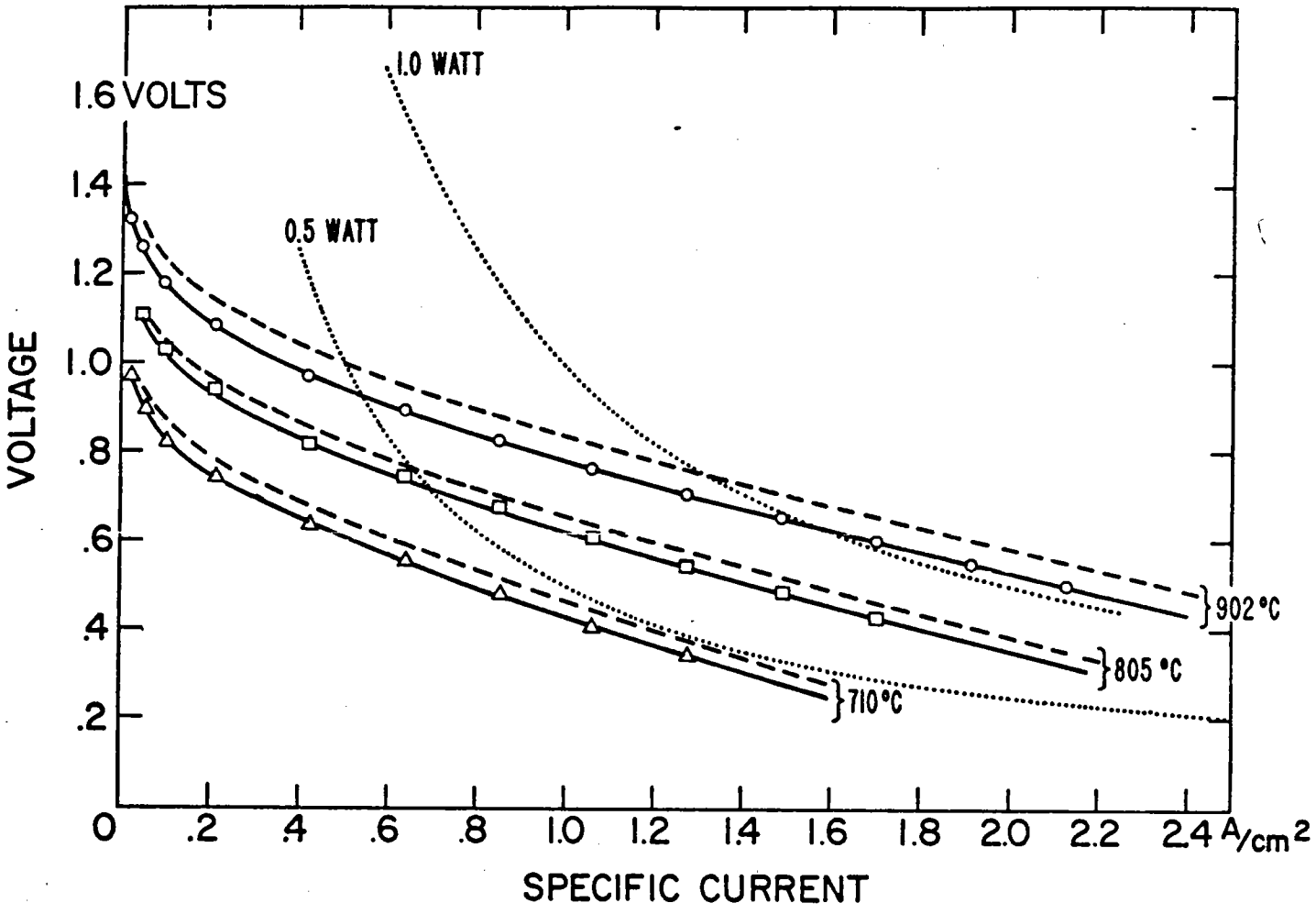
1.0 WATT
0.5 WATT
1.6 VOLTS
1.4
1.2
1.0
.8
.6
.4
.2
VOLTAGE
902 °C
805 °C
710 °C
0
.2
.4
.6
.8
1.0
1.2
1.4
1.6
1.8
2.0
2.2
2.4 A/cm²
SPECIFIC CURRENT

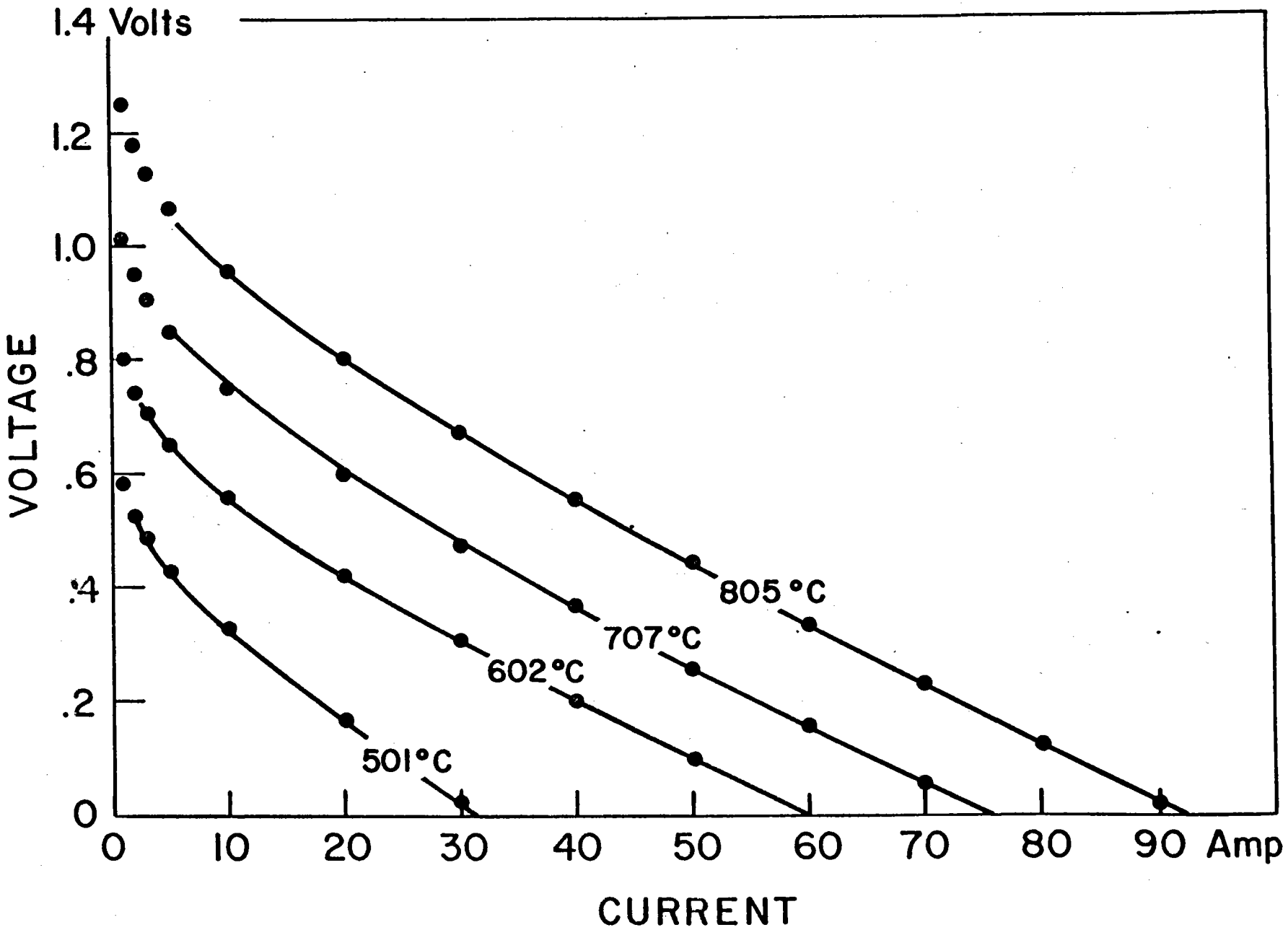

FIGURE 2. Experimental Voltage-Current data for a Sodium Heat Engine cell operating at different values of the high temperature, T_2. This cell had an electrode area of 115 cm^2. and reached an efficiency of 19%.

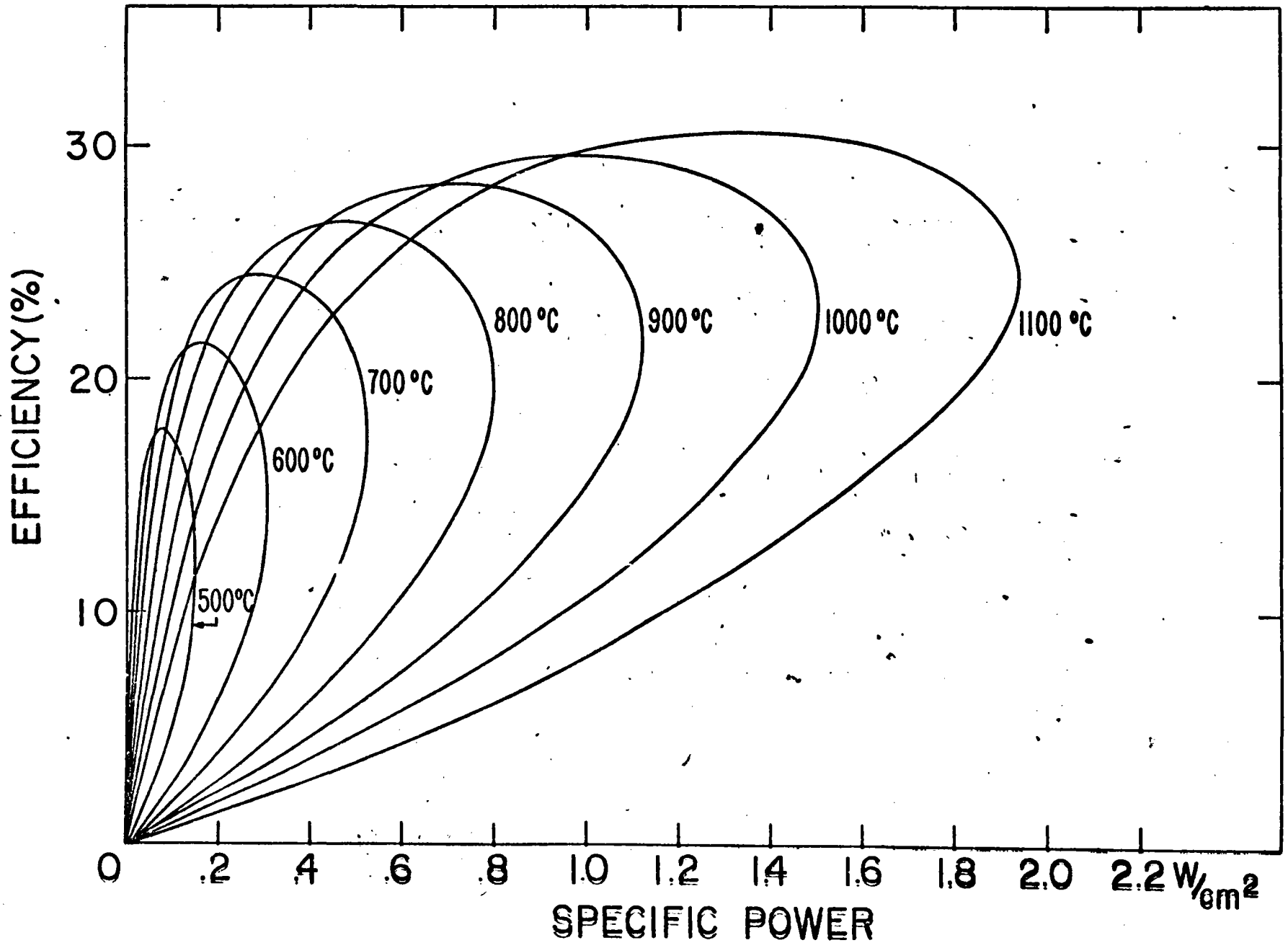
EFFICIENCY (%)
30
20
10
0
.2
.4
.6
.8
1.0
1.2
1.4
1.6
1.8
2.0
2.2 W/cm²
SPECIFIC POWER
500°C
600°C
700°C
800°C
900°C
1000°C
1100°C

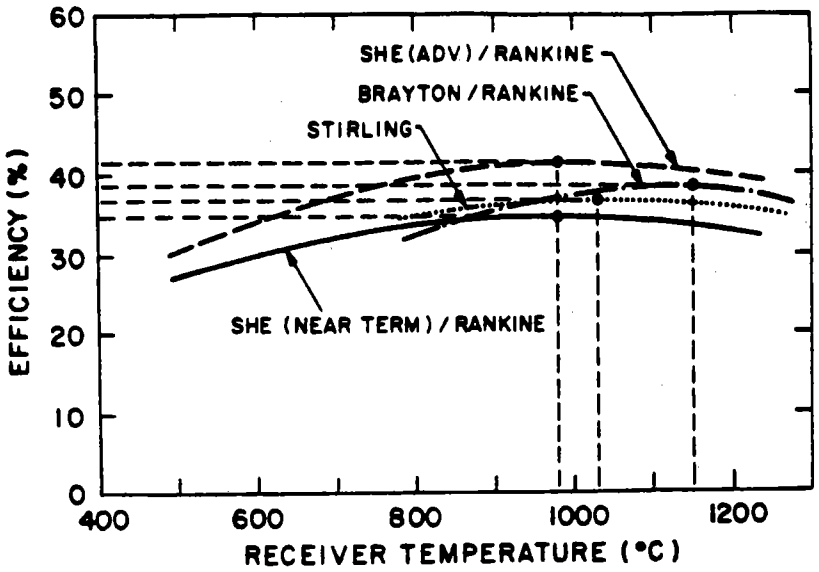
SHE(ADV)/RANKINE
BRAYTON/RANKINE
STIRLING
SHE (NEAR TERM)/RANKINE
EFFICIENCY (%)
RECEIVER TEMPERATURE (°C)
0
10
20
30
40
50
60
400
600
800
1000
1200

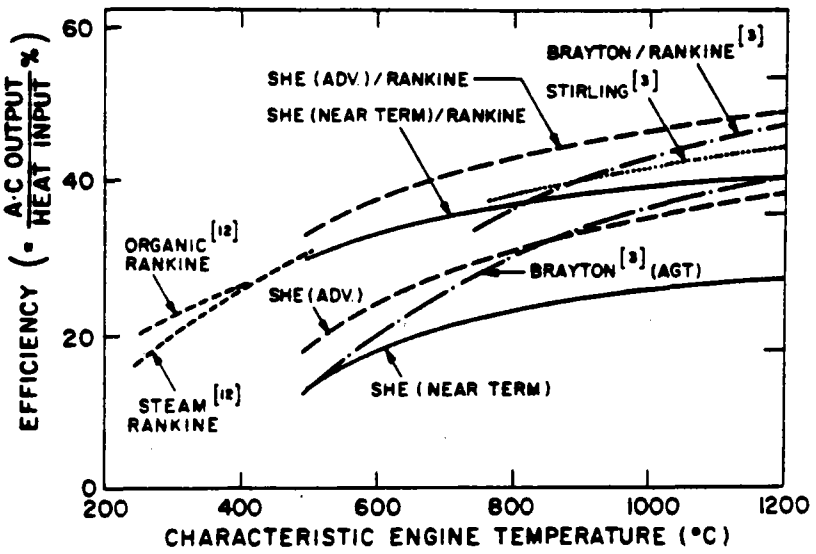
BRAYTON/RANKINE [3]
SHE (ADV.)/RANKINE
STIRLING [3]
SHE (NEAR TERM)/RANKINE
ORGANIC RANKINE [12]
BRAYTON [3] (AGT)
SHE (ADV.)
STEAM RANKINE [12]
SHE (NEAR TERM)
EFFICIENCY (= A·C OUTPUT / HEAT INPUT %)
CHARACTERISTIC ENGINE TEMPERATURE (°C)
0
20
40
60
200
400
600
800
1000
1200

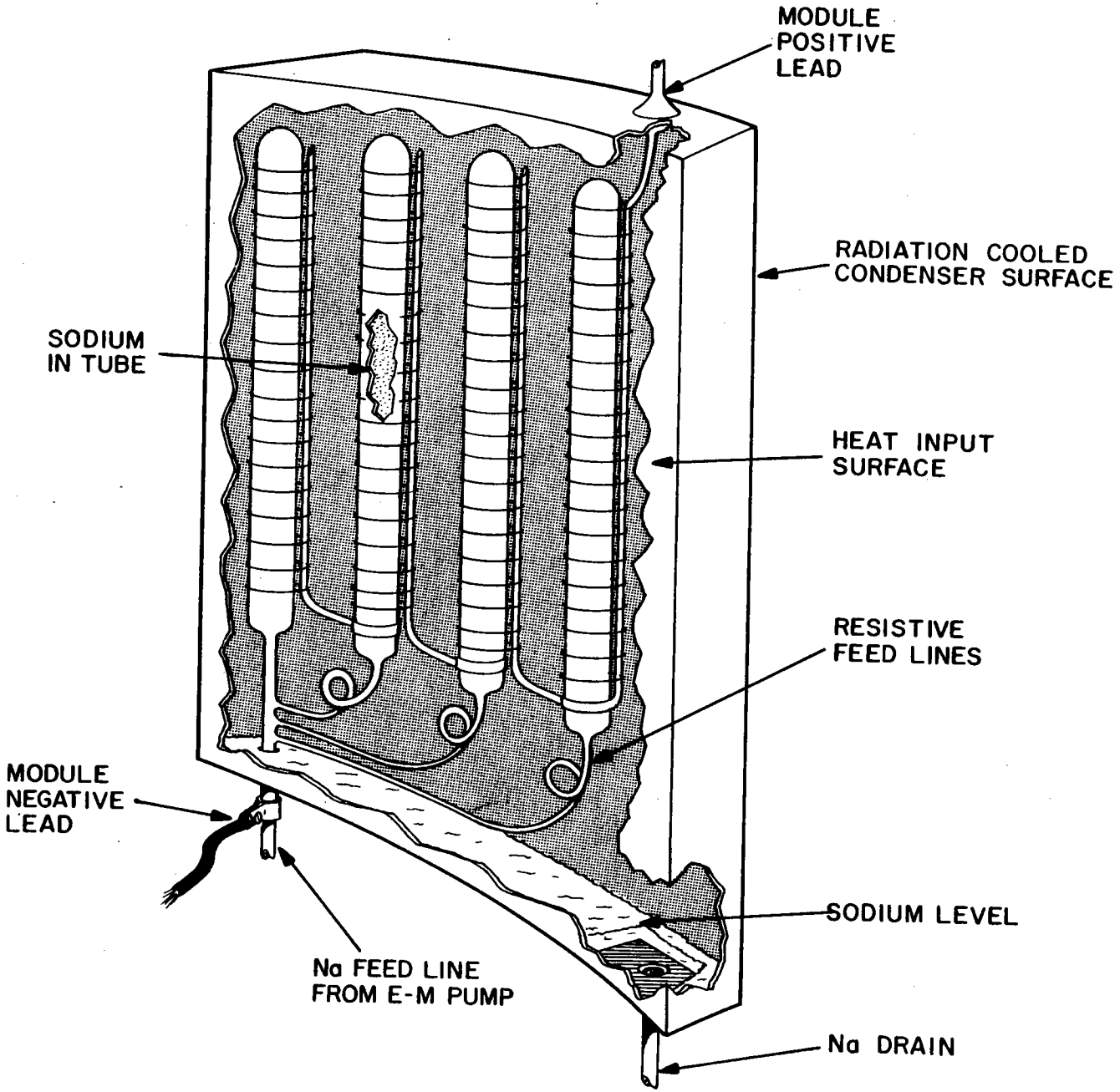
MODULE
POSITIVE
LEAD
RADIATION COOLED
CONDENSER SURFACE
SODIUM
IN TUBE
HEAT INPUT
SURFACE
RESISTIVE
FEED LINES
MODULE
NEGATIVE
LEAD
SODIUM LEVEL
Na FEED LINE
FROM E-M PUMP
Na DRAIN

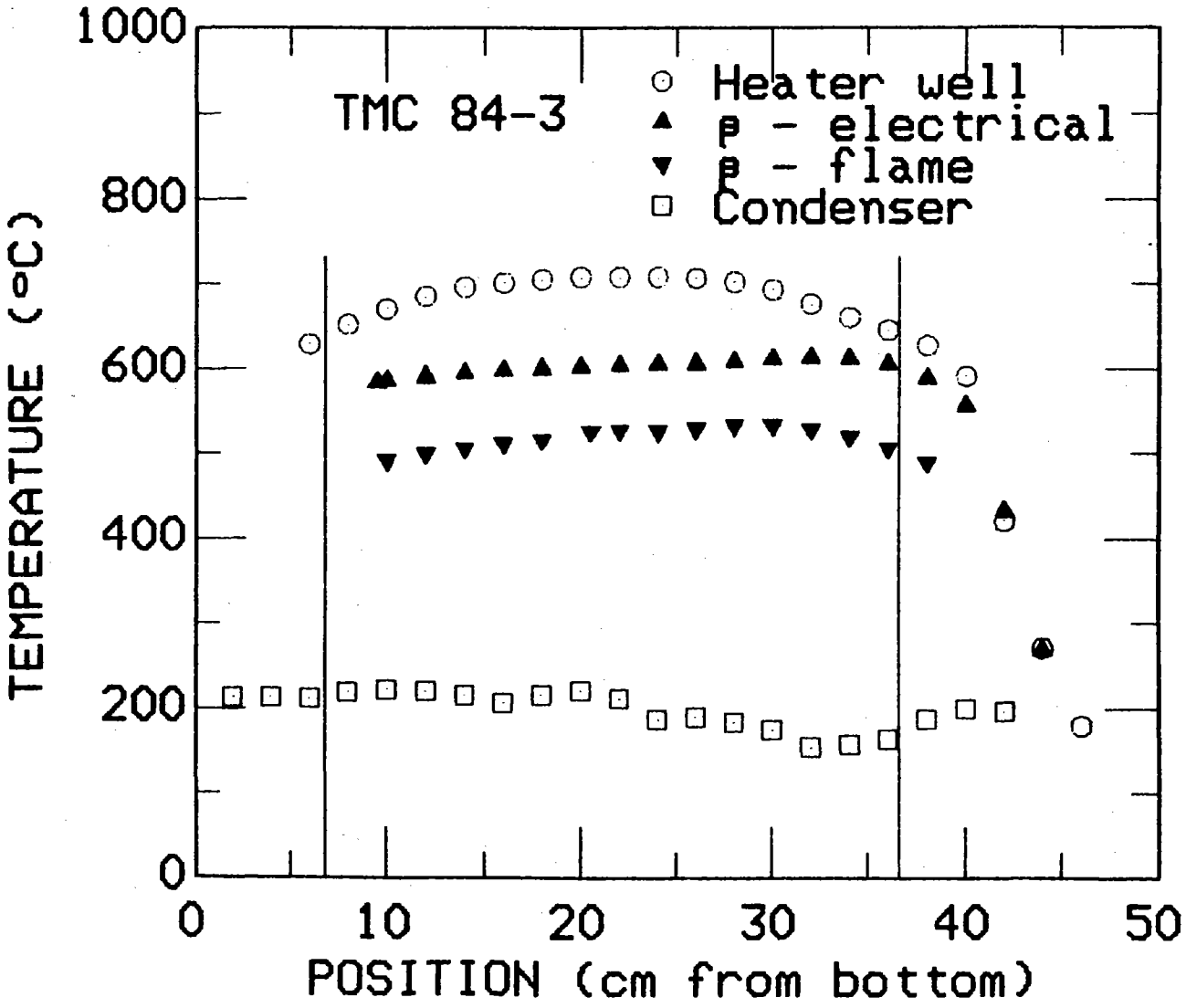
TMC 84-3
Heater well
β - electrical
β - flame
Condenser
TEMPERATURE (°C)
1000
800
600
400
200
0
0
10
20
30
40
50
POSITION (cm from bottom)

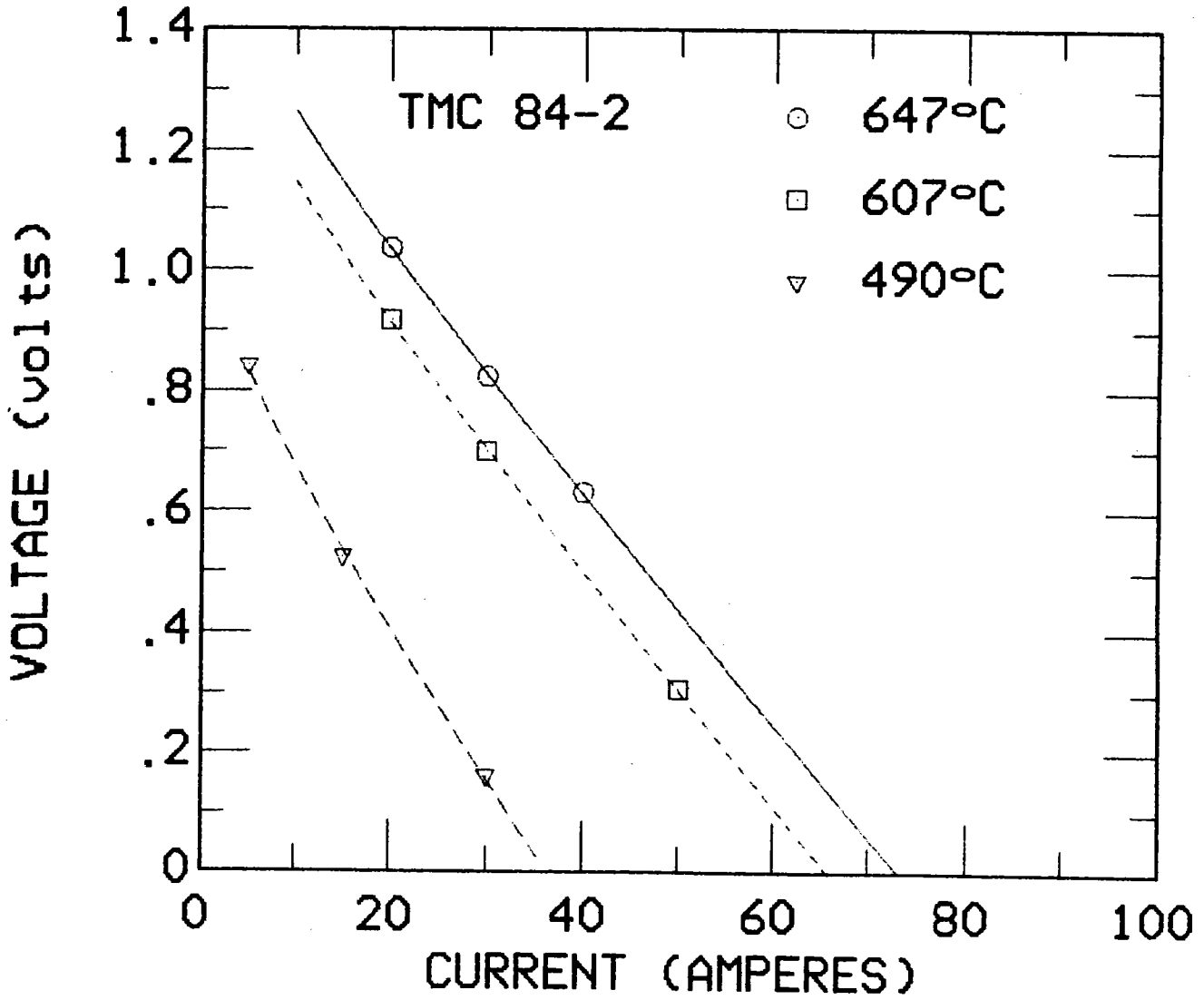
TMC 84-2
647°C
607°C
490°C
VOLTAGE (volts)
1.4
1.2
1.0
.8
.6
.4
.2
0
0
20
40
60
80
100
CURRENT (AMPERES)

SOLAR THERMIONIC ENERGY CONVERSION

Dave Lieb and Gabor Miskolczy
Thermo Electron Corporation

SOLAR THERMIONIC ENERGY CONVERSION

BACKGROUND

Thermionic energy converters are remarkably simple and environmentally clean devices for converting heat to electricity. A metal electrode, the emitter, is heated until electrons "boil" from its surface. The emitted electrons cross a narrow interelectrode gap and "condense" on the collector. This flow of electrons constitutes an electric current that delivers power to a load.

Research into this technology conducted over a number of years has led both to greatly increased understanding of the underlying physics of this phenomenon and to practical electricity-producing devices which proved themselves suitable for astronautical applications.

By the year 1980 the technology of building thermionic converters with silicon-carbide tungsten emitter hot shells, manufactured by chemical vapor deposition, was sufficiently advanced to result in a life test of 5,000 hours at an emitter temperature of 1650 K. In the same year, another life test began which culminated in 12,500 hours in 1982. This test was run at an emitter temperature of 1730 K. Thus, both the longevity of the converters and the operating temperature of the emitters were increased throughout the program.

The barrier index achieved by these first generation devices has also been improved, to the point where values as low as 2.1 eV are routinely obtained and values even below 2.0 eV are sometimes observed.

These achievements were largely realized because of significant advances in chemical vapor deposition (CVD) technology for the fabrication of such converters. A technique was developed to make a composite hot shell and emitter structure consisting of a unique combination of a CVD tungsten emitter protected by a CVD silicon carbide envelope, with a graphite interlayer. During the demonstrated operating life of 12,500 hours at an emitter temperature of 1730 K, no life-limiting interactions were revealed (i.e., by post test examination). These CVD structures also have shown excellent thermal shock resistance, surviving quenching from 1800 K by both liquid nitrogen and water.

Thermionic converters are not highly efficient electricity generators compared to conventional methods of generation, such as fossil fuel or nuclear power stations. Today's converters have electrical efficiencies a little above ten percent, with efficiencies of approximately twice that amount believed achievable by fully mature technology. By contrast, conventional and other developmental technologies for power generation typically are 30- to 40-percent efficient. For this reason, thermionic conversion is not attractive as a stand-alone system for power generation.

However, perhaps the key fact about thermionic converters is their ability to reject their waste energy at temperatures high enough to be useful as inputs to other generating technologies (i.e., in so-called "topping" applications) or directly to industrial processes (i.e., in cogeneration applications). Thus, by designing thermionic modules to serve as initial stages in cogeneration or power generation systems, highly efficient and economical systems can potentially be developed. The converter cost is approximately 200$/kW.

SOLAR EXPERIMENT

A one-inch CVD converter was solar tested in 1981 in a central receiver heliostat array at the Advanced Components Test Facility at the Georgia Institue of Technology. The test examined heat flux cycling, control of the operating point, and mounting arrangements. The converter was mounted directly in the solar image with no cavity. The input heat flux was 40-60 W/cm^2. The converter performance was comparable to combustion measurements made on the same diode. Thermal cycling caused no problems with converter operation. The converter showed no degradation after the test.

The converter proved to be easy to control during solar heating. The temperatures of the emitter, collector flange, and reservoir were stable. These temperatures were easily varied within their operating range while optimizing the converter performance. Rapid thermal cycling (by closing the shutters or by passing clouds) caused no problems. The converter returned to its operating point after each cycle.

The maximum emitter temperature that could be reached in this test was about 1400 K. This limitation restricted the amount of converter testing that could be done. Solar-heated converter performance at emitter temperatures up to 1800 K should be evaluated. The limited emitter temperature was caused by two solvable problems: 1) too low a maximum heat flux and 2) no solar cavity. The heat flux levels were back to normal at the ACTF shortly after the test. A solar cavity would most likely be utilized in any further thermionic testing. The CVD converter showed no signs of degradation after the test. Future tests with high heat flux levels and adequate solar cavities should lead to higher operating temperatures and more efficient thermionic performance.

THERMIONIC CONVERSION

- NO MOVING PARTS
- HIGH TEMPERATURE OPERATION IN AIR (1750 K)
- HIGH HEAT FLUX CAPABILITY (240 W/CM^2)
- HIGH POWER DENSITY (>10 W/CM^3)
- HIGH HEAT REJECTION TEMPERATURE, SUITABLE FOR TOPPING (1000 K)
- DEMONSTRATED LONG OPERATING LIFE (>12,000 HRS)
- THERMAL SHOCK RESISTANT

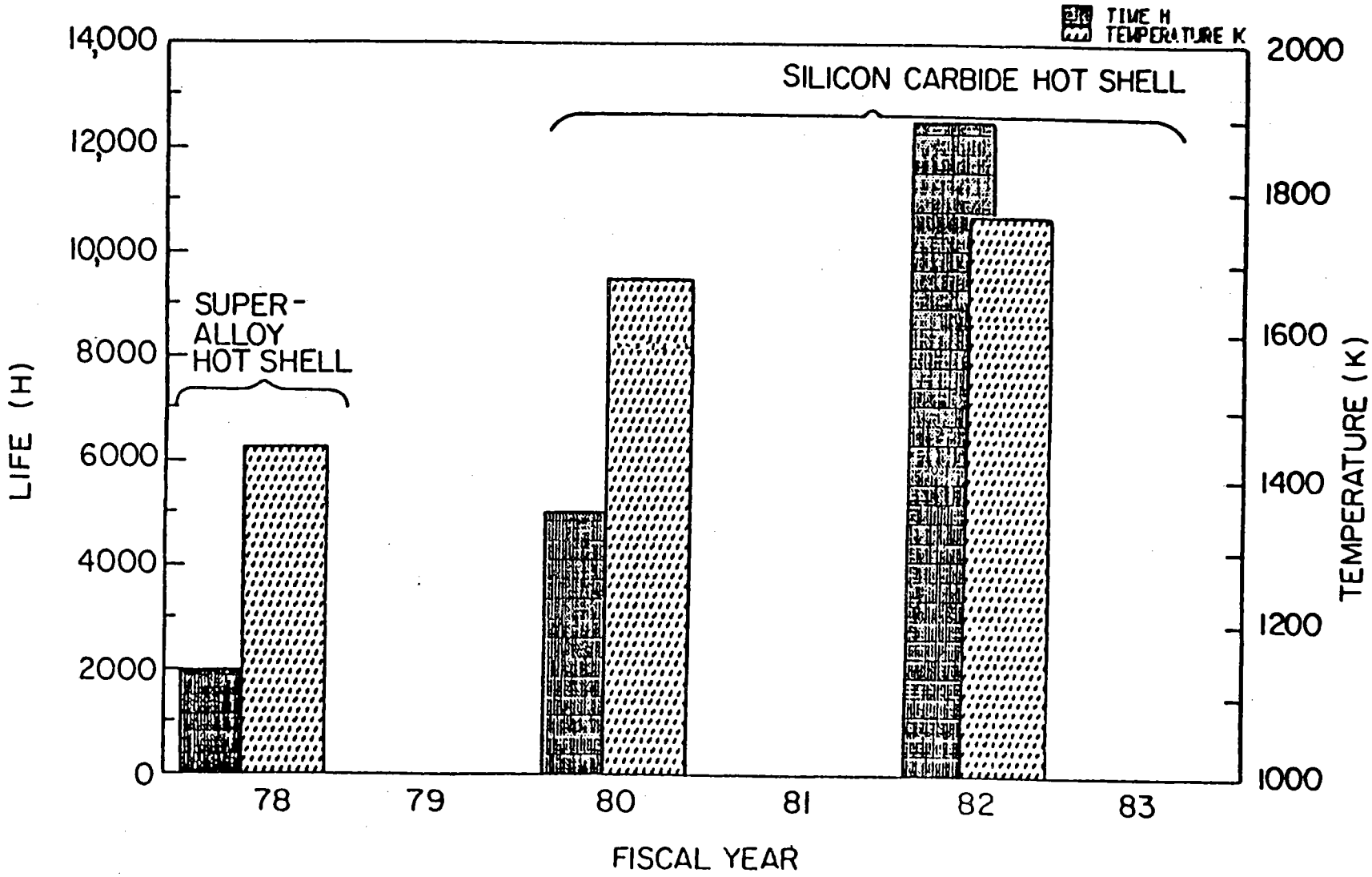

Exhibit A-1.1

Progress in Increasing Lifetime and Operating Temperatures of Flame-Heated Converters

THERMIONIC APPLICATIONS

- STEAM GENERATION TOPPING
  - HIGH HEAT FLUX INPUT
  - SYSTEM EFFICIENCY IMPROVED 20 POINTS
- ELECTROLYSIS PLANTS
  - HIGH CURRENT, LOW VOLTAGE D.C.POWER
  - THERMAL ENERGY FOR REACTION TEMPERATURE
- IRRIGATION OF REMOTE FIELDS
  - TOPPING OF ORGANIC RANKINE
  - D.C. POWER FOR PUMPS

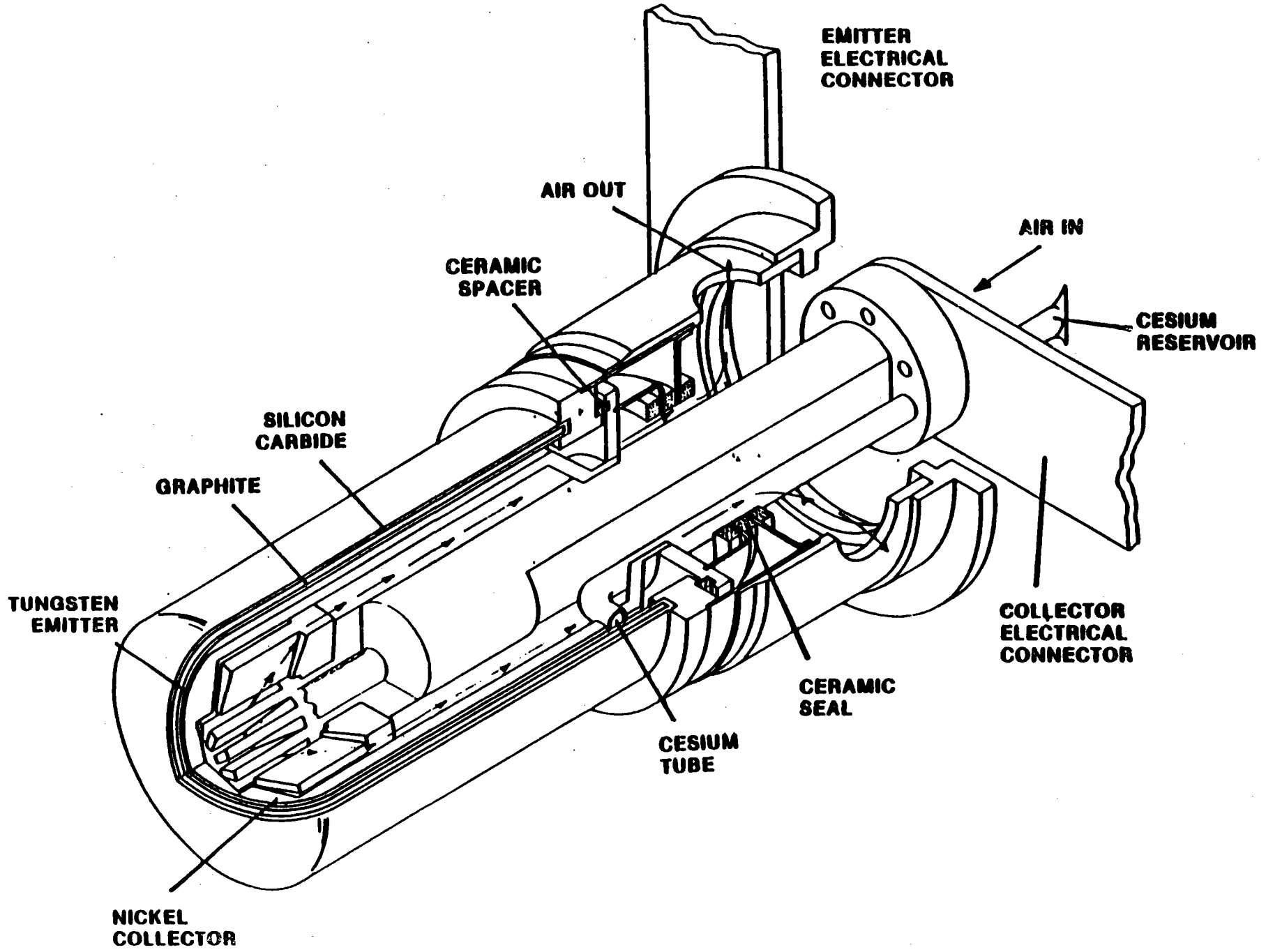

Two-Inch Torispherical Design, CVD Hot Shell

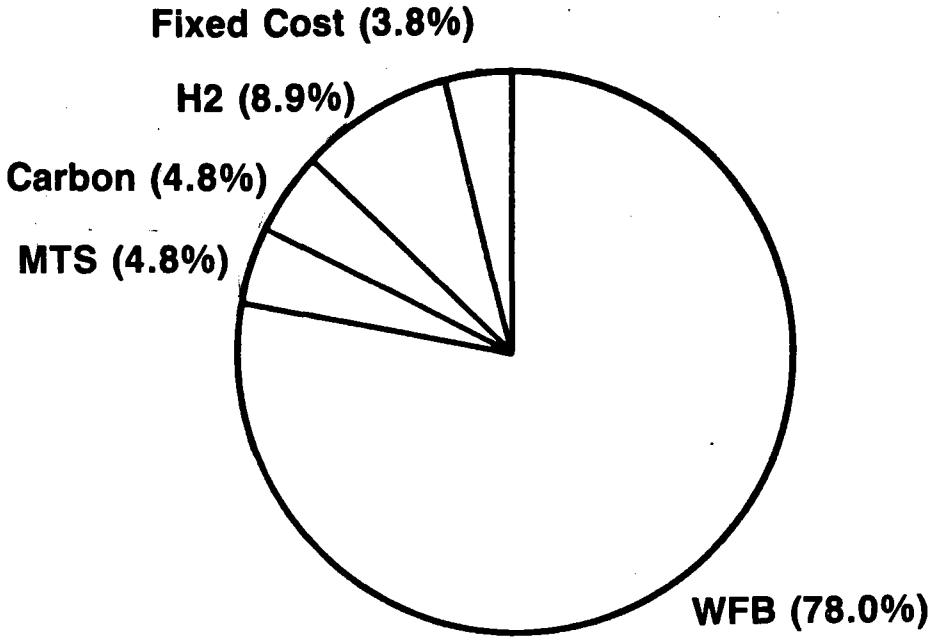

(A) EMITTER SUBASSEMBLY

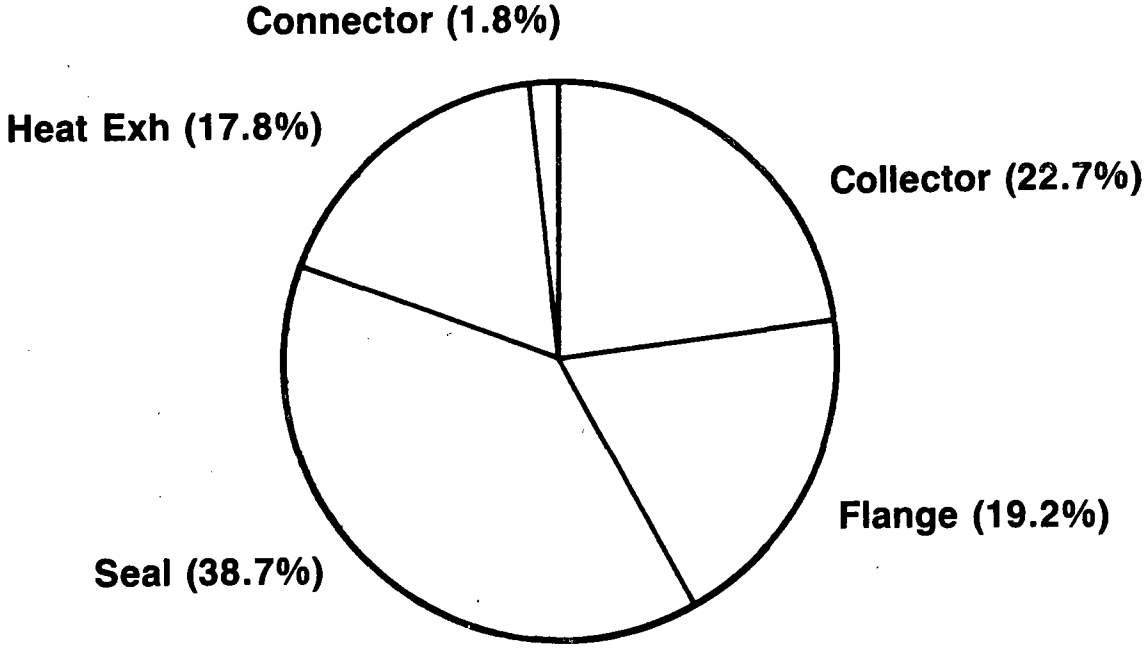

(B) COLLECTOR SUBASSEMBLY

8411-5

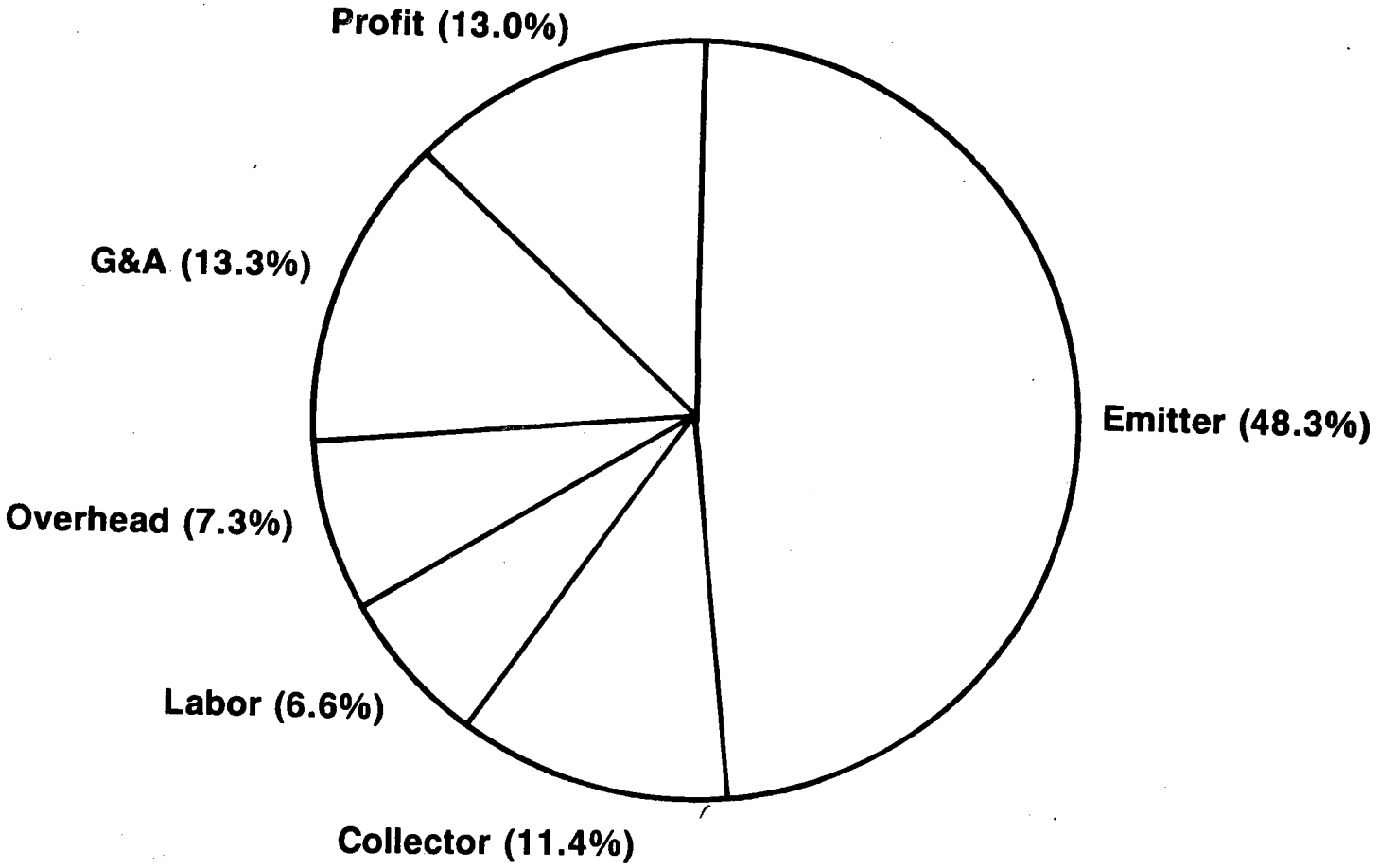
Profit (13.0%)
G&A (13.3%)
Emitter (48.3%)
Overhead (7.3%)
Labor (6.6%)
Collector (11.4%)

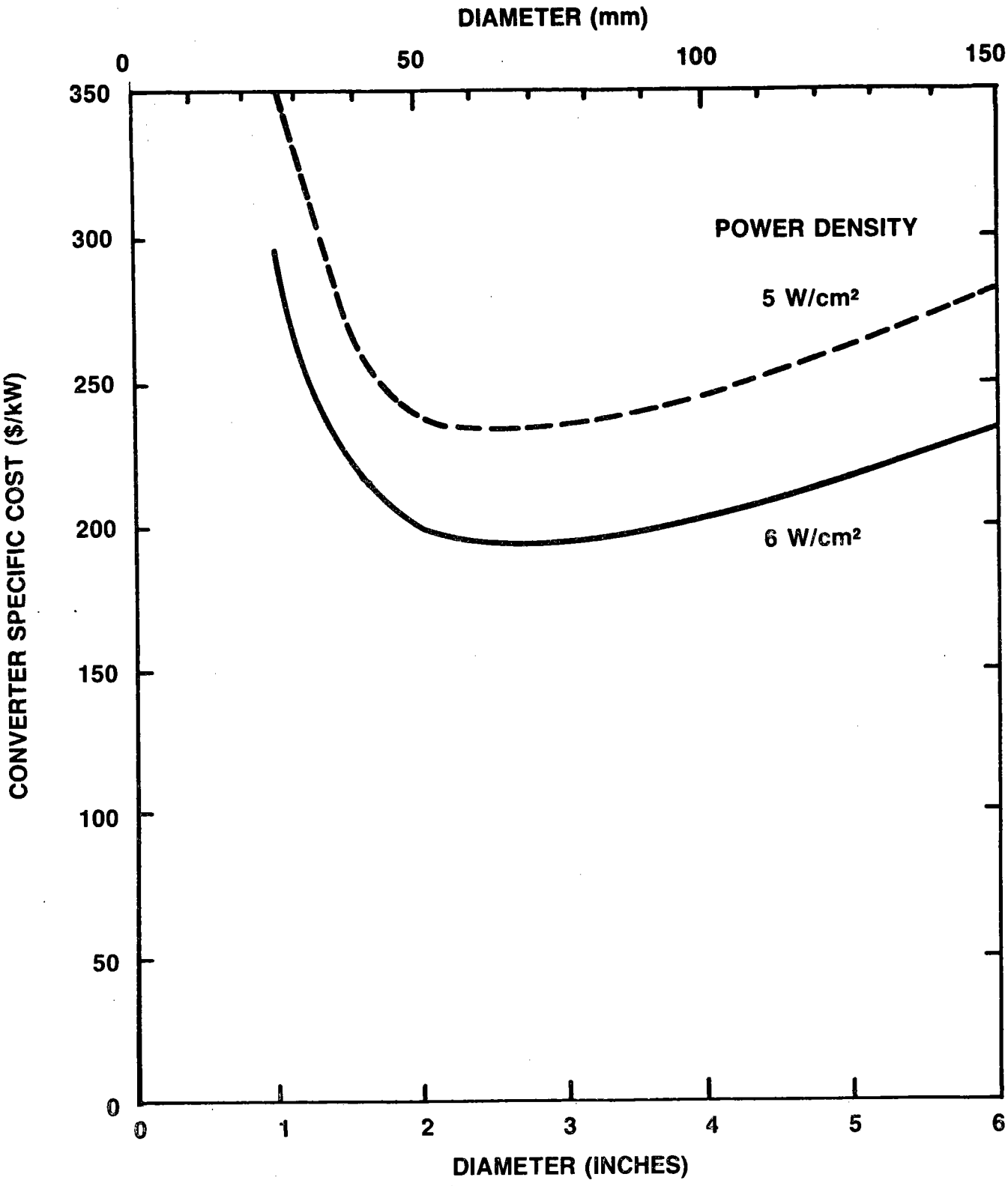
DIAMETER (mm)
0
50
100
150
350
300
250
200
150
100
50
0
CONVERTER SPECIFIC COST ($/kW)
POWER DENSITY
5 W/cm²
6 W/cm²
0
1
2
3
4
5
6
DIAMETER (INCHES)

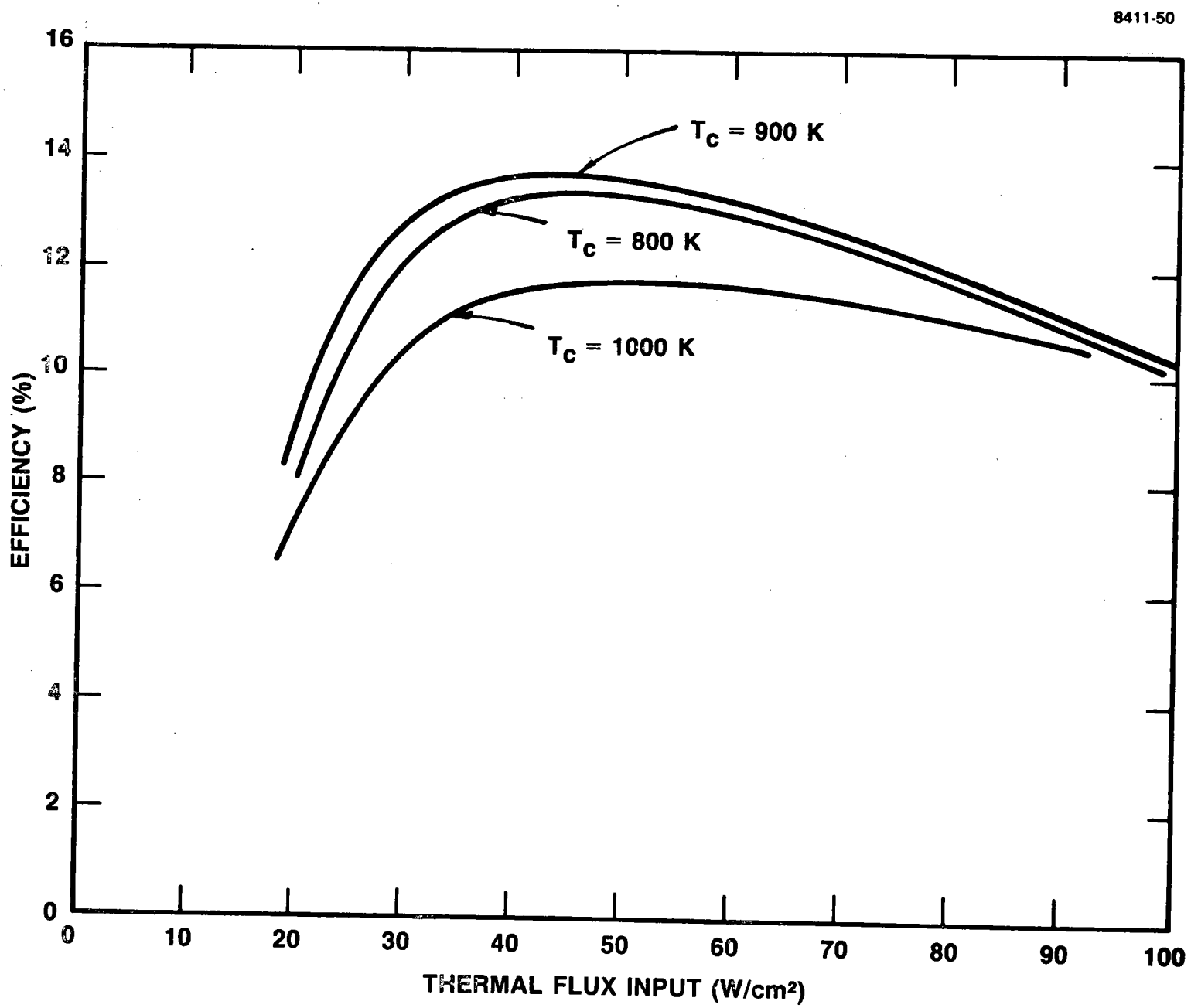
8411-50
16
14
12
10
8
6
4
2
0
EFFICIENCY (%)
T_c = 900 K
T_c = 800 K
T_c = 1000 K
0
10
20
30
40
50
60
70
80
90
100
THERMAL FLUX INPUT (W/cm²)

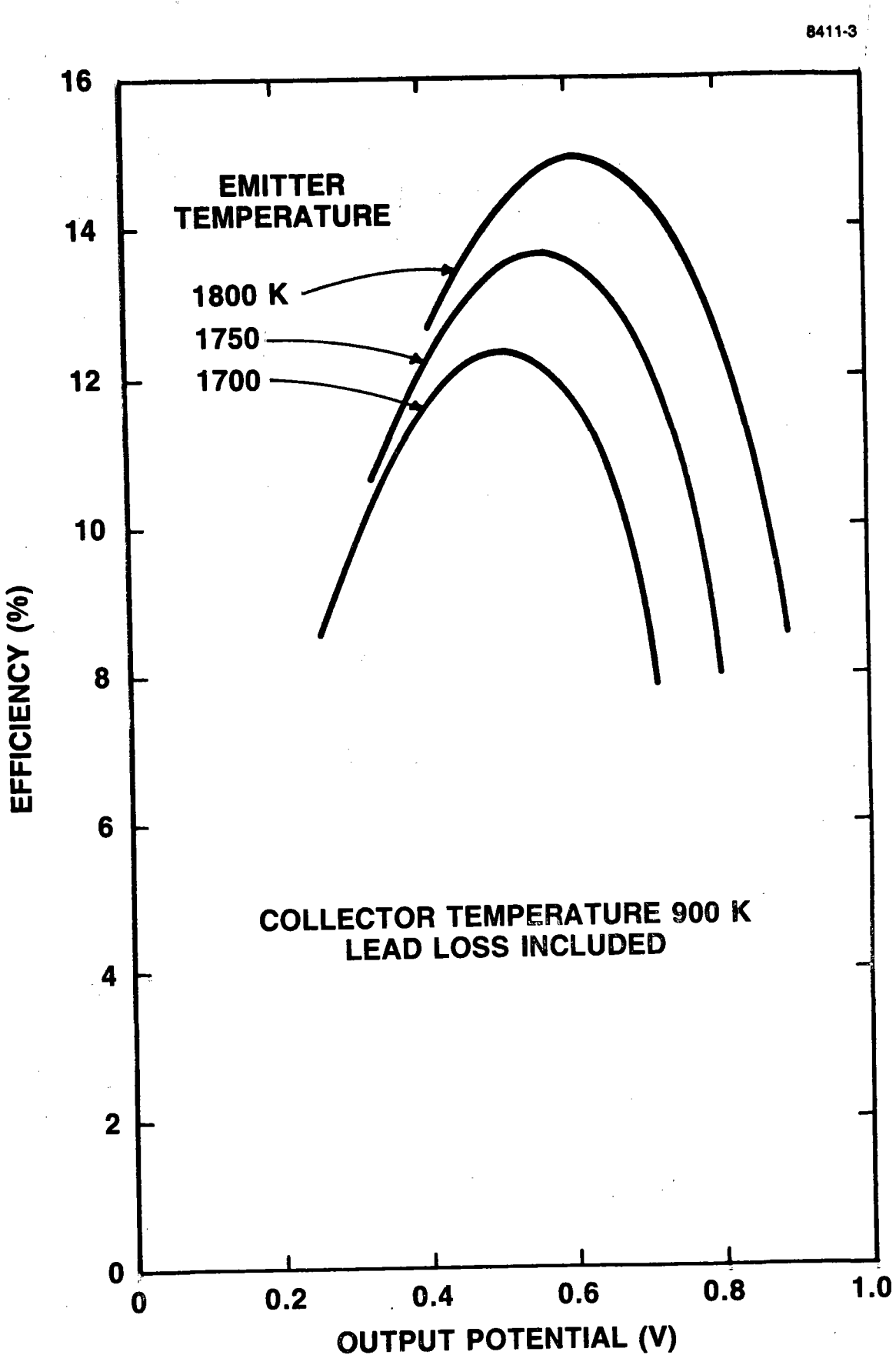
8411-3
16
14
12
10
8
6
4
2
0
EFFICIENCY (%)
EMITTER
TEMPERATURE
1800 K
1750
1700
COLLECTOR TEMPERATURE 900 K
LEAD LOSS INCLUDED
0
0.2
0.4
0.6
0.8
1.0
OUTPUT POTENTIAL (V)

SOLAR CONVERTER EXPERIMENTS

- OBJECTIVES
  1. SOLAR HEATING OF SiC CONVERTER
  2. EXAMINE CONTROL CHARACTERISTICS
  3. TEST CYCLING BEHAVIOR
  4. OPERATE CONVERTER WITH HIGH HEAT FLUX

- TEST FEATURES
  1. DIRECT SOLAR IMAGE (NO CAVITY)
  2. CALORIMETER FOR INCIDENT FLUX
  3. ELECTRICAL HEATING FOR RESERVOIR AND FLANGE
  4. AIR-COOLED COLLECTOR
  5. AC SWEEP AND DC I-V CHARACTERISTICS

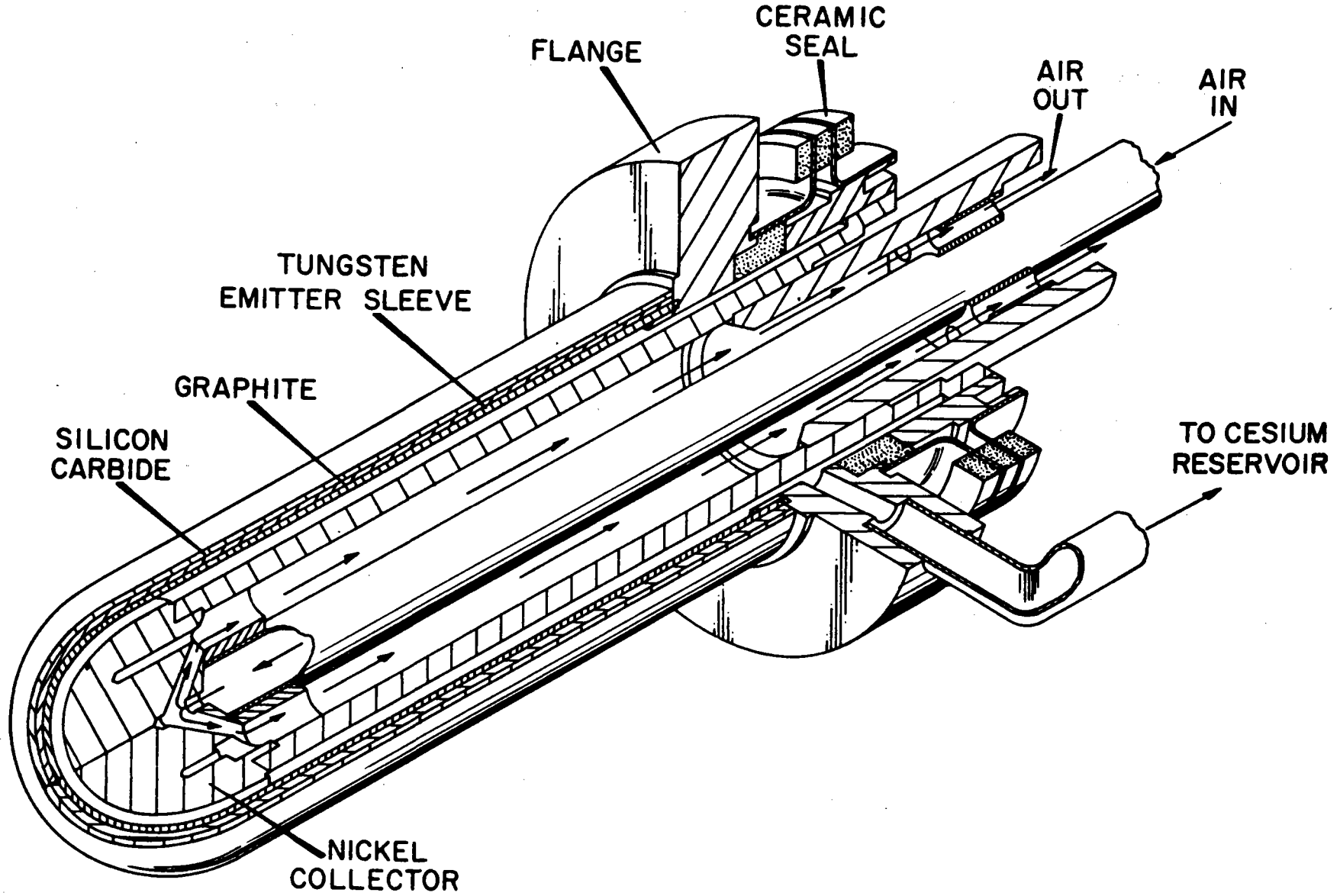

Figure III-1. Thermionic Converter with Composite CVD Hot Shell-Emitter (Silicon Carbide-Graphite-Tungsten)

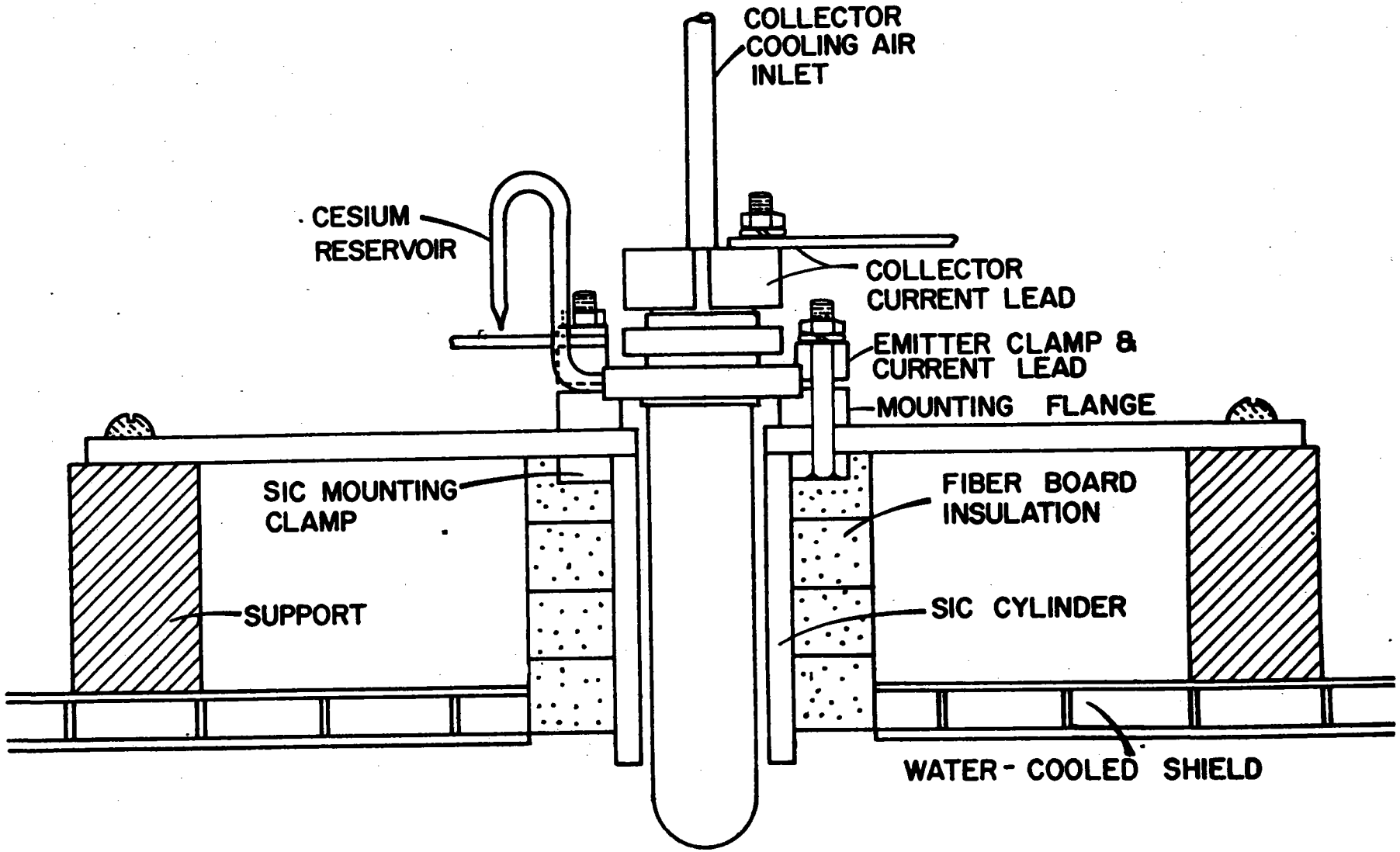

Figure IV-1. Mounting Fixture and Converter

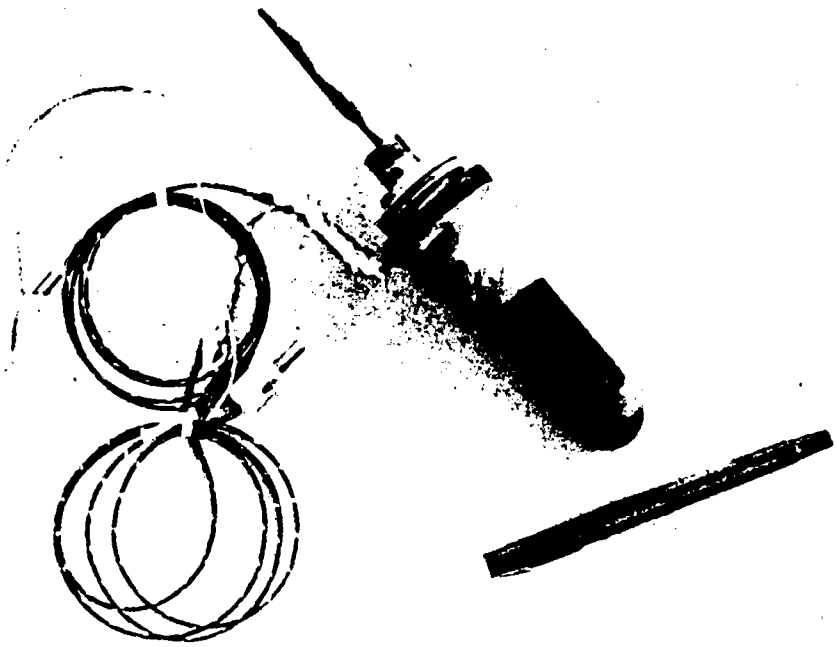

Figure III-2. Silicon Carbide Thermionic Converter

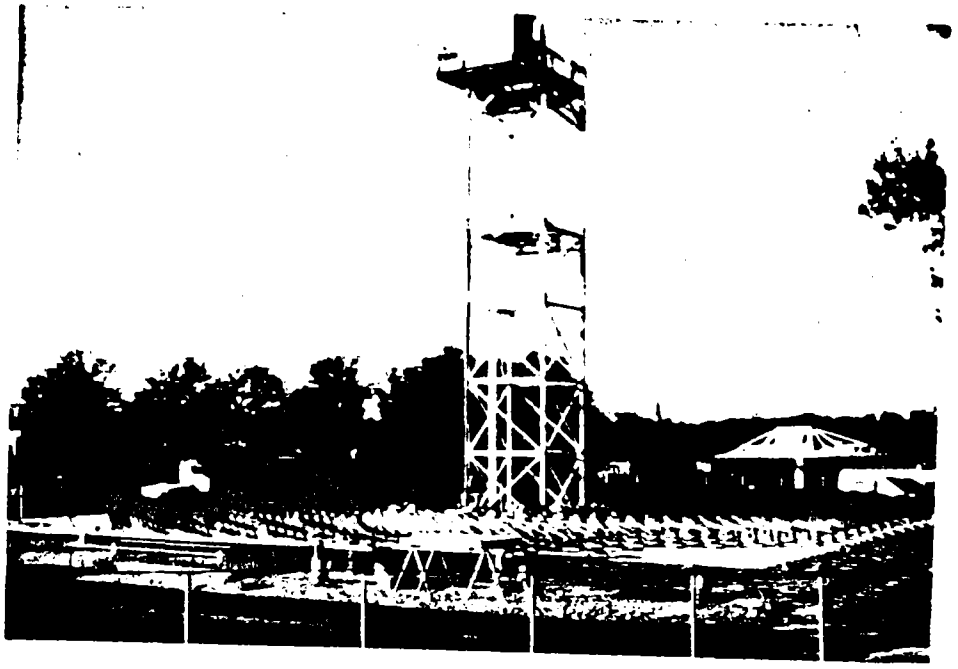

Figure II-1. Department of Energy Advanced Components Test Facility at the Georgia Institute of Technology

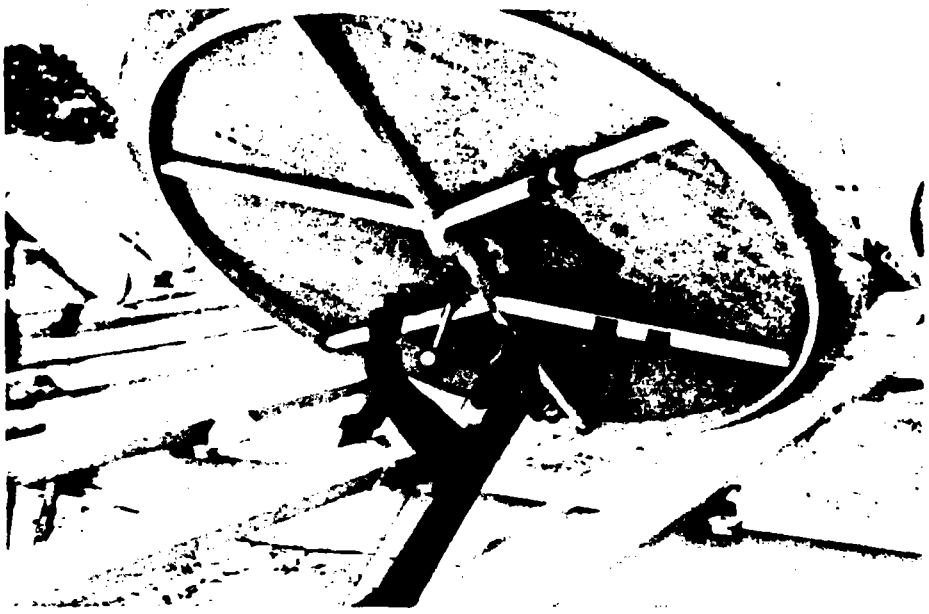

Figure II-5. Heliostat Detail

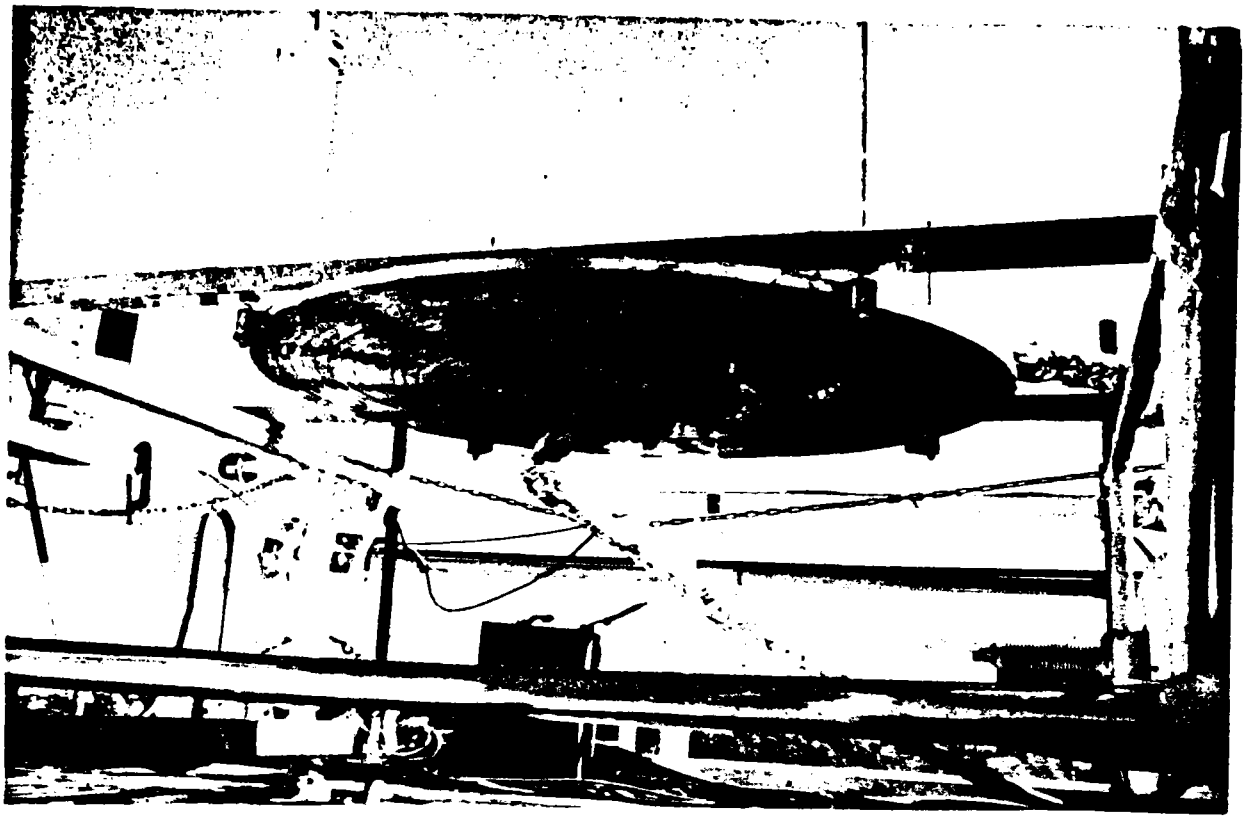

Figure IV-7. Adjustable Mount and Water-Cooled Shield on Solar Tower

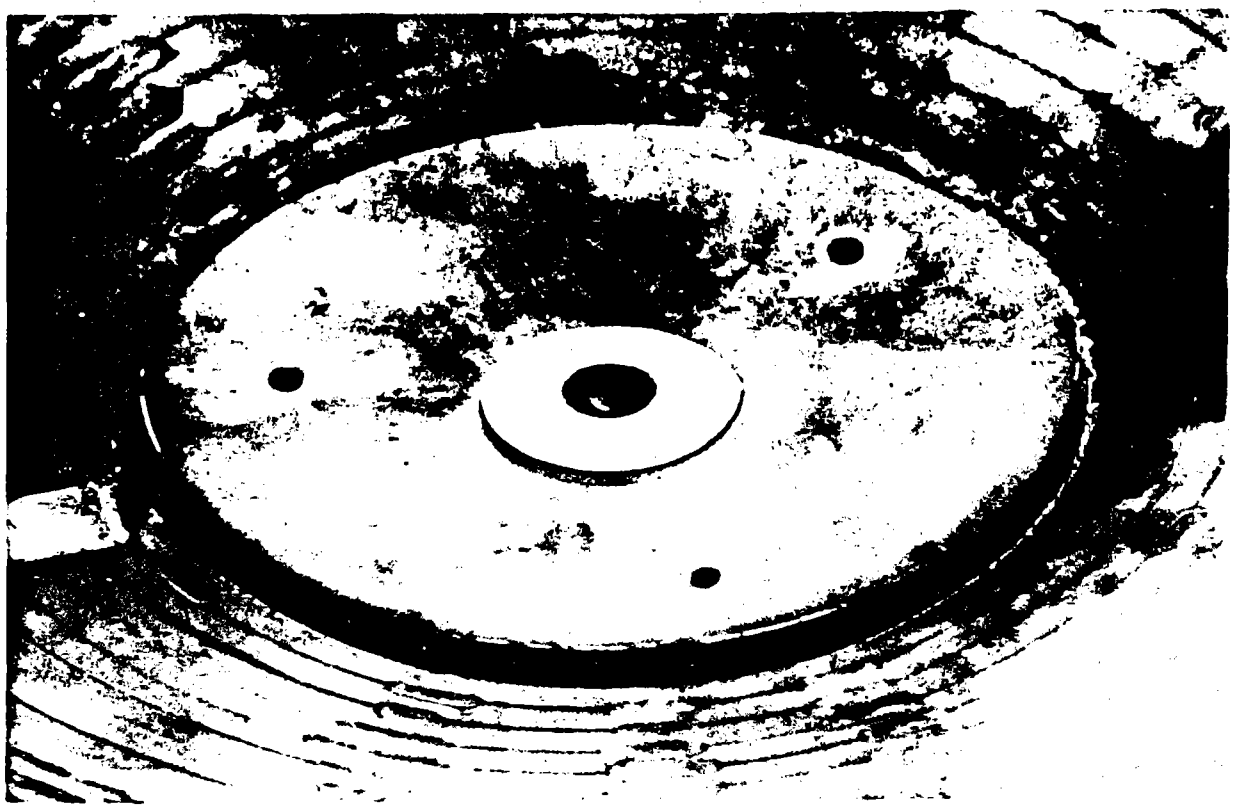

Figure IV-6. View from Beneath Water-Cooled Shield Showing Converter, Insulation, and Calorimeters

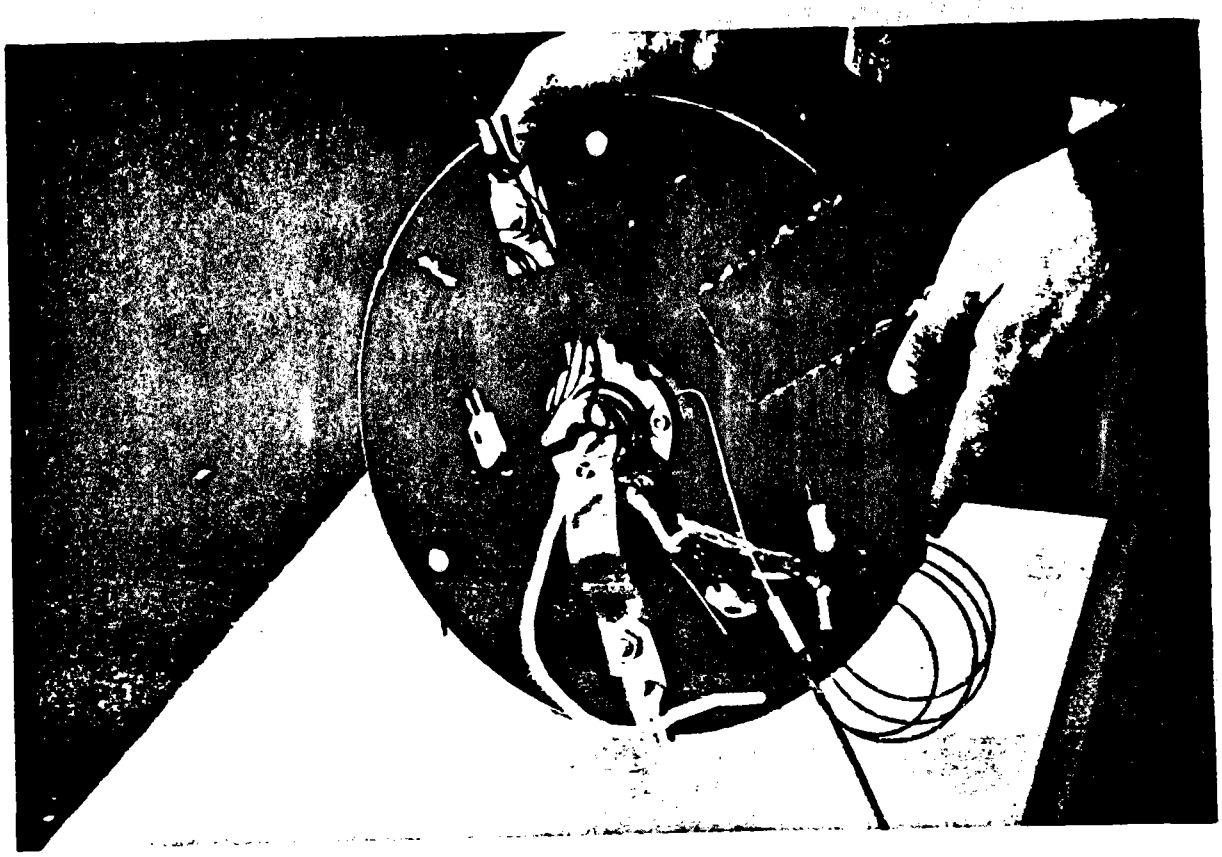

Figure IV-3. Solar Converter Fixture (Back Side)

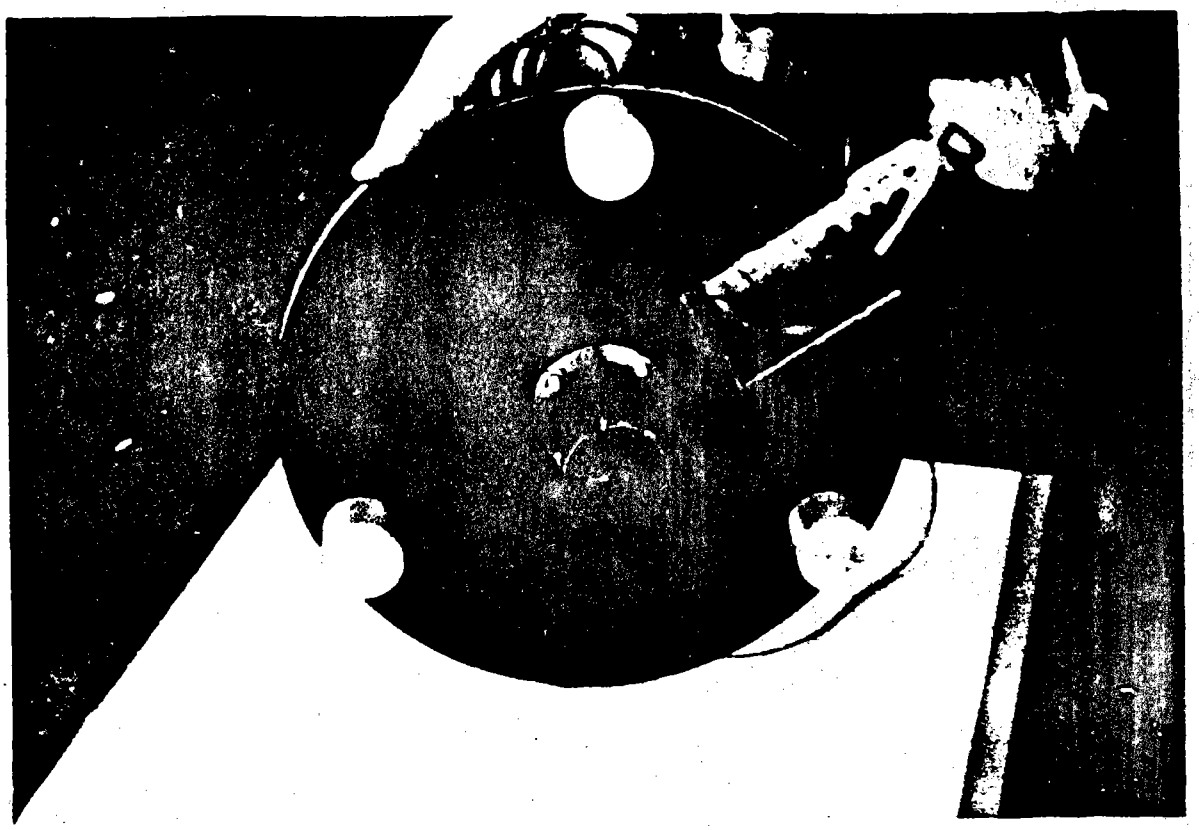

Figure IV-2. Solar Converter Fixture (Front Side)

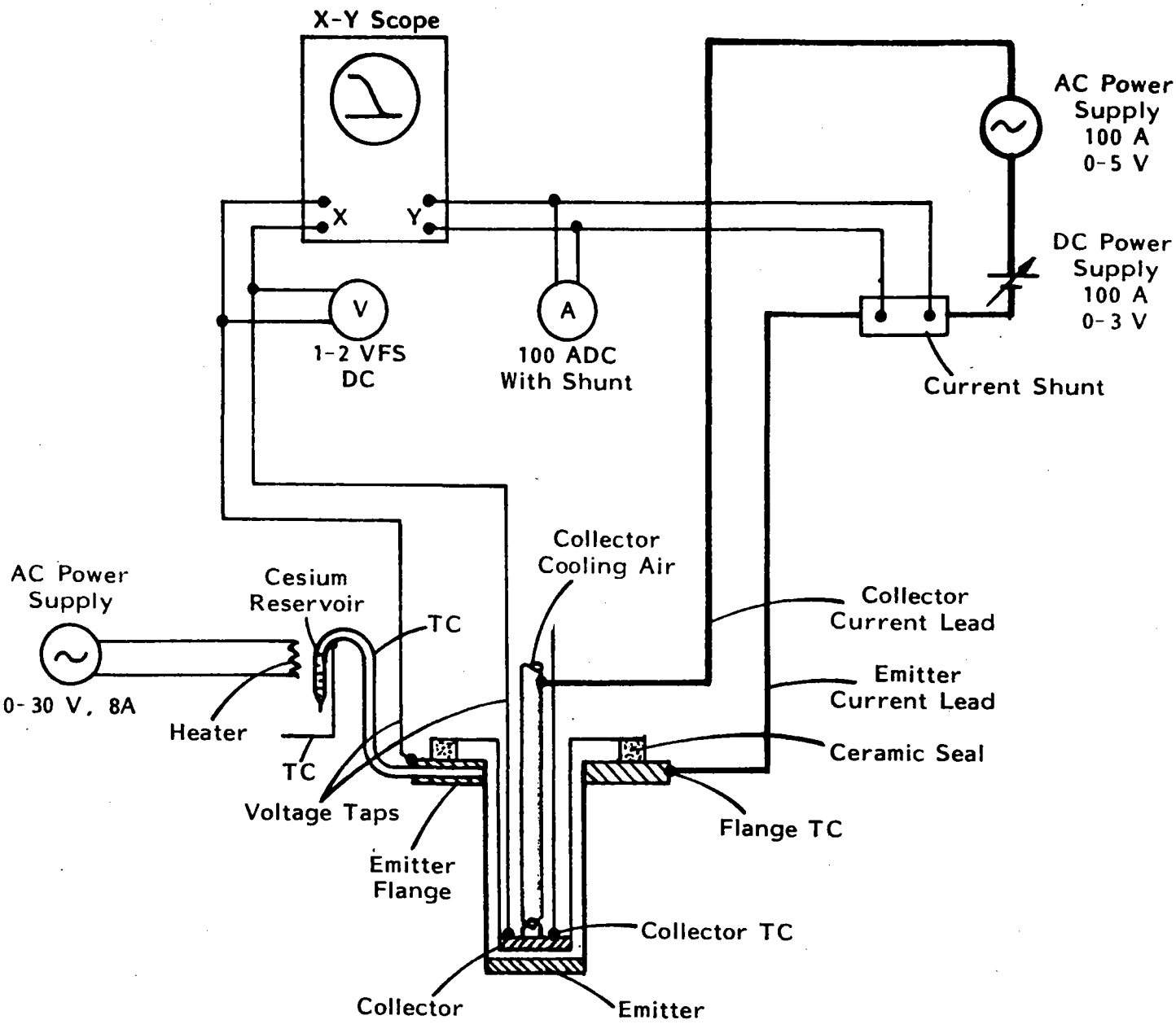

Note: All TC's Type K

Figure IV-5. Schematic Diagram of Converter Test

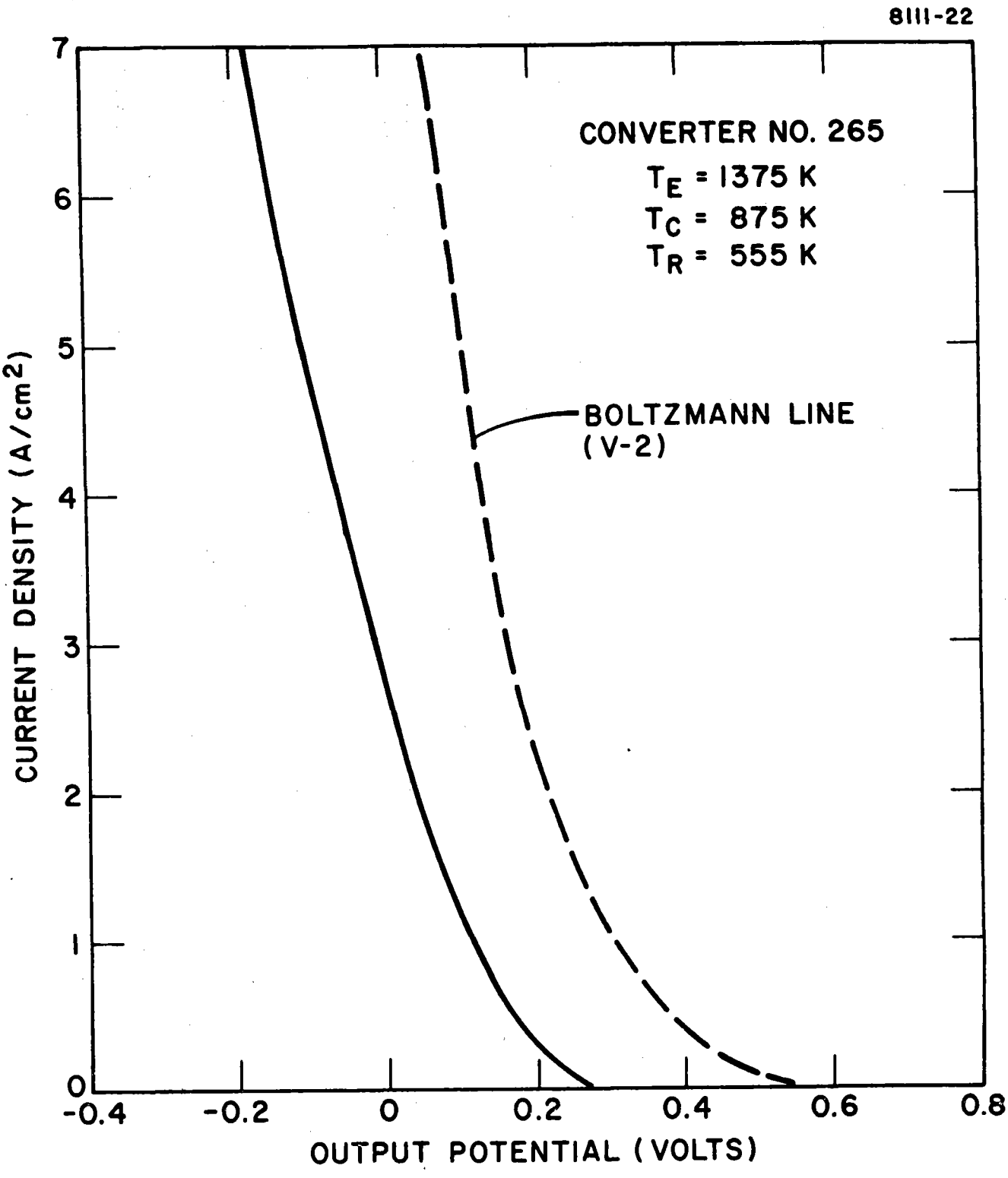

Figure V-1. Optimized Converter Performance AC Sweep

SOLAR TEST RESULTS

- RAPID CYCLING DUE TO CLOUDS CAUSED NO PROBLEMS
- HEAT FLUX INPUT MAXIMUM WAS 40-60 W/cm
- POWER OUTPUT 1.8 WATTS AT 1400 K
- HIGH TEMPERATURES REQUIRE CAVITY RECEIVER
- CONVERTER WITHSTOOD TEST WITH NO DEGRADATION

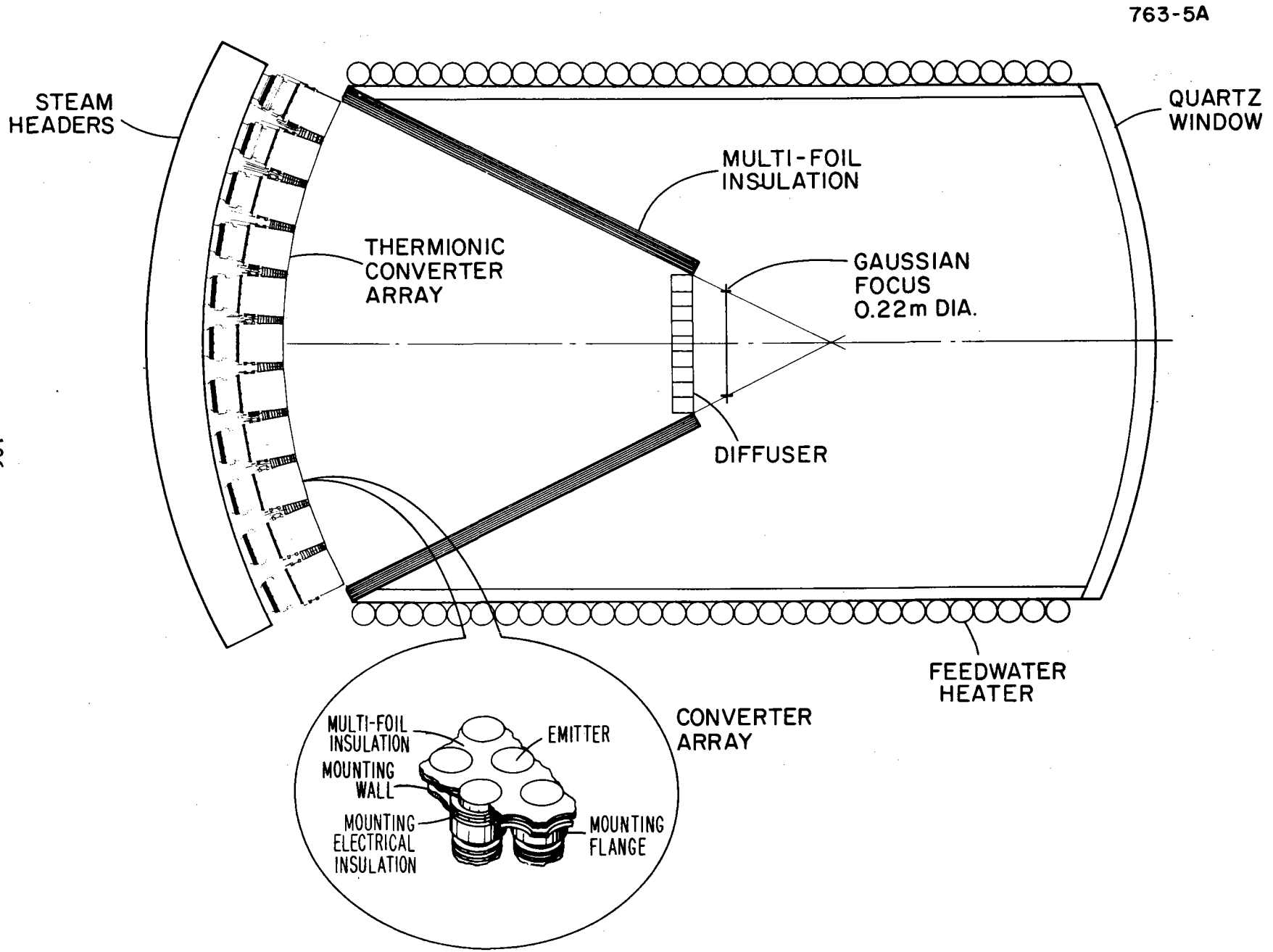
763-5A
STEAM HEADERS
QUARTZ WINDOW
MULTI-FOIL INSULATION
THERMIONIC CONVERTER ARRAY
GAUSSIAN FOCUS 0.22m DIA.
DIFFUSER
FEEDWATER HEATER
CONVERTER ARRAY
MULTI-FOIL INSULATION
EMITTER
MOUNTING WALL
MOUNTING ELECTRICAL INSULATION
MOUNTING FLANGE

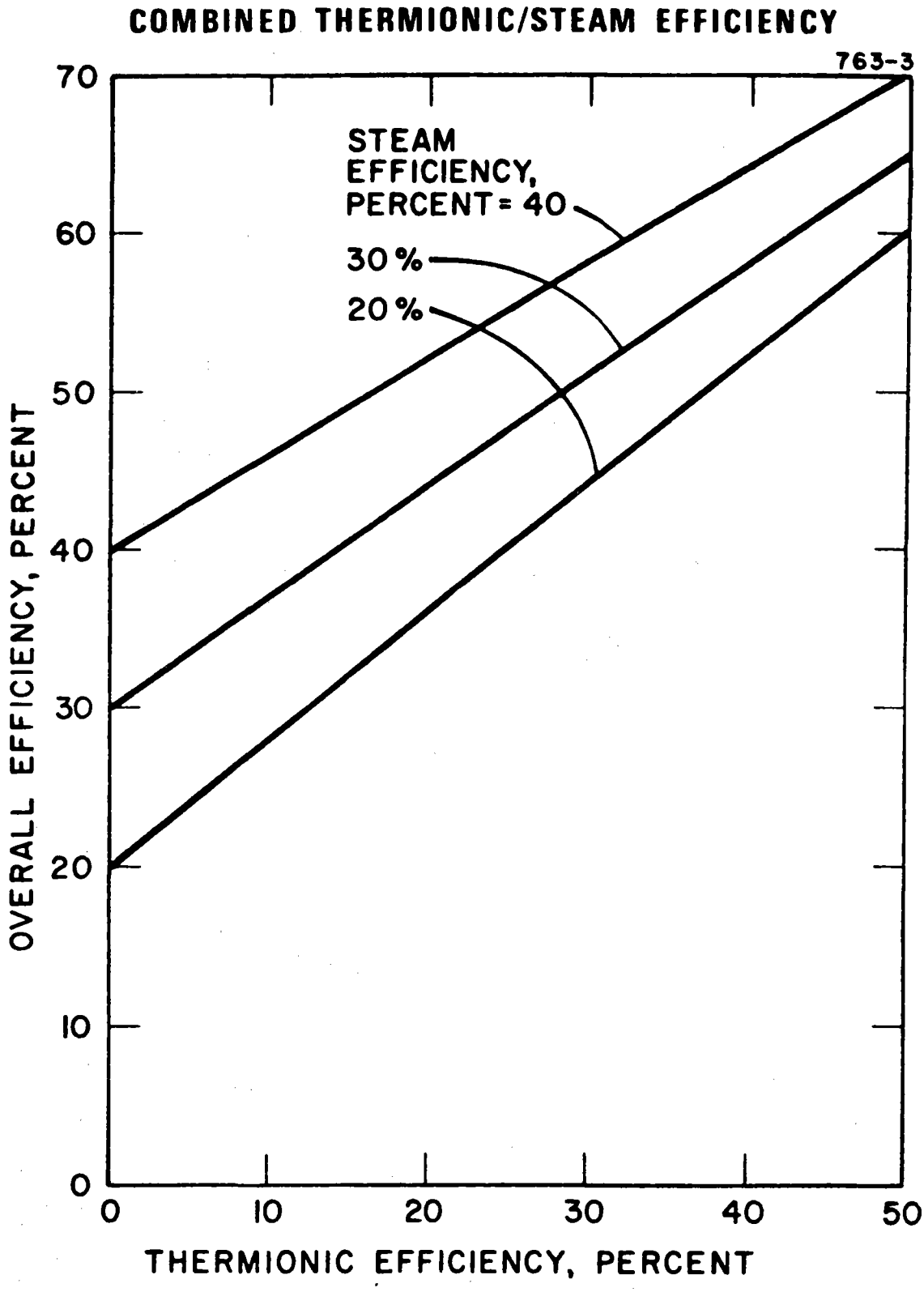

Figure II-1. Overall Efficiency of Combined Thermionic/Steam Cycle

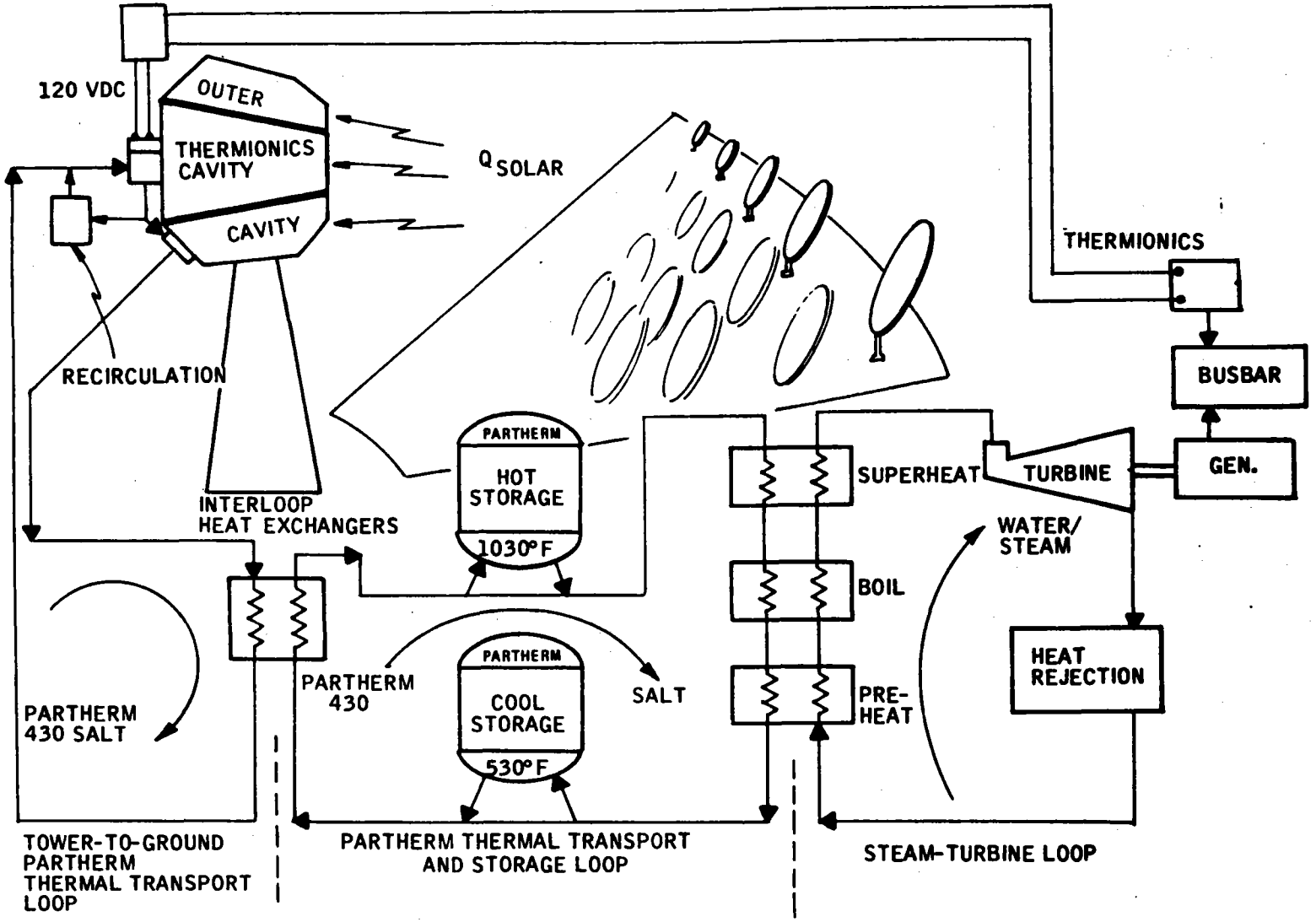

Figure 2-7. Commercial Plant Concept

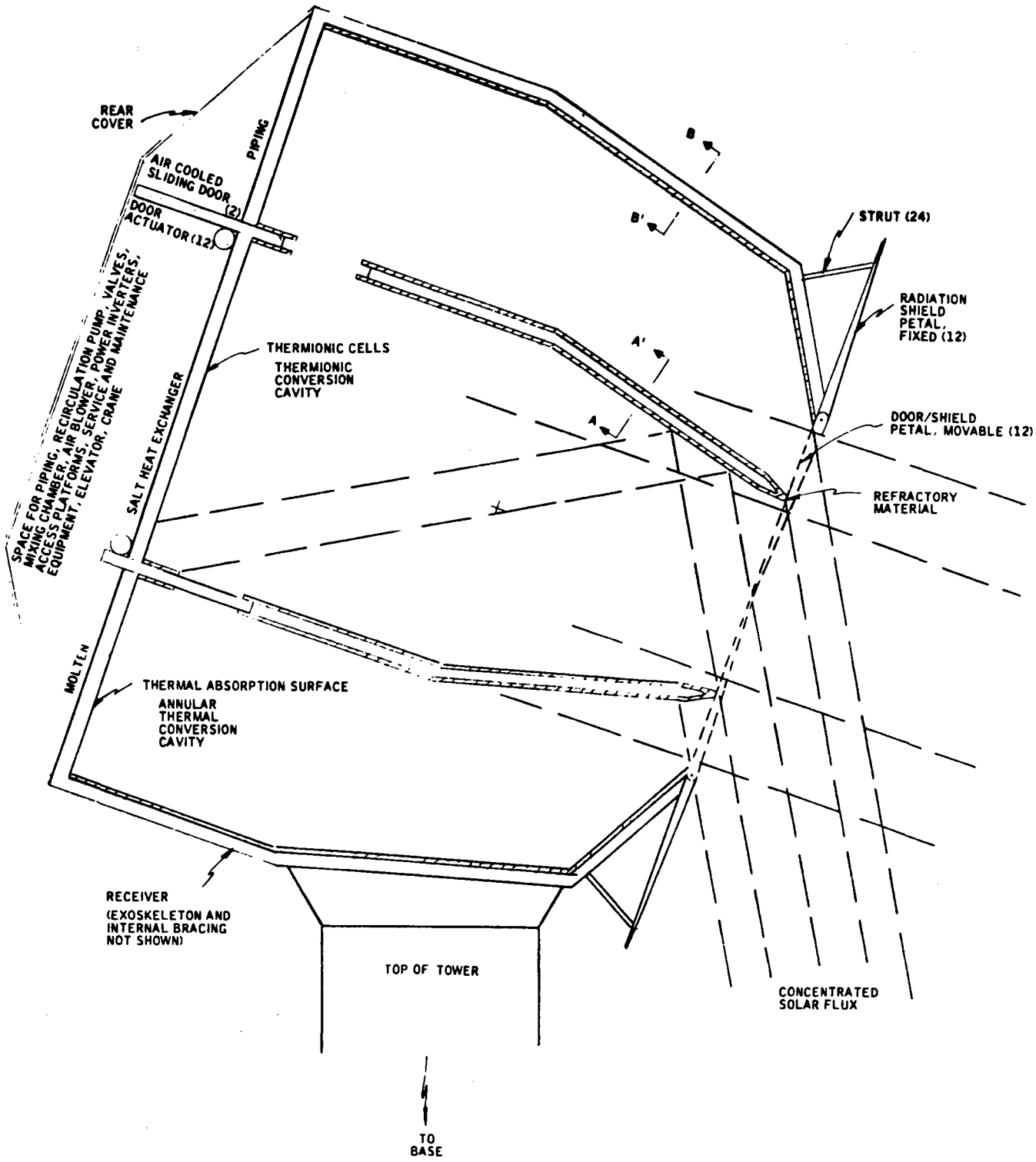

Figure 2-17. The Receiver Atop the Tower

41057-1

HIGH TEMPERATURE THERMOELECTRIC CONVERSION

Charles Wood
Jet Propulsion Laboratory

HIGH-TEMPERATURE THERMOELECTRIC ENERGY CONVERSION

Charles Wood

Jet Propulsion Laboratory
California Institute of Technology
Pasadena, CA 91109

The maximum efficiency (η) for the conversion of heat to electrical energy using a thermoelectric couple with a hot junction at temperature T_1 and a cold junction at temperature T_0 is given by[1]

$$\eta = \left(\frac{T_1-T_0}{T_1}\right)\left(\frac{M-1}{M+T_0/T_1}\right)$$

where $M = [1+Z(T_1+T_0)/2]^{1/2}$ and $Z = \alpha^2/\rho\kappa = \alpha^2\sigma/\kappa$. Z is a materials parameter called the figure of merit of the thermocouple. It is a function of the Seebeck coefficient, α, the electrical resistivity, ρ, or conductivity, σ, and the total thermal conductivity, κ, of each the leg of the thermocouple. The thermodynamic efficiency of an ideal reversible engine, the first factor of Eq. (1), is reduced by the irreversible losses of heat conduction and Joule heating in the thermocouple, accounted for in the second factor. Obviously, increasing the hot junction temperature, T_1, and the figure of merit, Z, both increase the conversion efficiency. The dimensions of Z are deg^{-1}. Thermoelectrics are generally characterized by the value of the dimensionless parameter ZT, since the efficiency is a function of Z (T_1+T_0).

Semiconductors, as distinct from metals or insulators, have the highest Z values. Therefore they are used for thermoelectric energy conversion. Metals are excellent conductors but their Seebeck coefficients are too low. Insulators can have high Seebeck coefficients but are too electrically resistive. A good compromise can be made by choosing highly-doped semiconductors with α and σ values intermediate between the properties of insulators and metals.

One class of refractory materials receiving considerable attention for high temperature thermoelectric energy conversion is the rare-earth chalcogenides. Rare-earth chalcogenides generally form the following binary compounds: RX, R_3X_4 - R_2X_3, RX_2, where R represents the rare-earth and X the chalcogenide atoms S, Se, or Te. Only compounds in the homogenous range R_3X_4 - R_2X_3 have been extensively investigated for high-temperature thermoelectric applications. There are often two and sometimes three polymorphic modifications of the solid solutions R_3X_4 - R_2X_3: (i) a low-temperature (<900 - 1000°C) orthorhombic α-phase; (ii) an intermediate temperature (900 to 1300°C) tetragonal β-phase; and (iii) a high temperature (>1300°C) cubic (Th_3P_4) metastable γ-phase. In the cubic Th_3P_4 structure it is convenient to designate the unit cell as $4(R_{3-x}V_xX_4)$ where V is a rare-earth vacancy. For R_2X_3 compounds 1/3 of the 12 rare-earth sites are vacant, i.e., x = 1/3. For the R_3X_4 compounds there are no vacant sites, i.e., x = 0. Each $R_{3-x}V_xX_4$ unit provides (1-3x) electrons for conduction. Hence R_2X_3 (X = 1/3) is an insulator and R_3X_4 (X = 0) is a metal.

Degenerate semiconductors for thermoelectric applications are produced from hot-pressed powders of $R_{3-x}X_4$ compounds with varying degrees of excess rare-earth atoms.[2] These stoichoimetries have been found to yield degenerate wide band-gap

semiconductors, with electrical conductivities of ~10^3 ohm^{-1} cm^{-1}, carrier concentrations greater than ~10^{20} cm^{-3} and charge carrier mobilities of ~ 1 to 10 cm^2/volt sec.

Lattice thermal conductivities (κ_{ph}) of the $R_{3-x}X_4$ compounds are generally low, in the range 0.005 to 0.01 watt/cm-deg.[3] This results from three factors. First, the Debye temperatures, θ_D, are anomalously low fractions of the melting temperatures, θ_D ~200-400 K, with $\kappa_{ph} \alpha \theta^3_D$. Secondly, these are complicated crystal structures with a fairly large number of atoms (28) per unit cell. Since there are 3 degrees of freedom and 3 acoustic modes per unit cell the number of optic modes, is N = 3 x 28-3. Examination of the dispersion curves, ω versus k, shows that these optic modes of vibration have very low propogation velocities. Therefore, the majority of phonons are optical and have low velocities. Thirdly, the rare-earth ion vacancies produce disorder which, inhibits thermal transport.

Rare-earth chalcogenides behave as highly-degenerate n-type semiconductors over most of the composition range R_3X_4 to R_2X_3. However, the large values of effective mass and the small values of the mobility suggest that the conduction band is somewhat narrow.

For itinerant motion a material's figure of merit is essentially determined by a simple combination of its transport parameters. Namely, $Z \alpha m^{*3/2} \mu/\kappa$, where m^* and μ are, respectively, the carrier's effective mass and mobility and κ is the material's thermal conductivity.[4] Since the thermal conductivities of the $R_{3-x}X_4$ materials are close to one another it is only the numerator of this expression for Z which varies much between materials. The values of m^* and μ for various R_3X_4 compounds have been tabulated[5] and suggest that $La_{3-x}S_4$ and $La_{3-x}Te_4$ have the greatest potential for high Z values. This is supported by the work of Golikova and Rudnik,[6] Zhuze et al.[5] and Luguev and Smirnov's data.[7] We have succeeded in obtaining, at temperatures of ~1000°C, Z values of ~0.5 x $10^{-3}K^{-1}$ for $La_{3-x}S_4$ and values is excess of 1 x $10^{-3}K^{-1}$ for $La_{3-x}Te_4$ and are currently endeavoring to make p-type rare-earth chalcogenides of equivalent quality. There are initial indications of electron Hall mobilities in excess of the commonly occurring values of ~3.5 cm^2/Vs in $La_{3-x}S_4$ at room-temperature. In view of the proportionality between Z and μ this result holds promise of even higher Z values. It should be noted that despite many attempts to place a theoretical upper limit on Z no such limit has been found.

1. A.F. Joffe, Semiconductor Thermoelements and Thermoelectric Cooling (Infosearch Limited, London 1957).
2. The author is indebted to L. Danielson and V. Raag, TECO, Waltham, MA who produced the hot-pressed samples and made many of the physical measurements.
3. I.A. Smirnov, Phys. Stat. Sol. (a) 14, 363 (1972).
4. H.J. Goldsmid and R.W. Douglas, Brit. J. Appl. Phys. 5, 386 (1954).
5. V.P. Zhuze, V.M. Sergeeva and O.A. Golikova, Sov. Phys. Solid State 11, 2071 (1971); 13, 6689 (1971).
6. O.A. Golikova and I.M. Rudnik, Izv. Akad. Nauk, SSSR Neorg. Mater. 14, 17 (1978).
7. S.M. Luguev and I.A. Smirnov, Sov. Phys. Solid State 19, 707 (1977).

HIGH TEMPERATURE THERMOELECTRIC ENERGY CONVERSION

JPL

Charles Wood

JET PROPULSION LABORATORY

A C K N O W L E D G E M E N T S

JPL

A. LOCKWOOD
A. ZOLTAN
D. ZOLTAN
J. PARKER

GA TECHNOLOGIES

N. ELSNER
G. REYNOLDS
J. NORMAN

TECO CORP.

V. RAAG
L. DANIELSON

SANDIA NATIONAL LABORATORIES

D. EMIN
E. VENTURINI
L. AZEVEDO
B. MOROSIN
G. SAMARA
M. MOSS

JPL

FIGURE OF MERIT

MAXIMUM EFFICIENCY η = $\frac{\text{ELECTRICAL ENERGY DELIVERED TO EXTERNAL CIRCUIT}}{\text{ENERGY CONSUMED FROM HEAT SOURCE}}$

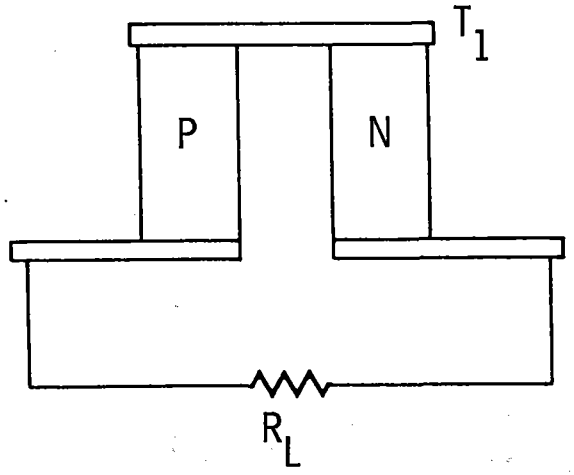

$$= \left(\frac{T_1 - T_0}{T_1}\right) \quad X \quad \left(\frac{M - 1}{M + \frac{T_0}{T_1}}\right)$$

$$\simeq 1/4\, Z(T_1 - T_0)$$

WHERE M = $\sqrt{1 + 1/2\, Z\,(T_1 + T_0)}$

AND FIGURE OF MERIT Z = $\frac{a^2 \sigma}{K}$

JPL

SEEBECK COEFFICIENT:

$$\alpha = \frac{k}{e}\left|A + \ell\eta\,\frac{Ne\mu}{\sigma}\right|$$

As $\sigma\uparrow$ $\alpha\downarrow$

THERMAL CONDUCTIVITY:

$$K = K_{ph} + K_{eL}$$

As $\sigma\uparrow$ $K_{eL}\uparrow$

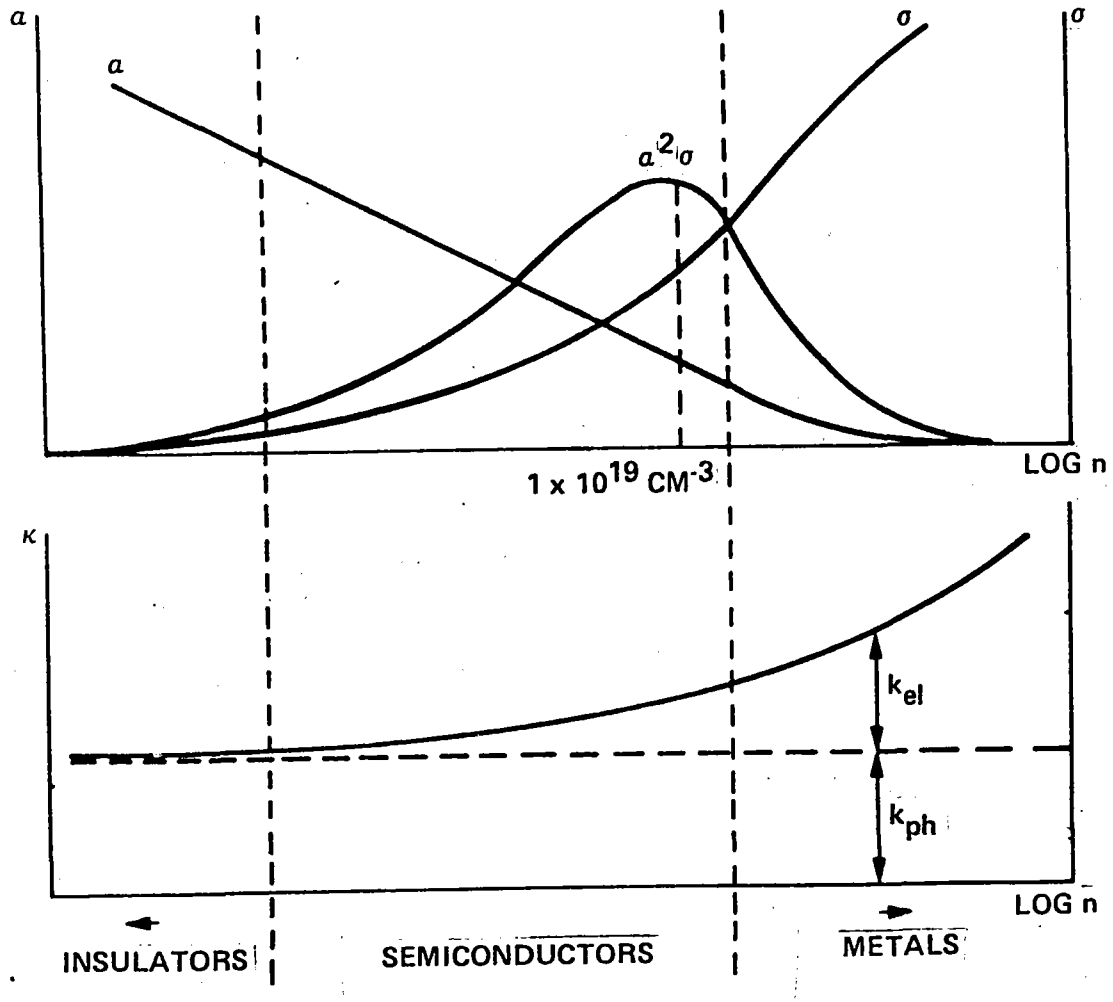
a
a
σ
σ
a^2/σ
1×10^{19} CM^{-3}
LOG n
κ
k_{el}
k_{ph}
LOG n
INSULATORS
SEMICONDUCTORS
METALS

BASIC PARAMETERS AFFECTING Z

$$Z = \frac{a^2 \sigma}{K_T}$$

$$a^2 \sigma \sim m^{*3/2} \mu$$

$m^* \mu$ IS RELATED TO SCATTERING MECHANISM

i) IONIZED IMPURITY SCATTERING:

$$m^{*1/2} \mu = \text{const.}$$

$\therefore$ Z ↑ AS m^* ↑

ii) HIGH TEMPERATURE POLAR OPTICAL MODE SCATTERING

$$m^{*3/2} \mu = \text{const.}$$

$\therefore$ Z INDEPENDENT OF m^*

iii) ACOUSTICAL-MODE LATTICE SCATTERING:

$$m^{*5/2} \mu = \text{const.}$$

$\therefore$ Z ↑ AS m^* ↓

BASIC PARAMETERS AFFECTING Z (cont)

$$K_T = K_{ph} + K_{el}$$

(LEIBFRIED AND SCHLÖMANN)

$$K_{ph} \sim \frac{\bar{M}a\,\theta^3}{T_\gamma^{\,2}}$$

- HEAVY ATOMIC MASS RESULTS IN LOW K_{ph}

EQUIVALENTLY:

$$K_{ph} \sim \frac{1}{3} C_v v \frac{a}{\alpha\gamma T}$$

(DUGDALE AND MACDONALD)

EQUIVALENTLY:

$$K_{ph}\,T \sim \frac{T_m^{\,3/2}\,\rho^{\,2/3}}{A^{7/6}}$$

(KEYES)

GENERALLY $T_m \downarrow$ AS $A \uparrow$

Lattice Thermal Conductivity Plotted Against Mean Atomic Weight for Covalent and Ionic Crystals

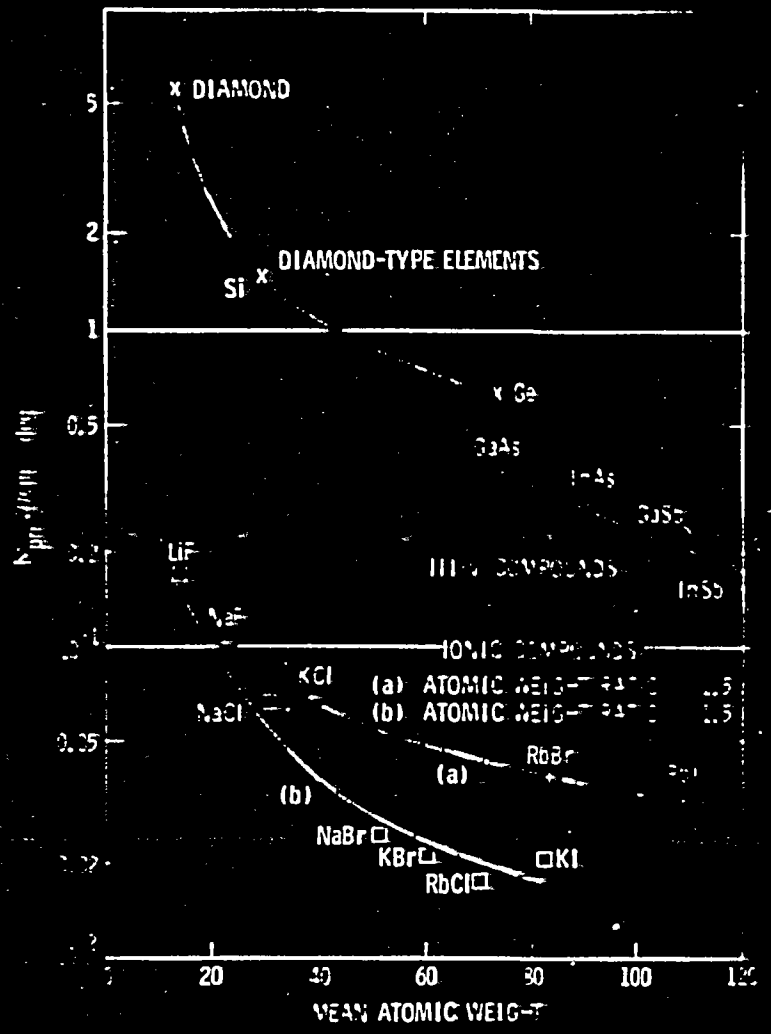

STEP-2-7
9-23-82

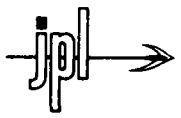

MATERIAL REQUIREMENTS

- $\kappa_{el} \sim \kappa_{ph}$
- ACOUSTIC-MODE LATTICE SCATTERING
- HIGH MOBILITY
- HIGH ATOMIC MASS
- LARGE ATOMIC MASS RATIO

FIGURE-OF-MERIT OF SELECTED THERMOELECTRIC MATERIALS

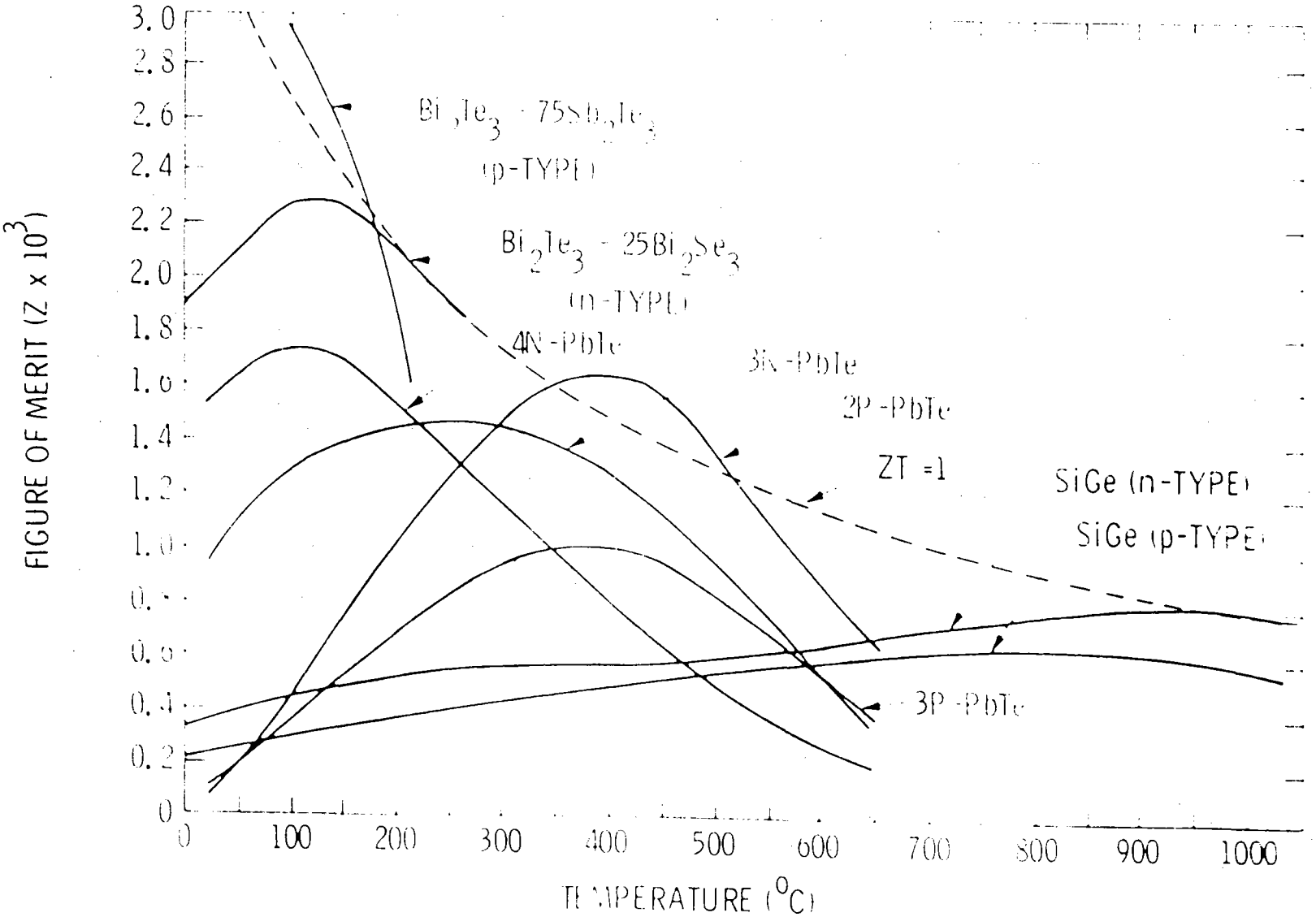

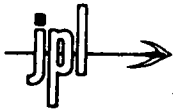

RARE EARTH CHALCOGENIDES: R_3X_4 - R_2X_3

28 LATTICE SITES/UNIT CELL: 4 $8R_{3-x}V_xX_4$)

(V IS RARE EARTH VACANCY)

X = 1/3 R_2X_3 HAS 4/3 VACANCIES/UNIT CELL

2 R^{3+} IONS CONTRIBUTE 6e

3 X^{2-} IONS ACCEPT 6e

∴ INSULATOR

X = 0 R_3X_4 HAS NO VACANCIES

3 R^{3+} IONS CONTRIBUTE 9e

4 X^{2-} IONS ACCEPT 8e

∴ SEMIMETAL

JPL PROPERTIES OF RARE EARTH CHALCOGENIDES*
(ROOM TEMPERATURE)

COMPOUND	MOBILITY (μ) (cm^2/V-sec)	EFFECTIVE MASS (m*)	$m^{*3/2}\mu$
La_3S_4	3.5	3.6	23.9
Ce_3S_4	3.1	2.8	14.5
Na_3S_4	3.2	2.7	14.2
Pr_3Se_4	2.6	2.6	10.9
La_3Te_4	11.5	1.8	27.8
Ce_3Te_4	4.2	2.1	12.8
Pr_3Te_4	6.2	1.6	12.5
Nd_3Te_4	5.0	2.0	14.1

*ZHUZE ET AL SOV. PHYS. SOL. STATE 13 6689 (1971)

JPL

PHASE DIAGRAM OF La-S*

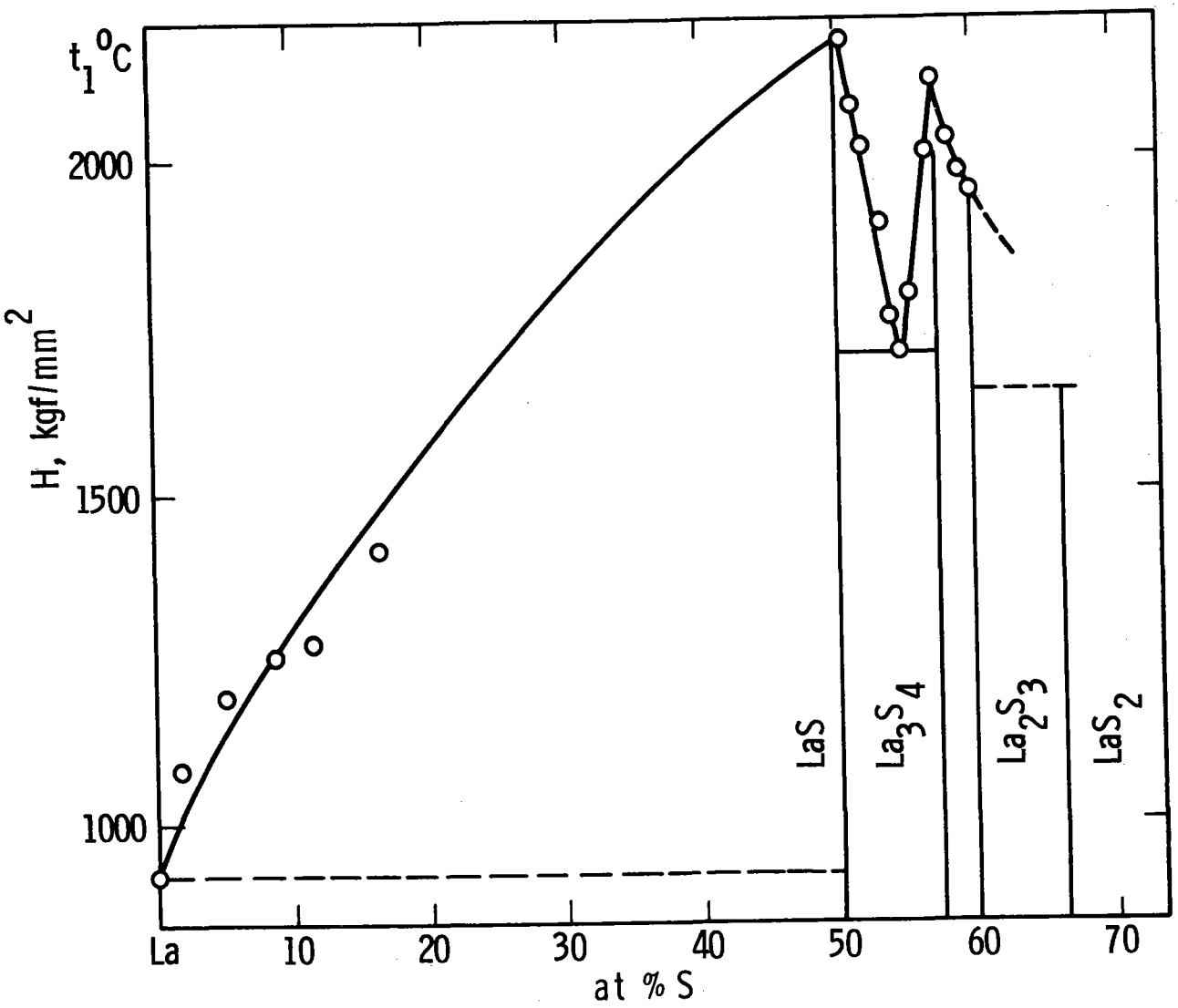

*K.E. MIRONOV et al. IZV. AKAD. NAUK SSSR
14 641(1978)

JPL SEEBECK COEFFICIENTS OF LANTHANUM SULFIDES

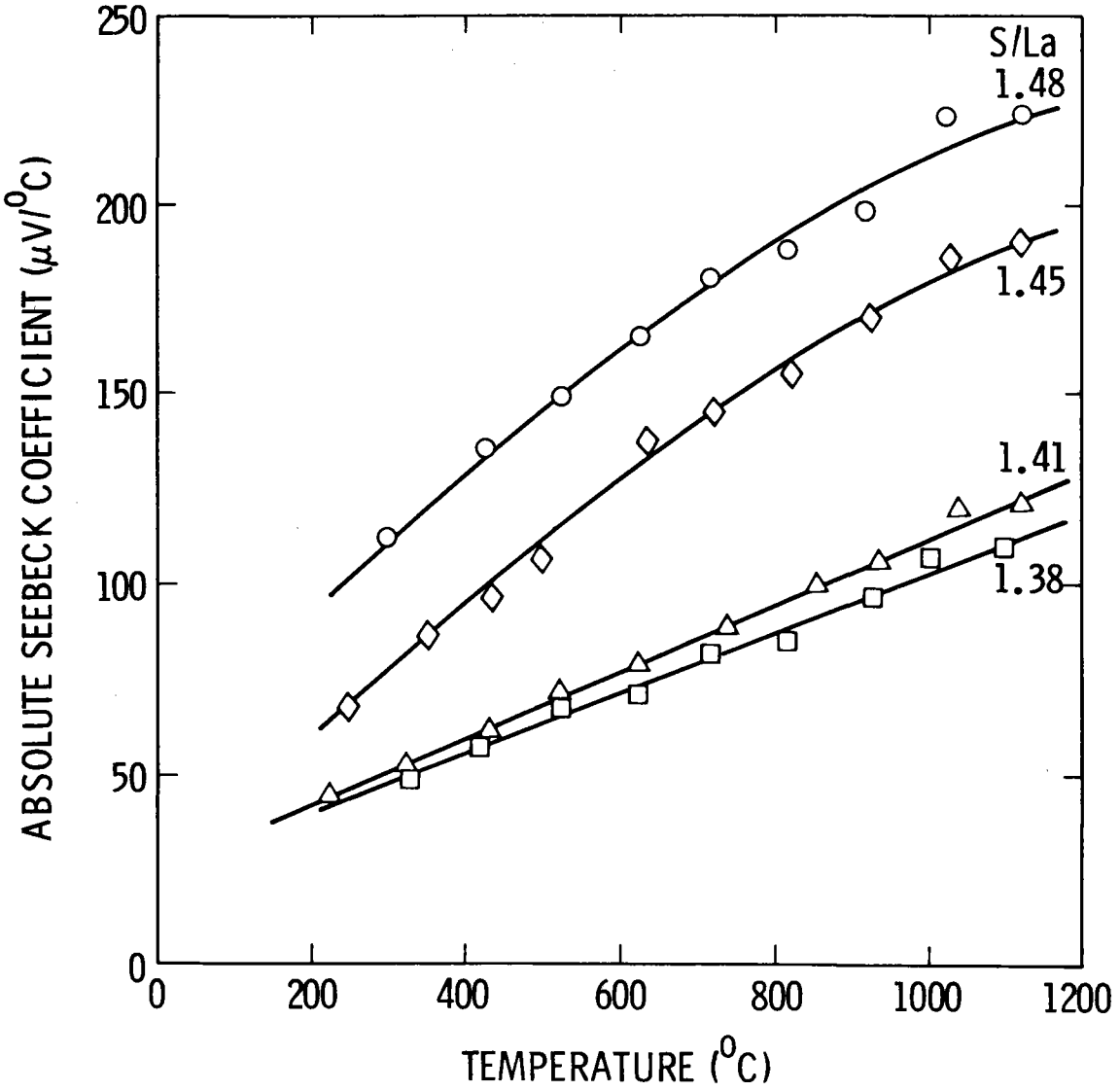

JPL ELECTRICAL RESISTIVITIES OF LANTHANUM SULFIDES

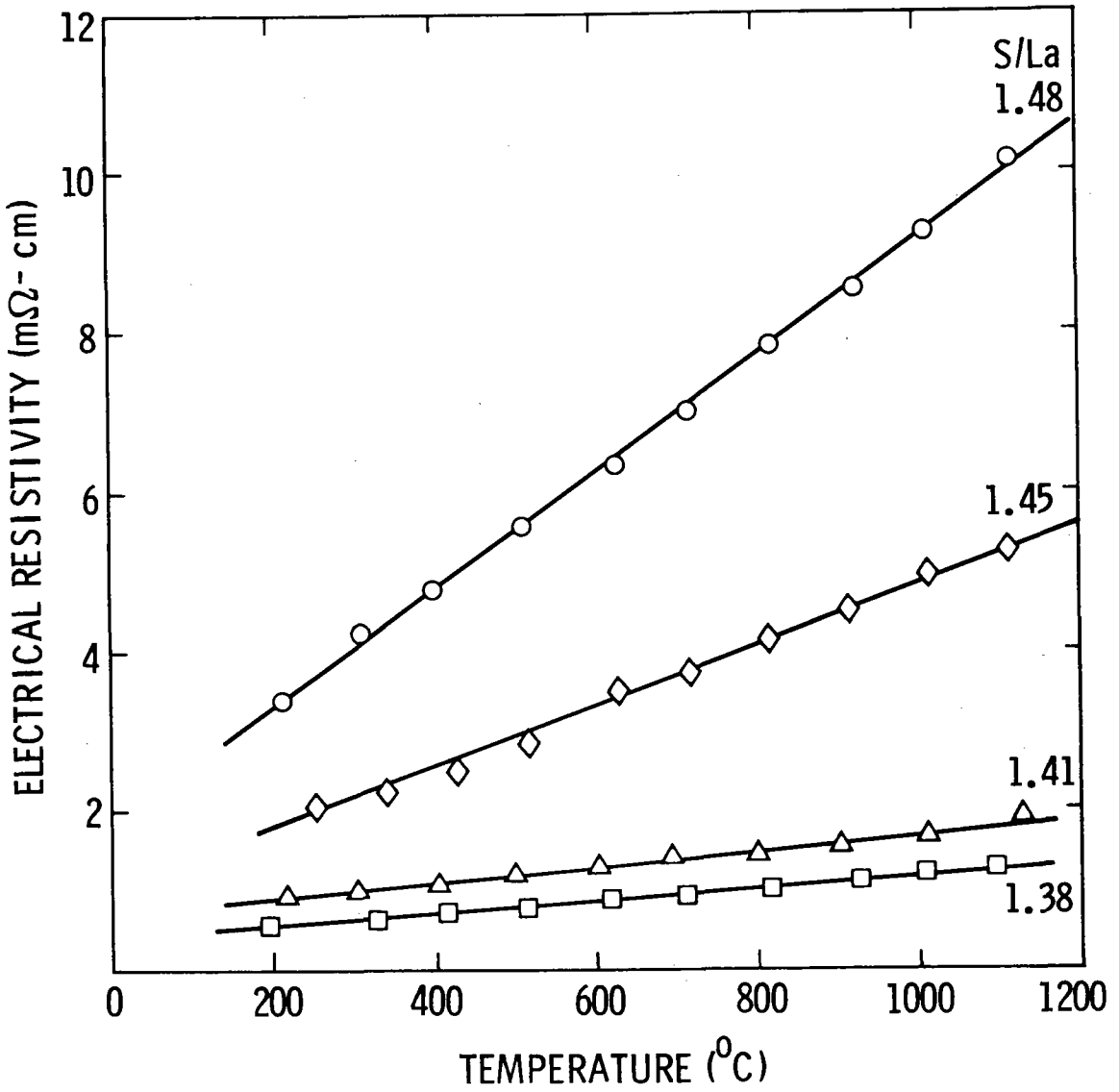

JPL

$LaS_{1.41}$: HALL EFFECT

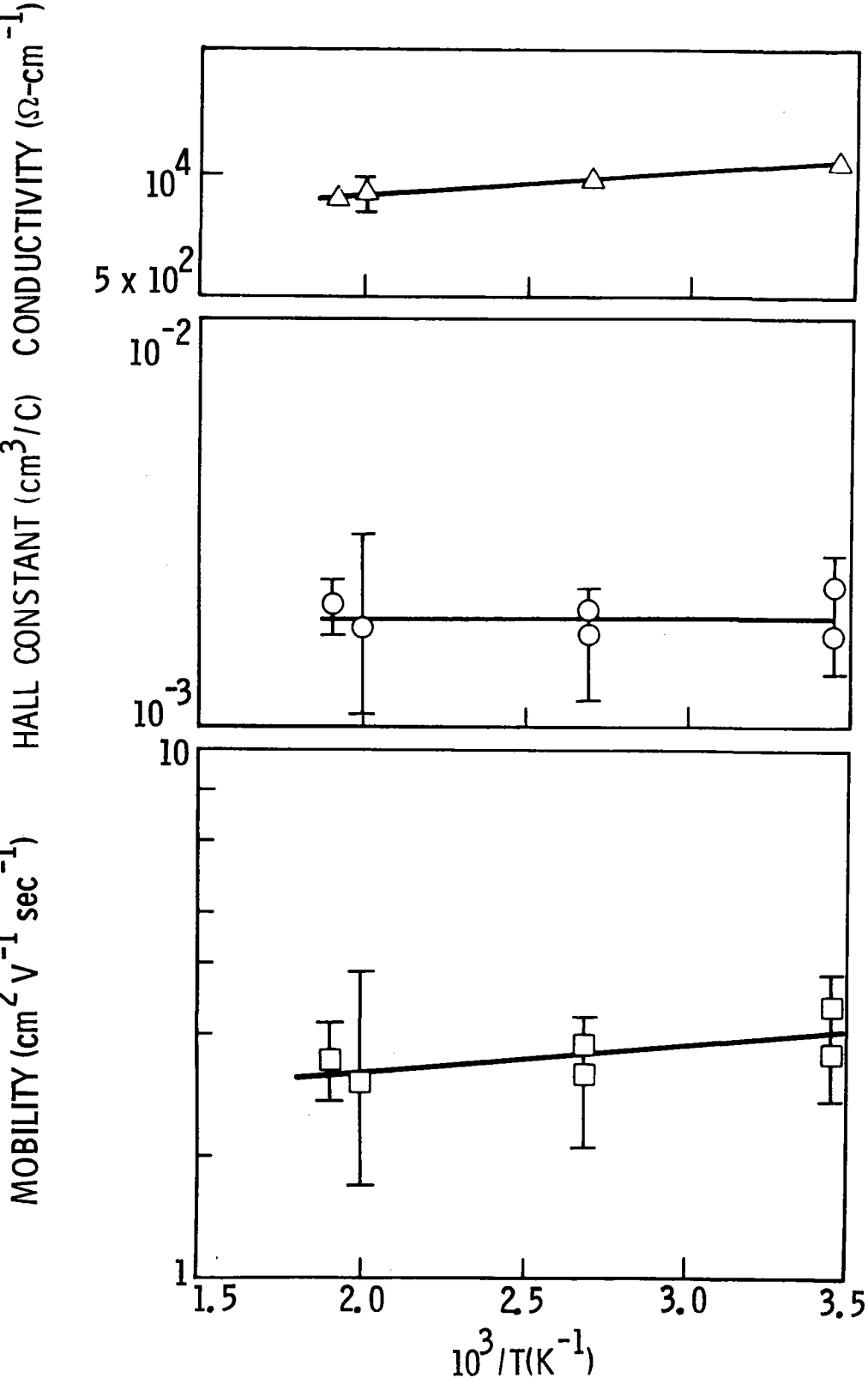

JPL

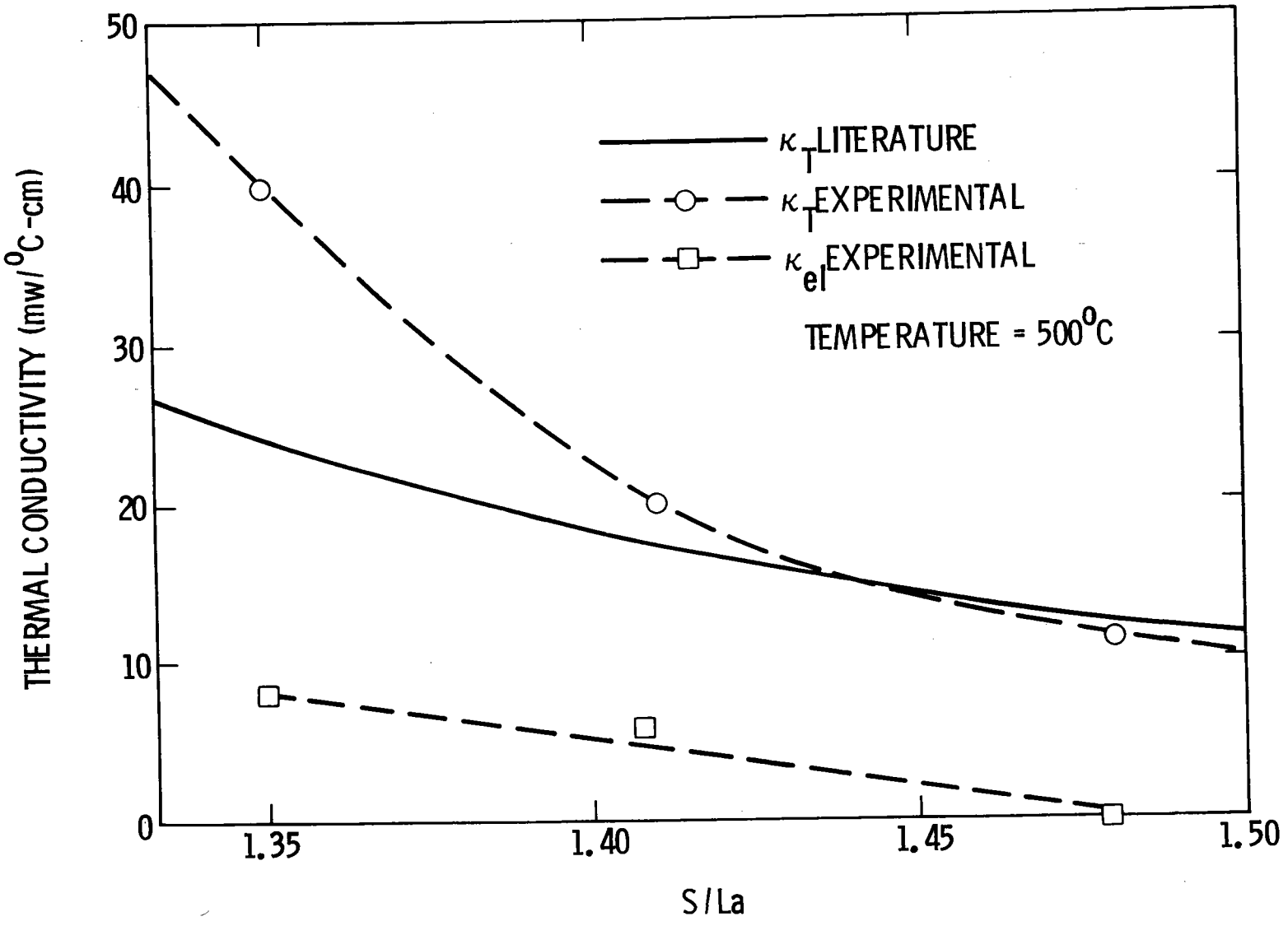
50
40
30
20
10
0
1.35
1.40
1.45
1.50
S/La
THERMAL CONDUCTIVITY (mw/°C-cm)
κ_T LITERATURE
κ_T EXPERIMENTAL
κ_{el} EXPERIMENTAL
TEMPERATURE = 500°C

JPL

FIGURE OF MERIT OF La CHALCOGENIDES

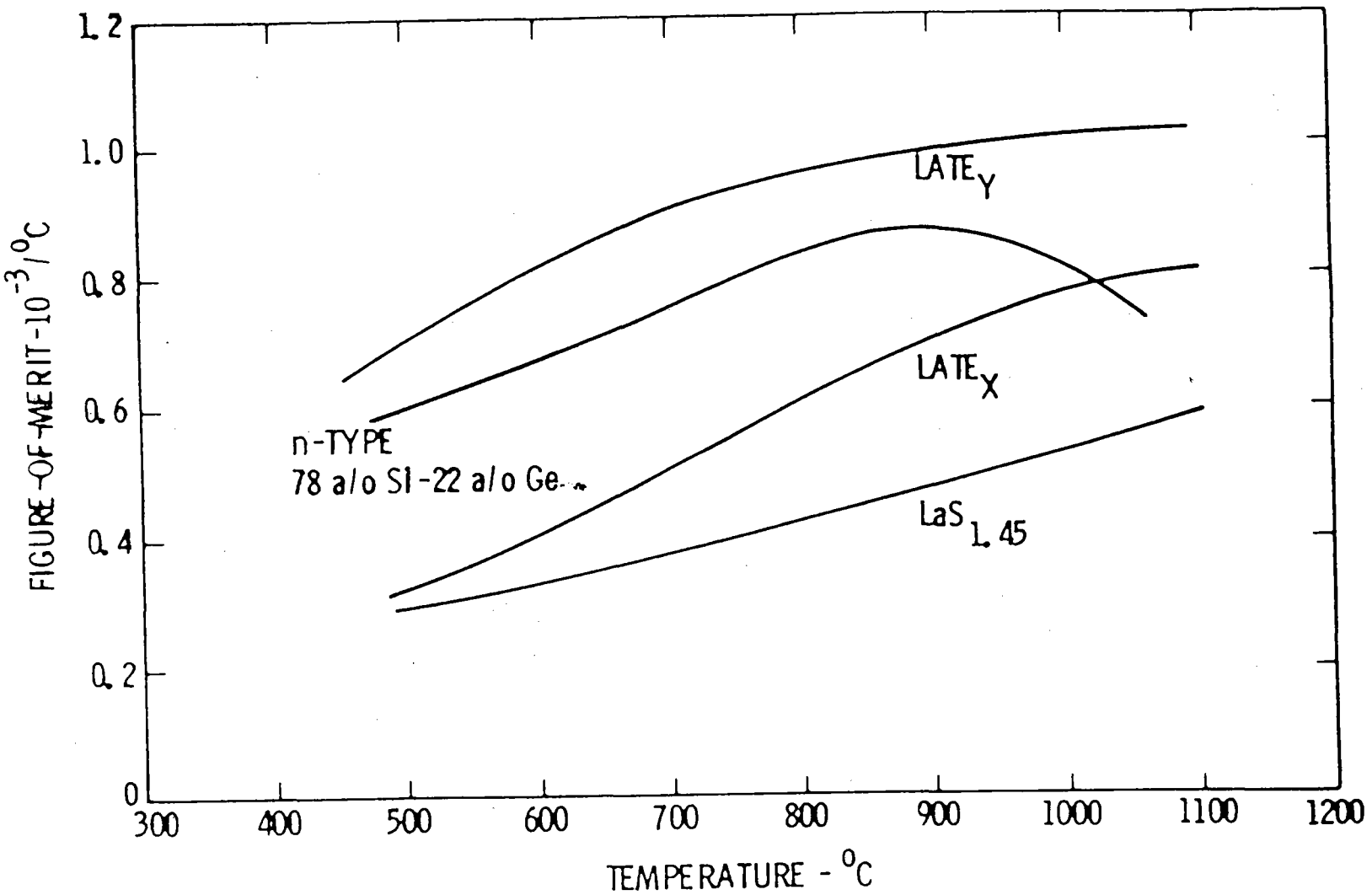

JPL

$La_{3-x}S_4 \quad 0 \leqslant X \leqslant 1/3$

- N - LEG
- REFRACTORY
- LOW VAPOR PRESSURE
- COMPOSITION CONTROLS CARRIER CONC
- DEGENERATE LOW T - OPTIMIZED HIGH T
- LOW K
  - LATTICE VACANCIES
  - 28 ATOMS/UNIT CELL

MAGNETIC HEAT ENGINES

Lance D. Kirol
Idaho National Engineering Laboratory

Magnetic Heat Engines

Principles of Operation. Thermal energy counters magnetic order, so for a given applied magnetic field, magnetization decreases as temperature increases. This phenomena makes the operation of magnetic heat engines possible. Heat is converted into work via changes in entropy which occur upon magnetization; at any given temperature, entropy of magnetized material is less than the entropy of unmagnetized material. This is analogous to pressure changes of a gas; for any temperature, entropy of the gas decreases with increasing pressure. With magnetic cycles, applied magnetic field plays the role of pressure in reducing entropy. Change in entropy upon application of a magnetic field is maximum at the Curie temperature, as is the slope of the magnetization-temperature curve, as shown in Figure 1. Magnetic heat engines must be operated near the Curie temperature of the working material, but materials are available with virtually any Curie temperature to 1400K.

Several types of magnetic heat engines are possible. A thermomagnetic generator (Figure 2) converts heat to electricity without a mechanical interface. A block of magnetic material is placed in a magnetic circuit, and wound with a conducting coil. Temperature of the magnetic material is cycled, causing a cyclic change in flux. The coil encloses a time varient magnetic flux, so a voltage is induced in the winding. Thermomagnetic generators utilize only very small field changes and are probably the least promising type of magnetic heat engine.

Figure 3 shows a very simple magnetic heat engine to produce shaft work. It consists of a toroid of magnetic working material which is free to rotate through a magnetic field. Toroid material is heated in the field and cooled outside. Once rotation is started in one direction (counterclockwise in Figure 3), material leaving the field is warmer than material entering. Cold material is more magnetic (more strongly attracted into the field) so a net torque is produced. The efficiency of this type of device can be greatly improved by recuperation, whereby heat is recovered during cooling of the toroid and is used to preheat material entering the field. Figure 4 shows a recuperative Brayton cycle rotary magnetic heat engine. The rotor consists of parallel flat disks of magnetic working material. Regenerator fluid is pumped counter to disk rotation, flowing between the disks. In the field change regions (1-2 and 3-4) fluid exits the rotor to allow adiabatic magnetization and demagnetization. Ericsson and Stirling cycles can be executed by increasing heat transfer in the field change regions to give isothermal field changes.

Mechanical means are used to vary the magnetic field seen by a reference volume in the rotor of the heat engine discussed above. Electrical field variation is also possible, as illustrated by the recuperative field modulation heat pump shown in Figure 5. Thermodynamics are identical to a rotary recuperative machine. A magnetic heat engine of this type would convert heat directly to magnetic field energy of the superconducting magnets, which is easily drawn off as electrical energy.

Performance. Major irreversibilities of magnetic heat engines are listed in Figure 6. Recuperative heat transfer is large compared to heat flow through the engine, and this heat transfer across non-zero temperature difference is one source of irreversibility. Variation in specific heat between magnetized and unmagnetized working material reduces the amount of heat which can be recuperated and lowers efficiency. This is probably the major heat engine irreversibility, but may be compensated for by proper material selection and field variation during regeneration.

Predicted performance for a rotary heat engine with different working materials is shown in Figure 7. Results are presented as thermal efficiency versus power output from a unit mass of working material. Each curve represents a specific machine operating at different speeds. These cycles operate with a 350°F source and 9T field change. Gadolinium and $Y_2(FeCo)_{17}$ do not exhibit exceptional performance, but a hypothetical material with constant specific heat results in efficiency close to the Carnot limit. Such performance should be possible with real materials and optimum magnetic field profiles.

Status and History. The concept of a magnetic heat engine is not new, as shown in Figure 8. Both Edison and Tesla held patents for magnetic energy conversion devices. Four studies of thermomagnetic generators were made during the 1940's and 50's, and two theoretical studies of other nonregenerative magnetic heat engines were performed during the 60's. Most recent work on magnetic cycles is focused on cryogenic refrigeration. Magnetic cycles appear to offer improved efficiency and reduced cost compared to gas compression refrigeration. The INEL is currently investigating the feasibility of high temperature magnetic heat pumps for industrial applications, and performed one small study of recuperative magnetic heat engines.

Renewed interest in magnetic cycles (mostly refrigeration) is occurring because of the availability of superconducting magnets to produce the high magnetic fields required, and because rare earth elements needed to tailor magnetic properties are now available, (Figure 9). Need for efficient cryocoolers and energy conversion devices is also stimulating interest.

Problems and concerns with different types of heat engines are listed in Figure 10. The major problem with the rotary mechanical design is developing a magnet system to give the optimum field profile. There appear to be no technical roadblocks, but cost may be quite high. Concerns with regenerator fluid pumping and torque transmission appear to be solvable. A.C. losses in the superconducting magnet is the major concern with field modulation devices. These losses result in heat generation in the superconducting magnet at 4.2K, and every unit of heat removed at this temperature requires 400 units of work at the cryogenic refrigeration system.

The many advantages of Magnetic Cycles over conventional equipment are listed in Figure 11. The greatest advantage is the potential to approach Carnot efficiency since truly isothermal entropy changes are possible and Stirling and Ericsson cycles can be easily implemented. (Magnetic field is more easily controlled than pressure in conventional Stirling cycles.) Magnetic Brayton cycles are also possible, and are particularly suited to sensible heat sources.

Application. Magnetic cycles can be used any place conventional heat pumps or heat engines are used. They may cost more than other conversion schemes, but their high efficiency can offset some increased cost by reducing the required size of the heat source and heat sink. Magnetic devices show no economy of scale (except the cryocooler to cool the superconducting magnets, which can be shared between several heat engines) so modular or distributed power generation is possible.

REFERENCES

1. L. D. Kirol, J. I. Mills, K. S. Fullmer, and J. N. Zabriskie, Magnetic Heat Pump Feasibility Assessment, Report EGG-2343, October 1984.

2. L. D. Kirol, Magnetic Heat Engine Preliminary Feasibility Study, Report EGG-SE-6718, November 1984.

3. J. A. Barclay and W. A. Steyert, Magnetic Refrigerator Development, Electric Power Research Institute Report EPRI EL-1757, April 1981.

4. L. D. Kirol and J. I. Mills, "Numerical Analysis of Thermomagnetic Generators", JAP, 56, 3, August 1, 1984, pp. 824-828.

5. L. D. Kirol, J. I. Mills, and D. H. VanHaaften, Thermomagnetic Generator, Report EG&G-SE-6442, November 1983.

6. G. V. Brown "Basic Principles and Possible Configurations of Magnetic Heat Pumps", ASHRAE Transactions, 87, 2, 1981.

7. G. V. Brown, "Magnetic Heat Pumping Near Room Temperature", JAP,47,8, August 1976, pp. 3673-3680.

8. H. Oesterreicher and F. T. Parker, "Magnetic Cooling Near Curie Temperatures Above 300K", JAP,55, 12, June 15, 1984, pp. 4334-4338.

9. W. P. Pratt, Jr., S. S. Rosenblum, W. A. Steyert, and J. A. Barclay, "A Continuous Demagnetization Refrigerator Operating Near 2K and a Study of Magnetic Refrigerants", Cryogenics, 17, 12, December 1977 pp. 689-693.

10. J. A. Barclay, O. Moze, L. Paterson, "A Reciprocating Magnetic Refrigerator for 2-4K operation: Initial Results", JAP, 50, 9, September 1979, pp. 5870-5877.

11. G. J. Van Der Maas and W. J. Purvis, "Curie Point Motor", American Journal of Physics, 24, 3, March 1956, pp. 176-177.

12. F. Brailsford, "Theory of a Ferromagnetic Heat Engine", Proc IEE,111, 9, September 1964, pp. 1602-1606.

13. R. E. Rosensweig, J. W. Nestor, and R. S. Timmins, "Ferrohydrodynamic Fluids for Direct Conversion of Heat Energy", AIChE Conference on Materials Associated with Direct Energy Conversion, London, June 13-17, 1965, pp. 95-110.

14. R. E. Rosensweig, "Theory of an Improved Thermomagnetic Generator", Proc. IEE, 114, 3, March 1967, pp. 405-409.

15. J. E. Elliott, "Thermomagnetic Generator" JAP, 30, 11, November 1959, pp. 1774-1777.

16. L. Brillouin and H. P. Iskenderian, "Thermomagnetic Generator", Electrical Communication, 25, 1948, pp. 300-311.

Significance of Curie Temperature (T_c)

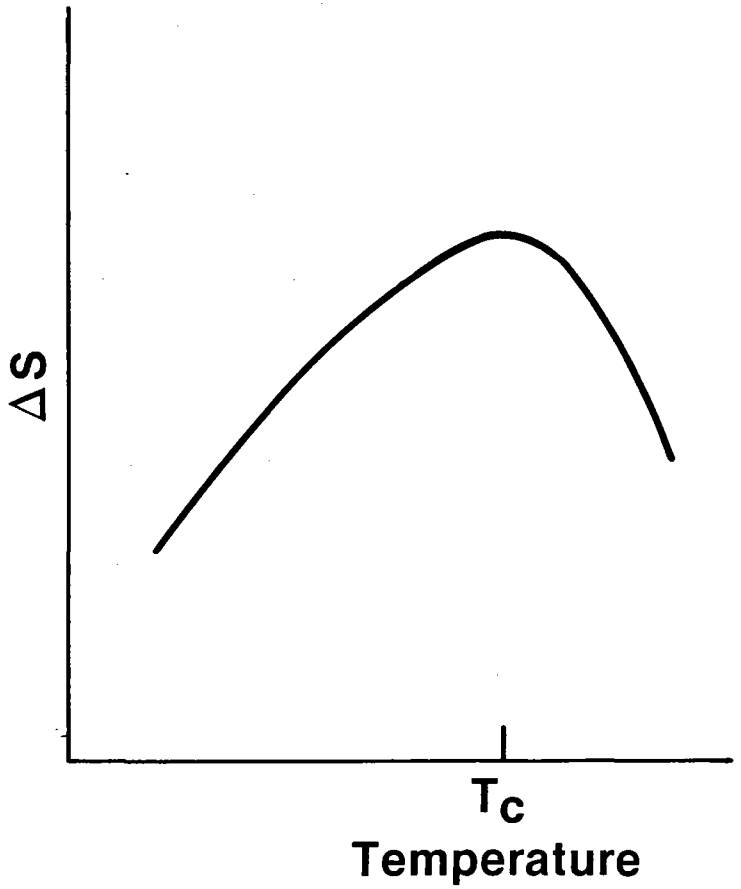

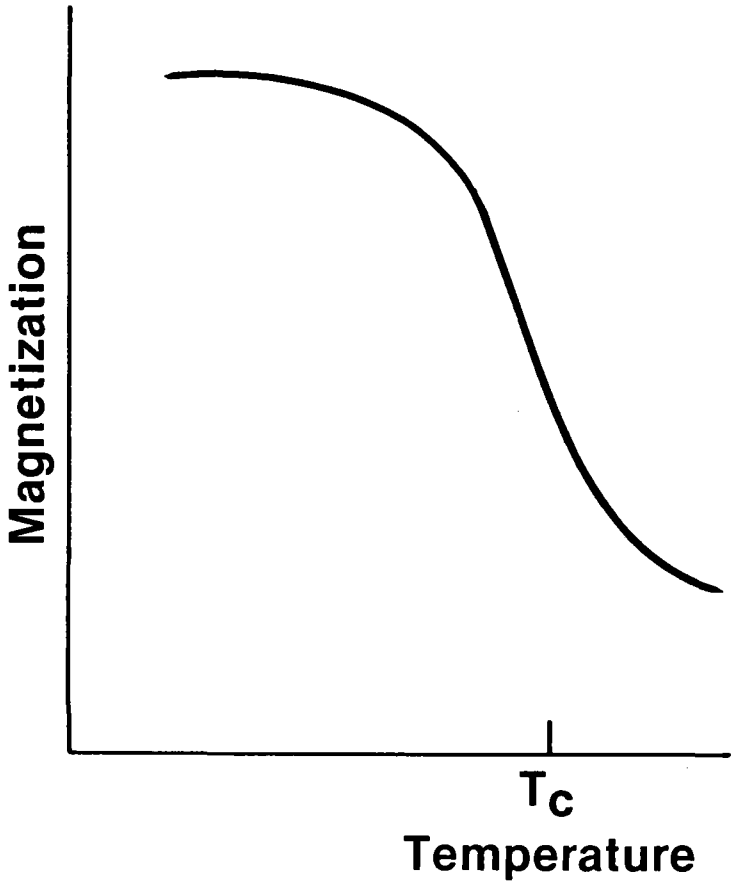

S4 11 678

Figure 1.

Thermomagnetic Generator Schematic

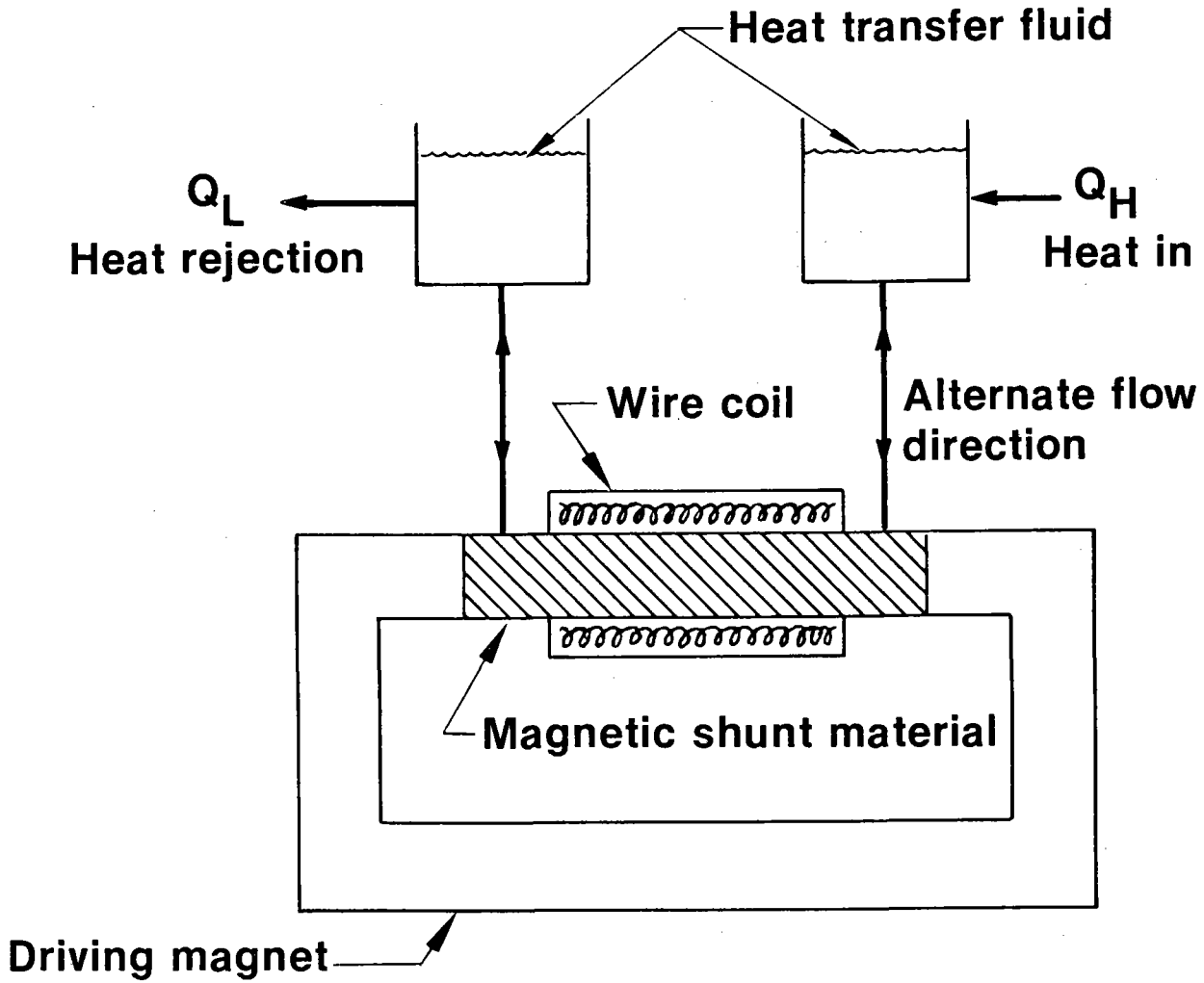

Figure 2.

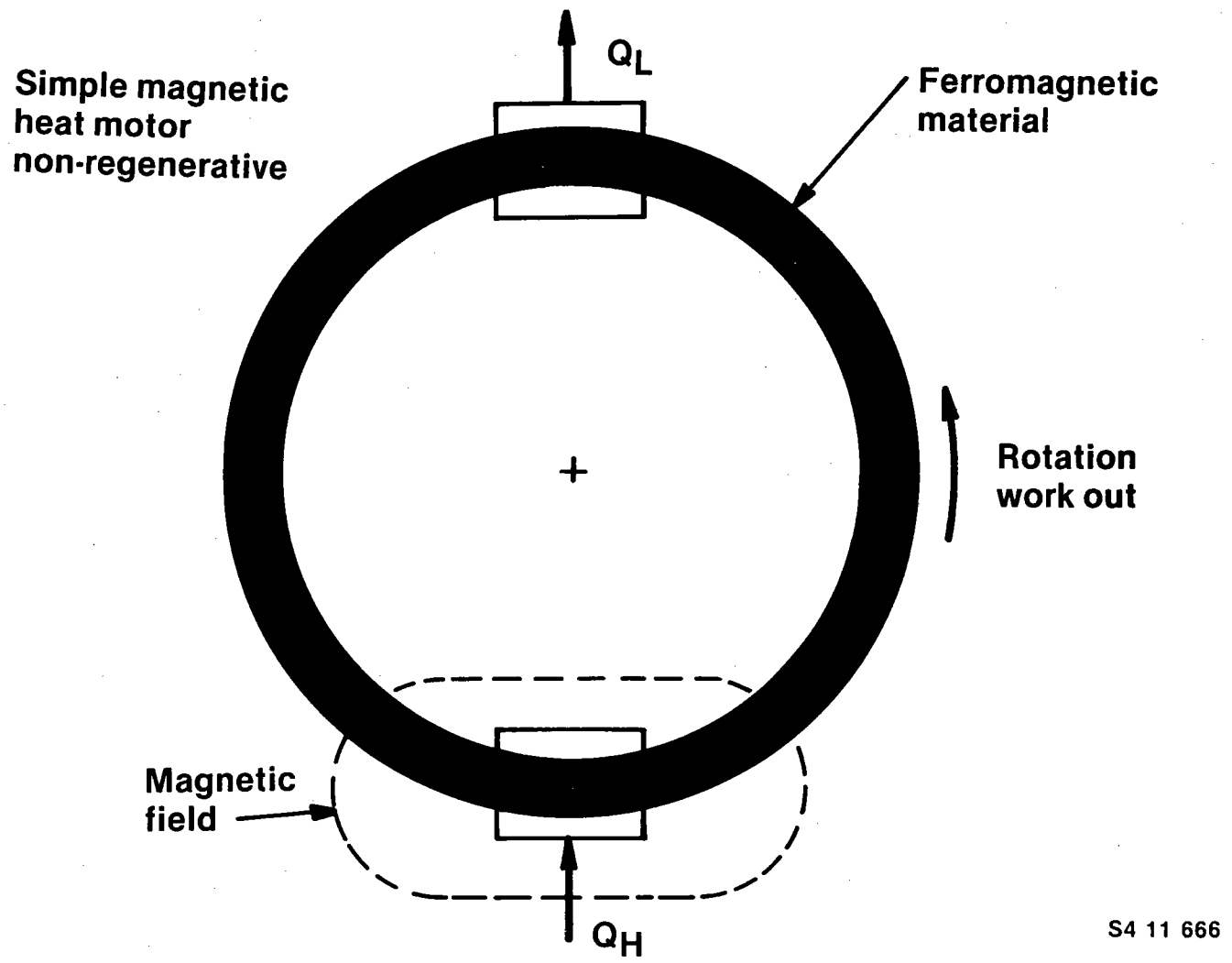
Simple magnetic
heat motor
non-regenerative
Q_L
Ferromagnetic
material
Rotation
work out
Magnetic
field
Q_H
S4 11 666

Figure 3.

Brayton Cycle Rotary Magnetic Heat Engine

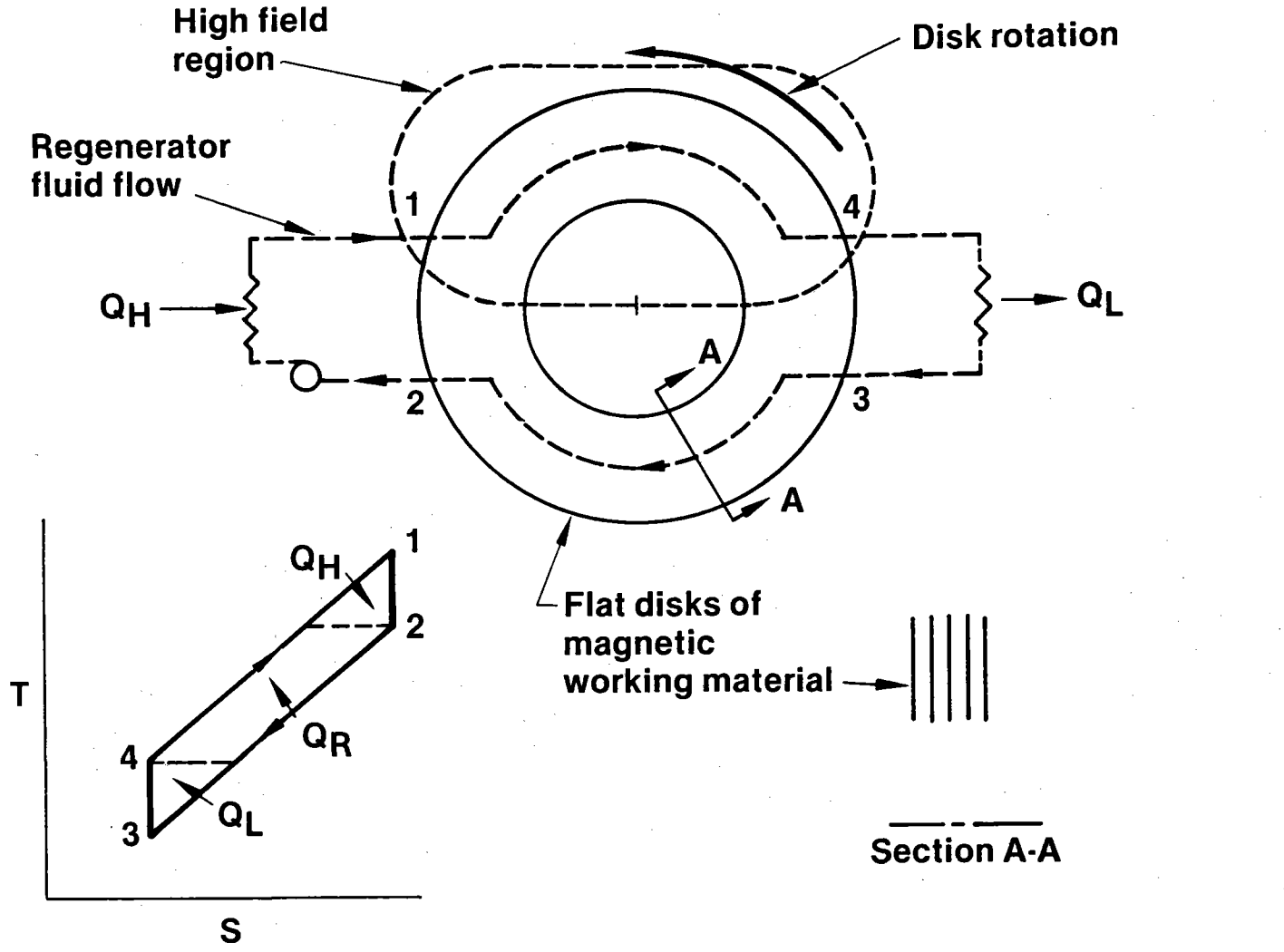

S4 11 669

Figure 4.

Recuperative Modulating Field Heat Pump

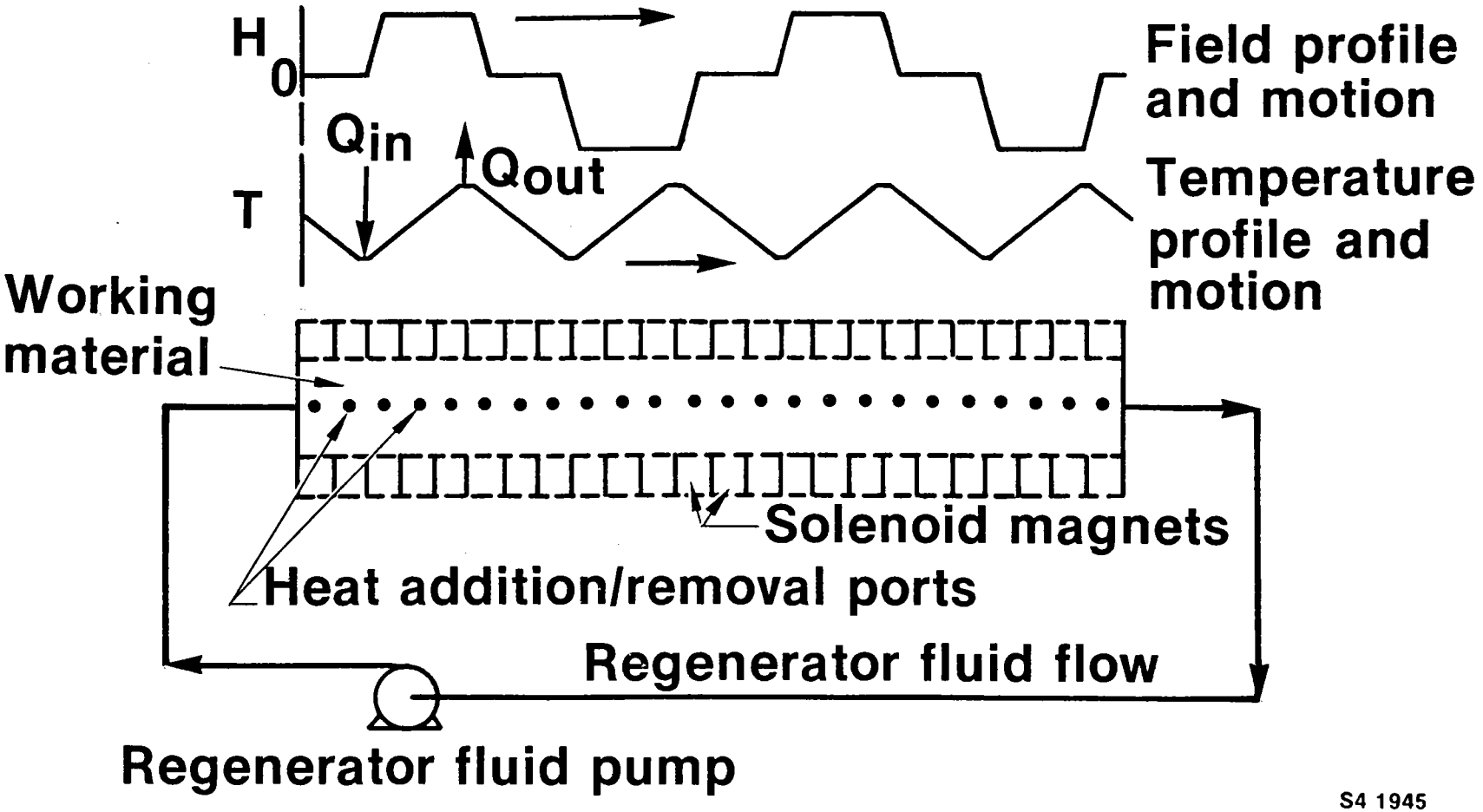

Figure 5.

Irreversibilities

- Heat transfer
- Specific heat variation
- Frictional heat generation
- Regenerator fluid mixing
- Conduction

Figure 6.

S4 1928

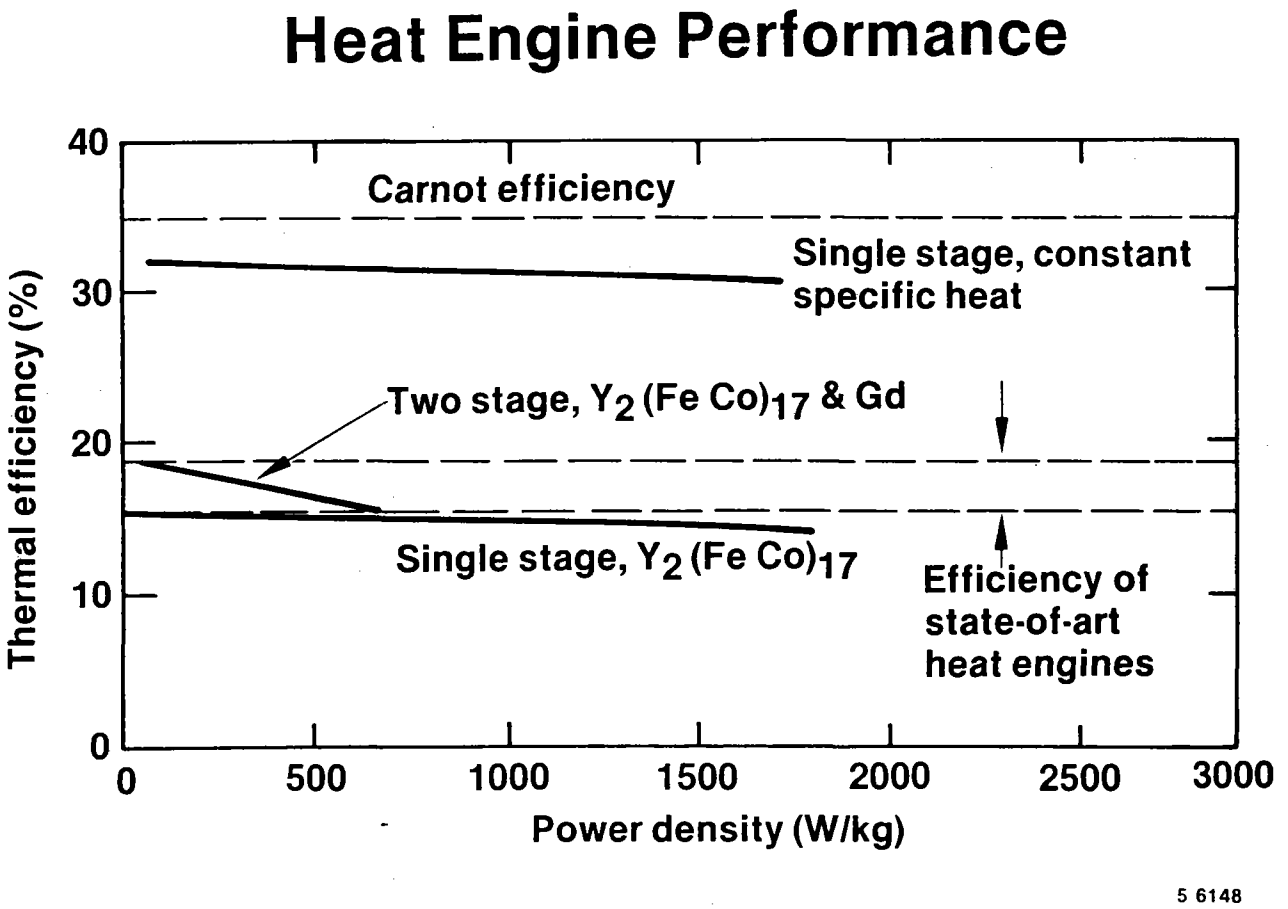
Heat Engine Performance
Thermal efficiency (%)
40
30
20
10
0
Carnot efficiency
Single stage, constant specific heat
Two stage, $Y_2(Fe\ Co)_{17}$ & Gd
Single stage, $Y_2(Fe\ Co)_{17}$
Efficiency of state-of-art heat engines
0
500
1000
1500
2000
2500
3000
Power density (W/kg)
5 6148

Figure 7.

Magnetic Heat Engine History

- Patents by Edison and Tesla
- Studies of TMG's in 1940's and 50's were not optimistic
- Non-regenerative permanent magnet heat engines have been built
- Most magnetic cycle work involves cryogenic refrigeration
  - — Batch cooling near absolute zero for 50 years
  - — Brown (1976) - reciprocal refrigerator
  - — Steyert and Barclay - reciprocal and rotary refrigerators
  - — INEL studying high temperature magnetic heat pumps

5 6150

Figure 8.

Magnetic Energy Cycles

Reasons for Current Interest

1. Superconducting magnet availability
2. Bulk separation of rare earth elements
3. Need for cost effective means to utilize low grade heat
4. Need for efficient means to cool superconducting equipment (power lines, generators, line filters, NMR machines, SCSC, etc.)
5. Inherent efficiency, simplicity, and compactness of magnetic cycle machines

S4 11 672

Figure 9.

Problems and Concerns

- Reciprocal mechanical
  - — ΔT for storage reduces regenerator effectiveness
  - — Regenerator fluid mixing
  - — Pumping work into regenerator fluid
  - — AC losses in magnets

- Rotary mechanical
  - — Adequate field change, profile and magnet cost
  - — Specific heat imbalances
  - — Getting heat in and out
  - — Pumping regenerator fluid
  - — Transmitting sufficient torque

- Field modulation
  - — Energy loss in non-superconducting components
  - — Energy storage
  - — Field change rate
  - — AC losses in magnets

5 6149

Figure 10.

Magnetic Energy Cycle Advantages

1. Flexible
   - Many thermodynamic cycles possible
   - Any temperature span from – 453°F to 2060°F
   - Improved efficiency at part load
2. Efficient - approaches carnot limits
3. Solid working material - reduces pressure comtainment and freezing problems
4. Simple and low cost (if superconducting magnet costs drop)
5. Modular units possible - no economy of scale

S4 11 671

Figure 11.

Possible Applications

1. Cryogenic refrigeration
2. Residential and commercial space conditioning
3. Industrial heat pumps
4. Solar engines and refrigeration
5. Geothermal well-head generators
6. Space and ocean power converters
7. Fusion reactor power converters
8. Efficient and economic heat engines

S4 11 701

Figure 12.

INTRINSICALLY IRREVERSIBLE ACOUSTIC HEAT ENGINES

G. W. Swift, A. Migliori, T. Hofler, J. C. Wheatley
Los Alamos National Laboratory

Intrinsically Irreversible Acoustic Heat Engines

G. W. Swift, A. Migliori, T. Hofler, J. C. Wheatley
Condensed Matter & Thermal Physics Group
Los Alamos National Laboratory, Los Alamos, NM 87545

In a demonstration of an intrinsically irreversible acoustic heat engine, a tube containing a stack of plates is heated at one end and cooled at the other, producing sound at the lowest resonant frequency of the tube. As outlined in Fig. 1, the engine works because the air in the stack of plates is mostly about a thermal penetration depth from the nearest plate, so that the acoustic motion of the air causes it to experience temperature oscillations that are phased with respect to the acoustic pressure oscillations in such a way that net work is done by the air. We call such engines "intrinsically irreversible" because the necessary phasing is caused by the rather poor thermal contact between the plate and the gas a thermal penetration depth away. Not only prime movers but also heat pumps and refrigerators can be designed. The references summarize our current understanding of these phenomena. The agreement between our theoretical work (based on work of N. Rott) and measurements we've made with engines using both air and helium gas thermoacoustic working fluids is good, so we believe we understand these engines well.

Three projects we're currently working on are an acoustic cryocooler, a "beer cooler", and a liquid sodium acoustic primer mover. The acoustic cryocooler, shown in Fig. 2, functions as a refrigerator driven by a modified loudspeaker. A loudspeaker piston P drives the fundamental acoustic resonance in the helium gas in a resonator T-V; heat is thereby pumped from a cold heat exchanger C through a stack of plates S to a hot heat exchanger H. Temperature differences of 100° C and cooling powers of a fraction of a Watt are typical of the results we are getting with this device. The "beer cooler", shown in Fig. 3, is a heat-driven refrigerator designed to absorb heat from a high temperature source, reject heat at room temperature, and thereby remove heat from a load (the beer) just below room temperature. Again, helium gas in a resonator is used; one stack of plates produces sound from heat and another stack uses that sound to refrigerate. The numbers in Fig. 3 are calculated values; this engine is now being assembled.

The liquid sodium acoustic prime mover, the most difficult of our current projects, is shown very schematically in Fig. 4. The thermoacoustic working substance will be liquid sodium instead of a gas. The model engine we are building will have a 1 kHz resonator about a meter long and 10 cm^2 in cross section and should absorb about 5 kW of heat at 700°C, reject about 4 kW at 100°C, and produce about 1 kW of acoustic power. The acoustic power will be converted to electric power either magnetohydrodynamically or by means of a variable reluctance generator (we're experimenting with both) with a high efficiency.

Liquid sodium is an excellent working substance for this kind of engine, for a number of reasons. Its high density (compared to a gas) leads to high power density in the engine. Its low Prandtl number (0.004 at 700°C) makes viscous losses small. Its high electrical conductivity makes magnetohydrodynamic conversion of acoustic power to electric power possible. And its thermal expansion coefficient, while only about a quarter that of a gas, is still adequately large.

We have completed extensive, detailed calculations of the behavior of this engine, and are now assembling components. Although our experience with thermoacoustics in gases has given us confidence in our understanding, our approach, especially toward the liquid sodium engine, is still oriented toward study of fundamental principles rather than optimally engineered designs for specific applications.

REFERENCES

"Theory and Calculations for an Intrinsically Irreversible Acoustic Prime Mover Using Liquid Sodium as Primary Working Fluid," G. W. Swift, A. Migliori, T. Hofler, and John Wheatley, submitted to J. Acoust. Soc. Am.

"Understanding Some Simple Phenomena in Thermoacoustics with Applications to Acoustical Heat Engines." John Wheatley, T. Hofler, G. W. Swift, and A. Migliori, Am. J. Phys., in press.

"An Intrinsically Irreversible Thermoacoustic Heat Engine." J. C. Wheatley, T. Hofler, G. W. Swift, and A. Migliori, J. Acoust. Soc. Am. 74, 153 (1983).

"Experiments with an Intrinsically Irreversible Acoustic Heat Engine," J. C. Wheatley, T. Hofler, G. W. Swift, and A. Migliori, Phys. Rev. Lett. 50, 499 (1983).

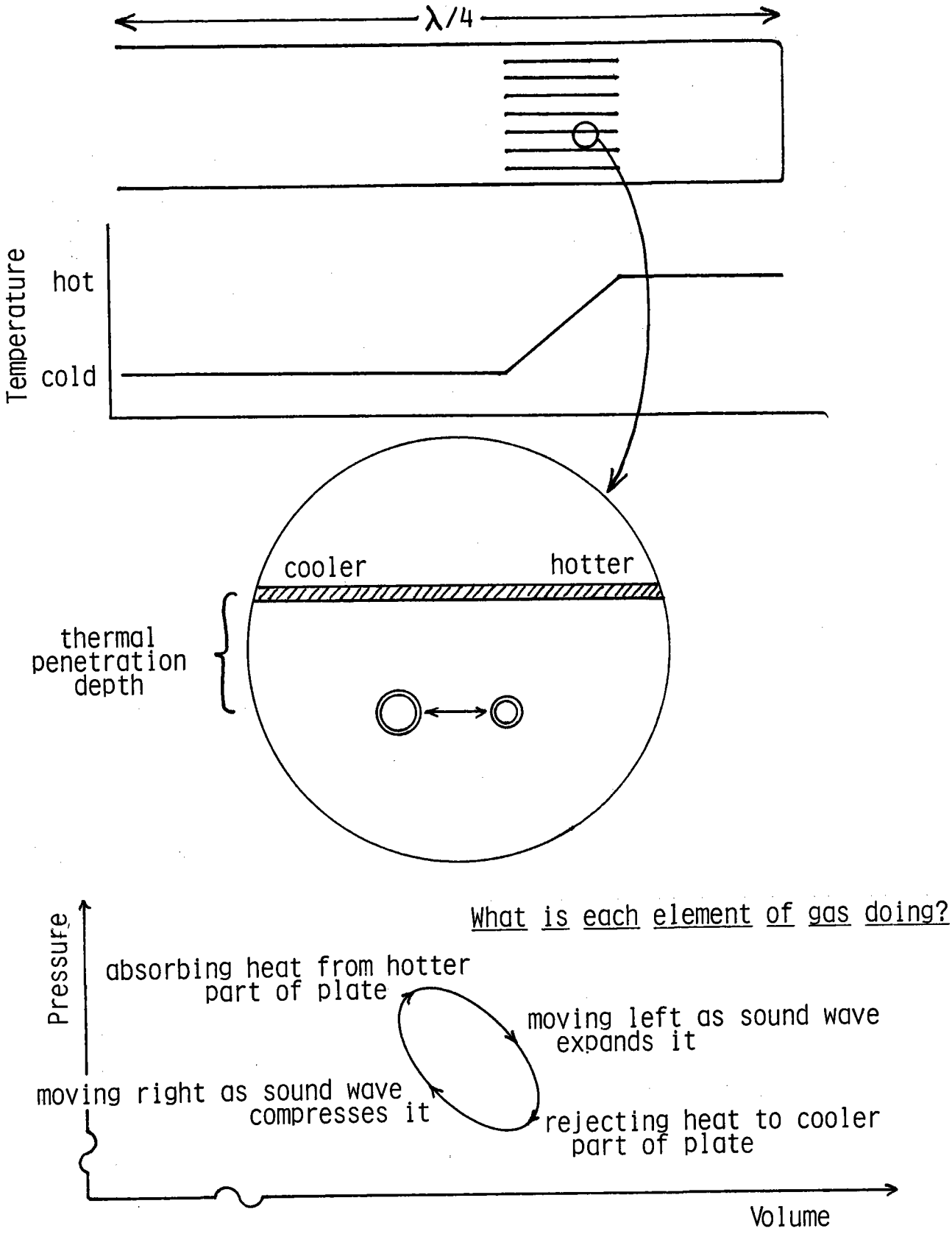

Fig. 1. The demonstration, and how such engines work.

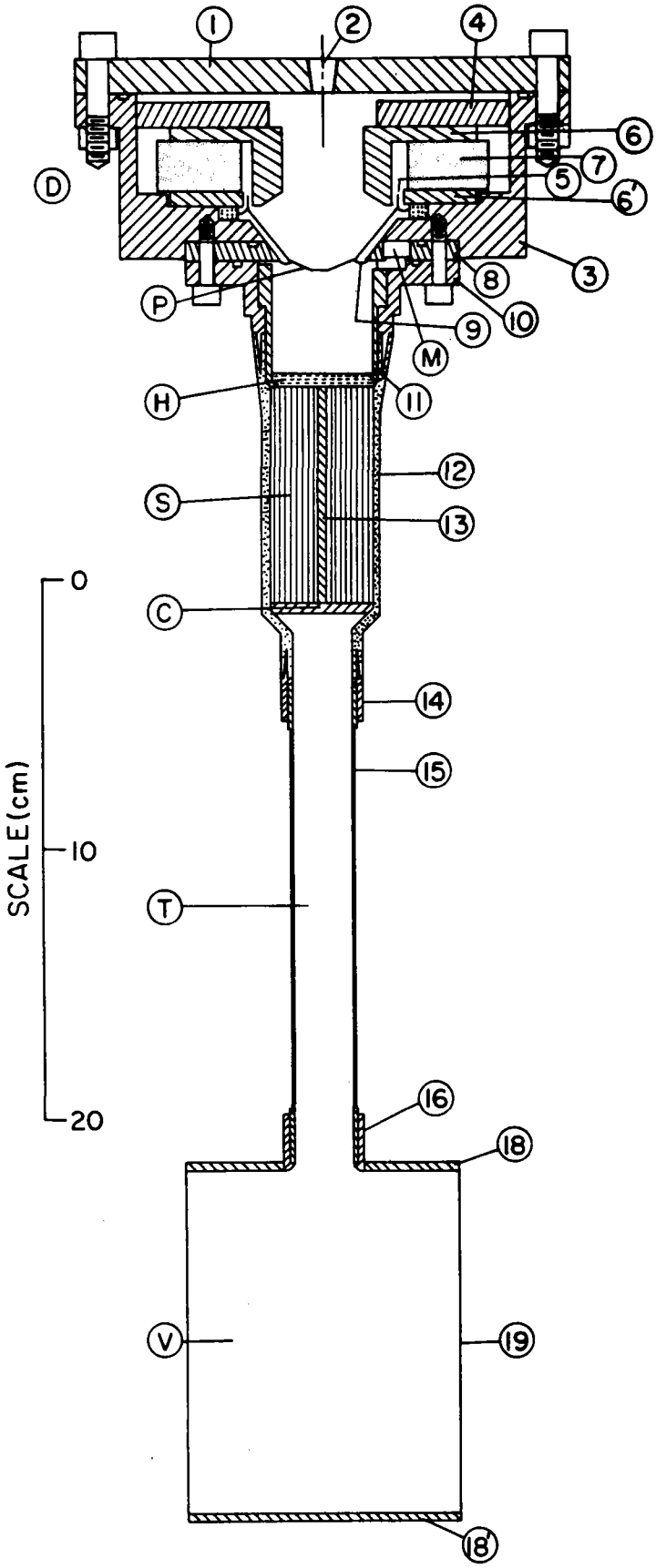

Fig. 2. Acoustic cryocooler.

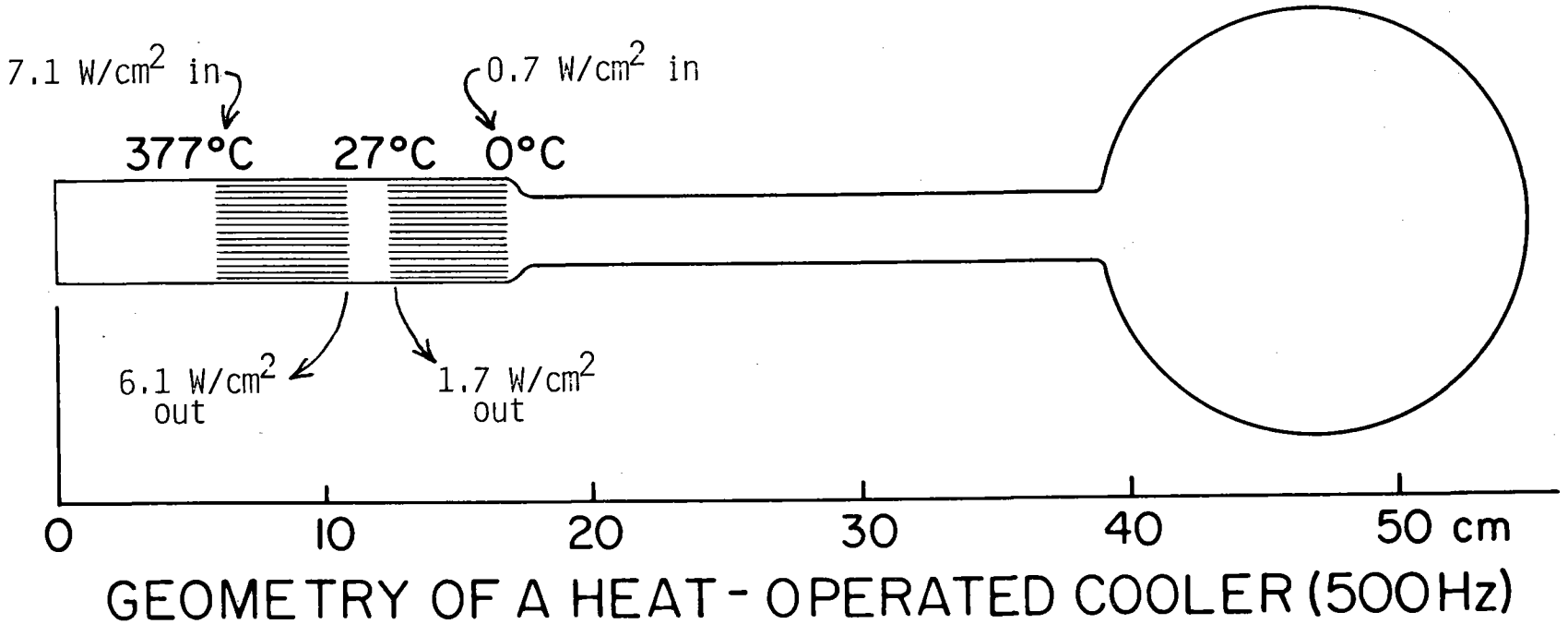

Fig. 3. "Beer cooler" design.

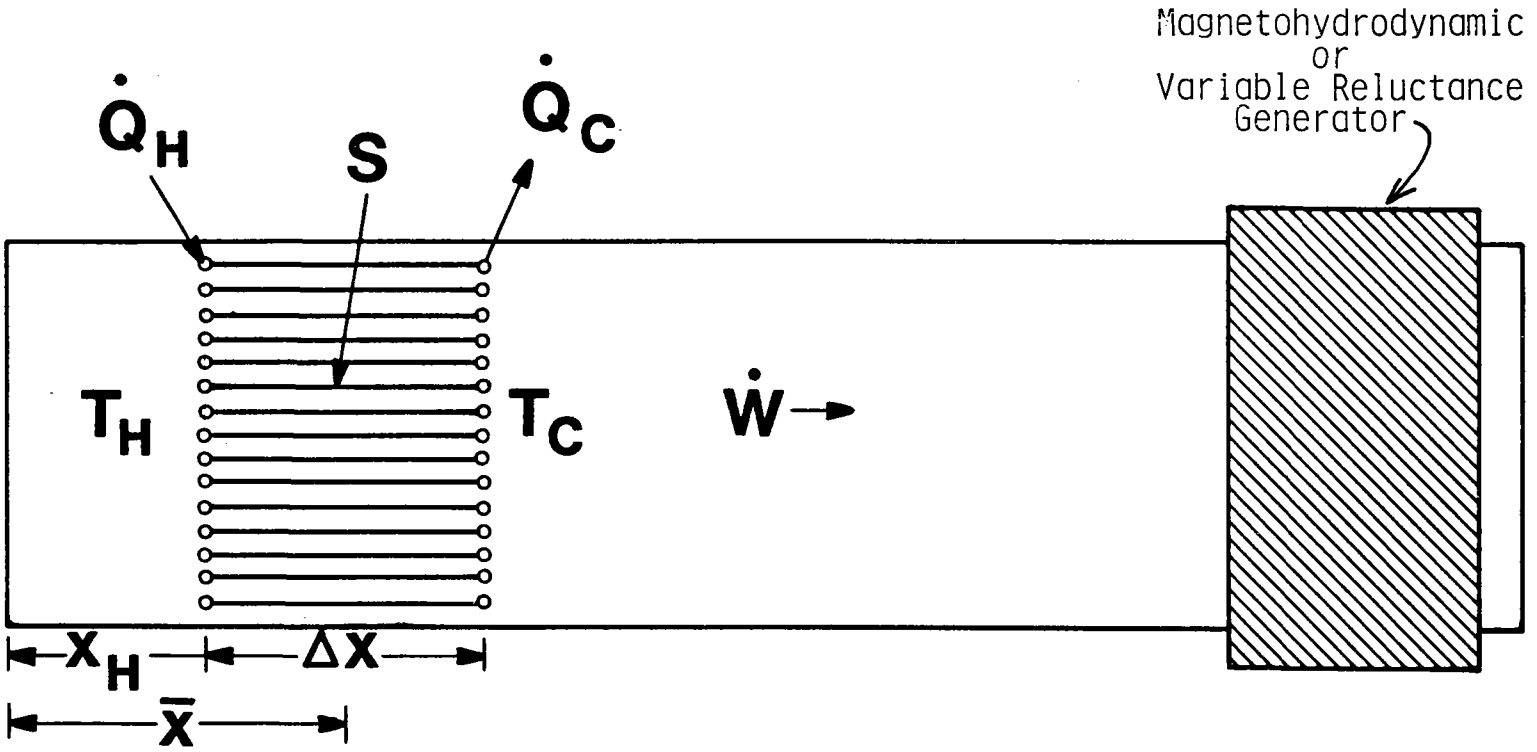

Fig. 4. Schematic, liquid sodium acoustic prime mover.

THERMODYNAMICS OF HEAT ENGINES IN FINITE TIME

Peter Salamon
San Diego State University

Thermodynamics of Heat Engines in Finite Time

Peter Salamon
Department of Mathematical Sciences
San Diego State University
San Diego, CA 92182

The research described below begins with a search for in-principle limitations imposed on the operation of heat engines by the constraint of operation in finite time[1]. The subject of thermodynamics was based on similar searches using idealized heat engines. For real operation, one would like a decompostion of a process into its reversible, intrinsically irreversible, and waste components[2]. While it is tempting to include all the known kinds of irreversibilities in attempting this task, and several authors[2,3] have done so, their results are difficult to obtain and interpret. Furthermore such results lack the generality which characterizes the classical work.

One avenue of approach has succeeded however in moving onto a plane of generality which vies the classical results. It is this direction that I describe below. While its roots are once again in heat engines, this approach can now be applied to virtually any process and promises to change our understanding of the energetics of physico-chemical phenomena.

This approach begins by considering heat engines which come equipped with perfect coupling between work reservoirs and the working fluid. It further assumes that the working fluid and the reservoirs are each in internal equilibrium at well defined temperatures throughout the process. The remaining dissipation is therefore due to coupling between the working fluid and the heat reservoirs. A theory built on these assumptions can provide in-principle bounds by showing a certain amount of dissipation to be necessary even if other aspects of the process were completely idealized.

The theory of Carnot type engines (i.e. engines working between two fixed temperature heat reservoirs) was worked out[4] and resulted in a robust comparison between various optimal operations. This was an important step, since in finite time operation it is not even à priori clear what the appropriate objective function should be. It turns out (see figure) that the efficiency is a poor indicator of merit, while all reasonable optimizations lie somewhere between the extremes of minimizing entropy production (equivalently loss of availability) and maximizing power. Effort then focused on these extremes and both problems have been solved for purely thermal losses in a heat engine using an arbitrary working fluid thermally coupled to a reservoir whose temperature can vary in an arbitrary fashion.

For maximum power it was found[5] that the power output cannot exceed the variance of the product of the conductance to the reservoirs and the square root of the reservoir temperature. When only two reservoir temperatures are used, this reduces to the results of Curzon and Ahlborn[3]. As an example in which the reservoir temperature varies continuously, the bound gives about one milliwatt per square centimeter for the power available from diurnal variations in ambient temperature.

The problem of a pumped working fluid which receives thermal energy at a known rate $f(t)$ gave a very similar bound for available power. Such power is given by the variance of the square root of the pumped thermal energy $f(t)$ plus the conductance times the reservoir temperature[5]. This result should have direct implications for solar conversion, but such implications remain to be explored.

The problem of minimum dissipation as measured by entropy production or availability loss have also been solved[6]. The minimum entropy produced must exceed the square of the variation in the entropy of the working fluid divided by the conductance and the cycle time. This minimum dissipation was later interpreted as the minimum loss associated with forcing the

working fluid to traverse a certain sequence of states in a given time[7].

The general problem of getting a thermodynamic system to traverse a given sequence of states in a given time turns out to be intimately related to distance traversed in a thermodynamic geometry defined on the set of equilibrium states of the system. The dissipation must exceed the square of such distance multiplied by the ratio of the mean time scale on which the system responds to the total time of the process[7]. While this geometry appears to depend on equilibrium, it in fact extends all the way to the quantum mechanical level[8]. The conditions that all participating systems be in internal equilibrium may therefore serve merely to define the level of analysis which must be pursued, and not to limit its generality.

The results above show us a route to the understanding of the intrinsic irreversibility accompanying the finite time evolution of a thermodynamic system. Similar general results for extracting maximum power have not yet been found. It seems clear however that there exists interesting physics in a careful examination of the limits to the achievable.

REFERENCES

1 B. Andresen, P. Salamon, and R. S. Berry, Phys Today, September 1984.
B. Andresen, R. S. Berry, M. J. Ondrechen, Acc. Chem. Res., 17, 226 (1984).
2 B. Andresen, P. Salamon, and R. S. Berry, J. Chem. Phys., 66, 1571 (1977).
3 F. L. Curzon and B. Ahlborn, Am. J. Phys., 43, 22 (1975).
M. H. Rubin, Phys. Rev. A, 19, 1272 (1979); 19, 1277 (1979); 22, 1741 (1980).
Y. B. Band, O. Kafri, and P. Salamon, J. Appl. Phys., 53, 8 (1982).
M. Mozurkewich and R. S. Berry, Proc. Natl. Acad. Sci., U.S.A., 78, 1986 (1981); J. Appl. Phys., 53, 34 (1982).
4 P. Salamon and A. Nitzan, J. Chem. Phys., 74, 3546 (1981).
5 Y. B. Band, O. Kafri, and P. Salamon, J. Appl. Phys., 53, 197 (1982).
6 P. Salamon, A. Nitzan, B. Andresen, and R. S. Berry, Phys. Rev. A, 21, 2115 (1980).
7 P. Salamon and R. S. Berry, Phys. Rev. Lett., 51, 1127 (1983).
J. D. Nulton, P. Salamon, and B. Andresen, "Quasistatic Processes as step equilibrations," submitted for publication, J. Chem. Phys..
8 W. K. Wootters, Phys. Rev. D, 23, 357 (1981).
P. Salamon, J. D. Nulton, and R. S. Berry, "Thermodynamic Length in Statistical Mechanics," to appear, J. Chem. Phys..

Heat Engines in Finite Time

Search for in-principle limits to operation.

TRICYCLE SPACE

(Q_{in}, Q_{out}, W)

Form a vector space.

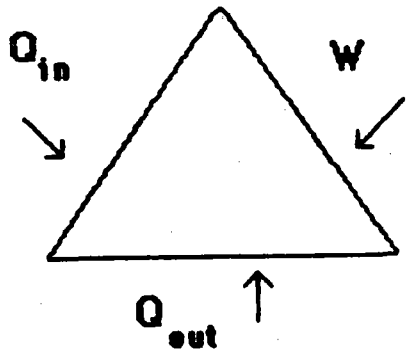

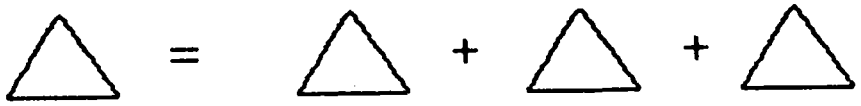

Real | Reversible | Intrinsic Irreversibility | Waste

Constraints of Finite Time Operation

Intrinsic Irreversibility | Thermal | Other

Finite time **Finite heat transfer rate**

Perfect coupling to work source

no inertia
no friction

SERI.1

Carnot Type Engines

Work between two constant temperature heat reservoirs.

The right parameter : σ = entropy carried by working fluid

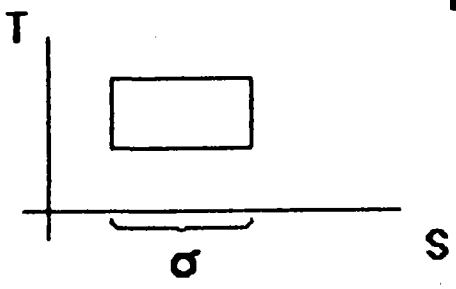

Easy optimizations T constant for heat exchange

τ = 0 for adiabats

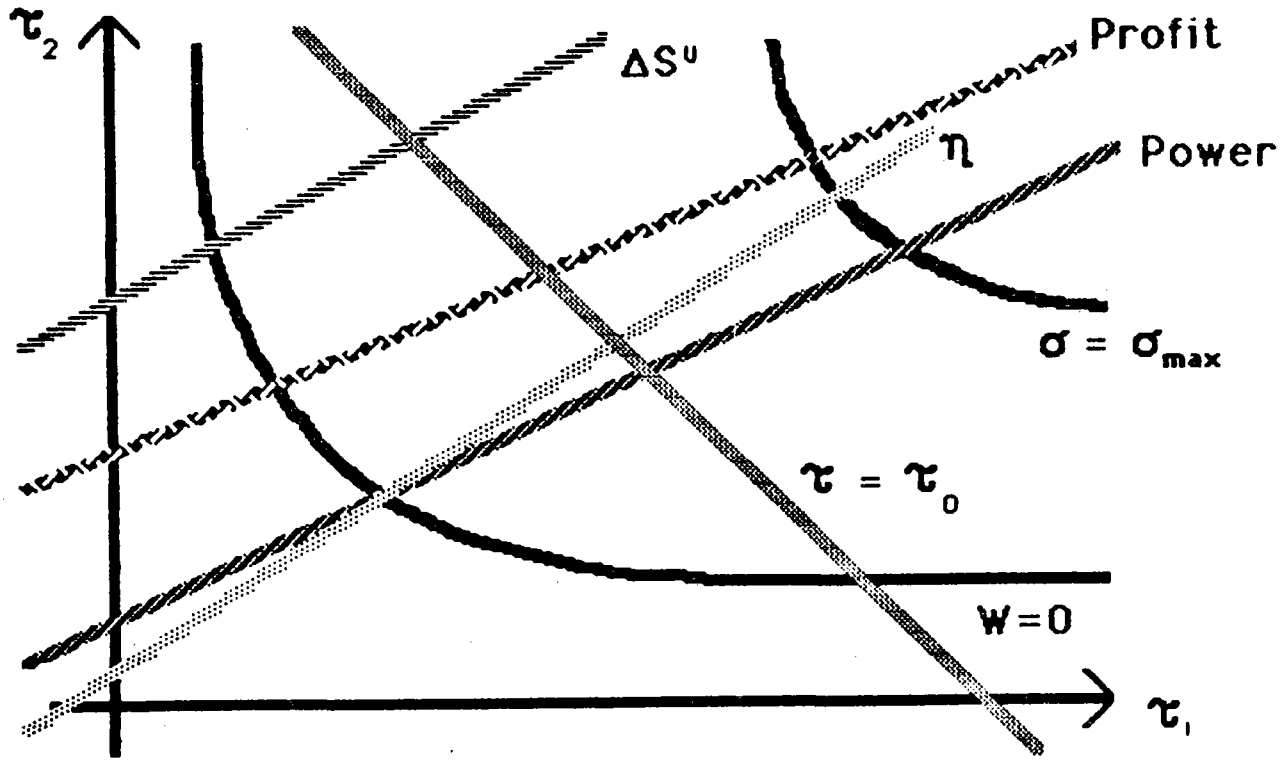

SERI.2

Min — Max

ΔS^* — Power

Cost of time

Either extreme holds new physics in the tradition of Carnot.

Both problems have been solved for an arbitrary working fluid working between arbitrary reservoirs

MAXIMUM POWER

$$\text{POWER} \leq \text{Variance}\ \left(\sqrt{\kappa T^{ex}}\right)$$

$$= \langle \kappa T^{ex} \rangle - \langle \sqrt{\kappa T^{ex}} \rangle^2$$

where $\langle\ \rangle$ indicates time average.

When T^{ex} alternates between two constant temperatures, this reduces to

$$\text{POWER} \leq \kappa \left(\sqrt{T_1} - \sqrt{T_2}\right)^2$$

$$\eta_{\substack{\text{Max} \\ \text{Power}}} = 1 - \sqrt{\frac{T_1}{T_2}}$$

Curzon
Ahlborn
1975

SER1.3

PUMPED WORKING FLUID

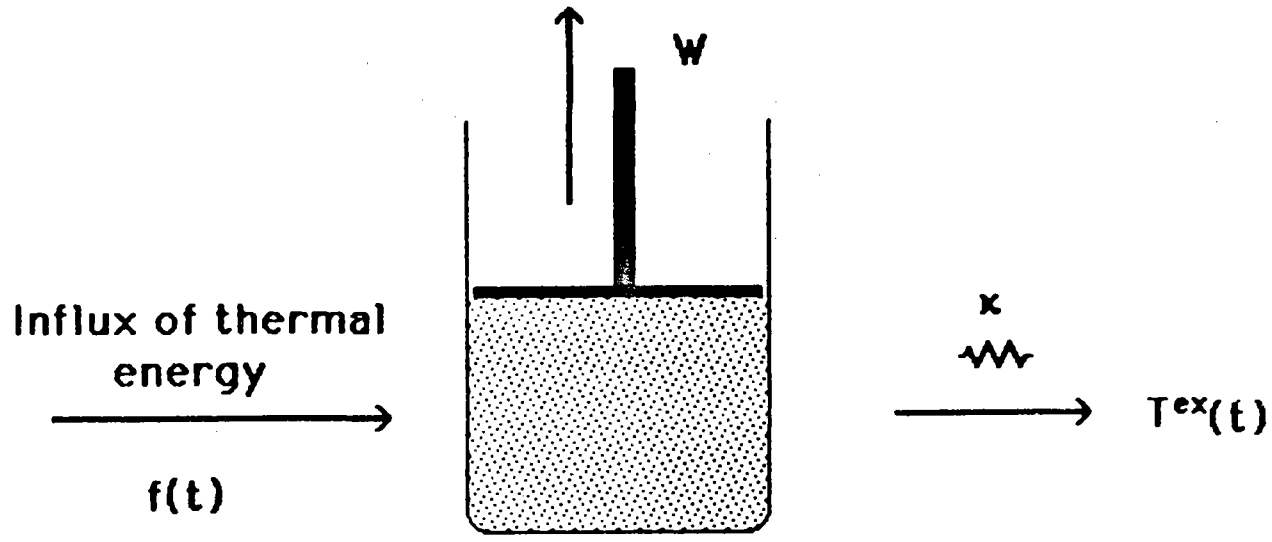

POWER ≤ Variance $\left(\sqrt{f+xT^{ex}}\right)$

Yardstick for assessing quality of operation.

MINIMUM ΔS^u

$$\frac{\Delta S^u}{\tau} \geq \frac{(\text{variation } \sigma)^2}{K\,\tau^2}$$

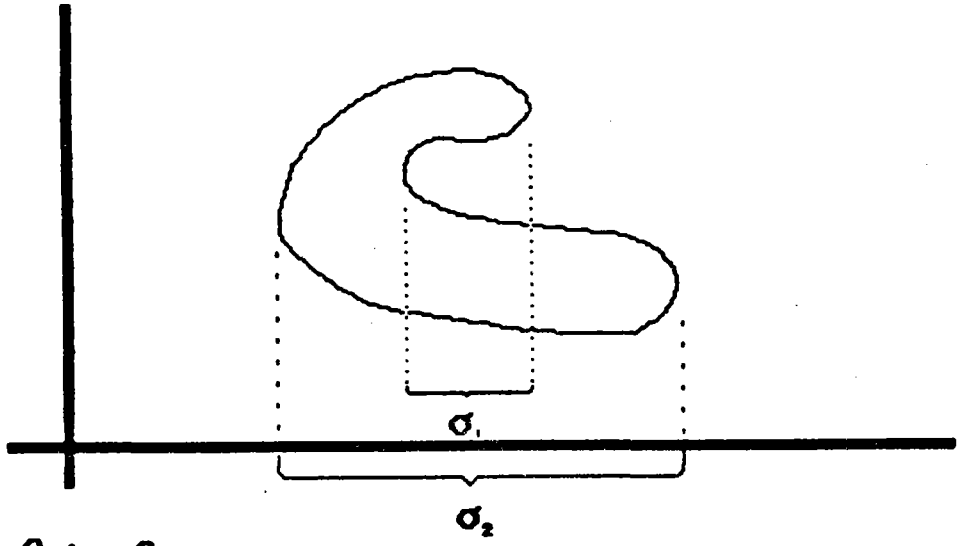

variation $\sigma = 2\sigma_1 + 2\sigma_2$

SERI.4

In retrospect we can see that bounds on dissipation are geometric in nature and result from forcing the working fluid to traverse its sequence of states.

$$\Delta S^u \geq L_s^2 \varepsilon / \tau$$

$$\Delta A^u \geq L_u^2 \varepsilon / \tau$$

where

S^u = Entropy of the universe.

A^u = Availability of universe.

L_s = Thermodynamic length from entropy metric.

L_u = Thermodynamic length from energy metric.

ε = Mean relaxation time.

τ = Total time of the process.

Obtained by optimizing rate along path.

Goes with the metaphor

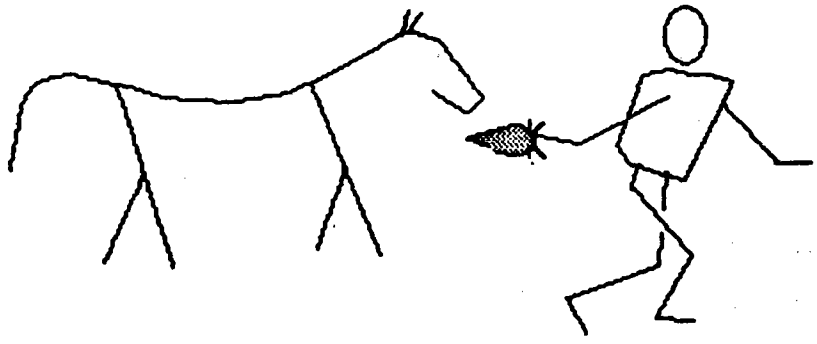

SERI.5

Geometry

Use of bound needs: distances
geometric relaxation times

Statistical mechanical distance = number of statistically distinguishable states

Quantum mechanical distance = angle in Hilbert space

Geometric relaxation times = ordinary relaxation times for slow process

Search for spectral probes of ϵ and relations to time correlations.

Constraints increase distance

Equations of state (active constraints) needed.

Simple systems (e.g. ideal gas) distances and relaxation times known.

COMPOSITE SYSTEM PROBLEM

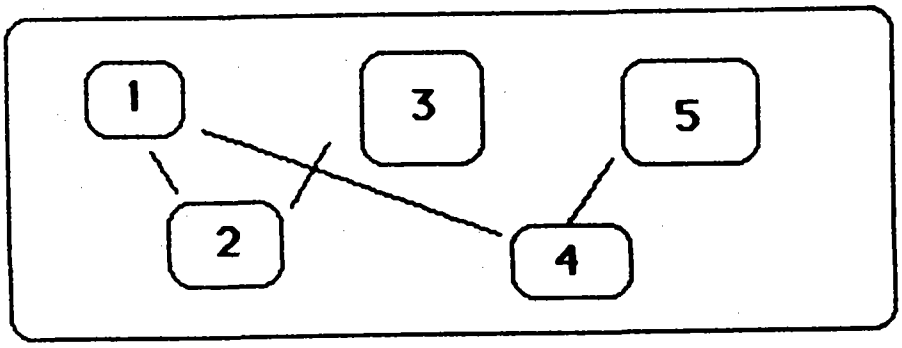

Each subsystem evolves endoreversibly.

(This defines subsystems.)

$$\Delta S^{u} \geq \frac{1}{2} \sum_{i} L^{2}_{s_i} \varepsilon_i / \tau$$

Deviation from this bound provides measure of mismatch.

Range of simply computable bounds

Given: τ

initial and final states

path followed by the system

total fluxes between any pair of subsystems

Can pinpoint potential savings

Real = Reversible + Intrinsic Irreversibility + Waste

Achievable modulo the freedom to do "surgery".

Achievable if enough control.

Should be tried for solar converters.

ELECTROTHERMODYNAMIC EQUATIONS OF A CHARGED AEROSOL GENERATOR

Alvin Marks
Phototherm, Inc.

ELECTROTHERMODYNAMIC EQUATIONS OF A CHARGED AEROSOL GENERATOR

Alvin M. Marks
Advanced Research Development, Inc
P.O. Box 189
Athol, MA 01331

ABSTRACT

An electrothermodynamic (ETD) generator and a compressor is described for use in a Marks/Ericsson Cycle. New equations are derived based on varying the electric charge distribution along the flow axis and new principles based thereon are used in the generator design.

1. INTRODUCTION

A charged aerosol whose charge distribution varies along the flow axis is discussed, by means of which several orders of magnitude of increased electric power and current and decreased voltage is obtained in converting heat/kinetic power to electric power. A charged liquid tin droplet/nitrogen aerosol is used for heat/electric power conversion at about 1800°K. A charged water droplet/nitrogen aerosol is used in the electrothermodynamic compressor at 300°K. This Marks/Ericsson Cycle has a theoretical efficiency of 83%, and a practical efficiency of 60% to 70%. Other cycle components are not here considered. This new ETD generator is known as model 84 ME.

2. BACKGROUND

The background [1] and bibliography [2] of electrothermodynamic (ETD) generators has previously been given. This reports further studies with previously described Methods III [3] and IV [4].

3. DESCRIPTION

Figure 1 shows a cross section of the 84 ME electrothermodynamic generator, a diagram of the electrical connections, the outer curve for the surface of the converging duct, and the inner curve for the surface of the charged aerosol-gas.

In figure 1, a straight duct 1 contains a flowing gas 2 passing into a converging duct 3 and through orifice

FIG. 1

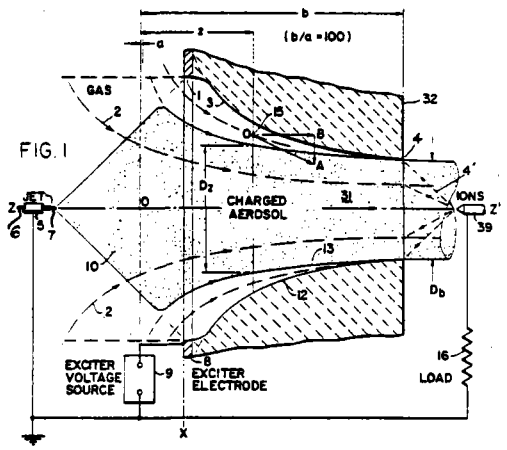

4. A small diameter tube 5 within the duct 1 contains a flowing conductive liquid 6, such as molten tin, Wood's metal, mercury, water, an alcohol, etc. which issues as a liquid jet 7. A voltage source 9 applies an electric field between the jet 7 and the exciter electrode 8. The liquid jet breaks into a large number of small diameter charged liquid droplets. The charged aerosol has a diameter d_a less than the duct diameter D_a, at z=a. Duct 3 converges along an outer curve 12. The charged aerosol expands to diameter d_a at z=a, and converges along an inner surface, which nests within the duct surface. The converging gas stream line has a velocity vector OA, which is resolved into an axial vector velocity component OB, and a normal vector velocity component BA directed towards the z axis, which causes the charged aerosol to be pinched toward the duct axis; and separate from the duct wall 3. This avoids wetting the wall and causing a "short". Duct convergence causes the charged aerosol-gas velocity to increase.

Figure 2 shows a graph of velocity ratio (U_z/U_b) vs. distance ratio (z/b).

FIG.2

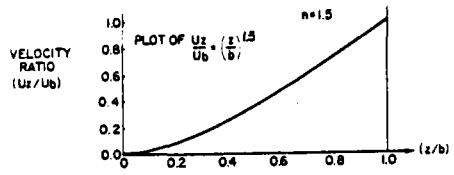

FIG.3

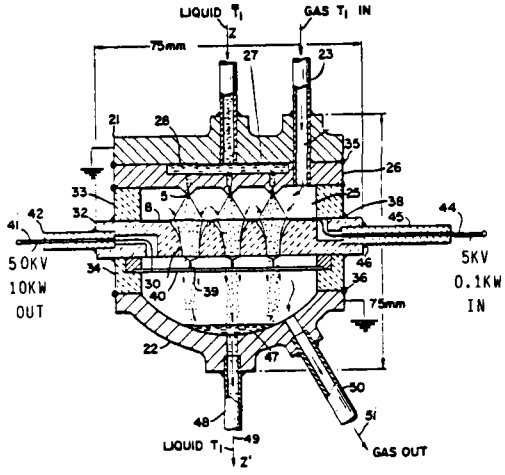

Figure 3 shows a cross-sectional view of the 84 ME electrothermodynamic generator comprising a 9 element array. Each element generates about 1100 watts; the total output is about 10KW @ 100,000 volts and 0.1 amp D.C.. The generator, one component in a Marks/Ericsson Cycle [4], is maintained at its operating temperature T_1 in a furnace; for example 1800°K.

The generator comprises two stainless steel end plates 21 and 22 which are at ground potential. An inlet pipe 23 supplies a gas; for example, air, nitrogen, or other suitable gas or mixture of gases through the entrance port 24 of the end plate 21 to a common chamber 25 in which the gas is temporarily held at a supply pressure, for example 120 atmospheres and at T_1 = 1800°K. The end plate 21 is welded to an intermediate plate 26, which contains a chamber 27 between the two plates. The chamber 27 receives the conductive liquid 28, which enters the chamber at a temperature T_1; for example 2400°K, and at a pump pressure of for example 130 atmospheres. The end plates hold together all the members including the insulating discs, 32, 33 and 34.

The electrothermodynamic power conversion occurs in the ducts 30 which contain charged aerosols 31 within the duct surfaces, formed in a 10mm thick sapphire plate 32. Sapphire is a preferred insulator, non-reactive at these temperatures. At lower temperatures other materials such as quartz may be used, Sapphire-metal joints have been described [5].

The charged aerosols 31 are discharged by ions of opposite sign 4' emitted from points 39. After discharge the neutral droplets no longer repel each other, and coalesce into the liquid which is circulated through the liquid pump and heating coils back to the generator at 28.

The gas enters the generator at pressure p_1 and temperature $T_a = T_1$ through tube 23 in end plate 21; and exits through tube 50 as a gas stream, now separated from the liquid, at pressure p_2 and temperature T_b. Each duct may produce about 1100 watts; a total of about 10KW for 9 ducts contained within a 7.5cm cube.

The electrothermodynamic cycle is substantially reversible.

About 17% of the electric power from the ETD Generator is supplied to the ETD compressor to compress the charged aerosol gas from p_2 to p_1, cooling it almost isothermally at 300°K by the charged water droplets; and increasing its velocity and kinetic power. After discharging the water droplets, the liquid is collected and sent to a heat exchanger heat-sink.

Gas is supplied to the ETD Compressor at pressure p_2 from the heat exchanger. Since its absolute temperature has decreased by the ratio 1800/300=6; the isothermal work done on the gas is decreased. If the ETD Generator has 12 modules producing 12KW at 1800°K, the compact compressor has 2 modules using 2KW.

4. TABLE OF SYMBOLS

Symbol	Description	Units
A	Area	m^2
C	Specific Heat	joules/kg^oK
D	Diameter of Duct	m
E	Electric Field Intensity	v/m
I	Current	amps
J	Exponent of area for the Duct Surface	
K	A Constant	
L	Length along Conversion Space = b-a	m
M	Mach No.	
N	Number	
P	Power	watts
R	Gas Constant - see constants, values of; a ratio	
T	Temperature	^oK
U	Velocity	m/s
V	Potential, electric	volts
a	Distance from origin at z=a	m
b	Distance from origin at z=b	m
d	Diameter of Charged Aerosol	m
e	Electron Charge, see constants	c
f	A Factor	
j	Exponent of (z/b) for cross sectional area of charged aerosol	
k	A Constant	
m	Mass	Kg
n	Exponent of (z/b) for velocity	
p	Pressure	N/m^2
r	Radius	m
z	A distance along the flow axis from origin	m
V	Volume	m^3
α	$\dot{m}_o/\dot{m}_g$	
δ	Density	Kg/m^3
δ_r	Relative density (δ/δ_1) at 273^oK	
γ	Ratio of specific heats c_p/c_v for gas	
ρ	Electric charge density	c/m^3
η	Efficiency P_e/P_q	
ζ	Electric field ratio (E/E_c) at incipient breakdown	
Ω	Molecular weight	
χ	Voltage ratio E_a/E_c	
χ	χ/ζ voltage ratio maximum	
Γ	χ/ζ^2 power ratio maximum	
Δ	Increase or decrease of a value	

Subscripts

L	Length
a	The distance z=a along conversion space z axis from origin
b	The distance z=b along conversion space z axis from origin
c	Constant area duct, constant velocity
d	Duct
e	Electric or Electron
g	Gas
k	Kinetic
o	Droplet
p	Pressure
q	Heat
r	Relative value
s	Sonic
v	Volume
1	Air, at standard conditions, 273^oK and 1 atmos.=1.01×10^5 N/m^2

Superscripts

•	Time Rate
–	Maximum value. When used thus $\bar{x}, \bar{r}$ these ratios are the values at incipient electric breakdown resulting from a n increase in the current by the ratio $1/\zeta$.

Constants, Values of:		Units
K_e	$\frac{1}{2}(\epsilon_0 b_1^2)(\Omega_1/\delta_1)$ $[(1/273\times8314)]=4.00\times10^{-4}$ a constant of the electric power conversion equation	
ϵ_0	8.854×10^{-12} dielectric constant of space	f/m
δ_1	1.273 density of air at 273^oK and 1 atm	Kg/m^3
b_1	3×10^6 electric breakdown field 273^oK, 1 atm, air.	V/m
Ω_1	28.97 average molecular weight of air	
R	8314/Ω, gas constant	joules/K^o-mol
e	1.601×10^{-19} electric charge of the electron	C
n_k	$1-(U_a/U_b)^2$ fraction of output kinetic power.	

5. MATHEMATICAL PHYSICS

5.1 Differential Equation of the Conversion Space.

The generalization of an earlier equation [6] uses a differential form of Gauss' equation. The charge density ρ and area A varies from z=a to z=b:

$$(d/dz)\,(A\,d\,V/dz) = -A\rho/\epsilon_o \qquad (1)$$

$$A_z = A_a(z/a)^j \qquad (2)$$

$$U_z = U_a(z/a)^n \qquad (3)$$

$$\rho_z = I/A_z U_z = (I/A_a U_a)(z/a)^{-(n+j)} =$$

$$\rho_a(z/a)^{-(n+j)} \qquad (4)$$

The differential equation obtained from (1) - (4) is:

$$(d/dz)[(z/a)^j(dV/dz)] = -\rho_a(z/a)^{-n} \qquad (5)$$

5.2 The Electric Field and Current Ratio

The equation (5) is integrated subject to E=dV/dz=0 at z=b. The equation for E is compared for various values of j and n to the Electric Field intensity E_a at z=a, the entrance to the conversion space, for a constant velocity gas in a constant area duct using the equation for E_a previously derived [7]:

$$E_c = -\rho L/\epsilon_o = IL/\epsilon_o UA \qquad (6)$$

$$E_b = b_1 K_a \delta_r = E_c = \overline{IL}/\epsilon_o UA \qquad (7)$$

The electric field intensity ratio ζ_a at z=a is:

$$\zeta_a = E/E_a = \frac{1}{(1-n)[(b/a)-1]}[(b/a)^{1-n}-1] \qquad (8)$$

For U increasing, n>0 and (b/a)>>1; from equation (8):

$$\zeta_a = \frac{1}{(1-n)}\left(\frac{a}{b}\right) \qquad (9)$$

The field ratio ζ_a is small; so large currents can be sustained without electric breakdown. For velocity decreasing n<0:

$$\zeta_a = \frac{1}{(1-n)}(b/a)^{-n} \qquad (10)$$

and the field ratio ζ_a is large. Hence it is preferred to use the conditions for (9). From (7) the maximum current $\overline{I}$ is limited by the breakdown field $E=E_b$. The electric field intensity at z=a is decreased by an increased velocity gradient, n>0; and from (9), the maximum current ratio is

$$(1/\zeta_a) = (n-1)(b/a) \qquad (11)$$

n should be as large as possible, limited by attainable values of (U_b/U_a)=1000. The useful maximum value of n is then, for (b/a)=100; from (3):

$$n = \ln(U_b/U_a)/\ln(b/a) =$$

$$\ln 1000/\ln 100 = 1.5 \qquad (12)$$

From (3) and (11) the current ratio is:

$$1/\zeta_a = (n-1)\,(U_b/U_a)^{1/n} \qquad (13)$$

For (U_b/U_a)=1000 the maximum value of $1/\zeta_a$ = 63.2 at n=1.2. Hence:

$$(b/a) = \ln^{-1}(1/1.2)\ln 1000 = 316 \qquad (14)$$

The variation of electric field intensity ratio ζ with (z/b), is obtained from (5) by integration subject to E=0 at (z/b)=1:

$$\zeta = \frac{1}{(n-1)[(b/a)-1]}(b/a)^{1-n-j}\left(\frac{z}{b}\right)^{-j}$$

$$\left[1-\left(\frac{z}{b}\right)^{1-n}\right] \qquad (15)$$

5.3 The Electric Voltage and Voltage Ratio

The voltage V from z=a to z=b is obtained by a second integration of equation (5), from equation (15), subject to the condition V=0 at z=a.

For comparison, the voltage V_c across L=b-a, for a constant area duct and a constant velocity charged aerosol, is used [7]:

$$V_c = \rho L^2/2\epsilon_o = IL^2/2\epsilon_o AU \qquad (16)$$

A voltage ratio x is defined, and derived from the second integration:

$$x \equiv V/V_c = \left\{\frac{2}{(1-n)[(b/a)-1]^2}\right\}$$

$$\left\{\frac{\left(\frac{b}{a}\right)^{2-n-j}\left(\frac{b}{a}\right)^{1-n}}{(1-j)} + \frac{1-\left(\frac{b}{a}\right)^{2-n-j}}{(2-n-j)}\right\} \qquad (17)$$

Equation (17) simplifies for $(b/a) \gg 1$ and $n > 1$:

$$\chi = [1/(1-j)(2-n-j)](\frac{a}{b})^{n+j} \qquad (18)$$

When the current I is increased to incipient electric breakdown by the current ratio $1/\zeta_a$ from (13); then $\bar{\chi} \equiv \chi/\zeta$ is the corresponding maximum voltage ratio. Hence from (13) and (18)

$$\bar{\chi} \equiv \chi/\zeta = [2(n-1)/(1-j)(2-n-j)](\frac{b}{a})^{-n-j} \qquad (19)$$

For $\bar{\chi}=1$, equation (19) requires these values:

$$\left.\begin{array}{l} n=1.5 \\ j=-0.635 \\ j+n=0.865 \end{array}\right\} \text{ for which } \begin{array}{l} \bar{\chi} = 1 \\ r = 50 \end{array} \qquad (20)$$

For $\bar{\chi}=2$, which may be a maximum useful value:

$$\left.\begin{array}{l} n=1.5 \\ j=-0.85 \\ j+n=0.65 \end{array}\right\} \text{ for which } \begin{array}{l} \bar{\chi} = 2 \\ r = 100 \end{array} \qquad (21)$$

For $n=1.2$, and $j = -0.45$, $\chi = 1$ and

$$1/\zeta = 63.2. \qquad (22)$$

For all values of $\bar{\chi}$, $\bar{\chi}=1$, $\bar{\chi}=2$, etc., the maximum current ratio $1/\zeta$ is the same, since from (13) it depends only on the value of n.

5.4 The Electric Power and the Power Ratio

The maximum power ratio is:

$$\bar{r} = \overline{IV}/I_c V_c = \chi/\zeta_a^2 = \bar{\chi}/\zeta_a \qquad (23)$$

5.5 The Duct Surface

The duct surface contains the flowing gas which converges toward an orifice of diameter D_b. Applying the continuity equation:

$$\dot{m}_g = \delta_a U_a A_a = \delta_b U_b A_b = \delta_z U_z A_z \qquad (24)$$

The equation of the duct surface curve in the YZ plane is derived from (2). J for the Duct surface distinguishes it from the j used for the charged aerosol surface.

$$(D_z/D_a)^2 = (A_z/A_a) =$$

$$(z/a)^J = (b/a)^J (z/b)^J \qquad (25)$$

$$r_z = r_b(z/b)^{J/2} \qquad (26)$$

5.6 The Charged Aerosol Surface

The gas and the charged aerosol mix and flow through the same orifice. The equation of the charged aerosol surface curve is derived similarly to the derivation for the duct curve (26) using a different value of j; but with the same orifice radius r_b at z=b:

$$r_{za} = r_b(z/b)^{j/2} \qquad (27)$$

The region of the duct curve (26) from $(z/b) = (a/b)$ to $(z/b) = 0.20$; and the region of the charged aerosol curve from $(z/b) = (a/b)$ to $(z/b) = 0.10$ are discarded. In these regions, the curves diverge rapidly to a large value. A duct entrance diameter $D_a = 10$mm and an orifice diameter of 3.7mm may be used.

5.7 Uncoupled Flow

The continuity equations (24) apply only to the gas in the duct but not to the charged aerosol. By "uncoupled flow" is meant that the area exponent for the duct J and the area exponent for the charged aerosol, j, have different values; but the gas and the charged aerosol, assumed to have a charged droplet of near zero mobility, are both subject to the same velocity gradient.

Figure 1 shows curve r_z vs. (z/b) for the duct surface, and the curve r_{za} vs. (z/b) for the charged aerosol surface; using J=-1.41 for the duct; and j=-0.65 for the curve of the charged aerosol surface, for (b/a)=100:

$$r_z = 1.85\ (z/b)^{-0.705} \qquad (28)$$

$$r_{za} = 1.85\ (z/b)^{-0.325} \qquad (29)$$

The velocity ratio curve of Figure (2) is plotted from

$$(U_z/U_b) = (z/b)^{1.5} \qquad (30)$$

5.8 Charged Aerosol Formation

In Figure 1, the liquid jet is at a greater temperature than the gas. The

electric field breaks the jet into small droplets charged by induction, and the charged droplets mutually repel each other. A sudden expansion occurs, resulting in a large value of n at the liquid jet. The maximum voltage generated in the cone $\bar{x}=0.0125$, calculated from (19), is small, exceeded by the voltage between the exciter ring 8 and the liquid jet 7, resulting in a large current. The electric power expended in the formation of the charged aerosol is 0.1-1% of the output electric power[8].

5.9 Isothermal Heat/Electric Power Conversion

The gas and the charged aerosol droplets enter the conversion space at the same temperature. As electric power is converted from the heat content of the charged aerosol gas along the conversion space, heat power is provided by the decrease in enthalpy of the gas as it cools by a temperature ΔT; that is $\Delta\dot{Q}_1 = \dot{m}_g C_p \Delta T$ (31)

and by the change in heat content of liquid droplets:

$$\Delta\dot{Q}_2 = \dot{m}_o C_o \Delta T = \alpha \dot{m}_g C_o \Delta T \quad (32)$$

The temperature changes ΔT in (31) and (32) are equal and simultaneous, and the total heat power provided to the gas is: $\Delta\dot{Q} = \Delta\dot{Q}_1 + \Delta\dot{Q}_2$ (33)

$$C_p = R\gamma/(\gamma-1) = (8314/\Omega)[\gamma/(\gamma-1)] \quad (34)$$

$$P_q = \Delta\dot{Q} = [\alpha C_o/R + \gamma/(\gamma-1)]\dot{m}_g R\Delta T \quad (35)$$

The heat power P_q provided to the gas is converted to electric power and to kinetic power, due to velocity increase. The kinetic power is small compared to the electric power output. The temperature of the gas and the charged droplets, and the gas pressure and density decrease.

For a gas and a metal droplet which have a temperature decrease $\Delta T \ll T$, the expansion is polytropic, almost isothermal [9]; from (35):

$$P_q = \dot{m}_g RT \ln(p_1/p_2) = \dot{m}_g R\Delta T\left[\frac{\alpha C_o}{R} + \frac{\gamma}{\gamma-1}\right] \quad (36)$$

$$\ln(p_1/p_1) = \left[\frac{\alpha C_o}{R} + \frac{\gamma}{\gamma-1}\right]\frac{\Delta T}{T} \quad (37)$$

If the liquid tin droplet and nitrogen heat contents are equal:

$$\alpha = (R/C_o)[\gamma/(\gamma-1)] = \frac{8314}{28 \times 218.4} \times \frac{1.4}{0.4} = 4.76 \quad (38)$$

Putting these values into (37) for $(p_1/p_2)=2$, $(\Delta T/T)=0.1$; the heat/electric power conversion is approximately isothermal; the electric power converted in a charged aerosol is [10]:

$$P_e = \tfrac{1}{2}\varepsilon_o b_1^2 (b_g K_a)^2 \delta_r^2 UA\Gamma \quad (39)$$

This equation may be expressed in terms of the mass flow rate, $\dot{m}_g$ with important consequences. In (39), multiply and divide through by the density δ, and by R; and use the lumped constant K_e to obtain:

$$\dot{m}_g = \delta AU = \delta \dot{V}_g \quad (40)$$

$$(\delta_r/\delta) = (1/28.97)(\Omega/\delta_1)(T/273) \quad (41)$$

$$P_e = K_e (b_g K_a)^2 \dot{m}_g RT\delta_r\Gamma = 4\times10^{-4}(b_g K_a)^2 \dot{m}_g RT\delta_r\Gamma \quad (42)$$

The equation for electrothermodynamic power conversion is:

$$P_q = \dot{m}_g RT \ln(\delta_1/\delta_2) = P_e + P_k \quad (43)$$

In (43), P_k is the heat power converted to kinetic power, and exhausted from the orifice at $(z/b) = 1$:

$$P_k = \tfrac{1}{2}(\dot{m}_o + \dot{m}_g)(U_b^2 - U_a^2) \quad (44)$$

$$P_k = \eta_k \tfrac{1}{2}\dot{m}_g(1+\alpha)U_b^2;\ \eta_k = 1 \text{ since } U_b \gg U_a \quad (45)$$

The sonic velocity U_s is:

$$U_s^2 = \gamma RT \quad (46)$$

For a charged aerosol gas, the sonic velocity is U_s^1

$$\tfrac{1}{2}(1+\alpha)\dot{m}_g U_s^1 = \tfrac{1}{2}\dot{m}_g U_s^2 \quad (47)$$

in terms of Mach No. M:

$$U_b = MU_s = (M/\sqrt{1+\alpha})U_s \quad (48)$$

$$P_k = \tfrac{1}{2}\dot{m}_g RT\gamma M^2 \text{ ; since } \eta_k = 1 \quad (49)$$

From (42), (43) and (49):

$$\dot{m}_g RT \ln(\delta_1/\delta_2) = K_e(b_g K_a)^2 \dot{m}_g RT \delta_r r + \tfrac{1}{2}\dot{m}_g RT \gamma M^2 \quad (50)$$

For P_k to be negligible:

$$\tfrac{1}{2}\gamma M^2 << \ln(\delta_1/\delta_2) \quad (51)$$

Subject to (51), this important criterion results:

$$\delta_r r = [1/K_e(b_g k_a)^2]\ln(\delta_1/\delta_2) \quad (52)$$

Example

Given gas: air, electric breakdown factor $b_g k_a = 1$ ambient or 0.5 at 1800°K (53)

Sonic velocity at 1800°K

$$U_s = (\gamma RT)^{\frac{1}{2}} = (1.4 \times \frac{8314}{28.97} \times 1800)^{\frac{1}{2}} = 850 \text{m/s} \quad (54)$$

Orifice velocity:

$$U_b = 0.2 U_s^{\,1} = 0.2 \times 850/(1+4.76)^{\frac{1}{2}} = 70.8 \text{m/s} \quad (55)$$

Gas density at orifice δ =

$$\Omega_r \delta_1 \frac{273}{T} \delta_r = 1 \times 1.273 \times \frac{273}{1800} \times 20 = 3.86 \text{Kg/m}^3 \quad (56)$$

The mass flow rate is decreased by the charged liquid tin droplets it contains. The area of orifice, for a diameter $D_b = 3.7$mm is:

$$A_b = \frac{\pi}{4}(3.7 \times 10^{-3})^2 = 1.075 \times 10^{-5} \text{m}^2 \quad (57)$$

$$\dot{m}_g = \delta_g A_b U_b = 3.86 \times 1.075 \times 10^{-5} \times 70.8 = 2.94 \times 10^{-3} \text{Kg/s} \quad (58)$$

From (43) the electric power output is

$$P_e = P_q - P_k = \eta P_q = \eta \dot{m}_g RT \ln(p_1/p_2) \quad (59)$$

for $\eta = 0.94$ and $(p_1/p_2) = 2.1$:

$$P_k = (1-\eta)P_q = 0.06 P_q \quad (60)$$

$$P_e = 0.94 \times 2.94 \times 10^{-3} \times \frac{8314}{29} \times 1800 \times \ln 2 = 1059 \text{ watts} \quad (61)$$

Using the criterion (52) to find δ_r:

$$\delta_r r = [1/k_e(b_g k_a)^2]\ln(p_1/p_2) = [\tfrac{1}{4} \times 10^4 \times 1]\ln 2.1 = 1854 \quad (62)$$

For $r = 50$, $\delta_r = 37$; and for $r = 100$, $\delta_r = 18.5$ For $\bar{x} = 1$, $\bar{x} = 2$, and $j = -0.635$ and -0.85 respectively; which implies that the charged aerosol surface curves vary; obtained by increasing or decreasing the exciter voltage, the load resistor 16, or the pressure ratio p_1/p_2.

5.10 Liquid/Gas Volume Flow Ratio

The liquid mass flow rate is:

$$\dot{m}_o = \alpha \dot{m}_g = \delta_o U_o A_o = \delta_o \dot{V}_o \quad (63)$$

$$\dot{V}_o = (\alpha/\delta_o)\dot{m}_g \quad (64)$$

From (40), (41) and (64):

$$R_{og} = [(\delta_1/\delta_o)\Omega_r 273]\,(\alpha \delta_r/T) \quad (65)$$

For these conditions the volume ratio R_{og} of liquid to gas is about 3/1000; but the mass ratio is 4.76.

5.11 Area and Diameter of the Liquid Jet Orifice

$$A_o = \dot{m}_o/\delta_o U_o = \alpha \dot{m}_g/\delta_o U \quad (66)$$

Example Given: $\dot{m}_g = 2.94 \times 10^{-3}$kg/s from (58); $\alpha = 4.76$ from (38); $\delta_o = 5750$ kg/m^3; and U_o = 10m/s, find A_o and D_o. From (66):

$$A_o = 4.76 \times 2.94 \times 10^{-3}/5750 \times 10 = 2.4 \times 10^{-7} \text{m}^2 \quad (67)$$

$$D_o = [\frac{4}{\pi} \times 2.4 \times 10^{-7}]^{\frac{1}{2}} = 5.5 \times 10^{-4} \text{m} = 0.5 \text{mm} \quad (68)$$

5.12 Jet Power Input:

$$P_o = \tfrac{1}{2}\dot{m}_o U_o^{\,2} = \tfrac{1}{2}\alpha \dot{m}_g U_o^{\,2} = \tfrac{1}{2} \times 4.76 \times 2.94 \times 10^{-3} \times 10^2 = 0.70 \text{ watts} \quad (69)$$

5.13 Droplet Diameter and Electric Charge

For optimum mobility [11] there is 1 electron per 100 Å Dia. droplet.

$$N_e = d_o/100 = d_o \times 10^{10}/100 = 10^8 d_o \quad (70)$$

$$\dot{N} = \dot{m}_o/(\pi/6)d_o^{\,3}\delta_o = \alpha \dot{m}_g/(\pi/6)d_o^{\,3}\delta_o \quad (71)$$

$$I = \dot{N} N_e e = [\alpha \dot{m}_g/(\pi/6)d^3{}_o \delta_o][10^8 d_o]e \quad (72)$$

$$d_o = 7.29 \times 10^{-8}(\alpha \dot{m}_g/I)^{\frac{1}{2}} \quad (73)$$

The droplet dia. d_o and the number of charges N_e per droplet is:

$$d_o = 7.29 \times 10^{-8}(4.76 \times 2.94 \times 10^{-3}/\times 10^{-3})^{\frac{1}{2}} = 0.84 \times 10^{-6} \text{m} = 0.84 \mu\text{m} \quad (74)$$

$$N_e = 0.84 \times 10^{-6} \times 10^8 = 84 \text{ electrons/droplets} \quad (75)$$

6. DISCUSSION

Figure 4 shows log power ratio Γ versus n for various values of j. The power ratio Γ increases rapidly as the velocity exponent n increases, with peaks at values of n according to the value of j;

FIG. 4

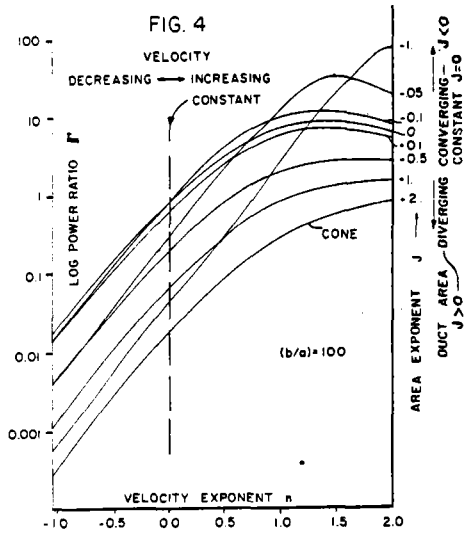

The power ratio curves show that in every case the peak occurs at increasing velocity ratio n>1.2, for (b/a)=100.

Figure 5 shows a graph of log current ratio $1/\xi_a$ versus n for various values of j.

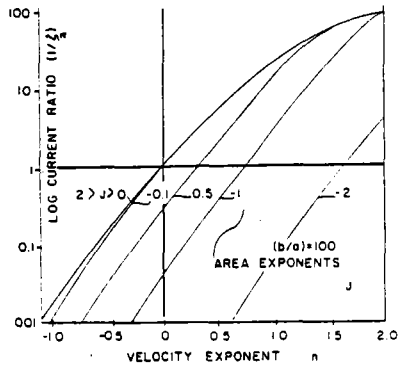

FIG. 5

Figure 5 shows that the current ratio increases with n. The increase occurs even for n<0 for decreasing velocity for straight or converging ducts j<0.

Figure 6 shows a graph of the log of maximum voltage ratio $\bar{x}$ versus n for various values of j. The maximum voltage ratio $\bar{x}$ is small for all values of n for j>0.5. For a cone j=+2, and $\bar{x}$=.01 for all values of n. For j=-0.5, $\bar{x}$=1, but decreases for j from -2 to -0.5.

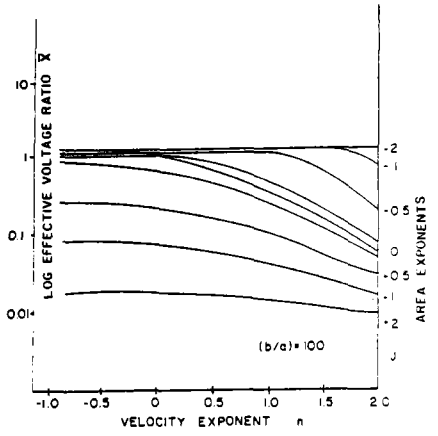

FIG. 6

Figure 7 shows a graph of the Electric Field Intensity Ratio (E/E_a) versus (z/b) for j=-0.1 and various values of n.

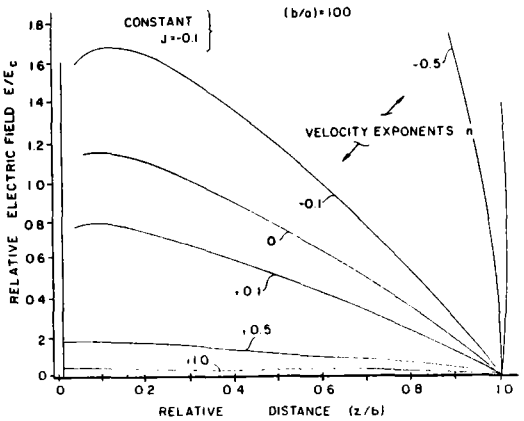

FIG 7

Figures 7 and 8 show the Relative Electric Field intensity ratio (E_z/E_a) versus (z/b) from 0 to 1 along the conversion space for j = -0.1, a slightly converging duct; Figure 8 with an expanded scale.

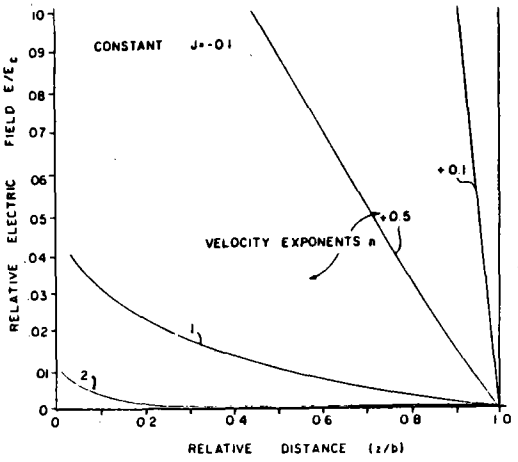

FIG 8

For increasing velocity ratio n>0.5 the peaks in (E_z/E_a) vs. (z/b) disappear, and for larger values of n>1.5 are flat for all (z/b). The greatest electric field intensity occurs at z=a for n>1.5.

Important results are summarized in Table 1 for various shapes of charged aerosol surfaces and velocity ratios.

7. SUMMARY

New electrothermodynamic equations of a charged aerosol are obtained by integrating the differential form of Gauss' law: $d/dz\,[A(dV/dz)] = -\rho A/\varepsilon_0$, where z is the distance along the flow axis from a to b and the electric charge density $\rho = I/AU$; the current I being constant, but the area A varying as the function $(z/a)^j$, and the velocity U varying as the function $(z/a)^n$.

Equations are derived for the electric field intensity, voltage, current and electric power output as functions of j, n, and (b/a). These equations are subjected to geometric and thermodynamic constraints yielding new and useful results, for divergent, constant area and convergent flows. Values of j, n and (b/a), and the corresponding thermodynamic variables, density, pressure and temperature are selected for an optimum configuration.

These new principles are applied to engineer a practical [12.5 KW, 50,000 volt D.C.] generator for use in a Marks/Ericsson Cycle. This compact electrothermodynamic power may be inverted to 120 volt, 60 Hz A.C. power.

8. REFERENCES

U.S. Patent 4,395,648 issued July 26, 1983 to Alvin M. Marks.

1. Background: Cols 2-8
2. Bibliography Cols 51 and 52
3. Method III Cols 31-44 Col 32 Equ. (122) and Col 34 Equ. (145)
4. Method IV Cols. 44, 45 Figs. 26, 28-30 incl.; Cols. 46-51 incl.
5. Col. 11, lines 38-48
6. Col. 32, Equ. (122)
7. Col. 52 ref. 7 also see Col 4 lines 10-30
8. Bottom Col 4, top Col 5
9. Col. 46, Equ. (197)
10. Col. 34, Equ. (145)
11. Col. 52, Refs. 7, 26

TABLE 1

Shows Peak Power, Voltage and Current Ratios: $\bar{\Gamma}$, $\bar{x}$ and $1/\zeta$ respectively, versus j and n for (b/a)=100; for various ducts.

j	n	Current Ratio $1/\zeta$	Volt Ratio $\bar{x}$	Power Ratio $\bar{\Gamma}$	Duct Shape
Equ. No		(11)	(19)	(23)	
1.99	4	297	0.005	1.50	Exp Cone
0.999	3.8	277	0.007	2.00	Expanding
0.50	1.6	63.5	0.055	3.49	Expanding
0.10	1.4	47.1	0.169	7.98	Expanding
0.00	1.4	47.1	0.217	10.2	Straight
-0.10	1.2	33.0	0.40	13.3	Converging
-0.50	1.5	50.0	1.00	50.0	Converging
-0.50	1.4	41.9	0.89	41.9	Converging
-0.999	2.0	100	0.99	99.5	Converging
-1.999	3.0	198	1.31	26.1	Hyperboloid

For larger values of (b/a), the power peaks are greater.

SCIENCE & MECHANICS

AMAZING TIN-AEROSOL GENERATOR

With a remarkable 70 percent efficiency, it can cut conventional fuel usage in half/BY JORMA HYYPIA

Electric power is something we all take pretty much for granted until a power outage turns off the lights, toaster, coffee pot, electric shaver, heating system, television, radio, and just about everything civilized people seem to need to make it through each day. Those are the times when we wish for our own, independent sources of electrical power that cannot be disrupted by a tree limb falling on a power line miles away. It's just possible that one day you will have your own electrical power plant—one that has virtually no moving parts, and that can convert any available source of heat into electrical power by means of an aerosol spray consisting of molten tin.

The Marks-Ericsson ETD Heat-to-Electric Power Generator described here just might be the answer. It promises remarkably high heat-to-power conversion efficiency (83 percent in theory and possibly 70 percent in practice), silent operation, virtually no maintenance problems, and low initial cost (only about 20

The artist's conception below shows what a Marks-Ericsson ETD generator for the home might look like. Such a unit could provide 15 kilowatts of power using oil, gas, wood or even solar energy.

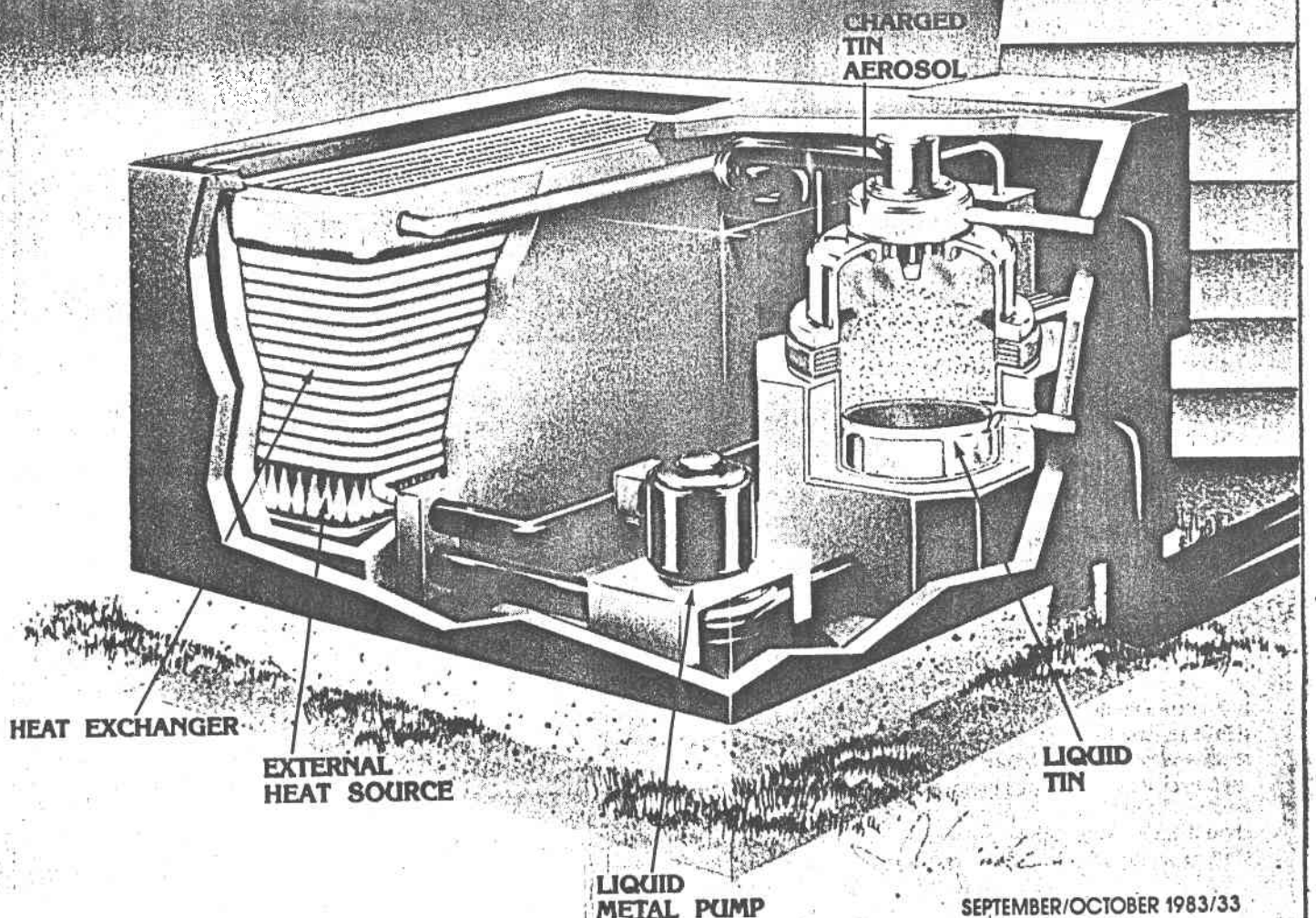

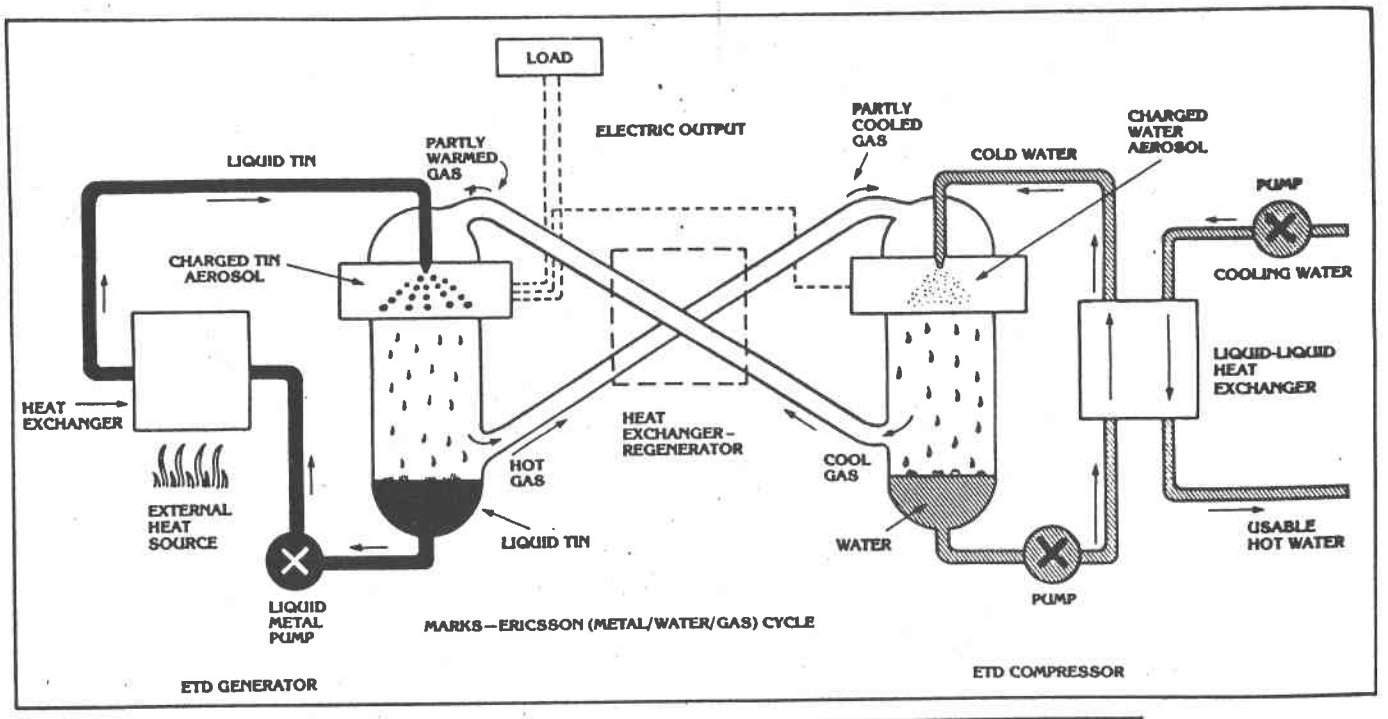

TIN-AEROSOL GENERATOR

percent of the cost of standard generators that require the use of such mechanical components as turbines and compressors). It also offers the potential of being fueled by any practical source of heat, including oil, gas, wood, and solar energy. The real kicker is that this system is claimed to provide twice as much electrical power per unit of heat as can any conventional generating system; put another way, there's the possibility of cutting electric power fuel requirements in half, according to the inventor.

This patented invention (pat. #4,395,648) is the brainchild of Alvin M. Marks, founder of Marks Polarized Corporation (Whitestone, NY), who has spent decades exploring the potentials of power generation using various applications of charged aerosols. (Much of the work has been supported by federal funding.) His primary inspiration was to generate electricity in much the same way that nature creates lightning using charged water particles in rapidly moving air. Although Mark's first experiments concentrated largely on similar water-aerosol systems, his current idea involves the injection of an aerosol, consisting of charged particles of molten metal (tin or gallium, for example), into a stream of hot, inert, nitrogen gas. Marks envisions use of 15-kilowatt units in private homes, and 200- to 300-kilowatt models to serve factories, offices and apartment houses.

Thermodynamic Primer. To better understand how heat can be converted directly—electrothermodynamically—into usable electricity, without need of conventional turbines and generators, we should touch very lightly on some established thermodynamic concepts.

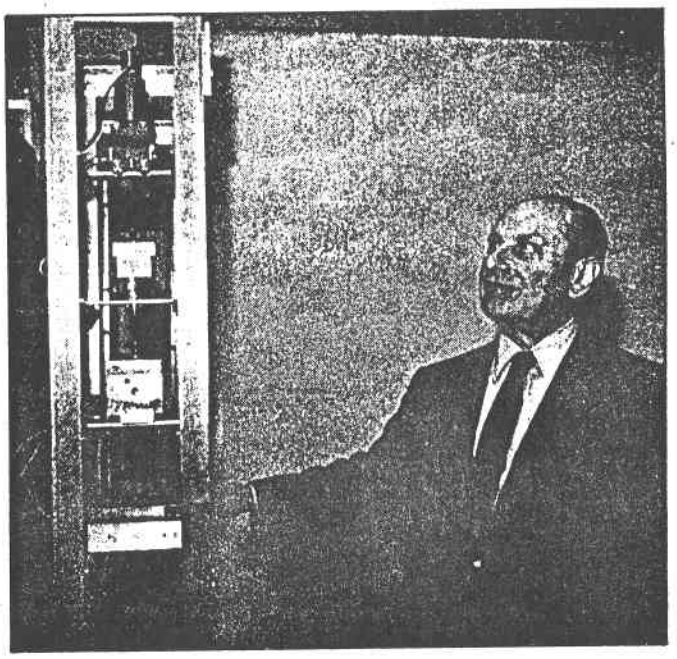

A diagram of the ETD, above, shows the cycles of molten tin, cold water and gas. See text of how they work to generate power. At left, inventor Alvin Marks poses beside a prototype of his revolutionary device.

First, it's helpful to think of heat in terms of "quantities" and "potentials" that are analogous to amperes and volts when dealing with electricity. Temperature in this case corresponds to volts while heat flow (measured in BTUs or joules per second, for example) corresponds to amperes.

In an electrical circuit, power is related to voltage; for instance it might be 120 volts across an operating motor. When dealing with heat, the potential (or driving force) is the *temperature drop* within the system. Bear this in mind when we discuss the low and high temperature stages in the Marks EDT system.

Those who have studied physics may be familiar with the so-called Carnot Cycle, a thermodynamic concept credited to a French physicist who lived around the turn of the 18th century. Carnot found that the theoretically ideal efficiency of any thermodynamic process is equal to the drop in temperature divided by the absolute temperature. In simple arithmetic terms, it therefore becomes obvious that as the temperature drop (the difference between the high and low temperatures in a system) is increased, division by the absolute temperature must yield a larger quotient. That quotient represents the efficiency of the system. Physics buffs should be interested to know that the Marks EDT generator, which is based largely upon the Carnot principle, holds promise of very high efficiency because it utilizes a much higher temperature drop than do other generating systems.

Marks, like all other modern scientists,

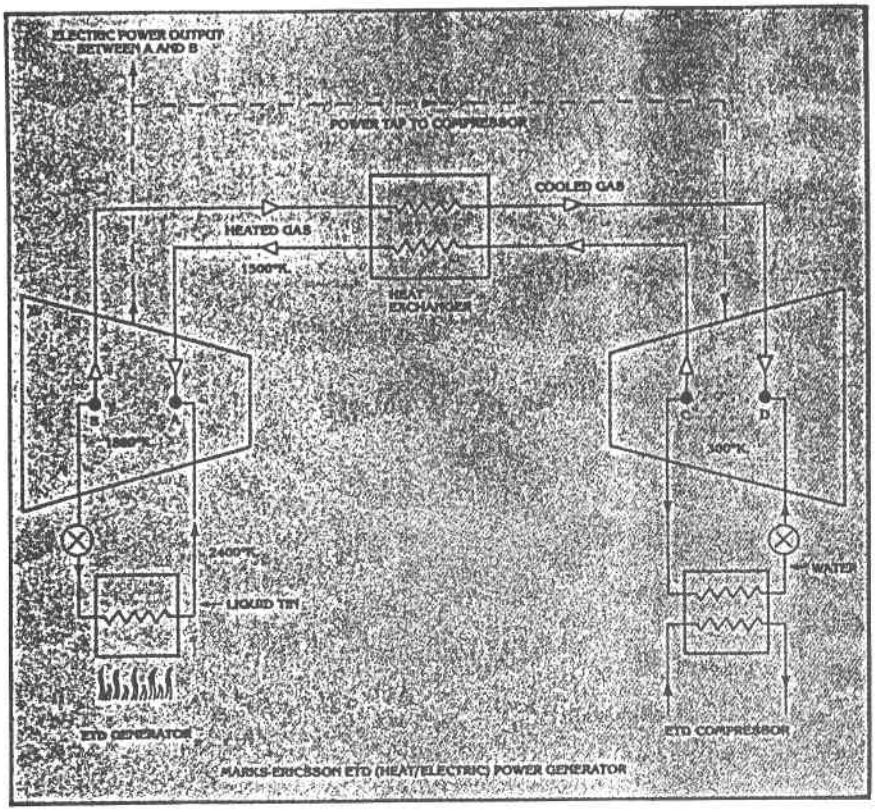

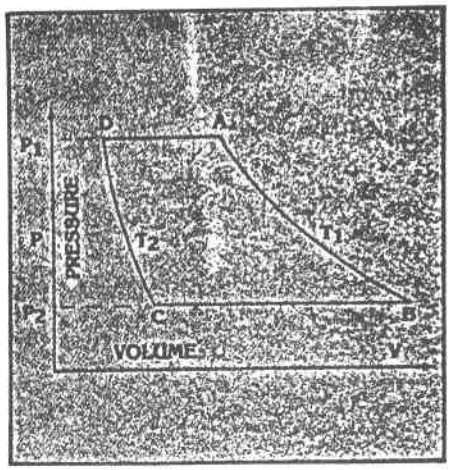

Thermodynamic characteristics of flow of nitrogen. P_1 indicates rising pressure, P_2 indicates rising pressure between D and A.

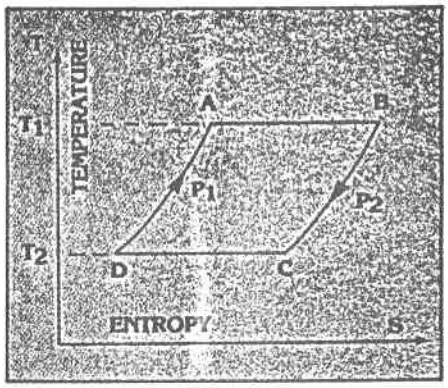

In this diagram, T_1 is 1,800° K in the gap between electrodes A and B. T_2 is 300° K between gas input (C) and gas output (D).

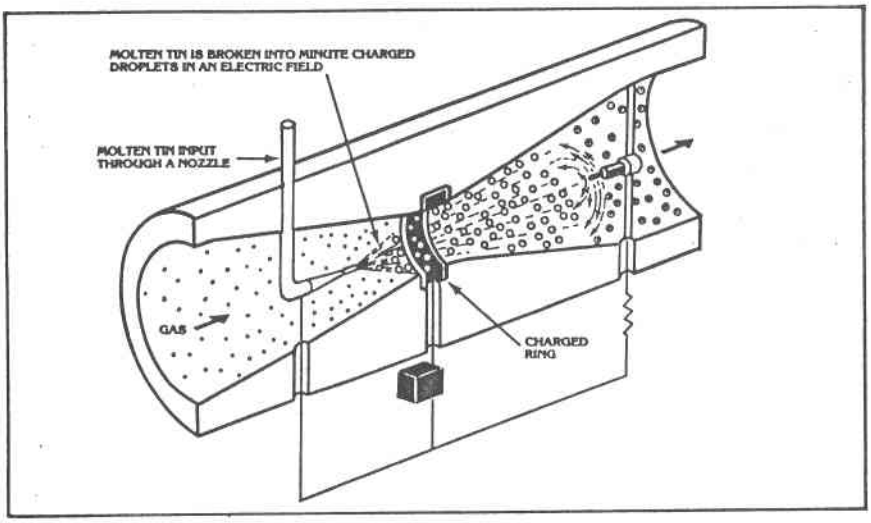

Schematic top left shows the basic thermodynamic requirements of the system. Nitrogen gas is heated to 1,500° K in the exchanger, then further heated to 2,400° K by the tin aerosol. Drawing at left shows how electrically charged aerosol particles are created. The droplets of molten tin pass through an electric field, gaining a positive charge. Usable generated power is tapped from input/output sides of system.

builds upon the works of others. In this case he gives due credit to yet another pioneer, John Ericsson, a Swedish engineer who invented a "caloric engine" back about 1833. Since the present invention is based upon a well-known "Ericsson Cycle," it is called the Marks-Ericsson ETD (electrothermodynamic) Heat/Electric Power Generator. The Ericsson cycle describes a thermodynamic system in which there is a "hot" end and a "cool" end. In such a system gas is expanded isothermally (basically without temperature change) at the hot end in order to do work, and then isothermally compressed at the low temperature end of the system. There is a constant flow of gas between the hot and cool ends of the gaseous system.

Let's try to visualize all that a little more clearly. Assume that we have a cylinder of gas that is maintained at a constant temperature of, say, 500° C by controlled addition of heat. As more heat is supplied, the gas continues to expand and do work at constant temperature. Now imagine the same situation in reverse. Assume the system at this "low" end is kept near room temperature. If the gas is compressed it naturally tends to heat up. However, since the gas enclosure can be cooled with circulating cold water, it is possible to compress gas at constant temperature by simply removing excess heat. This type of two-stage system provides isothermal expansion at the hot end to do work, and simultaneous isothermal compression at the cool end.

To successfully apply this basic Ericsson concept to creation of a workable power generating device it is necessary to circulate the gas, from generator to compressor and vice versa, through a heat exchanger that is stabilized at a constant temperature. If one were to cool the gas without exchanging heat along the line, the process would be very inefficient. Ericsson proposed energy-conserving heat exchange by means of a cross-flow of gas. What Marks has done is to replace an imagined "piston" at the hot end of the system with a charged metal aerosol (liquid tin). Water is used at the cool end of the system. The tin/water combination is ideal because both substances are nontoxic and do not react chemically with each other.

(Continued on page 128)

TIN-AEROSOL GENERATOR

(Continued from page 35)

ETD Generator. Let's trace what happens, beginning with the pool of liquid tin at the bottom of the ETD generator stage. A liquid metal pump moves the tin through a coil in a heat exchanger to which heat is added from any convenient external source. It could even be solar energy. This boosts the temperature of the tin to 2,400° Kelvin (about 3,860° Fahrenheit). The hot tin is sprayed through a nozzle into a flow of nitrogen gas inside the generator reaction chamber. During this process the tiny tin droplets are electrically charged by means of an externally-powered charging system.

The temperature of the incoming nitrogen gas (point A) is 1,500° K (about 2,240° F). The hotter tin boosts the kinetic power of the gas by raising its temperature to a constantly maintained 1,800° K (2,780° F). As the gas expands isothermally, it generates an electric potential which is tapped off at points A and B. The tin droplets fall back down to the liquid tin pool for recycling. Meanwhile the expanded, still hot gas is exhausted to a heat exchanger-regenerator located between the generator and compressor stages. Here heat from the generator exhaust is partially transferred to an opposing flow of gas headed for the generator input.

A small amount of electrical power is needed to give the tin aerosol its electrical charge, but the power used for this purpose is negligible when compared to the output of usable power. The charged aerosol creates its own "space charge" which results in an electrical potential "hill" against which the charged particles do work in the generator to create the heat-to-electricity energy transformation.

ETD Compressor. Note that the ETD compressor stage bears a marked resemblance to the generator stage. The main differences are the relatively low temperature of 300° K (about 80° F) and circulation of water rather than tin. Water from the compressor's pool is pumped through a heat exchanger to cool it by means of an external supply of cold water. The exhausted hot water can be used for any purpose, for example to meet normal hot water needs in a private home. The cooled water is pumped into the compressor reaction chamber through a nozzle. The water droplets that comprise the aerosol spray are electrically charged at this time.

As the already partly cooled nitrogen gas exhausted from the generator stage enters the compression chamber, it is cooled further by the water aerosol. This temperature reduction of course causes a reduction (compression) of the gas volume. During this process the cooling water, which becomes hot as it absorbs heat from the gas, drops back down to the pool for recycling. The cooled nitrogen gas flows out of the compressor system, through the central heat exchanger where it is once again heated to 1,500° K, and back again to the generator.

Note that gas compression requires no moving mechanical devices aside from the pumps used to circulate water through the compressor heat exchanger. Compression is accomplished smoothly and silently by electrothermodynamic means.

In like manner, the electrothermodynamic generator functions without turbines or other mechanical components other than the liquid metal circulating pump. About the only required maintenance, says Marks, is to periodically change the electrodes.

High efficiency is one of the primary advantages of this ETD system, according to the inventor. Note that the temperature difference between the generator and compressor stages is 1,500° K. The classic equation used to calculate the theoretically ideal efficiency of a heat engine is $T\text{-}T_0/T$. In this case it is (1,800°-300°)/1,800°, or 1,500 divided by 1,800, which is 0.83. Multiply by 100 to get 83 percent efficiency. Of course, in the real world nothing is perfect so this degree of efficiency is not realizable in practice. However, Marks says the true efficiency should be around 70 percent which would represent a dramatic advance over most present-day cycles which are rated at 33 percent efficiency at most.

How does the Marks-Ericsson ETD system stack up against other pioneering approaches to energy generation? Magnetohydrodynamic (MHD) systems have been researched intensively in recent years, but these require extremely high temperatures and the necessarily huge and complex installations are very costly. MHD systems are still a very long way from practical application, says Marks. The Marks-Ericsson system, by contrast, uses a much lower and more manageable temperature range.

More conventional steam plants are relatively inefficient because they must work at still lower temperatures. Also, turbines tend to be troublesome because they are very expensive and the blades just do not stand up to stresses imposed by high temperatures. The Marks system, as already noted, eliminates entirely such expensive and potentially troublesome components. The Marks ETD system does not require the use of high operating pressures, hence heavy-duty construction is unnecessary. This also helps reduce costs.

All in all, the Marks system promises to greatly reduce both investment and fuel costs; this indicates lower prices for consumers of electricity and/or better profits for utility industries that might switch to this system. Marks plans to license equipment manufacturers who should enjoy a "tremendous advantage" over present day turbine manufacturers who must compete against foreign manufacturers throughout the world.

How soon will we be seeing the Marks-Ericsson system in our homes? That's still an unanswerable question because much more development and promotional work lies ahead. But one thing is certain. If this concept proves to be as practical as Marks believes it is, the reaction of the established power utility industry should be something to behold! **S&M**

HOT WATER

(Continued from page 94)

a Heat Saver Plus system can save a homeowner more than half the cost of heating water using a conventional electric water heater. Annual savings are estimated at $200 to $400 depending upon local utility rates. In terms of "average family hot water usage," the payback period is put at two to five years; however, payback is even faster in an area where the homeowner qualifies for state tax credits and/or rebates from local utilities.

Furnace-Heated Systems. Perhaps your home still has an old-fashioned hot water heating system which includes a domestic hot water heating coil inside the furnace boiler. The problem with this type of system is that, if heat is demanded by the home radiator system while you are taking a shower, your supply of hot water may peter out almost completely until the room thermostat clicks off again. One solution is to turn down the room thermostat before showering; however, it's too easy to forget to reset it after the shower, until the home begins to feel cold.

A better solution to that problem is a water heater that can be added to an Amana (Amana, IA) gas-fueled furnace. When the water heater thermostat calls for replenishment of hot water in an adjacent storage tank, a diverter valve in the furnace cuts off room heating and reroutes a heat-transporting glycol-water mixture to a heat exchanger in the water heater. Thus there is no competition between space and domestic water heating. **S&M**

MANUFACTURERS' ADDRESSES

Resources Conservations, Inc.
P.O. Box 71
Greenwich, CT 06830

Chronomite Laboratories, Inc.
21011 South Figueroa
Carson, CA 90745

The Tankless Heater Corp.
Melrose Square
Greenwich, CT 06830

Mor-Flo Industries, Inc.
18450 South Miles Road
Cleveland, OH 44128

ELECTROHYDRODYNAMIC GENERATOR FOR USE WITH DISSIMILAR FLUIDS

T. H. Gawain and O. Biblarz
Naval Postgraduate School

ELECTROHYDRODYNAMIC (EHD) GENERATOR FOR USE WITH DISSIMILAR FLUIDS

T. H. Gawain
O. Biblarz

Naval Postgraduate School, Monterey, California

ABSTRACT

An electrohydrodynamic generator (EHD) design employing dissimilar fluids for the primary and secondary fluids is proposed. The electrical working section is disposed after the condenser/separator and before the ejector pump. The primary fluid vapor does not pass through the electrical working section, thereby avoiding many difficulties of the previous designs.

DESCRIPTION

An EHD generator uses the flow of a carrier fluid, normally a gas, in which are entrained a very large number of very fine and well distributed solid or liquid particles as in an aerosol. The particles are charged at an injector as the gas is caused to flow through an electrical working section by imposition of a suitable pressure drop. In the electrical working section the charged particles move through an electric field which exerts forces upon them in a direction and sense opposed to the general fluid motion. The gas stream does work on the charged particles in moving them against the resistance of the electrical forces. This work done creates a difference in electric potential between an injector electrode upstream and a collector electrode downstream. Electrical power is provided to an external electrical load which is connected between the electrodes.

Typically, an EHD generator is implemented using a condensible primary fluid which undergoes a Rankine cycle and a secondary fluid, typically a gas or vapor, which serves as the carrier fluid and which augments the volumetric flow through the electrical working section. While the primary and secondary fluid may be either identical or

different, the overall performance of the ejector pump is greatly enhanced by using a fluid of high molecular weight for the primary and a fluid of low molecular weight for the secondary. A typical primary secondary fluid combination is fluorcarbon/air. The performance is also critically limited by the maximum electrical field that the fluid medium can withstand without electrical breakdown.

In previous state-of-the-art EHD generator designs, the electrical working section either coincides with the ejector pump or immediately follows it. The schematic drawings of Figs. 1 and 2 illustrate a new EDH generator design in which the electrical working section is located after the condenser/separator and just prior to the ejector pump. In the horizontal, recirculating system shown in the Figures, the arrows indicate the direction of fluid flow. The high molecular weight primary fluid is injected by an ejector pump 10 into the seondary fluid which is circulating in the generator. The combined fluids then pass through a condenser/separator represented by fins 12 where the primary fluid is condensed and separated from the fluid flow. The condensed primary fluid is returned to the ejector pump 10 by a gravity return (not shown). The ejector thus serves purley the purpose of pumping the secondary fluid.

The fluid medium, which now consists entirely of the secondary gas or vapor with droplets of primary fluid and/or a suitable solid suspension, flows into the electrical working section. The particles are charged at injector electrode 14 and are transported downstream against an electric field to a collector electrode 16 to provide electrical power to an external load represented by resistor 18.

ADVANTAGES AND FEATURES

The present EHD generator design has the following advantages over the previous designs:

1. The curcially important breakdown strength in the electrical working section may be kept at its highest value because the medium in the working section consists entirely of the secondary fluid with droplets of primary fluid or a suitable solid suspension. Breakdown qualities need not be degraded by the presence of significant amount of primary fluid vapor as they can be in the previous state of the art.

2. Possible difficulties relating to aerosol condensation rates of primary vapor and optimum particle size in the electrical working section are voided when primary vapor is used as the source of the aerosol to be charged.

3. Possible chemical degradation of the primary vapor in passing through the corona discharge at the injector are avoided (particularly true for high molecular weight organic vapors).

4. The thermodynamic cycle of the primary fluid is freed from restrictions relating to the amount of moisture in the primary jet. This additional degree of freedom may be exploited to better optimize the cycle and thereby achieve a higher overall generator efficiency.

5. The flow in the electrical working section will be considerably less perturbed than at the ejector or condensor where mass and momentum mixing and unmixing are required. This leads to smoother flow conditions and more controllable generator parameters.

ELECTROHYDRODYNAMIC (EHD) GENERATOR FOR USE WITH DISSIMILAR FLUIDS

T. H. Gawain, O. Biblarz

Naval Postgraduate School, Monterey, California

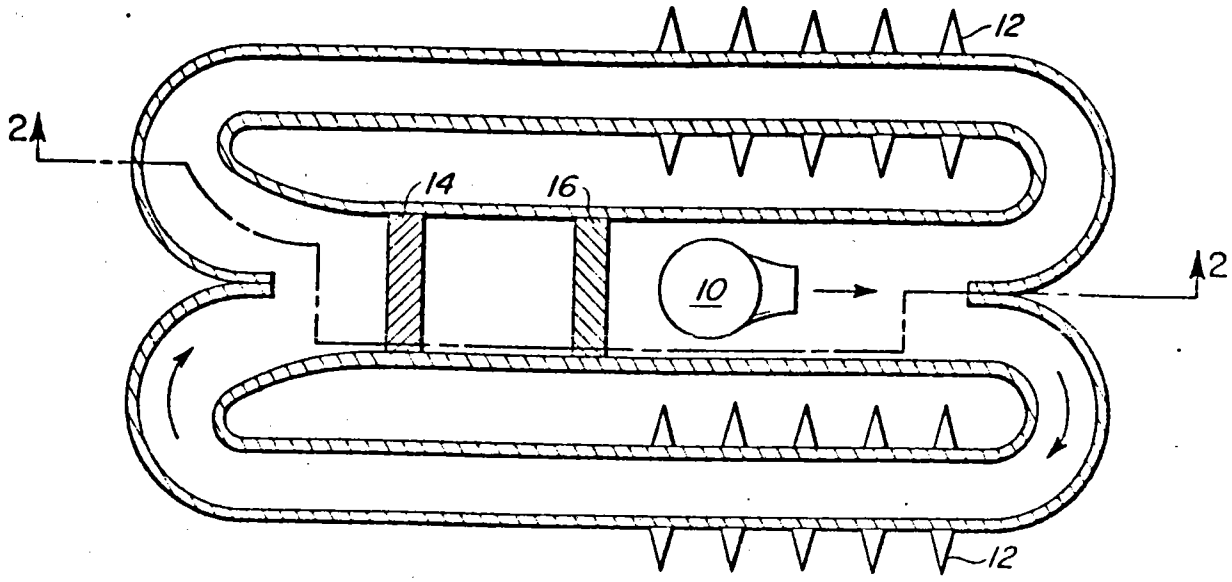

Fig. 1

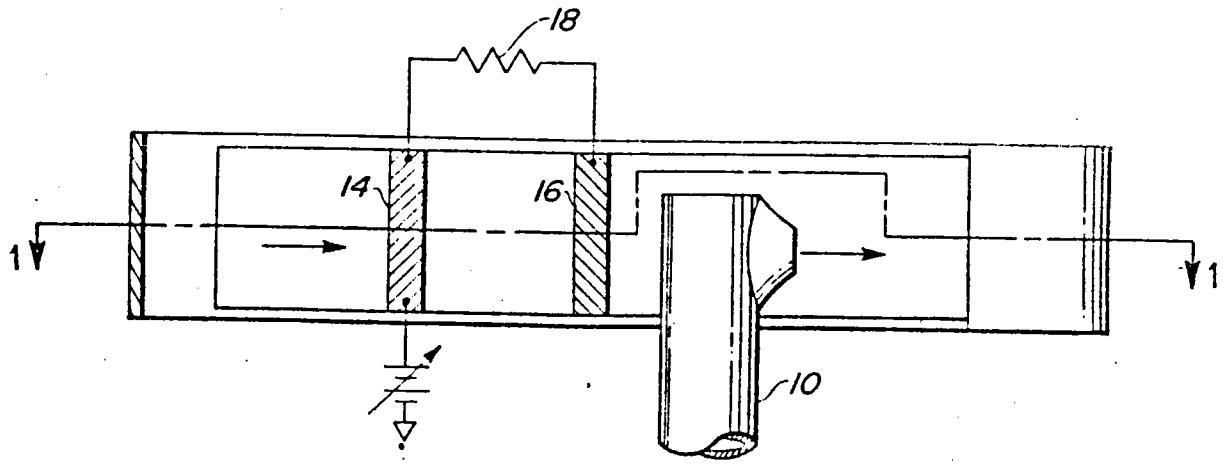

Fig. 2 "PRIMARY FLUID"

LIQUID METAL MHD CONVERSION FOR SOLAR THERMAL SYSTEMS

William Jackson
HMJ Corporation

LIQUID METAL MHD CONVERSION FOR SOLAR THERMAL SYSTEMS

By

William D. Jackson
HMJ Corporation
P.O. Box 15128
Chevy Chase, MD 20815

1. INTRODUCTION

The science of magnetohydrodynamics (MHD) deals with the interaction of electrically conducting fluids with electromagnetic fields. The fluids may be liquid metals, electrolytes, two-phase flows comprising a gas or vapor with a continuously connected conducting liquid phase, a slightly ionized gas (or plasma) or a fully ionized plasma. The application of MHD to electric power power generation[1] involves the driving of one of these conducting fluids through a magnetic field with appropriate electrode or inductive coupling circuits. The motionally induced electromotive force causes current to flow in an electric circuit and so deliver power to a load appropriately matched through a power conditioning system.

In 1936, Karlowitz first pointed out that MHD conversion could provide the basis for a heat engine converting the enthalpy of the working fluid directly to electrical form provided only that the working fluid is a sufficiently good electrical conductor to ensure that the generated power substantially exceeds the losses per unit volume.

2. BACKGROUND

Most of the effort of MHD power generation follows Karlowitz and is centered on slightly ionized gases produced by the seeding of combustion products with readily ionized materials such as potassium carbonate. This electrically

conducting working fluid is expanded through a DC magnetic field on a once through or open cycle basis. Lack of understanding of conductivity phenomena in these gases delayed demonstration of this effect until 1959. There has since been a major development effort on large machines of this type to operate under electric utility conditions and also to provide large pulses of electric power.

The first attempt to demonstrate motionally induced MHD was by Faraday in 1832 and involved the use of a liquid, the River Thames and the earth's magnetic field. Until the 1920's, MHD effects were basically treated as a laboratory curiosities involving experiments with electrolytes or liquid metals, usually mercury in the latter case. The decade of the 1920's was notable both because it marked the beginning of the systematic study of the science of MHD primarily for astrophysical and geophysical applications but also because it included the first proposals and developments of the MHD interaction for pumping and measuring the flow of electrically conducting liquids. This work was subsequently applied to the pumping of liquid metals in nuclear installations by electromagnetic or MHD pumps.

The use of a liquid metal as a heat transfer in nuclear reactors and difficulties with obtaining conductivity in combustion products led in the 1950's to proposals for these metals as MHD working fluids. It was realized that this opened up a wholly new temperature range for MHD systems below that appropriate to any type of plasma while retaining the inherent feature of eliminating highly stressed new power components.

While operating a device similar to an MHD pump but in a generating mode offers one possible approach (i.e., a mechanical to electrical converter), it is possible to operate a liquid metal MHD (LMMHD) device as a heat engine by creating a two-phase flow with a suitable gas or vapor and ensuring that the liquid phase is continuous (i.e., gas bubbles embedded in a liquid) for electrical conductivity purposes. Operation may be either with a Brayton or Rankine cycle,

depending on the temperature range and working fluids selected and a recirculating or closed cycle system is almost always assumed. It was also recognized that the use of a liquid conducting system offered the possibility of direct AC generation in contrast to plasma systems which thus far, because of magnetic Reynolds number considerations, are limited to DC generation in a manner analogous to that of a linear homopolar machine.[2]

3. DEVELOPMENT OF LMMHD

The first discussion of pure liquid metal MHD converters was given by Mawardi[3] in 1955 and the flow conditions were thoroughly analyzed by Harris[4] in 1959. The initial proposal for obtaining thermodynamic acceleration of the liquid stream in an MHD converter was to use the condensing-ejector type of pump frequently employed for feedwater, particularly on railroad locomotives.[5,6] Experimental studies by Brown[5] confirmed the feasibility of the approach but showed that the efficiency is limited due to the slippage between the liquid and the driving vapor phase during the acceleration process. As its designation indicates, this is basically a single-fluid cycle with condensation occurring after acceleration and the poor performance has been traced to this requirement.

In 1960 Elliott[7] devised a heat engine cycle in which heated lithium is mixed with cesium to form a cesium vapor/liquid lithium two-phase flow. This flow is accelerated and the two streams separated on a flat plate separator so that an essentially liquid stream passes through a DC type of MHD converter. Jackson and Pierson[8] conducted extensive studies of the induction type of AC converter and this was adopted by Elliott and adapted for his cycle. The Elliott cycle, shown in Fig. 1 was intended to be coupled to a SNAP-50 reactor to provide a power source for deep space missions. Extensive experimental and analytical investigations were conducted until 1973 when lack of an established mission led to the program being phased out at the Jet Propulsion Laboratory (JPL). Results from this program are well documented in the literature.

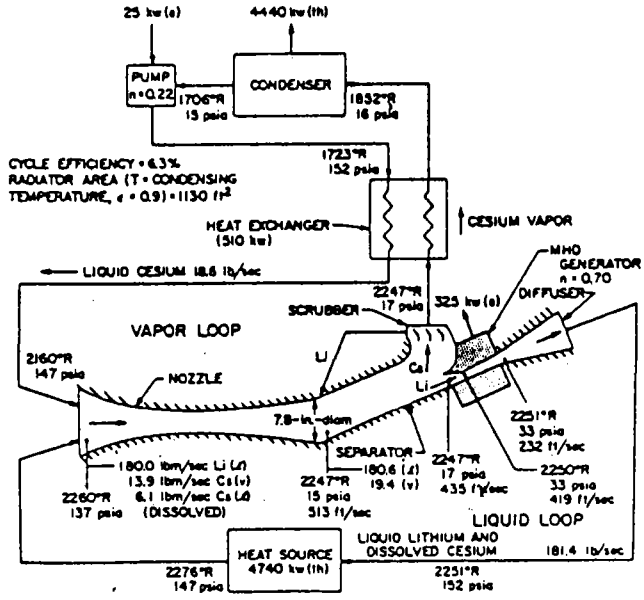

Fig. 1 Elliott two-fluid cycle with liquid stream MHD Generator.

Note: The conditions given in this Figure are for a typical SNAP-50 reactor system.

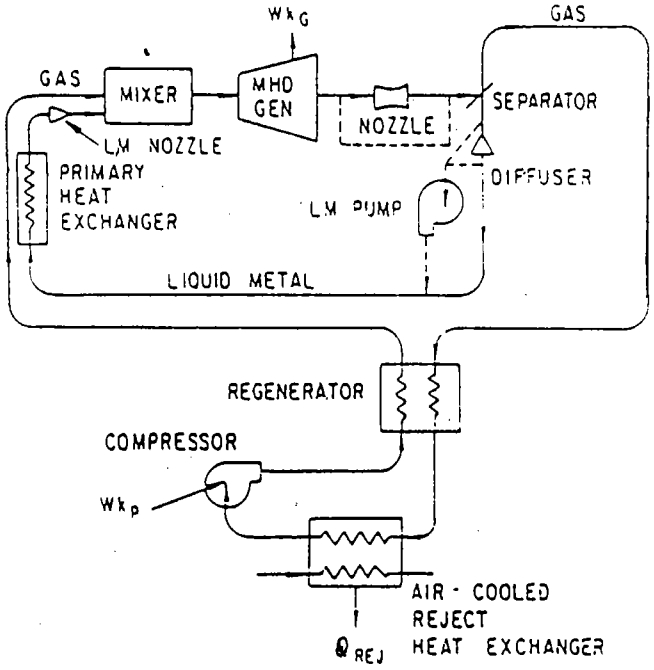

Fig. 2 Schematic of two-fluid cycle with bi-phase expansion engine MHD generator.

The first proposal to expand a two-phase mixture in an MHD generator duct was made by Bidard[9] in France in 1960 and this initiated investigations which have continued to the present time. In 1962, Petrick[10] pointed out that the attractive features of the Elliott cycle could be retained and the advantage of employing an MHD heat engine gained if the MHD generator was moved to a position between the nozzle and the separator (Fig. 2). This approach has formed the basis for a sustained effort at the Argonne National Laboratory (ANL) on LMMHD. From the applications viewpoint a major focus was electric power for submarine propulsion but space and terrestrial applications also received considerable attention. Many valuable experimental investigations were conducted and these are also well documented in the literature.

The liquid metal type of MHD has also been the subject of extensive investigations in the Soviet Union by both Velikov and his co-workers at the Kurchatov Institute and by Shelkov and Speilrain at the Institute of High Temperatures. At the Latvian Institute for Physics, Leilpeter has reported extensively on induction type generators and Aladiev and his co-workers at the Krzhizhonovsky Power Institute have also reported extensively on LMMHD. This USSR work is fully documented and readily available in international literature. Later a number of concepts were developed for higher temperature solar applications, specifically for parabolic solar troughs and for central solar tower. Detailed perimetric studies demonstrated that highest performance can be achieved with dual cycles in which the MHD system performs the topping cycle and a turbine (steam or gas) system performs the bottoming cycle.

4. APPLICATIONS

A high temperature liquid metal cooled reactor (SNAP) was favored as the energy source for deep space missions and LMMHD was initially considered as a candidate conversion system on account of its temperature compatibility and absence of highly stressed rotating components. Significant reductions in radiator weight over rotating systems was shown to be possible with the Fig. 1 system. Decline of interest in the proposed application caused work to be shelved in the 1970's.

Consideration was also given to terrestrial applications involving both nuclear and fossil heat sources. The latter was included in the Energy Conversion Alternatives Study (ECAS) conducted by NASA for the Department of Interior during 1974-76. For central station applications, LMMHD was found

to be at a significant disadvantage with respect to competing systems[11] primarily because of the need for additional heat exchangers although subsequent work with an open cycle copper system[12] showed considerable promise.

In the late 1970's, Branover[13] pointed out that LMMHD was particularly suited to solar heat sources in which liquid metal served as the heat transfer medium and initiated a development effort aimed at small scale relatively low temperature Rankine cycle systems for isolated installations. Consideration is now being given to apply LMMHD to low temperature geothermal and reject heat sources.

5. CURRENT STATUS

In 1983, Pierson and Jackson pointed out that the high temperature range of LMMHD (above 900°F) was particularly promising for LMMHD conversion systems coupled to liquid metal solar power towers and that a Brayton cycle was appropriate for these conditions. As part of the Innovative Research Program in Solar-Thermal initiated by DOE/SFO and now being undertaken by SERI, the system efficiency obtainable in high temperature systems using the configuration of Fig. 2 was undertaken using a revised and improved computer model originally developed at ANL. Several cycles involving potassium and lithium were considered using the conditions of Table 1. The principal result is that the thermodynamic performance of LMMHD systems leads to overall thermal efficiences above those of conventional rotating machinery, i.e., above 33%, the projected efficiency for the Carissa Plain Solar Central Receiver Power Plant Project[15]. With reasonable extrapolation of component performance, sodium systems can reach 40% while lithium can raise this value to over 46% at 1400°F top temperature. A typical result is illustrated in Fig. 3.

The use of a liquid flow generator continues to be attractive because of the possibility of direct AC generation and improved cycles have been proposed to circumvent the condensing-ejector limitations or to improve further the Elliott cycle performance. The cycle of Fig. 4 has recently been advanced

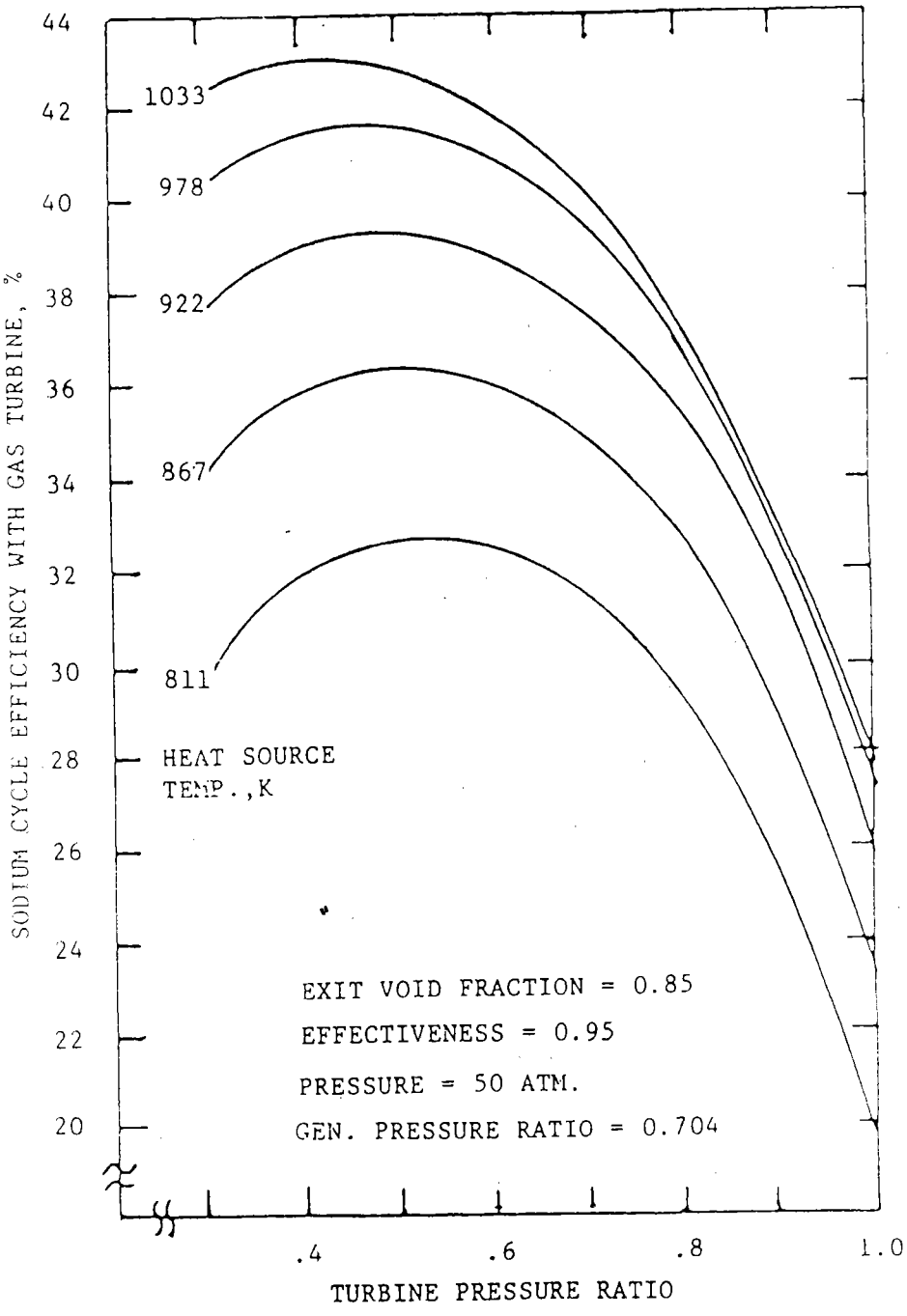

Figure 3. Sodium Cycle Efficiency Versus Turbine Pressure Ratio as a Function of Temperature for 0.704 Generator Pressure Ratio

by Branover and Petrick[16] and as shown is a Rankine cycle and can operate as either a Rankine or Brayton type cycle in a wide temperature range. Detailed parametric studies of these cycles have been performed at the Center for MHD Studies of Ben-Gurion University in Israel under sponsorship of Solmecs Corporation.[17] Those parametric studies yield very attractive performance characteristics, specifically for applications with parabolic troughs and central solar towers.

Lastly,[18] A feasibility study of a number of applications of this cycle called OMACON was performed by Solmecs USA in Chicago on behalf of Southern California Edison Co. This study includes a number of applications, but concentrates mainly on the central solar tower application; for this case a preconceptual design study and cost assessment for a 2 MW_e prototype OMACON module was performed. The conclusions of this study were quite positive. At the Center for MHD Studies of Ben-Gurion University, two complete OMACON-type systems - ER-4 and ETGAR-3, working with a heavy liquid metal and steam, are in advanced stages of testing. Power conditioning problems in Liquid Metal MHD systems are studied on behalf of Solmecs Corporation by Westinghouse R&D Center in Pittsburgh.

6. CONCLUSIONS

In the overall development process which begins with conceptual studies, proceeds through exploratory development and engineering development and continues to system and commercial demonstrations, LMMHD is still in the early stages of exploratory development. Experimental data are available to support the assumed component performance but additional testing, particularly at high temperatures, is required to obtain information necessary for engineering design purposes. System analysis has concentrated on the thermodynamic aspects of solar LMMHD systems. It has identified performance potential but has left cost and operational issues to future work. It has also identified those areas where engineering efforts are required both to establish actual component performance and to develop the engineering basis for the design, construction and demonstration of a complete system operationally acceptable to electric utilities.

Alternative concepts still require evaluation to determine their relative merits and preferred applications both from the points of view of power level and temperature. At this stage, it has been established that:

(1) LMMHD systems are compatible with solar central receivers using liquid metal as the heat transfer medium;
(2) they elminate the sodium/steam heat exchanger; and
(3) they offer significant increases in system efficiency over conventional turbo-machinery.

System analysis, cost studies and experimental engineering studies are urgently required to establish an engineering basis from which solar thermal LMMHD systems may be confidently evaluated.

7. REFERENCES

1. Jackson, W.D., "Critique of MHD Electrical Power Generation," Proc. 3rd Beer-Sheva Seminar on MHD Flows and Turbulence, AIAA, New York, NY 1982.

2. Jackson, W.D., Bidard, R., and Toschi, R., (Editors) "MHD Electrical Power Generation: 1972 Status Report," Chapter 3, Atomic Ener. Rev., Vol. 10, No. 3, IAEA, Vienna, 1972.

3. Mawardi, O.K., Unpublished lecture notes on MHD, Massachusetts Institute of Technology, Fall Semester, 1955.

4. Harris, L.P., Hydomagnetic Channel Flows, MIT Press, Cambridge, MA 1960.

5. Brown, G.A. and Levy, E.K., "Liquid Metal Magnetohydrodynamic Power Generation with Condensing Ejector Cycles," Paper No. SM-74/171, presented at International Symp. on MHD Electrical Power Generation, Salzburg, Austria, July 4-8, 1966.

6. Prem, L.L. "Analytical and Experimental Results of the Fluid Metal MHD Power Conversion Program," Paper No. SM-74/84, presented at International Symp. on MHD Electrical Power Generation, Salzburg, Austria, July 4-8, 1966.

7. Elliott, D.G. "Two-fluid Magnetohydrodynamic Cycle for Nuclear-Electric Power Conversion." TR32-116, Jet Propulsion Laboratory, Pasadena, CA, June 30, 1961; also ARS J., 32, 924-928 (1962).

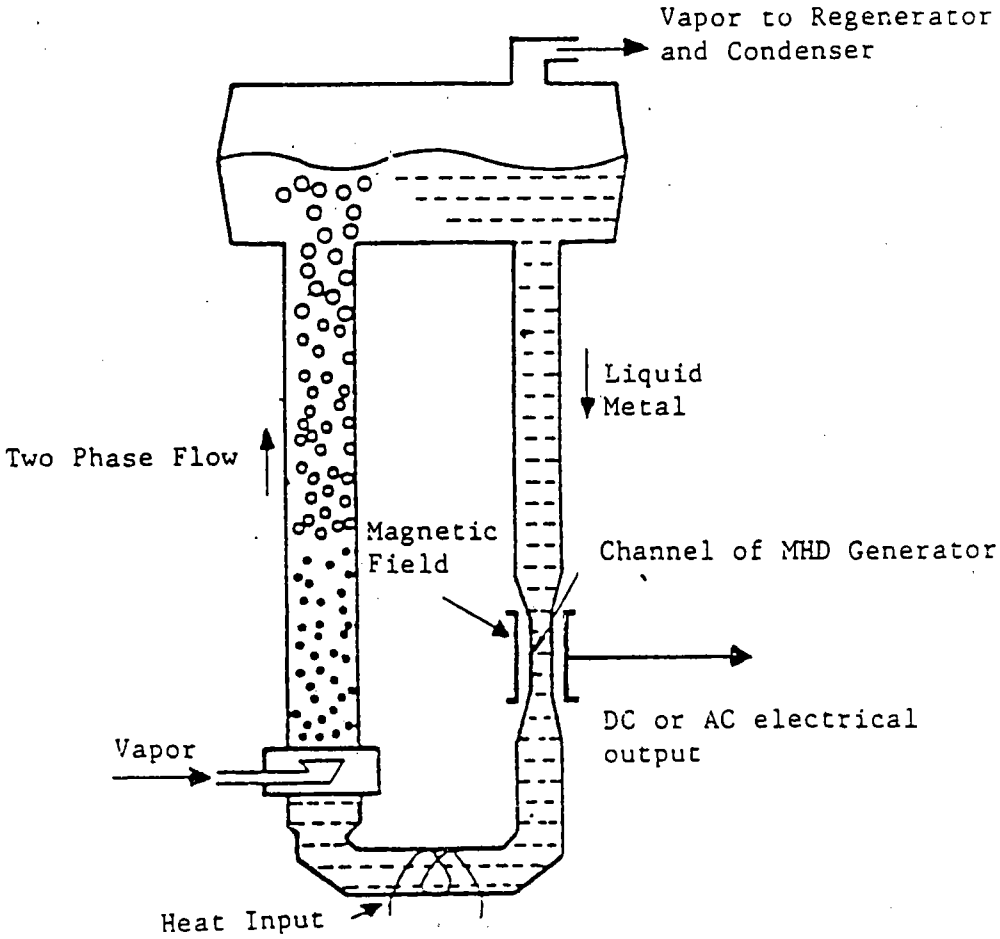

Fig. 4 Lift-pump gravity separator cycle schematic.

8. Jackson, W. D., Pierson, E. S., "Operating Characteristics of MHD Induction Generators" IEE Conference Report, Series No. 4, pp. 38-42, Proc. of International Symp. on Magnetohydrodynamic Power Generation, Newcastle-upon-Tyne, September 1962.

9. Bidard, R. and Sterlini, J., "Generator MHD Fonctionnant par Emulsion" - Electricity from MHD (c.r. Colloque, Salzburg, 1966), 2, SM-74/108 (1966),

10. Petrick, M., and Lee, K. Y., "Performance Characteristics of a Liquid-Metal MHD Generator." ANL-6870, Argonne National Laboratory, Argonne, IL, July 1964.

11. "Comparative Evaluation of Phase I Results from the Energy Conversion Alternatives Study (ECAS)", NASA TM-X-71855, February 1976.

12. Pierson, E. S., Cohen, D., and Grammel, S. J., "Liquid-Metal MHD for Solar and Coal," Proc. the Seventh International Conference on MHD Electrical Power Generation, Boston, MA, pp. 150-157, 1980.

13. Pierson, E. S., Branover, H., Fabris, G., Reed, C. B., "Solar Powered Liquid Metal Power Systems," Mechanical Engineering, 102, pp. 32-37, Oct. 1980.

14. Pierson, E. S., Jackson, W. D., Berry, G., Petrick, M., and Dennis, C., "Performance of Solar Thermal Systems with Liquid Metal MHD Conversion." Report No. 4MHDSA-DCE-P/84/R1, HMJ Corporation, Chevy Chase, MD, June 1984.

15. "Preliminary Design of the Carrisa Plain Solar Central Receiver Power Plant, Vol. 1, Executive Summary." DOE Report ESG-DOE 13404, Dec. 1983, prepared by Rockwell International Corporation under Contract DE-SFC03-82SF11674.

16. Petrick and H. Branover, "Liquid Metal MHD Power Generation - Its Evaluation and Status", In: Single and Multi-Phase Flow in an Electromagnetic Field, Progress in Astronautics and Aeronautics, Vol. 100, AIAA, 1985, pp. 371-400.

17. H. Branover et al., Status Report on Liquid Metal MHD Heat and Power Generation, System Applications Studies for Non-Nuclear Heat Sources, The Center for MHD Studies, Solmecs Ltd., Ben-Gurion University of the Negev, Israel, March 1986.

18. Performance of OMACON LMMHD Conversion Systems in Selected System Applications: Final Summary Report, submitted to Southern California Edison Company by Solmecs Corporation USA, December 1985.

RESPONSES TO QUESTIONNAIRES ON ENERGY CONVERSION CONCEPTS

SURFACE PLASMON CONVERSION

Anne Arrisan and Donald Chubb
NASA Lewis Research Center

1. What is the current status of the technology (theoretical, lab scale, moderate scale)?

   The concept as originally set forth has not yet been realized. Theoretical and experimental work on the key technical barriers is underway.

2. What are the major problems associated with full-scale operation?

   The main difficulties with the original concept are broadband coupling of light to surface plasmons, the plasmon range, coupling energy into the tunnel diodes, and extracting energy from the tunnel diodes.

3. What attributes of the technology make it particularly suitable for solar applications?

   The devices would be made of thin films which would provide for lightweight cells that are potentially radiation resistant.

4. What is the optimum temperature range for operation of the technology?

   This has not yet been determined.

5. What degree of concentration of solar light is required?

   The device would be used with a concentrator but the optimum degree of concentration has not been calculated.

6. What are the critical areas in which research is required to further the development of the technology for solar applications?

To overcome the problems of the original concept, new devices involving different tunnel diode configurations have been suggested.

7. Is research currently being funded in any of these areas?

Yes.

LEPCON LIGHT - ELECTRIC POWER CONVERSION

Alvin Marks and Edgar Bourke II
Phototherm Incorporated

1. What is the current status of the technology (theoretical, lab scale, moderate scale)?

   Theoretical
   U.S. Patent No. 4,445,050
   Additional Patent Applications

2. What are the major problems associated with full-scale operation?

   None Anticipated

3. What attributes of the technology make it particularly suitable for solar applications?

   Does not use Semiconductor Material. Uses low cost Materials, unlimited area, and a low cost/unit area. High efficiency: 80%. 50 ¢/watt investment cost. Output 500w/m^2.

4. What is the optimum temperature range for operation of the technology?

   Make of metals, glass, oxides - very stable from 200 degrees to 1000 degrees K; ambient temperature (300 degrees K) operation.

5. What degree of concentration of solar light is required?

   None- functions on direct sunlight, however it will function on concentrated

sunlight if temperature at Lepcon^{tm} Area is ambient 300 degrees K to 1000 degrees K.

6. What are the critical areas in which research is required to further the development of the technology for solar applications?

Fabrications and Testing of Submicron Arrays. Development testing and manufacturing of special production device (known as the Supersebter^{tm}) to make panels $1m^2$ in 100 sec.

7. Is research currently being funded in any of these areas?

Only very small private funds to date. We are seeking U.S. Government or private funds of 3 million, or more to R & D this technology.

LUMELOID LIGHT - ELECTRIC POWER CONVERSION

Alvin Marks and Edgar Bourke II
Phototherm Incorporated

1. What is the current status of the technology (theoretical, lab scale, moderate scale)?

   THEORETICAL
   Patent application filed.

2. What are the major problems associated with full-scale operation?

   The inventor has great experience in the large scale manufacture of Polarizing films. The cost shoulder is about $\$2\text{-}5/m^2$. The same equipment can be used. Only the composition differs.

3. What attributes of the technology make it particularly suitable for solar applications?

   Can be manufactured readily in plastic rolls and a large scale at a low cost per watt (1 ¢/watt). Can be used every where by everyone, making low cost affordable solar energy available.

4. What is the optimum temperature range for operation of the technology?

   Ambient

5. What degree of concentration of solar light is required?

   None

6. What are the critical areas in which research is required to further the development of the technology for solar applications?

Physical-chemical R & D on our composition and fabrication. Creation of a Special Lab to do this work.

7. Is research currently being funded in any of these areas?

No, except for small private funds. Substantial U.S. Government or private funds are needed. $3,000,000 or more to produce this technology.

BLACK BODY PUMPED LASERS

Walter Christiansen
University of Washington

1. What is the current status of the technology (theoretical, lab scale, moderate scale)?

   Lab scale

2. What are the major problems associated with full-scale operation?

   a Materials problem - useful materials must be focused with good transparency.
   b. Optical depth problem - requires the use of isotopes - not fully explored yet.
   c. Scaling to large powers not shown yet.

3. What attributes of the technology make it particularly suitable for solar applications?

   It is a mode direct conversion of sunlight to laser (work) than that assoc. with conversion to electricity first.

4. What is the optimum temperature range for operation of the technology?

   1500-2000°K (Blackbody temp.)

5. What degree of concentration of solar light is required?

   O (500 X)

6. What are the critical areas in which research is required to further the development of the technology for solar applications?

Materials - availability? & cost?
Large cheap concentrators are also required

7. Is research currently being funded in any of these areas?

In the case of my research, these areas are not funded.

PYROELECTRIC CONVERSION

Randall Olsen
Chromos Research Laboratories, Inc.

1. What is the current status of the technology (theoretical, lab scale, moderate scale)?

   Small Lab Scale 2 Watts (electrical) Demonstrated 1/10 of Carnot efficiency (1% overall)

2. What are the major problems associated with full-scale operation?

   Existing demonstrations have been performed with an expensive, brittle _____. Research is now concentrated on an inexpensive, flexible polymer.

3. What attributes of the technology make it particularly suitable for solar applications?

   Compact. Low temperature conversion. Inexpensive polymer ($50/lb or $0.10 watt). A low temperature heat engine. Completely controllable stress parameter (Electric field) 90% of Carnot efficiency possible at high power density.

4. What is the optimum temperature range for operation of the technology?

   Room temp. to 300°C. -Best range near term is 30°C to 140°C

5. What degree of concentration of solar light is required?

   Low

6. What are the critical areas in which research is required to further the development of the technology for solar applications?

Materials synthesis- In two years we have made a factor of 100 improvement in the conversion energy density of polymers. This has been with an available piezoelectric polymer. We need to tailor make a pyroelectric material to our specs.

7. Is research currently being funded in any of these areas?

Almost (materials measurements are being performed at our lab.) We are hoping to be able to start synthesis work in Oct. 85 on a Phase II SBIR [NASA].

REGENERABLE FUEL CELLS

Frank Ludwig
Hughes Aircraft Company

1. What is the current status of the technology (theoretical, lab scale, moderate scale)?

   Lab scale

2. What are the major problems associated with full-scale operation?

   Time and money for development.

3. What attributes of the technology make it particularly suitable for solar applications?

   Modular, no moving parts, very high efficiency, upper and lower temperatures ideal for terrestrial solar applications, "built-in" storage at the lower temperature, high power density, low cost

4. What is the optimum temperature range for operation of the technology?

   Varies depending on working fluid, but can be generally considered to be 100°-600°C, lower & upper temperatures.

5. What degree of concentration of solar light is required?

   Appropriate for 600°C receiver

6. What are the critical areas in which research is required to further the development of the technology for solar applications?

   Electrochemical power plant, working fluid types and properties, thermal regenerator design.

7. Is research currently being funded in any of these areas?

   Yes

SODIUM HEAT ENGINE (SHE)

Thomas K. Hunt
Ford Motor Company

Speaker: Thomas K. Hunt

Type of Technology: Sodium Heat Engine (SHE)

1. What is the current status of the technology (theoretical, lab scale, moderate scale)?

   The SHE is currently in lab scale testing - 100 to 200 Watt device will be tested in 1985.

2. What are the major problems associated with full-scale operation?

   Demonstration of high power performance for periods beyond a few thousand hours.

3. What attributes of the technology make it particularly suitable for solar applications?

   Efficiency is nearly independent of size and should reach 25 to 30%. High specific power output leads to low weight and small size. There are no moving parts and should have low maintenance.

4. What is the optimum temperature range for operation of the technology?

   Optimum 800 - 1000°C
   Minimum is ≃650°C
   Maximum is ≃1200°C

5. What degree of concentration of solar light is required?

   Parabolic dish ∿

6. What are the critical areas in which research is required to further the development of the technology for solar applications?

    1. Engineering development of complete systems - modularized with thermal impact designed for application.

    2. Electrode materials and preparation studies - durability testing.

    3. Performance studies at high condenser temperatures.

7. Is research currently being funded in any of these areas?

    - Research on #1 is being funded by DOE - Office of Industrial Programs.
    - Research on #2 has some funding at JPL but is not currently supported at Ford.
    - Research on #3 not currently under study.

SOLAR THERMIONIC ENERGY CONVERSION

Dave Lieb and Gabor Miskolczy
Thermo Electron Corporation

1. What is the current status of the technology (theoretical, lab scale, moderate scale)?

   Individual flame-fired converters have operated in the laboratory for 12,500 hours. Modules were operated with four converters in series. Solar operation was also demonstrated.

2. What are the major problems associated with full-scale operation?

   Cost estimates show thermionic cost $200 per kilowatt in quantities of 200,000. A moderate scale demonstration is needed to convince users.

3. What attributes of the technology make it particularly suitable for solar applications?

   High temperature, high heat flux operation possible (1750 to 1800 K, 60 to 100 W/cm^2)

4. What is the optimum temperature range for operation of the technology?

   1750 to 1800 K

5. What degree of concentration of solar light is required?

   1000 to 4000

6. What are the critical areas in which research is required to further the development of the technology for solar applications?

Solar receiver cavity design could increase the system efficiency. Thermionics rejects heat at 1000 K. This makes thermionics particularly effective as a topping cycle for lower temperature thermodynamic system. An attractive total system study and actual demonstration would make such a combined system attractive.

7. Is research currently being funded in any of these areas?

No

THERMOELECTRIC ENERGY CONVERSION

Charles Wood
Jet Propulsion Laboratory

1. What is the current status of the technology (theoretical, lab scale, moderate scale)?

   Full-scale.

2. What are the major problems associated with full-scale operation?

   None.

3. What attributes of the technology make it particularly suitable for solar applications?

   High temperature - high reliability.

4. What is the optimum temperature range for operation of the technology?

   Depends on material; ranges from room-temperature for Bi_2Te_3 type alloys to 1400° for B_4C type compounds.

5. What degree of concentration of solar light is required?

   Unknown.

6. What are the critical areas in which research is required to further the development of the technology for solar applications?

Improvement of conversion efficiency.

7. Is research currently being funded in any of these areas?

Yes, for radio-isotope and reactor heat conversion to electricity.

MAGNETIC HEAT ENGINES

Lance D. Kirol
Idaho National Engineering Laboratory

1. What is the current status of the technology (theoretical, lab scale, moderate scale)?

   Regenerative magnetic heat engines are strictly theoretical, but the phenomena has been demonstrated in magnetic refrigerators and non-regenerative magnetic torque motors and thermomagnetic generators. Overall, the technology is somewhere between theoretical and lab scale.

2. What are the major problems associated with full-scale operation?

   a. Designs which achieve adequate recouperation must be conceived and tested.
   b. Adequate magnetic field strength and profile must be achieved by proper superconducting magnet design.
   c. Methods to manufacture rotors of very think disks with thin spaces are required.

3. What attributes of the technology make it particularly suitable for solar applications?

   High efficiency (for reduced collector area) is the major attribute. Seventy percent of Carnot efficiency appears to be reasonably achievable. Other characteristics which may prove valuable are low speed operation and simple deisgn which should give reliable operation, suitable for remote sites. The solid working material make OTEC possible, esp. if high mag. field disrupts biofouling.

4. What is the optimum temperature range for operation of the technology?

   Working materials should be available for any operating temperature to 1400K. Specific applications have not been studied. For solar applications, there will be an economic optimum temperature based on required solar concentration, engine efficiency, and heat losses.

5. What degree of concentration of solar light is required?

   Must be determined as part of an economic study as above.

6. What are the critical areas in which research is required to further the development of the technology for solar applications?

   a. Working material identified and tested which give improved energy density and more parallel high and low field T-s lines.
   b. Magnet design to give the required field profiles.
   c. Parametric study to define optimum conditions of operation for solar applications.

7. Is research currently being funded in any of these areas?

   As part of INEL's magnetic heat pump program, we are performing magnet and field studies which will be directly applicable to magnetic heat engines. Heat pump working mateial studies are only slightly applicable to heat engines. No other magnetic heat engines research is being performed.

INTRINSICALLY IRREVERSIBLE ACOUSTIC HEAT ENGINES

G. W. Swift, A. Migliori, T. Hogler and J. C. Wheatley
Los Alamos National Laboratory

1. What is the current status of the technology (theoretical, lab scale, moderate scale)?

   Now in transition from theoretical to lab scale.

2. What are the major problems associated with full-scale operation?

   I think it's too soon to guess.

3. What attributes of the technology make it particularly suitable for solar applications?

   Reasonable efficiency; no moving parts; no critical dimensional tolerances, purities

4. What is the optimum temperature range for operation of the technology?

   The hotter, the better: 1/3 of Carnot's efficiency for 700°C, 0.4 of Carnot's efficiency for 1000°C

5. What degree of concentration of solar light is required?

   100 W/cm^2

6. What are the critical areas in which research is required to further the development

of the technology for solar applications?

This technology is in such an early stage of development that we have plenty of "critical areas" quite independent of the type of heat source!

7. Is research currently being funded in any of these areas?

CHARGED AEROSOL GENERATOR

Alvin Marks
Phototherm Incorporated

1. What is the current status of the technology (theoretical, lab scale, moderate scale)?

   Eight (8) previous U.S. Government contracts, (15) U.S. patents much Lab work. New breakthrough with Converging nozzle direct isothermal conversion using charged Tin/Nitrogen aerosol in a Marks/Ericsson Cycle 1500 degrees/-300 degrees K-83.3% Theor. Efficiency.

2. What are the major problems associated with full-scale operation?

   Minor compared to present systems. No moving parts except in the auxiliaries.

3. What attributes of the technology make it particularly suitable for solar applications?

   Can be operated with a Solar Tower or other concentrating means at greater temperature differentials and hence greater efficiency - real: about 70%, twice present steam/electic turbine, and lower cost/KW (20%)

4. What is the optimum temperature range for operation of the technology?

   1500 degrees-300 degrees K

5. What degree of concentration of solar light is required?

   Existing Solar Towers could be employed, or a smaller scale version.

6. What are the critical areas in which research is required to further the development of the technology for solar applications?

R & D on Tin/Nitrogen Aerosols in a Converging Nozzle to confirm new electrothermodynamic mathematical Equations and to build prototype.

7. Is research currently being funded in any of these areas?

No. Except for small private funds supporting theoretical and patent work.

ELECTROHYDRODYNAMIC GENERATOR FOR USE WITH DISSIMILAR FLUIDS

T. H. Gawain and O. Biblarz
Naval Postgraduate School

1. What is the current status of the technology (theoretical, lab scale, moderate scale)?

   THEORETICAL

2. What are the major problems associated with full-scale operation?

   a. Choice of primary/secondary fluids based on available working temperature range.
   b. Conception of a scheme to maximize breakdown strength of working section.

3. What attributes of the technology make it particularly suitable for solar applications?

   a. No moving parts
   b. Light weight
   c. Very high voltages
   d. Closed thermo. cycle (silent/non-polluting)
   e. Cycle uses heat content of radiation and thus more efficient

4. What is the optimum temperature range for operation of the technology?

   This can be dictated by available solar energy concentrators at this stage (see 6 below) of the research.

5. What degree of concentration of solar light is required?

This can be dictated by available solar energy concentrators at this stage (see 6 below) of the research.

6. What are the critical areas in which research is required to further the development of the technology for solar applications?

   a. Identify as either ground-based or space-based application.
   b. Identify realistic temperatures and energy fluxes.
   c. Select primary/secondary fluids to run thermodynamic analysis.

7. Is research currently being funded in any of these areas?

   No funding since 1981.

A HEAT PIPE RANKINE ENGINE

Y. K. Chuah, Frank Kreith and Robert Barber
Barber Nichols Engineering Company

1. What is the current status of the technology (theoretical, lab scale, moderate scale)?

   Theoretical - a new concept of power generation.

2. What are the major problems associated with full-scale operation?

   At present, it is investigated as a power generator with output in the range of 1 to 5 kW.

3. What attributes of the technology make it particularly suitable for solar applications?

   The evaporator can be shaped into a solar collector.

4. What is the optimum temperature range for operation of the technology?

   It can operate in various temperature ranges, higher temperatures will result in higher efficiency, but will be limited by hardwares.

5. What degree of concentration of solar light is required?

   Depending on the working fluid used, concentration as high as 1000 to 1 is possible, though the engine can also function without concentration of solar light.

6. What are the critical areas in which research is required to further the development of the technology for solar applications?

   The Heat Pipe Rankine Engine requires only low level technologies. It might be best at this point to build one and demonstrate that the engine can work.

7. Is research currently being funded in any of these areas?

   Research is currently being sought for.

LIQUID METAL MHD CONVERSION FOR SOLAR THERMAL SYSTEMS

William Jackson
HMJ Corporation

1. What is the current status of the technology (theoretical, lab scale, moderate scale)?

   Laboratory scale, (i.e., exploratory development or preliminary engineering investigations).

2. What are the major problems associated with full-scale operation?

   LMMHD is considered to be a modular system with current work being on a single essentially full scale module. Chief issues involve interconnection of modules for required power level and development of efficient DC/AC inversion.

3. What attributes of the technology make it particularly suitable for solar applications?

   Use of a liquid metal in the MHD system provides excellent coupling with solar power towers of other collectors using a liquid metal as the heat transfer system. The same liquid metal may be used for both heat transfer and MHD conversion thereby eliminating sodium, steam or other heat exchangers.

4. What is the optimum temperature range for operation of the technology?

   Rejection temperature can be ambient. Upper limit of operating temperature is set by the boiling point of appropriate liquid metals such as sodium or lithium. Analysis indicates upper temperature range to be between 800 and 1500°F. For other applications, operation to 1800°F has been considered.

5. What degree of concentration of solar light is required?

Sufficient to achieve the conditions stipulated in 4. above.

6. What are the critical areas in which research is required to further the development of the technology for solar applications?

a. System analysis, especially performance optimization, cost comparison and off-peak performance;
b. determination of receiver configuration for LMMHD conditions;
c. electrical power conditioning;
d. attainable component performance (especially 2-phase flow components);
e. economic evaluation.

7. Is research currently being funded in any of these areas?

It is understood that Southern California Edison Company is funding a liquid metal MHD evaluation for low temperature geothermal and waste heat utilization. Analytical studies are being conducted at the University of Grenoble, France on LMMHD space power systems. An experimental low temperature loop is being operated at the Ben Gurion University, Beer-Sheva, Israel. No other research is presently being funded, either for solar thermal or other applications.

EVALUATION OF ENERGY CONVERSION TECHNOLOGIES FOR SOLAR APPLICATIONS

EVALUATION OF DIRECT ENERGY CONVERSION TECHNOLOGIES FOR SOLAR APPLICATIONS

Our evaluation of the various conversion technologies that were discussed by the participants of the workshop sought to determine the maturity of the technology as well as the characteristics of the technology that would affect its interface with the solar resource. We grouped the direct conversion technologies into three categories of maturity: conceptual, which means the idea has not yet been proven feasible (although it may appear to have potential from a solar point of view); feasible, which means the idea has been proven with laboratory or bench scale demonstrations but insufficient data exists for a complete assessment; and operational, which means that prototypes of the idea have been built and sufficient data exists for a complete assessment.

A summary of our evaluation of the characteristics of each technology is given in Table 2. Our ability to evaluate the characteristics of the technology is directly linked to the maturity of technology. The evaluations presented in Table 2 represent our best estimate of the current state of the art of each technology, but it should be emphasized that this information will rapidly become outdated as each technology develops from the conceptual to the operational stage. The categories considered in our evaluation include operating temperature, efficiency, input energy density, power density, circulating heat ratio, working fluid, cost effective size, toughness, and energy storage capability.

The input and output temperatures determine the theoretical limits on conversion efficiency (the greater the difference and the higher the input temperature, the greater the conversion efficiency. In addition, the magnitude of the input temperature influences the efficiency of the receiver (the higher the temperature, the lower the efficiency) and the output temperature determines the possibilities for cogeneration or use as a topping cycle.

The conversion efficiency directly impacts the capital cost of a solar conversion system through the size of the collector (the higher the efficiency, the lower the collector size for a given output). The efficiency also impacts the size of the conversion equipment but this is usually of secondary importance for a solar system.

The input energy density indicates the degree to which solar energy should be concentrated before applying it to the various conversion technologies (one sun approximately equals 500 W/m^2). Parabolic trough collectors can concentrate solar energy by a factor of 15-50, while solar central receiver systems concentrate by a factor of 1000-3000, and dishes a factor of 500-3000. Thus, the input energy flux required by a conversion technology indicates the type of solar concentrator it might be suitable to match with.

The power density indicates the size of the conversion device required for given output. A small, lightweight unit would be suitable for mounting on a dish for use as a distributed power source, while a large, heavy unit would be more suitable for a solar central receiver system.

The circulating heat ratio is the ratio of sensible heat flowing through the working fluid per cycle of operation to the work output per cycle. This ratio is low for engines that involve a first order phase change (latent heat) but high for engines that involve heating and cooling a mass of material. When the circulating heat ratio is high a recuperative heat exchanger is called for to increase cycle efficiency. This adds complexity to the conversion technology.

Table 2. Characteristics of Direct Energy Conversion Technologies

Techaology	Maturity	T_{in}(°C)	T_{out}(°C)	η	Energy Density (W/cm^2)	Power Density (W/cm^2)	Cir. Working Heat Ratio	Fluid	Cost Effect. Size	Storage Toughness	Capability	Comments
Thermoelectric	Operational	Up to 1499°C	Ambient	Low	?	?	Low	None	Modular	Good	None	Efficiency low with current materials
Thermomagnetic	Conceptual	Up to 1100°C	Ambient	0.7 η_c	?	?	High	None	Modular	?	Storage in magnetic field.	Requires superconducting magnets
Pyroelectric	Ceramic feasible	Up to 300°C	Ambient	1/16 × η_c	?	?	High	None	Modular	?	None	Ceramic system demonstrated
	Polymer-conceptual			1/2 × η_c								
Magnetohydrodyaamic	Feasible	400°C-800°C	Ambient	0.6-0.8η_c	?	?	Moderate	Liquid Metal	Modular	?	None	May require superconducting magnets
Electrohydrodynamic	Conceptual	1200°C	Ambient	0.7?	?	?	Moderate	Tin droplets in air	?	?	None	Few moving parts
Thermoacoustic	Feasible	700°C-100°C	100°C	0.4 × η_c	100	?	Moderate	Liquid sodium	Modular	Good	None	
Thermionic	Operational	1500°C	700°C	0.1-0.2	60-100	10	Low	None	Modular	Good	None	1.25×10^4 hrs @1730 K. Liquid N_2 and H_2O quench from 1800°K.
Sodium Heat Engine	Feasible	700°C-1000°C	200°C	0.25-0.3	?	?	Low	Liquid sodium	1-10KW	Good	None	8W system demonstrated
Regenerable Fuel Cell	Conceptual/ Feasible	80-1200	20-500	0.05-0.2	0.005-0.5	?	High	Aqueous solutions molten salts	Modular	Good	Internal chemical storage	no system has shown more than a small fraction of Carnot efficiency.
Surface Plasmon	Conceptual	X	X	0.4?	?	?	Low	None	Modular	?	None	
Submicron Antenna/ Rectifier	Conceptual	X	X	0.8?	?	?	Low	Conduction electrons	Modular	?	None	
Black Body Laser	Feasible	X	X	?	?	?	Low	None	Modular	?	None	

The working fluid of the cycle has an impact on cost and lifetime. Exotic materials, materials that must be contained at high pressure or that are corrosive, imply high cost and short lifetime.

The cost effective size is determined by economies of scale inherent in each technology. Some direct conversion technologies have no inherent economies of scale and thus lend themselves to modular construction. These technologies could be sized for a parabolic dish receiver.

By toughness we mean ability to withstand thermal shock and cycling. The solar resource is inherently time varying. If a direct conversion technology is "tough" then it is a candidate for integration with a receiver. If it is not, then it must be buffered by thermal storage or an auxiliary source of heat to keep it at operating temperature when the sun is not shining.

If a solar driven conversion process is to stand alone, then energy storage of some kind must be used to supply heat when the sun is not shining. Some technologies interface well with energy storage, indeed they may provide inherent storage in the way they operate. Others pose potential problems for storage such as high temperature or corrosive working fluids.

Out of all of the technologies that were considered by the workshop, only thermoelectric and thermionic conversion can be considered to be fully operational. The remaining technologies were evenly split as to level of maturity between the categories of "feasible" and "conceptual". Two of the technologies (Sodium Heat Engine and Regenerable Fuel Cell) are currently being funded by DOE to examine their potential for solar energy applications.

Several of the technologies do not operate over a large enough temperature range or have a high enough efficiency to serve as stand alone conversion systems. Thermoelectric conversion, pyroelectric conversion, thermionic conversion and the black body pumped laser all fall into this category. A thermoelectric conversion system could be built into the nonilluminated walls of a high temperature cavity receiver to take advantage of the high wall temperature caused by black body thermal radiation in the cavity. Pyroelectric conversion and thermionic conversion would work best as bottoming and topping cycles, respectively. Finally, the black body pumped laser would operate most effectively in a combined quantum/thermal conversion system where the laser light was used directly in a manufacturing process or converted to electricity by a photovoltaic array, with the remaining thermal energy in the cavity used to run a thermal conversion system. In this type of combined quantum/thermal conversion system, the band gap of the photovoltaic array could be tuned to exactly match the wavelength of the laser light, insuring virtually 100% conversion of the laser light to electricity.

CONCLUSIONS AND RECOMMENDATIONS FOR FUTURE RESEARCH

CONCLUSIONS AND RECOMMENDATIONS FOR FUTURE RESEARCH

From the workshop it is clear that a consistent basis for evaluating and comparing alternative conversion technologies for use in solar energy applications does not exist. The tabulation of the characteristics of the conversion technologies in Table 2 is in many cases incomplete. The values presented have been developed by investigators with different points of view and assumed constraints, and a number of the technologies are still conceptual or have received only limited laboratory evaluation. For this initial survey no attempt was made to make a complete assessment of the literature on each technology, and some of the tabulated information reflects the bias of the workshop presentor. Those technologies recognized as conceptual show in general more optimistic performance predictions than those that are more fully developed. Experience shows that projected values generally assume more conservative values as a technology nears fruition.

On the basis of the information available, it appears that none of the conversion technologies considered during the workshop offer a significant advantage as "stand alone" conversion devices relative to the current state-of-the-art Brayton, Rankine, or Stirling heat engine conversion systems. This observation, however, is based on limited and in some cases incomplete data. A definitive conclusion to address or dismiss further consideration of new conversion technologies for solar application requires a more sound analysis. The workshop results do not support a comprehensive program to evaluate each of the technologies presented. In considering alternative technologies, conversion efficiency is the primary characteristic of beneficial impact for solar application--solar energy economics are more strongly dominated by heliostat costs than conventional power systems are by fuel costs, and increased energy conversion efficiency tips the scales in favor of solar power. As a result it is recommended that an analysis of the efficiency of alternative conversion technologies be carried out from a consistent, fundamental, thermodynamic, and engineering basis to provide a common ground upon which to judge the comparative performance of the different technologies. By limiting the analysis to conversion efficiency, definitive results of primary impact for the evaluation of conversion alternatives to conventional heat engines and for topping cycles can be obtained in a study of well defined scope. It is recommended that the study use the existing literature as a point of departure but develop the results so that they can be understood in comparison with the intrinsic thermodynamic limits of thermal and quantum radiation conversion. For example: early treatments of thermophotovoltaic conversion, which neglected the fact that solar energy is a power source not an energy source, predicted unrealistic conversion efficiencies of 70%. Evaluation of the submicron antenna/reactifier should include a self-consistent analysis and not be limited to analogy with a microwave receiver, in view of the incoherent nature of the solar flux.

Even though the conversion technologies do not offer significant advantages as "stand alone" devices, three of the technologies are mature enough to consider their interface with the solar thermal resource in detail and at the same time possess proven or potential efficiencies great enough to inspire optimism that they may prove effective in combined cycle applications. These are thermionics, magnetohydrodynamics, and the sodium heat engine.

Thermionics has relatively low efficiency but its high outlet temperature indicates a possible application to cogeneration or as a topping cycle. The outlet temperature of the thermionic converter is just about the input temperature required of a heat engine using liquid sodium as the working fluid. This suggests a possible match with the sodium heat

engine, magnetohydrodynamics or thermoacoustics (when it is proven as a practical conversion scheme). The sodium heat engine and magnetohydrodynamics with sodium as the working fluid have input and output temperatures somewhat below thermionics but higher efficiencies. They too might be used for cogeneration or topping cycles although their efficiencies may be large enough for them to serve as primary power converters.

Thermoelectric conversion is a mature technology but has very low efficiency. Current efforts in this area (funded by NASA) are aimed at developing materials that will operate at high temperature with adequate efficiency.

Thermomagnetics and thermoacoustics are immature technologies with some potential for efficient operation at high temperature. Thermomagnetic materials with the potential for efficient operation at high temperature exist and the use of the thermomagnetic phenomena in refrigerators and heat pipes has been demonstrated. The concept of a thermomagnetic heat engine has not been demonstrated. The need for superconducting magnets and the high circulating power inherent in this concept implies a potentially high cost. The thermoacoustic engine is also conceptual but is calculated to perform efficiently at high temperature using liquid sodium as the working fluid. The simplicity of this concept implies potentially low cost. Further work is being funded by OER.

Pyroelectric conversion with known materials is limited to operating temperatures low enough to be attained with flat plate collectors and does not seem suitable for consideration by the solar technology program at this time. If materials capable of efficient operation at high temperature are ever developed then this technology might become attractive although the high circulating power inherent in this concept implies potentially high cost.

Electrohydrodynamic conversion is conceptual and cannot be evaluated in detail. The idea seems to have a close match with prior proposed concepts of high-temperature air receivers.

The nonquantum concepts for converting light directly to electricity considered by us may hold the greatest potential of all but their extremely conceptual nature implies that this potential will not be realized for a long time. Surface plasmon (and other electrooptic phenomena) conversion is being pursued by NASA. The submicron dipole antenna and diode rectifier is simple in principle and would probably work if it can be manufactured but its basic conversion efficiency has not been rigorously evaluated or demonstrated.

We also considered a way of thermally coupling to a quantum conversion system via black body radiation from a cavity receiver. We believe that this approach may have merit but past analyses have not been performed in a way that will allow consistent comparison with pure thermal, quantum, or combined quantum/thermal conversion.

Finally, the workshop contained a presentation of recent advances in the thermodynamics of heat engines operating in finite time. This includes the effects of time varying temperatures of heat sources and sinks. The solar thermal resource is inherently a time varying resource (regular diurnal and irregular short time fluctuations).

We specifically recommend the following areas for future research efforts:

1. Assess the position of thermionics, magnetohydrodynamics, the sodium heat engine, and the regenerable fuel cell as applied to cogeneration or topping cycles relative to the baseline technologies of Rankine, Brayton, or Stirling cycles. Initial steps would include conceptual configurations (i.e., thermionics topping a sodium heat engine with exhaust heat used for cogeneration or to drive a baseline bottoming cycle) and estimate of cost.

2. Monitor progress on thermoelectrics, thermomagnetics (the thermomagnetic heat pump), thermoacoustics, pyroelectrics, and electrohydrodynamics funded by others. Encourage the development of these technologies by defining the general operating characteristics that must be achieved before they can be considered for solar applications.

3. Estimate conversion efficiencies of electrohydrodynamic conversion used in conjunction with high-temperature air receivers.

4. Analyze black body coupling to quantum systems in a way consistent with previous analysis of thermal, quantum and combined thermal/quantum conversion.

5. Analyze the efficiency of alternative direct conversion technologies from a consistent, fundamental, thermodynamic and engineering basis to provide a common ground upon which to judge the comparative performance of the different technologies.

DISTRIBUTION LIST

3MCorporation
3M Center Building, 207-1W-08
St. Paul, MN 55101
Mr. David Hill
Mr. Burton A. Benson

ARCO Solar, Inc.
9315 Deering
Chatsworth, CA 91311
Mr. Jim Caldwell

Acurex Solar Corporation
485 Clyde Ave.
Mt. View, CA 94042
Mr. Don Duffy

Advanco Corporation
40701 Monterey Ave.
Palm Desert, CA 92260
Mr. Byron Washom

Allied Chemical Company
P.O. Box 1021R
Morristown, NJ 07960
Mr. Robert Armburst

Arizona Public Service Company
P.O. Box 21666
Phoenix, AZ 85036
Mr. Eric Weber

BDM Corporation
1801 Randolph SE
Albuquerque, NM 87106
Dr. J. Alcone

Babcock and Wilcox
91 Stirling Ave.
Barberton, OH 44203
Mr. Paul Elsbree

Barber-Nichols Engineering Co.
6325 W. 55th Ave.
Arvada, CO 80002
Mr. Robert Barber

Battelle Pacific NW Laboratory
P.O. Box 999
Richland, WA 99352
Dr. Ben Johnson
Dr. Kevin Drost
Mr. Tom A. Williams

Bechtel Corporation
P.O. Box 3965
San Francisco, CA 94119
Mr. Pascal DeLaquil

Black and Veatch Consulting Engineers
1500 Meadow Lake Parkway
Kansas City, MO 64114
Dr. Charles Grosskreutz

Bowman, Dr. Melvin
Consultant
360 Andanada
Los Alamos, NM 87544

Brandt, Dr. Richard
Consultant
University of Washington
Robert Hall
Seattle, WA 98195

Brookhaven National Laboratory
Department of Applied Sciences
Building 701
Upton, NY 11973
Dr. William Wilhelm

Brumleve, Mr. Tom
Consultant
1512 N. Gate Road
Walnut Creek, CA 94598

Burns and McDonnell
P.O. Box 173
Kansas City, MO 64141
Mr. Peter Steitz

Chronos Research Laboratories, Inc.
3025 Via Decaballo
Olivenhain, CA 92024
Randall B. Olsen

Colorado State University
Dept. of Civil Engineering
Ft. Collins, CO 80523
Dr. Jon Peterka

Dan-Ka Products, Inc.
3862 South Kalamath
Englewood, CO 80110
Mr. Daniel Sallis

Department of Energy/ALO
P.O. Box 1500
Albuquerque, NM 87115
Mr. Dean Graves
Mr. Joe Weisiger
Mr. Nyles Lackey

Department of Energy/HQ
Forrestal Building
1000 Independence Ave., SW
Washington, DC 20585
Dr. H. Coleman
Mr. S. Gronich
Mr. C. Mangold
Mr. M. Scheve
Mr. Frank Wilkins

Department of Energy/SAN
1333 Broadway
Oakland, CA 94536
Mr. Robert Hughey
Mr. William Lambert

Department of Energy/SAO
1617 Cole Blvd.
Golden, CO 80401
Mr. Jerry Bellows

Dow Chemical Company
Contract Research, Devel. and Engr.
Building 566
Midland, MI 48640
Mr. J. F. Mulloy

Dow Corning Corporation
Midland, MI 48640
Mr. G. A. Lane

EG&G Idaho, Inc.
MS/WCB-E3, Box 1625
Idaho Falls, ID 83414
Lance Kirol

El Paso Electric
P.O. Box 982
El Paso, TX 79960
Mr. James E. Brown

Electric Power Research Institute
P.O. Box 10412
Palo Alto, CA 94303
Mr. Donald Augenstein

England, Dr. Christopher
Consultant
Engineering Research Group
138 West Pomona Ave.
Morrovia, CA 91016

Entech, Incorporated
P.O. Box 612246
DFW Airport, TX 75261
Mr. Walter Hesse

Falconer Glass Industries, Inc.
500 South Work Street
Falconer, NY 14733-1787
Mr. Jack South

Farmland Industries
P.O. Box 69
Lawrence, KS 66044
Mr. John Prijatel

Ford Scientific Laboratory
Room 2016, Box 2053
Dearborn, MI 48121
Tom Hunt

Foster Wheeler Solar Development Corp.
12 Peach Tree Hill Road
Livingston, NJ 07070
Mr. Robert J. Zoschak

Gas Research Institute
8600 West Bryn Mawr Ave.
Chicago, IL 60631
Mr. Keith Davidson

Georgia Institute of Technology
Atlanta, GA 30332
Dr. Tom Brown

Georgia Power Company
7 Solar Circle
Shenandoah, GA 30265

HMJ Corporation
P.O. Box 15128
Chevy Chase, MD 20815
Mr. William D. Jackson

Hughes Aircraft Company E1/F150
P.O. Box 902
El Segundo, CA 90245
Frank Ludwid

Hughes Aircraft Company
Electric Optical Data Systems Group
El Segundo, CA 90245
Dr. Frank Ludwig

Jet Propulsion Laboratory
4800 Oak Grove Drive
Pasadena, CA 91109
Mr. William Owen

Jet Propulsion Laboratory
MS 277-102
4800 Oak Grove Drive
Pasadena, CA 91109
Charles Wood

LaJet Energy Company
P.O. Box 3599
Abilene, TX 79604
Mr. Monte McGlaum

Lawrence Berkeley Laboratory
Building 90-2024,
University of California
1 Cyclotron Road
Berkeley, CA 94720
Dr. Arlon Hunt

Los Alamos National Laboratory
Mail Stop: K764
Los Alamos, NM 87545
Greg Swift

Luz Engineering Corp.
15720 Ventura Blvd.
Suite 504
Encino, CA 91436
Dr. David Kearney

Martin Marietta
P.O. Box 179
Denver, CO 80201
Mr. Tom Tracey

McDonnell Douglas Astronautics Company
5301 Bolsa Ave.
Huntington Beach, CA 92647
Mr. Jim Rogan

Mechanical Technology, Inc.
968 Albany Shaker Road
Latham, NY 12110
Mr. H. M. Leibowtiz
Mr. G. R. Dochat

Meridian Corporation
5113 Leesburg Pike
Suite 700
Falls Church, VA 22041
Mr. Dinesh Kumar

Midwest Research Institute
425 Volker Blvd.
Kansas City, MO 64110
Mr. R. L. Martin
Mr. Jim Williamson

NASA Lewis Research Center
21000 Brookpark Road
Cleveland, OH 44135
Dr. Dennis Flood

NASA Lewis Research Center
Solar Conversion Branch
MS-302-2 21002 Brookpark Road
Cleveland, OH 44135
Donald Chubb

NASA-Johnson Space Center
NASA Road One - EPS
Houston, TX 77058
Mr. William Simon

National Bureau of Standards
Building 221, Room 252
Gaithersburg, MD 20899
Mr. Joseph Richmond

New Mexico State University
Physical Sciences Lab
P.O. Box 3548
Las Cruces, NM 88003
Mr. James McCrary

Olin Corporation
315 Knotter Drive
Cheshire, CT 06410-0586
Mr. Jack Rickly

Pacific Gas and Electric Company
3400 Crow Canyon Rd.
San Ramon, CA 94583
Mr. Gerry Braun
Mr. Joe Iannucci

Phototherm, Inc.
141 Canal Street
Nashua, NH 03060
Edgar R. Bourke

Power Kinetics, Inc.
1223 Peoples Ave.
Troy, NY 12180
Mr. Bob Rogers

Rockwell International Corp
Energy Technology Center
P.O. Box 1449
Canoga Park, CA 91304
Mr. W. L. Bigelow

Rockwell International
Energy Systems Group
8900 DeSoto Ave.
Canoga Park, CA 91304
Mr. Tom H. Springer

San Diego State University
Math Department
San Diego, CA 92182
Peter Salamon

Sanders Associates, Inc.
95 Canal Street
Nashua, NH 03010
Mr. Daniel J. Shine

Sandia Labs
Division 6222
Albuquerque, NM 87185
John Holmes

Sandia National Laboratories
Division 6227
P.O. Box 5800
Albuquerque, NM 87185
Jesus Martinez

Sandia National Laboratories
Solar Department 8453
Livermore, CA 94550
Mr. A Skinrood
Dr. R. A. Rinne

Sandia National Laboratories
Solar Energy Department 6220
P.O. Box 5800
Albuquerque, NM 87185
Mr. John Otts
Mr. James Leonard
Dr. Donald Schuler

Science Applications, Inc.
10401 Rosselle Street
San Diego, CA 92121
Dr. Barry Butler

Solar Energy Industries Association
1717 Massachusetts Ave. NW No. 503
Washington, DC 20036
Mr. Carlo La Porta
Mr. David Goren
Mr. Hal Seilstad

Solar Energy Research Institute
1617 Cole Blvd. Bldg. 15/3
Golden, CO 80401
Meir Carasso

Solar Energy Research Institute
1617 Cole Blvd., Bldg. 16/2
Golden, CO 80401
Helena Chum

Solar Energy Research Institute
1617 Cole Blvd.
Golden, CO 80401
Mr. B. P. Gupta
Dr. L. J. Shannon

Solar Energy Research Institute
1617 Cole Blvd. Bldg. 15/3
Golden, CO 80401
Bim Gupta

Solar Energy Research Institute
1617 Cole Blvd. Bldg. 15/3
Golden, CO 80401
David H. Johnson

Solar Energy Research Institute
1617 Cole Blvd. Bldg. 15/3
Golden, CO 80401
Elizabeth Fisher

Solar Energy Research Institute
1617 Cole Blvd. Bldg. 15/3
Golden, CO 80401
Gerry Nix

Solar Energy Research Institute
1617 Cole Blvd. Bldg. 15/3
Golden, CO 80401
Kuang-Yu Wang

Solar Kinetics, Inc.
P.O. Box 47045
Dallas, TX 75247
Mr. Gus Hutchison

Southern Research Institute
2244 Walnut Grove Ave.
Rosemead, CA 91770
Mr. Joe Reeves

Southwest Research Institute
6220 Culebra Road
San Antonio, TX 78238
Mr. Danny M. Deffenbaugh

Stirling Thermal Motors, Inc.
2841 Boardwalk
Ann Arbor, MI 48104
Mr. Benjamin Ziph

Texas Tech University
Dept. of Electrical Engineering
Lubbock, TX 79409
Mr. Edgar A. O'Hair
Physics Department
Ms. Virginia K. Agarwal

Thermo Electron Corporation
101-1st Avenue
Waltham, MA 02254
Gabor Miskolczy

U.S. Department of Energy
ECUT Porgram, CE-142
Forrestal Bldg., 5E-091
1000 Independence Ave., S.W.
Washington, DC 20585
Marvin Gunn

U.S. Department of Energy
STT Program, CE-314
Forrestal Bldg., 5H-041
1000 Independence Ave., S.W.
Washington, DC 20585
Frank Wilkins

United Technologies Research Center
Silver Lane
East Hartford, CT 06108
Alan Haught

University of Arizona
College of Engineering
Tucson, AZ 85721
Dr. Kumar Ramohalli

University of Arizona
Dept. of Electrical Engineering
Tucson, AZ 85721
Dr. Roger Jones

University of Chicago
Enrico Ferni Institute
5640 S. Ellis Ave.
Chicago, IL 60637
Dr. R. Winston
Dr. J. O'Gallagher

University of Dayton Research Institute
300 College Park, KL102
Dayton, OH 45469
Dr. Barry H. Dellinger

University of Hawaii at Manoa
Hawaii Natural Energy Institute
Homes Hall Room 246
2540 Dole Street
Honolulu, HI 96822
Dr. Mike Antal

University of Houston
4800 Calhoun
106 SPA Building
Houston, TX 77004
Dr. Alvin Hildebrandt
Dr. Lorin Vant-Hull

University of Illinois
Dept. of Mechanical and Industrial Engineering
1206 W. Green Street
Urbana, IL 61801
Dr. Art Clausing

University of Kansas Center for Research
2291 Irving Hill Drive
Lawrence, KS 66045
Mr. David Martin

University of Minnesota
Dept. of Mechanical Engineering
Minneapolis, MN 55455
Dr. Edward Fletcher

University of New Hampshire and College of Engineering and Physical Sciences
Kingsbury Hall - 260
Durham, NH 03824
Dr. V. K. Mathur

University of New Mexico
Department of Mechanical Engineering
Albuquerque, NM 87131
Mr. M. W. Wilden
Mr. W. A. Gross

University of Washington, Seattle
Dept. of Aeronautics & Astronautics
Seattle, WA 98195
Walter Christiansen

Wichita State University
Mechanical Engineering Dept.
Wichita, KS 67208
Mr. James A. Harris

Demichelis, F. and Minetti-Mezzetti, E., "A Solar Thermophotovoltaic Converter," *Solar Cells*, 1 (1979/80): 395-403.

Duomarco, J.L. and Kaplow, Roy, "MIT Industrial Liason Program Report," Boston: Massachussetts Institute of Technology [1981]. (Mimeographed.)

Kim, Chang Wook, and Schwartz, Richard J., "A p-i-n Thermo-Photovoltaic Diode," *IEEE Transactions on Electron Devices* Vol ed-16, no. 7 (July 1969): 657-663.

Rabl, Ari, "Comparison of Solar Concentrators," *Solar Energy* (1975): 93-111.

Swanson, R.M., and Bracewell, R.N., *Silicon Photovoltaic Cells in Thermophotovoltaic Conversion.* Stanford: Stanford Electronics Laboratories, [1977].

Swanson, Richard M, "A Proposed Thermophotovoltaic Solar Energy Conversion System," *Proceedings of the IEEE* Vol 67, no. 3 (March 1979): 446-47.

Vasil'ev, A.M., "Thermophotovoltaic Conversion Efficiency," Trans. *Teplofizika Vysokikh Temperatur* Vol 5, no. 2 (March-April 1967).

Weaver, Willard R. and Lee, Ja H., "A Solar Simulator-Pumped Gas Laser for the Direct Conversion of Solar Energy," *16th IECEC* V.1 (August 1981): 84-88.

Wedlock, Bruce D., "Thermo-Photo-Voltaic Energy Conversion," *Proceedings of the IEEE* (May 1963): 694-98.

White, David C., and Wedlock, Bruce D., and Blair, John, "Recent Advance in Thermal Energy Conversion," *Session on Thermal Energy Conversion:* 125-32.

ELECTROHYDRODYNAMIC CONVERSION

Gawain, T.H. and Biblarz, O., "Electrohydrodynamic (EHD) Generator for Use with Dissimilar Fluids," *Navy Technical Disclosure Buletin* V.9(1) (September 1976). Navy Cat. No. 3714; Navy Case No. 65,382.

Gram, David, "Inventor Targets Poor," *The Morning Union.*

Marks, Alvin M., "Device for Conversion of Light Power to Electronic Power," *United States Patent* No. 4, 445,050 (April 24, 1984).

Marks, Alvin M., "Electrothermodynamic Equations of a Charged Aerosol Generator," *19th IECEC* V.1 (August 1984): 43-51.

Marks, Alvin M., "Space Satellite Power System Presentation" (typewritten).

Phototherm, Inc., "Lepcon/Elcon Defense System," presentation of Dr. Alvin Mark's invention. (Typewritten.)

"Alumni Focus: Alvin M. Marks' New Solar Power Converter," *At Cooper Union* 8 (Spring and Summer 1984): 26.

"Amazing Tin-Aerosol Generator," *Science & Mechanics* September-October 1983.

"Athol Inventor Uses Sun Power to Cook Food," *The Morning Union* 14 July 1984.

"Energy Digest," *Science Digest* (August 1984): 21.

Science Digest, January 1984; p. 50.

"Scientist's Idea for Cheap Electricity," *The Boston Herald*, 26 December 1984.

"Technology," *Robb Report* VIII (September 1984): 30.

Chum, H. "Review of Thermally Regenerative Electrochemical Systems," SERI/TR-332-416, Golden, Colorado, 1981.

Hsu, M.S.S and Reed, T.B., "Electrochemical Power and Hydrogen Generation from High Temperature Electrolytic Cells," *11th IECEC*.

Subramanian, K. and Hunt, T.K., "Solar Residential Total Energy System Using the Sodium Heat Engine--A Concept Study," *17th IECEC* V.3 (August 1982): 1474-80.

IRREVERSIBLE HEAT ENGINES

Andresen, Bjarne; Salamon, Peter; and Berry, R. Stephen, "Thermodynamics in finite time," *Physics Today*, September 1984, pp. 62-70.

Salamon, P., Band, Y.B., and Kafri, O., "Maximum power from a cycling working fluid," *Journal of Applied Physics* 53(1), (January 1982): 197-202.

Salamon, Peter and Nitzan, Abrahan, "Finite time optimizations of a Newton's law Carnot cycle," *Journal of Chemical Physics* 74(6) (March 1981): 3546-560.

Salamon, Peter; Nitzan, Abrahan; Andersen, Bjarne; and Berry, R. Stephen, "Minimum entropy production and the optimization of heat engines," *Physical Review A* 21(6) (June 1980): 2115-129.

Swift, G.W., Migliori, A., Hofler, T., and Wheatley, John, "Theory and Calculations for an Intrinsically Ireversible Acoustic Prime Mover Using Liquid Sodium as Primary Working Fluid," submitted to J. Alcoust. Soc. Am.

Wheatley, J.C., Hofler, T., Swift, G.W., and Migliori, A., "An Intrinsically Irreversible Thermoacoustic Heat Engine." J. Acoust. Soc. Am. *74*, 153 (1983).

Wheatley, J.C., Hofler, T., Swift, G.W., and Migliori, A., "Experiments with an Intrinsically Irreversible Acoustic Heat Engine." Phys. Rev. Lett. *50*, 499 (1983).

Wheatley, John, Hofler, T., Swift, G.W., and Migliori, A., "Understanding Some Simple Phenomena in Thermoacoustics with Applications to Acoustical Heat Engines." Am. J. Phys., in press.

Bidard, R. and Sterlini, J., "Generateur MHD Fonctionnant par Emulsion" - Electricity from MHD (c.r. Colloque, Salzburg, 1966), 2, SM-74/108 (1966), 107.

Brown, G.A. and Levy, E.K., "Liquid Metal Magnetohydrodynamic Power Generation with Condensing Ejector Cycles," Paper No. SM-74/171, presented at International Symp. on MHD Electrical Power Generation, Salzburg, Austria, July 4-8, 1966.

Elliott, D.G., "Two-fluid Magnetohydrodynamic Cycle for Nuclear-Electric Power Conversion." TR32-116, Jet Propulsion Laboratory, Pasadena, CA, June 30, 1961; also ARS J., 32, 924-928 (1962).

Free, John, "NOW: liquid-metal MHD," *Popular Science* (July 1985) p. 54.

Hals, F. et al., Kessler, R., Westra, L., Zar, J., Morgan, W., and Bozzuto, C., "Results from Conceptual Design Study of Potential Early Commercial MHD/Stream Power Plants," *16th IECEC* V.2 (August 1981): 1493-98.

Harris, L.P., *Hydomagnetic Channel Flows*, MIT Press, Cambridge, MA 1960.

Jackson, W.D., "Critique of MHD Electrical Power Generation," Proc. 3rd Beer-Sheva Seminar on MHD Flows and Turbulence, AIAA, New York, NY 1982.

Jackson, W.D., Bidard, R., and Toschi, R., (Editors) "MHD Electrical Power Generation: 1972 Status Report," Chapter 3, Atomic Ener. Rev., Vol. 10, No. 3, IAEA, Vienna, 1972.

Jackson, W.D. and Pierson, E.S., "Operating Characteristics of MHD Induction Generators," IEE Conference Report, Series No. 4, pp. 38-42, Proc. of International Symp. on Magnetohydrodynamic Power Generation, Newcastle-upon-Tyne, September 1962.

Mawardi, O.K., Unpublished lecture notes on MHD, Massachusetts Institute of Technology, Fall Semester, 1955.

Petrick, M. and Lee, K.Y., "Performance Characteristics of a Liquid-Metal MHD Generator." ANL-6870, Argonne National Laboratory, Argonne, IL, July 1964.

Petty, S., Enos, G., Kessler, R., and Swallom, D., "MHD Generator Performance Comparisons Between Coal and Ash Firing," *16th IECEC* V.1 (August 1983): 118-24.

Pierson, E.S., Branover, H., Fabris, G., and Reed, C.B., "Solar Powered Liquid Metal Power Systems," *Mechanical Engineering*, 102, pp. 32-37, October 1980.

Pierson, E.S., Cohen, D., and Grammel, S.J., "Liquid-Metal MHD for Solar and Coal," Proc. the Seventh International Conference on MHD Electrical Power Generation, Boston, MA, pp. 150-157, 1980.

Pierson, E.S., Jackson, W.D., Berry, G., Petrick, M., and Dennis, C., "Performance of Solar Thermal Systems with Liquid Metal MHD Conversion." Report No. 4MHDSA-DCE-P/84/R1, HMJ Corporation, Chevy Chase, MD, June 1984.

Prem, L.L., "Analytical and Experimental Results of the Fluid Metal MHD Power Conversion Program," Paper No. SM-74/84, presented at International Symp. on MHD Electrical Power Generation, Salzburg, Austria, July 4-8, 1966.

"Comparative Evaluation of Phase I Results from the Energy Conversion Alternatives Study (ECAS)", NASA TM-X-71855, February 1976.

"Preliminary Design of the Carrisa Plain Silar Central Receiver Power Plant, Vol. 1, Executive Summary." DOE Report ESG-DOE 13404, December 1983, prepared by Rockwell International Corporation under Contract DE-SFCO3-82SF11674.

PYROELECTRIC CONVERSION

Beam, B.H., "An exploratory study of thermoelectrostatic power generation for space flight applications," NASA TN-D336 (1960).

Beam, B.H., Fry, J. and Russel, L., "Experiments on radiant energy conversion using thin dielectric films,: *Progress in Astronautics and Aeronautics*, Vol. 16, Space Power Systems Engineering, Editors: G. Szego and J. Taylor, Academic Press, 1964.

Das, R., Krauthamer, S., and Frank, H., "Application of Electrochemical Energy Storage Systems," *17th IECEC* V.2 (August 1982): 620-24.

De Young, R.J., Stripling, J., Enderson, T.M., Humes, D.H., Davis, W.T., and Conway, E.J., "Laser and Solar-Photovoltaic Space Power Systems Comparison--Part II," *19th IECEC* V.1 (August 1984): 339-344.

Drummond, J.E., "Dielectric Power Conversion," *10th IECEC* (August 1975): 569-75.

Furukawa, T., Date, M., Fukada, E., Tajitsu, Y. and Chiba, A., "Ferroelectric behavior in the copolymer of vinylidene fluoride and trifluorocthylene," Jap. J. Appl. Phys. *19* (1980).

Furukawa, T., Johnson, G.E., Bair, H.E., Tajitsu, Y., Chiba, A. and Fukada, E., "Ferroelectric phase transition in a copolymer of of vinylidene fluoride and trifluorethylene," Jap. J. Appl. Phys. 19 (1980).

Gonzalo, J.A., "Ferroelectric materials as energy converters," Ferroelectrics *11*, 423 (1976).

Hicks, J.C., Jones, T.E., Burgener, M.L. and Olsen, R.B., "High temperature hysteresis in polyvinylidene fluoride," Ferroelectrics Letters, *44* pp. 89-92 (1982).

Higashihata, Y., Sako, J. and Yagi, T., "Piezoelectricity of vinylidene fluoride-trifluorethylene copolymers," Ferroelectrics, *32*, 85 (1981).

Lines, M.E. and Glass, A.M., ***Principles and Applications of Ferroelectrics and Related Materials***, Clarendon, Oxford (1977).

Margosian, P.M., "Parametric study of a thermoelectrostatic generator for space applications," Lewis Research Center, NASA, Cleveland, Ohio, Jan. 4, 1965.

Olsen, Randall B., "Pyroelectric Conversion in Space," *19th IECEC* V.1 (August 1984): 224-28.

Olsen, R.B., "Ferroelectric conversion of heat to electrical energy--a demonstration," J. Energy, p. 91 March/April (1982).

Olsen, R.B., "Condensed state heat engines," DOE workshop on thermally regenerative electrochemical systems (TRES), Alexandria, Virginia, Dec. 3-4 (1981).

Olsen, R.B., "Pyroelectric conversion in space," *19th IECEC* (1984) p. 224.

Olsen, R.B., Briscoe, J.M., Bruno, D.A. and Butler, W.F., "A pyroelectric energy converter which employs regeneration," Ferroelectrics *38*, 975 (1981).

Olsen, R.B., Briscoe, J.M. and Bruno, D.A., "Performance of a 1-watt pyroelectric converter," *17th IECEC* (1982).

Olsen, R.B. and Brown, D.D., "High efficiency direct conversion of heat to electrical energy-related pyroelectric measurements," Ferroelectrics *40* pp. 17-27 (1982).

Olsen, R.B., Bruno, D.A. and Briscoe, J.M., "Pyroelectric conversion cycles," submitted to J. Appl. Phys.

Olsen, R.B., Bruno, D.A., Briscoe, J.M. and Dullea, J., "Cascaded pyroelectric energy converter," Ferroelectrics (in press).

Olsen, R.B., Bruno, D.A., Briscoe, J.M. and Jacobs, W.E., "Quasi-irreversible changes in the polarization of vinylidene flouride-trifluoroethylene," submitted to Ferroelectrics Letters.

Olsen, R.B., Bruno, D.A., Briscoe, J.M. and Jacobs, W.E., "Pyroelectric conversion cycle of vinylidene fluoride-trifluoroethylene," J. Appl. Phys. (in press).

Olsen, R.B., Butler, W.F., Drummond, J.E., Bruno, D.A. and Briscoe, J.M., "Heat flow in a pyroelectric converter," submitted to IECEC (1985).

Olsen, R.B., Butler, W.F., Payne, D.A., Tuttle, B.A. and Held, P.C., "Observation of a polarocaloric (electrocaloric) effect of 20 in lead zirconate modified with Sn^{4+} and Ti^{4+}," Phys. Rev. Lett. *45* p. 1436 (1980).

Olsen, R.B. and Evans, D., "Pyroelectric Energy Conversion--Hysteresis Loss and Temperature Sensitivity of a Ferroelectric Material," J. Appl. Phys. *54* p 5941 (1983).

Olsen, R.B., Hicks, J.C., Broadhurst, M.G. and Davis, G.T., Temperature Dependent Ferroelectric Hysteresis Study of Poly(vinylidene fluoride) App. Phys. Let., *43*, 127-129 (1983).

Sawyer, C.B. and Tower, C.H., Phys. Rev. *35*, pp. 269-273 (1930).

Yamada, T. and Kitayama, T., "Ferroelectric properties of vinylidene fluoride-trifluoroethylene copolymers," J. Appl. Phys. *52*, 6863 (1981).

Yamaka, T., Ueda, T. and Kitayama, T., "Ferroelectric-to-paraelectric phase transition of vinylidene fluoride-trifluorethylene copolymer," J. Appl. Phys. *52*, 2 (1981).

"Method and apparatus for pyroelectric power conversion," U.S. Patent No. 4,425,540 (1984).

THERMIONIC CONVERSION

Goodale, Douglass; Lieb, David; and Neale, Douglas, "Solar Thermionic Energy Converter Experiment," *17th IECEC* V.4 (August 1982): 1924-28.

Goodale, Douglass; Reagon, Peter; Lieb, David; and Huffman, Fred, "Thermionic Converters for Terrestrial Applications," *17th IECEC* V.4 (August 1984): 1913-17.

Goodale, D.B. and Miskolczy, "Combustion Converter Design Evolution," *19th IECEC* V.4 (August 1984): 2270-75.

Miskolczy, G.; Goodale, D.; Moffat, A.; and Gentile, A., "Design and Construction of Thermionic Cogeneration Burner Module," *19th IECEC* V.4 (August 1984): 2260-64.

THERMOELECTRIC CONVERSION

Cole, Terry, "Thermoelectric Energy Conversion with Solid Electrolytes," *Science* September 1983, pp. 915-920.

Zoltun, D.; Word, C.; and Stapfer, G., "Measurement of Seebeck Coefficient Using a Light Pulse," *19th IECEC* V.4 (August 1984): 2241-43.

THERMOMAGNETIC CONVERSION

Barclay, J.A., Moze, O. and Paterson, L., "A Reciprocating Magnetic Refrigerator for 2-4K operation: Initial Results," *JAP, 50*, 9, September 1979, pp. 5870-5877.

Barclay, J.A. and Steyert, W.A., ***Magnetic Refrigerator Development***, Electric Power Research Institute Report EPRI EL-1757, April 1981.

Brailsford, F., "Theory of a Ferromagnetic Heat Engine," *Proc IEE,111*, 9, September 1964, pp. 1602-1606.

Brillouin, L. and Iskenderian, H.P., "Thermomagnetic Generator," *Electrical Communication, 25*, 1948, pp. 300-311.

Brown, G.V., "Basic Principles and Possible Configurations of Magnetic Heat Pumps," *ASHRAE Transactions, 87*, 2, 1981.

Brown, G.V., "Magnetic Heat Pumping Near Room Temperature," *JAP, 47*, 8, August 1976, pp. 3673-3680.

Elliott, J.E., "Thermomagnetic Generator," *JAP, 30*, 11, November 1959, pp. 1774-1777.

Kirol, L.D., ***Magnetic Heat Engine Preliminary Feasibility Study***, Report EGG-SE-6718, November 1984.

Kirol, L.D. and Mills, J.I., "Numerical Analysis of Thermomagnetic Generators," *JAP, 56*, 3, August 1, 1984, pp. 824-828.

Kirol, L.D. and Mills, J.I., "Thermomagnetic Generator," *19th IECEC* V.3 (August 1984): 1361-68.

Kirol, L.D. and Mills, J.I., "Rotary Magnetic Heat Pump," *19th IECEC* V.3 (August 1984): 1350-57.

Kirol, L.D., Mills, J.I., Fullmer, K.S. and Zabriskie, J.N., ***Magnetic Heat Pump Feasibility Assessment***, Report EGG-2343, October 1984.

Kirol, L.D., Mills, J.I. and VanHaaften, D.H., ***Thermomagnetic Generator***, Report EG&G-SE-6442, November 1983.

Mills, J.I., Kirol, L.D. and VanHaaften, D.H., "Magnetic Heat Pump Cycles for Industrial Waste Heat Recovery," *19th IECEC* V.3 (August 1984): 1369-74.

Oesterreicher, H. and Parker, F.T., "Magnetic Cooling Near Curie Temperatures Above 300K," *JAP, 55*, 12, June 15, 1984, pp. 4334-4338.

Pratt, Jr., W.P., Rosenblum, S.S., Steyert, W.A. and Barclay, J.A., "A Continuous Demagnetization Refrigerator Operating Near 2K an a Study of Magnetic Refrigerants," *Cryogenics, 17*, 12, December 1977, pp. 689-693.

Rosenweig, R.E., "Theory of an Improved Thermomagnetic Generator," *Proc. IEE, 114*, 3, March 1967, pp. 405-409.

Rosenweig, R.E., Nestor, J.W. and Timmins, R.S., "Ferrohydrodynamic Fluids for Direct Conversion of Heat Energy," *AIChE Conference on Materials Associated with Direct Energy Conversion*, London, June 13-17, 1965, pp. 95-110.

Van Der Maas, G.J. and Purvis, W.J., "Curie Point Motor," *American Journal of Physics, 24*, 3, March 1956, pp. 176-177.

Almstrom, Sten-Haken, Bratt, Christer, Nelving, Hans-Goran, "Control Ststems for United Stirling 4-95 Engine in Solar Application," *16th IECEC* V.2 (August 1981): 1883-93.

Anderson, L.M., Proc. 17th Intersociety Energy Conversion Engineering Conference, pp. *125*-130 (1982); and Proc. 16th IEEE Photovoltaic Specialists Conference, pp. *371*-377 (1982).

Anderson, Lynn Marie, "A New Strategy for Efficient Solar Energy Conversion: Parallel-Processing with Surface Plasmons," *17th IECEC* V.1 (August 1982): 125-30.

Baker, N., Lynch, F., Mejia, L. and Olavson, L., "A Hydride Fuel System for Hydrogen Powered Mine Vehicles," *19th IECEC* V.3 (August 1984): 1421-28.

Baron, S., "The Embedded Energy Costs in Solar Energy Systems," *19th IECEC* V.2 (August 1984): 1009-1014.

Bevilacqua, S. and Gislon, R., "A Central Tower Solar Test Facility (RM/CTSTF)," *16th IECEC* V.2 (August 1981): 1742-45.

Bilgen, E., Galindo, J. and Baykara, S.Z., "Experimental Study of hydrogen Production by Direct Decomposition of Water," *16th IECEC* V.2 (August 1983): 564-68.

Boda, F.P., "The SCSE Organic Rankine Engine," *16th IECEC* V.2 (August 1981): 1371-74.

Bronicki, L., "Twenty Years of Experience with Organic Rankine Cycle Turbines--Their Applicability and Use in Energy Conservation and Alternative Energy Systems," *17th IECEC* V.2 (August 1982): 1118-21.

Brown, D.R., Huber, H.D. and Reilly, R.W., "Aquastor: A Computer Model for Cost Analysis of Aquifer Thermal Energy Storage Coupled with District Heating or Cooling Systems," *17th IECEC* V.4 (August 1982): 2012-18.

Galloway, Terry R., "New Developments in Energy Recovery with Organic Rankine Bottoming Cycles," *16th IECEC* V.2 (August 1983): 662-67.

Grant, S., Johnson, S.D. and Smith, D.C., "Technical Developments in Molten Salt Solar Central Receiver Systems," *18th IECEC* V.3 (August 1984): 1716-19.

Hall, D.G., NASA Grant NAG 3-414 (University of Rochester) 1983-1985; Holland, W.R. and Hall, D.G., Phys. Rev. B*27*, 7765 (1983); Holland, W.R. and Hall, D.G., Phys. Rev. Lett. *52* 1041 (1984).

Hildebrandt, Alvin F., "Receiver Design Considerations for Solar Central Receiver Hydrogen Production," *18th IECEC* V.3 (August 1984): 1720-26.

Hofer, D.A. and Pierce, B.L., "Dynamic Performance Analysis for the Solar Hybrid Repowering of the El Paso Electric Company Newman Unit #1," *16th IECEC* V.2 (August 1981): 1776-81.

Hunt, A.J., Ayer, J., Hull, P., Miller, F., Russo, R. and Yuen, W., "Solar Radiant

Processing of Gas-Particle Systems for Producing Useful Fuels and Chemicals," Berkeley: Lawrence Berkeley Laboratory. (Mimeographed.)

Laakso, J.H. and Kimmerman, D.K., "System Design for a Commercial Solar Brayton Cycle Central Receiver Water Desalination Plant," *16th IECEC* V.2 (August 1981): 1810-15.

Lambe, J. and McCarthy, S.L., Phys. Rev. Lett. *37*, 923 (1976).

Lin, S., Parker, G.H. and Stella, M.E., "Solar Hydrogen System Design Considerations," *16th IECEC* V.2 (August 1981): 1430-35.

Maloney, T.J., Solar Energy Mat. *4*, 359 (1981).

Nix, R.G., "A Heat-Pumped Thermochemical Energy Storage System," *16th IECEC* V.4 (August 1983): 1812-817.

Rajeshwar, Krishnan and Dubow, Joel B., "Molten Salt Electrolytes for Photoelectrochemical Applications" *16th IECEC* V.1 (August 1981): 779-82.

Rault, D. and Hertzbert, A., "Radiative Energy Receiver for High Performance Energy Conversion Cycles," *17th IECEC* V.2 (August 1982): 113-18.

Schreiber, J.D. and Carty, R.H., "Parametric Study of the Cadmium Thermoelectrochemical Hydrogen Cycle" *16th IECEC* V.2 (August 1981): 1415-19.

Sincerbox, G.T. and Gordon II, J.C., App. Optics 20' 1491 (1981); Philpott M.R. and Swalen, J.D., J. Chem. Phys. *69*, 2912 (1978); Philpott, M.R., Brillante, A., Pockrang, I.R. and Swalen, J.D., Ml. Cryst. Liq. Cryst. *50*, (1979).

Stegeman, G.I. and Burke, J.J., NASA Grant NAG 3-392 (Univerisity of Arizona) 1983-1985 and Stegeman, G.I., Wallis, R.F. and Maradudin, A.A., "Excitation of Surface Polaritons by End-fire Coupling" paper JH3, Proc. Am. Phys. Soc, March 1983.

Stegeman, G.I. and Burke, J.J., NASA Grant NAG 3-392 (University of Arizona) 1983-1985; Stegeman, G.I., Burke, J.J. and Hall, D.G., Appl. Phys. Lett. *41*, 906 (1982); Stegeman, G.I. and Burke J.J., Appl. Phys. Lett. *43*, 221 (1983).

Stegeman, G.I. and Burke, J.J., NASA Grant NAG 3-392 (University of Arizona) 1983.

Surette, R.G., Moore, A.E. and Pauckert, R.P., "Design, Fabrication, and Initial Testing of Solar One Receiver," *17th IECEC* V.2 (August 1982): 1463-67.

Tanaka, M. and Yanagihara, S., "Mechanical Engineering Laboratory," *16th IECEC* V.1 (August 1981): 12-17.

Wood, P., "Central Station Advanced Power Conditioning: Technology, Utility Interface, and Performance," *19th IECEC* V.4 (August 1984): 2216-19.

Yuen, Walter W. and Hunt, Arlon J., "On the Heat Transfer Charactristics of Gas-Particle Mixture under Direct Radiant Heating," Santa Barbara: University of California and Berkeley: Lawrence Berkeley Laboratory. (Mimographed.)

For a complete discussion of surface plasmons see Raether, H., *Excitation of Plasmons and Interband Transitions by Electrons*, Spring Tracts in Modern Physics, Vol. 88 (Springer Verlag, NY 1980).

For a review and extensive bibliography see Dawson, P., Walmsley, D.G., Quinn, H.A. and Ferguson, A.J.L., Phys. Rev. *B* 30, 3164 (1984).